

UNILATERAL BREAST CANCER-RELATED
LYMPHEDEMA DIAGNOSIS AND MONITORING SYSTEM
USING BIOIMPEDANCE ANALYSIS ON A SMARTPHONE
APPLICATION

SYARIFAH AISYAH BINTI SYED IBRAHIM

FACULTY OF ENGINEERING
UNIVERSITI MALAYA
KUALA LUMPUR

2024

**UNILATERAL BREAST CANCER-RELATED
LYMPHEDEMA DIAGNOSIS AND MONITORING
SYSTEM USING BIOIMPEDANCE ANALYSIS ON A
SMARTPHONE APPLICATION**

SYARIFAH AISYAH BINTI SYED IBRAHIM

**THESIS SUBMITTED IN FULFILMENT OF THE
REQUIREMENTS FOR THE DEGREE OF MASTER OF
ENGINEERING SCIENCE**

**FACULTY OF ENGINEERING
UNIVERSITI MALAYA
KUALA LUMPUR**

2024

UNIVERSITI MALAYA
ORIGINAL LITERARY WORK DECLARATION

Name of Candidate: Syarifah Aisyah binti Syed Ibrahim

Matric No: KGA170004 / 17013974/4

Name of Degree: Master of Engineering Science

Title of Project Paper/Research Report/Dissertation/Thesis ("this Work"):

Development of Unilateral Breast Cancer-Related Lymphedema Diagnosis and Monitoring System Using Bioimpedance Analysis and Smartphone Application

Field of Study: Biomedical Engineering (NEC 520: Engineering & Engineering Trades)

I do solemnly and sincerely declare that:

- (1) I am the sole author/writer of this Work;
- (2) This Work is original;
- (3) Any use of any work in which copyright exists was done by way of fair dealing and for permitted purposes and any excerpt or extract from, or reference to or reproduction of any copyright work has been disclosed expressly and sufficiently and the title of the Work and its authorship have been acknowledged in this Work;
- (4) I do not have any actual knowledge nor do I ought reasonably to know that the making of this work constitutes an infringement of any copyright work;
- (5) I hereby assign all and every rights in the copyright to this Work to the Universiti Malaya ("UM"), who henceforth shall be owner of the copyright in this Work and that any reproduction or use in any form or by any means whatsoever is prohibited without the written consent of UM having been first had and obtained;
- (6) I am fully aware that if in the course of making this Work I have infringed any copyright whether intentionally or otherwise, I may be subject to legal action or any other action as may be determined by UM.

Candidate's Signature

Date: 21 February 2024

Subscribed and solemnly declared before,

Witness's Signature

Date: 22 February 2024

Name:

Designation:

ABSTRACT

Lymphedema resulting from breast cancer treatment can significantly impact the quality of life for affected individuals. Early diagnosis and continuous monitoring of lymphedema are crucial for effective management. However, current methods are inconvenient, expensive, and limited accessibility.

This thesis presents the development of a portable system for diagnosing and monitoring unilateral breast cancer-related lymphedema (UBCRL) using bioimpedance analysis (BIA) and a smartphone application.

The developed UBRCL system utilises BIA technique via bioimpedance spectroscopy frequency analysis. The bioimpedance analyser includes an impedance analyser unit (AD5941), isolating capacitors (0.47 μF), limiting resistors (1 k Ω), electrostatic discharge protection unit, calibration resistors (1 k Ω), and ADuCM3029 microcontroller. The AD5941 embeds an AC voltage signal generator, high-precision current meter, differential voltage meter, and Discrete Fourier transform (DFT). The DFT processes measured data, calculating real and imaginary parts, while the ADuCM3029 microcontroller computes bioimpedance values. The system applies tetrapolar electrode configuration for uniform current distribution and eliminates skin contact impedance. Frequencies from 5 kHz to 200 kHz with 400 μA are delivered to the upper limbs through source electrodes. Resultant bioimpedance measurements are captured using sense electrodes. The bioimpedance measurements are wirelessly transmitted to a smartphone application via Bluetooth. Data is sent to the Google Cloud Function to extrapolate Cole parameters, specifically the resistance at zero frequency (R_0), and evaluate inter-arm R_0 ratio. The R_0 ratio is stored in Firestore database and on the app, aiding UBCRL diagnosis and monitoring. The smartphone application was developed using the Flutter framework. The app functions to initiate measurements with the bioimpedance analyser and provides a user interface for diagnosing and monitoring UBCRL. The UBCRL system was tested

and validated using passive loads and clinical validation involving 45 healthy participants and 100 unilateral BCRL patients. The results were compared with established devices: LCR meter and Quadscan 4000.

The validation results using passive loads against an LCR meter demonstrated high accuracy and precision with 0.5% error, 0.01 standard deviation, 0.08% precision, and R-squared value of 0.999. Validation results compared with Quadscan 4000 showed negligible difference ($p > 0.05$), indicating high similarity with the commercial device. The clinical validation showed that the developed UBCRL system could differentiate between healthy and lymphedema-affected upper limbs. The R_0 ratios were significantly different between healthy participants and stage 0 and those with stage 1 ($p < 0.001$) and stage 2 ($p < 0.001$) lymphedema. The UBCRL detection threshold in Malaysia was identified as 1.077 for dominant affected and 1.047 for non-dominant affected individuals. Mean and standard deviation dominant affected individuals were: stage 0 (1.034 ± 0.021), stage 1 (1.145 ± 0.035), stage 2 (1.394 ± 0.090). For non-dominant affected individuals: stage 0 (0.989 ± 0.029), stage 1 (0.989 ± 0.014), stage 2 (1.447 ± 0.712).

These findings demonstrate the potential of the developed UBCRL system for diagnosis, monitoring and effective treatment management of UBCRL. The system is non-invasive, portable and affordable, increasing access particularly in resource-limited settings.

Keywords: unilateral breast cancer-related lymphedema, bioimpedance analyser, diagnosis, monitoring, rehabilitation,

ABSTRAK

Limfedema akibat daripada rawatan kanser payudara boleh memberi kesan ketara kepada kualiti hidup bagi individu yang terjejas. Diagnosis awal dan pemantauan berterusan lymphedema adalah penting untuk pengurusan yang berkesan. Walau bagaimanapun, kaedah semasa menyusahkan, mahal dan kebolehcapaian terhad.

Tesis ini membentangkan pembangunan sistem mudah alih untuk mendiagnosis dan memantau lymphedema berkaitan kanser payudara unilateral (UBCRL) menggunakan analisis bioimpedans (BIA) dan aplikasi telefon pintar.

Sistem UBRCL yang dibangunkan menggunakan teknik BIA melalui analisis frekuensi spektroskopi bioimpedans. Penganalisis bioimpedans termasuk unit penganalisis impedans (AD5941), kapasitor pengasingan ($0.47 \mu\text{F}$), perintang pengehad ($1 \text{ k}\Omega$), unit perlindungan nyahcas elektrostatik, perintang penentukuran ($1 \text{ k}\Omega$), dan pengawal mikro ADuCM3029. AD5941 membenamkan penjana isyarat voltan AC, meter arus ketepatan tinggi, meter voltan pembezaan dan transformasi Discrete Fourier (DFT). DFT memproses data yang diukur, mengira bahagian sebenar dan khayalan, manakala mikropengawal ADuCM3029 mengira nilai bioimpedans. Sistem ini menggunakan konfigurasi elektrod tetrapolar untuk pengagihan arus seragam dan menghapuskan galangan sentuhan kulit. Frekuensi dari 5 kHz hingga 200 kHz dengan $400 \mu\text{A}$ dihantar ke anggota atas melalui elektrod sumber. Pengukuran bioimpedans terhasil ditangkap menggunakan elektrod deria. Pengukuran bioimpedans dihantar secara wayarles ke aplikasi telefon pintar melalui Bluetooth. Data dihantar ke Fungsi Awan Google untuk mengekstrapolasi parameter Cole, khususnya rintangan pada frekuensi sifar (R_0) dan menilai nisbah R_0 antara lengan. Nisbah R_0 disimpan dalam pangkalan data Firestore dan pada apl, membantu diagnosis dan pemantauan UBCRL. Aplikasi telefon pintar telah dibangunkan menggunakan rangka kerja Flutter. Aplikasi ini berfungsi untuk memulakan pengukuran dengan penganalisis bioimpedans dan menyediakan antara muka pengguna

untuk mendiagnosis dan memantau UBCRL. Sistem UBCRL telah diuji dan disahkan menggunakan beban pasif dan pengesahan klinikal yang melibatkan 45 peserta yang sihat dan 100 pesakit BCRL unilateral. Hasilnya dibandingkan dengan peranti sedia ada: meter LCR dan Quadscan 4000.

Keputusan pengesahan menggunakan beban pasif terhadap meter LCR menunjukkan ketepatan dan kejituan yang tinggi dengan ralat 0.5%, sisihan piawai 0.01, ketepatan 0.08% dan nilai kuasa dua R sebanyak 0.999. Keputusan pengesahan berbanding dengan Quadscan 4000 menunjukkan perbezaan yang boleh diabaikan ($p > 0.05$), menunjukkan persamaan yang tinggi dengan peranti komersial. Pengesahan klinikal menunjukkan bahawa sistem UBCRL yang dibangunkan boleh membezakan antara anggota atas yang sihat dan terkena lymphedema. Nisbah R0 adalah berbeza dengan ketara antara peserta yang sihat dan peringkat 0 dan mereka yang mempunyai limfedema peringkat 1 ($p < 0.001$) dan peringkat 2 ($p < 0.001$). Ambang pengesanan UBCRL di Malaysia dikenal pasti sebagai 1.077 untuk individu terjejas dominan dan 1.047 untuk individu terjejas bukan dominan. Min dan sisihan piawai individu yang dominan terjejas ialah: peringkat 0 (1.034 ± 0.021), peringkat 1 (1.145 ± 0.035), peringkat 2 (1.394 ± 0.090). Bagi individu yang tidak dominan terjejas: peringkat 0 (0.989 ± 0.029), peringkat 1 (0.989 ± 0.014), peringkat 2 (1.447 ± 0.712).

Penemuan ini menunjukkan potensi sistem UBCRL yang dibangunkan untuk diagnosis, pemantauan dan pengurusan rawatan UBCRL yang berkesan. Sistem ini tidak invasif, mudah alih dan berpatutan, meningkatkan akses terutamanya dalam tetapan terhad sumber.

Keywords: lymphedema yang berkaitan dengan kanser payudara unilateral, mesin analisis impedans, diagnosis, pemantauan, rehabilitasi

ACKNOWLEDGEMENTS

Alhamdulillah, all praise to Allah S.W.T for His blessings I am able to write this section, finally. This master's journey has been long and challenging, and I am filled with happiness as I finally submit my thesis.

First and foremost, I want to express my deepest gratitude to my parents. Their unwavering love, support, patience, and encouragement throughout this chapter of my life. Thank you, Ma and Ba for being the biggest cheerleaders.

I would like to extend my heartfelt gratitude to my supervisors, Prof. Ir. Dr. Fatimah Ibrahim, and Prof. Jongman Cho, for their invaluable guidance, expertise, and continuous support. Your mentorship has shaped my research and academic growth.

I am indebted to Prof. Dr. Nur Aishah Mohd Taib for her support and collaboration in the medical aspects of lymphedema. The staff and patients of the Lymphedema Rehabilitation, Department of Rehabilitation, University of Malaya Medical Center for their assistance, participation, and contributions to the success of this research.

My sincere appreciation goes to my family and friends who volunteered their time and support. Your involvement and willingness to contribute have been immensely helpful and deeply appreciated.

I am grateful to the members of the Centre for Innovation in Medical Engineering. Special thanks to Mr. Karunan, Ms. Nurhaslina, Dr. Teh Swe Jyan, Dr. Nurul Fauzani, Dr. Adam, and Ms. Elyana for your spirits and encouragement when I needed it the most.

To all those who have been a part of my master's journey, whether mentioned or not, thank you from the bottom of my heart.

TABLE OF CONTENTS

Abstract	iii
Abstrak	v
Acknowledgements	vii
Table of Contents	viii
List of Figures	xiv
List of Tables.....	xix
List of Symbols and Abbreviations.....	xxi
List of Appendices	xxiii
CHAPTER 1: INTRODUCTION.....	24
1.1 Overview.....	24
1.2 Objectives	26
1.3 Scope of Work	27
1.4 Thesis Organisation	27
CHAPTER 2: LITERATURE REVIEW.....	30
2.1 Introduction.....	30
2.2 Breast Anatomy and Physiology	30
2.3 Breast Diseases	31
2.4 Breast Cancer.....	31
2.4.1 Symptoms of Breast Cancer	31
2.4.2 Diagnosis of Breast Cancer	33
2.4.3 Types of Breast Cancer	35
2.4.4 Stages of breast cancer	38
2.4.5 Types of Breast Cancer Treatment.....	39

2.4.5.1	Surgery	40
2.4.5.2	Lymph Node Removal and Analysis	41
2.4.5.3	Radiation Therapy	43
2.4.5.4	Systemic Therapy	43
2.4.6	Complications of Breast Cancer Treatment	44
2.5	Breast Cancer-related Lymphedema (BCRL)	45
2.5.1	Stages of BCRL	46
2.5.2	Current BCRL Clinical Diagnosis and Monitoring	49
2.5.2.1	Water Displacement	50
2.5.2.2	Circumferential Limb Measurement	51
2.5.2.3	Palpation	54
2.5.2.4	Tonometry	54
2.5.2.5	Perometry	56
2.5.2.6	Lymphoscintigraphy	57
2.5.2.7	Bioelectrical Impedance Analysis	58
2.6	Bioelectrical Impedance Analysis and Breast Cancer-Related Lymphedema (BCRL)	60
2.6.1	Fundamental of Bioelectrical Impedance Analysis Technique	60
2.6.2	Frequency Analysis Methods for Breast Cancer-Related Lymphedema Assessment	63
2.6.2.1	Single Frequency Bioimpedance Analysis	64
2.6.2.2	Multiple Frequencies Bioimpedance Analysis	64
2.6.2.3	Bioelectrical Impedance Spectroscopy	65
2.6.3	Measurement Protocol	70
2.6.3.1	Preliminary Measurement Preparations	70
2.6.3.2	Measurement Posture	70

2.6.3.3	Whole-body Versus Segmental Body Bioimpedance Measurement	71
2.6.4	Electrodes	74
2.6.4.1	Types of Surface Electrodes.....	74
2.6.4.2	Electrode Design and Configuration	76
2.6.5	Sources of Artifacts and Noise in Bioimpedance Measurements	78
2.6.6	Quantitative Evaluation of Lymphedema Using BIA	79
2.6.7	Validity of BIA in Lymphedema Assessment.....	83
2.6.8	Commercial Bioelectrical Impedance Analyser.....	87
2.7	Design of Bioelectrical Impedance Instrumentation	90
2.7.1	Testing and Validation	98
2.8	Bioelectrical Impedance Portable Application	99
2.9	Smartphone Application	100
2.9.1	Frameworks	103
2.10	Medical Device Standards	104
2.10.1	Medical Device Standards for Bioimpedance Analyser.....	104
2.10.1.1	ISO 13485	104
2.10.1.2	IEC 60601	104
2.10.2	Medical Device Standards for Smartphone Application.....	105
2.10.2.1	ISO 14971	105
2.10.2.2	IEC 62366-1	106
2.10.2.3	ISO 9241-210	106
2.11	Statistical Analysis.....	106
2.12	Summary.....	108
CHAPTER 3: METHODOLOGY.....		111
3.1	Introduction.....	111

3.2	Development of Hardware Module	115
3.2.1	Microcontroller.....	115
3.2.2	Bioimpedance Analyser	115
3.2.2.1	Impedance Analyser Unit.....	119
3.2.2.2	Isolation Capacitors.....	120
3.2.2.3	Current Limit Resistor.....	120
3.2.2.4	Transimpedance Amplifier Gain Resistor.....	121
3.2.2.5	Calibration Resistor.....	123
3.2.2.6	Electrostatic Discharge Protection Unit.....	123
3.2.3	Power Supply Unit	123
3.2.4	Electrodes	123
3.3	Development of Software Module.....	124
3.3.1	Development of Smartphone Application Module	124
3.3.2	Development of Firmware Module	126
3.3.3	Development of Cloud Server Module.....	128
3.3.4	Estimation of Cole Parameters	128
3.4	System Integration and Data Acquisition.....	129
3.4.1	Microcontroller.....	129
3.4.2	Bluetooth	129
3.5	Testing and Validation of the Unilateral BCRL System	131
3.5.1	Testing and Validation with Passive Loads	131
3.5.1.1	Resistors	132
3.5.1.2	Capacitors.....	132
3.5.1.3	Electrical Circuit Model of Human Upper Arm.....	133
3.5.2	Validation with Healthy Participants	134
3.5.3	Clinical Validation	134

3.5.3.1	Ethics Application	134
3.5.3.2	Selection of Participant	134
3.5.3.3	Study Protocol	136
3.5.3.4	Clinical Measurements	136
3.5.4	Determination of Unilateral Upper Limb Lymphedema Detection Threshold.....	137
CHAPTER 4: RESULTS & DISCUSSION.....		139
4.1	Introduction.....	139
4.2	Development of Hardware Module	139
4.2.1	Microcontroller.....	139
4.2.2	Bioimpedance analyser.....	140
4.2.3	Power Supply Unit	143
4.2.4	Electrodes	143
4.2.5	3D Casing	144
4.3	Development of Software Module.....	148
4.3.1	Development of Smartphone Application Module	148
4.3.1.1	Smartphone Application Screens	149
4.3.1.2	Smartphone Application Screens and Navigation Flowchart for Lymphedema Measurement	160
4.3.2	Development of Firmware Module	161
4.3.3	Development of Cloud Server Module.....	162
4.3.3.1	Cloud Functions	163
4.3.3.2	Firestore Database	164
4.3.4	Estimation of Cole Parameters	166
4.4	System Integration and Data Acquisition	170
4.4.1	Microcontroller.....	170

4.4.2	Bluetooth	171
4.5	Testing and Validation of the Unilateral BCRL System	172
4.5.1	Testing and Validation with Passive Loads	172
4.5.1.1	Resistors	172
4.5.1.2	Capacitors	175
4.5.1.3	Electrical Circuit Model of Human Upper Arm.....	176
4.5.2	Validation with Healthy Participants	181
4.5.3	Estimation of Cole Parameters on Healthy Participant and UBCRL patient 182	
4.5.4	Clinical Validation	188
4.5.4.1	Ethics Application	188
4.5.4.2	Selection of Participants	188
4.5.4.3	Clinical Measurements	189
4.5.5	Determination of Unilateral Upper Limb Lymphedema Detection Threshold.....	192
4.6	Cost Analysis.....	195
4.7	Comparison with Commercial BIA Analysers	196
4.8	Summary.....	199

CHAPTER 5: CONCLUSIONS AND RECOMMENDATION FOR FUTURE WORK 202

5.1	Conclusion.....	202
5.2	Limitation and Recommendation for Future Work	203
	References	204
	List of Publications and Papers Presented	226
	Appendix: ETHICS APPROVAL.....	227

LIST OF FIGURES

Figure 2.1: Breast anatomy and lymph nodes.....	30
Figure 2.2: Signs and symptoms of breast cancer (Thomas, 2023)	32
Figure 2.3: Breast mammography.....	33
Figure 2.4: Breast ultrasound	34
Figure 2.5: Comparison of normal and abnormal breast MRI images.....	35
Figure 2.6: Ductal Carcinoma in Situ (DCIS).....	36
Figure 2.7: Inflammatory Breast Cancer (IBC)	37
Figure 2.8: Lumpectomy.....	40
Figure 2.9: Mastectomy	41
Figure 2.10: Sentinel lymph node biopsy	42
Figure 2.11: Axillary lymph node dissection.....	42
Figure 2.12: Radiation therapy.....	43
Figure 2.13: Stages of BCRL (Cheng, Chang, & Patel, 2021)	47
Figure 2.14: Water displacement (Karlsson, Johansson, Nilsson-Wikmar, & Brogårdh, 2022)	50
Figure 2.15: Five marks used by physiotherapists for circumference measurements (Gjorup, Zerahn, & Hendel, 2010).....	52
Figure 2.16: Tonometry (Zaleska, Olszewski, Durlík, Kaczmarek, & Freidenrich, 2018)	55
Figure 2.17: Perometry.....	56
Figure 2.18: Lymphoscintigraphy of upper limb lymphedema (Barbieux et al., 2023) .	57
Figure 2.19: Cylinder model as a representation of human body	62
Figure 2.20: Current flow in biological tissue (Scagliusi et al., 2023)	63
Figure 2.21: Fricke’s equivalent electrical circuit model.....	65

Figure 2.22: Cole plot (T. Cole, 2018).....	66
Figure 2.23: Whole-body and segmental bioimpedance measurement (Mialich et al., 2014)	72
Figure 2.24: Two-electrode bioimpedance measurement	76
Figure 2.25: Four-electrode bioimpedance measurement.....	76
Figure 2.26: Interpretation of L-Dex scores.....	83
Figure 2.27: Block diagram of the BIS instrumentation system by Santoso <i>et al.</i> (2020)	91
Figure 2.28: Block diagram of the BIS instrumentation system by Ain <i>et al.</i> (2021)	92
Figure 2.29: AD5933 impedance analyser system by Simic <i>et al.</i> (2013).....	93
Figure 2.30: Schematic of the Load-in-the-Loop current source (AFE-1) (Noveletto et al., 2016)	95
Figure 2.31: Schematic of the Mirrored Howland-Modified current source (AFE-2) (Noveletto et al., 2016).....	95
Figure 2.32: AD5941 bioimpedance instrumentation block diagram.....	96
Figure 2.33: BIA instrumentation hardware block diagram by Tonello <i>et al.</i> (2023)	97
Figure 2.34: Prototype of the portable and wearable BIA system (Hegarty-Craver et al., 2015)	100
Figure 2.35: BIA system and smartphone application by Krzesinki <i>et al.</i> (2021).....	100
Figure 2.36: Elements of the measurement prototype for monitoring changes in body volume due to oedema by Scagliusi <i>et al.</i> (2023)	101
Figure 2.37: User tongue application (UTAP) developed by Luo <i>et al.</i> (2021)	102
Figure 2.38: Daily obesity management system proposed by A. Choi <i>et al.</i> (2015)	102
Figure 3.1: Research methodology flowchart	112
Figure 3.2: Unilateral BCRL diagnosis and monitoring system	113
Figure 3.3: Unilateral BCRL diagnosis and monitoring system block diagram	114
Figure 3.4: Bioimpedance analyser module block diagram.....	116

Figure 3.5: Schematic diagram of the developed bioimpedance analyser (Part 1).....	117
Figure 3.6: Schematic diagram of the developed bioimpedance analyser (Part 2).....	118
Figure 3.7: AD5941 pin configuration.....	119
Figure 3.8: Overall current flow in transimpedance amplifier.....	121
Figure 3.9: Smartphone application operation flowchart.....	125
Figure 3.10: ADuCM3029 and AD5941 firmware flowchart.....	127
Figure 3.11: Bioimpedance spectroscopy data processing flowchart.....	128
Figure 3.12: Bluetooth process flowchart.....	130
Figure 3.13: Electrodes connection to the impedance under measure.....	132
Figure 3.14: Electrode placement on the participant.....	136
Figure 4.1: Hardware module board diagram.....	141
Figure 4.2: Hardware module PCB.....	142
Figure 4.3: Bioimpedance electrodes cables.....	144
Figure 4.4: Mobilymph bottom part drawing and dimension (mm).....	145
Figure 4.5: Mobilymph top part drawing and dimension (mm).....	146
Figure 4.6: Mobilymph enclosure.....	147
Figure 4.7: The Home screen of the Mobilymph smartphone application.....	149
Figure 4.8: The Progress screen of the Mobilymph smartphone application.....	151
Figure 4.9: The Ready to Measure screen of Mobilymph smartphone application.....	153
Figure 4.10: The Measure screen of Mobilymph smartphone application.....	155
Figure 4.11: The Results screen of Mobilymph smartphone application.....	157
Figure 4.12: The Profile screen of Mobilymph smartphone application.....	159
Figure 4.13: Smartphone application screens and navigation flowchart to start lymphedema measurement.....	160
Figure 4.14: Firmware development progress in Tera Term.....	162

Figure 4.15: Cloud function logs	164
Figure 4.16: Organization of Firestore Database for lymphedema measurement data.	165
Figure 4.17: Query builder in Firestore Database.....	166
Figure 4.18: NLLS results and R-squared value in PyCharm.....	167
Figure 4.19: Resistance versus frequency of a parallel RC circuit	168
Figure 4.20: Resistance versus imaginary of a parallel RC circuit.....	168
Figure 4.21: Estimated resistance (R_0 and R_∞) of a parallel RC circuit.....	169
Figure 4.22: Cole – Cole plot of a parallel RC circuit	169
Figure 4.23: UART communication test using Tera Term	170
Figure 4.24: Bluetooth communication between smartphone application and nRF52840	171
Figure 4.25: Resistance estimation and Impedance plane (Cole – Cole plot) of Set 1.	179
Figure 4.26: Resistance estimation and Impedance plane (Cole – Cole plot) of Set 2.	179
Figure 4.27: Resistance estimation and Impedance plane (Cole – Cole plot) of Set 3.	180
Figure 4.28: Resistance versus frequency of a healthy participant (Subject 45) upper limb	184
Figure 4.29: Resistance versus imaginary of a healthy participant (Subject 45) upper limb	184
Figure 4.30: Estimated resistance (R_0 and R_∞) of a healthy participant (Subject 45) upper limb	185
Figure 4.31: Cole – Cole plot of a healthy participant (Subject 45) upper limb.....	185
Figure 4.32: Resistance versus frequency of a UBCRL Stage 1 patient (Subject 98) upper limb	186
Figure 4.33: Resistance versus imaginary of a UBCRL Stage 1 (Subject 98) upper limb	186
Figure 4.34: Estimated resistance (R_0 and R_∞) of a UBCRL Stage 1 (Subject 98) upper limb	187
Figure 4.35: Cole – Cole plot of a UBCRL Stage 1 (Subject 98) upper limb	187

Figure 4.36: Inter-arm R_0 ratios in healthy and UBC participants with different stages of BCRL 191

Universiti Malaya

LIST OF TABLES

Table 2.1: Description and characteristics of stages in BCRL.....	48
Table 2.2: Comparison of advantages and disadvantages of BCRL diagnosis methods	59
Table 2.3: Normative inter-limb ratios and lymphedema detection threshold	81
Table 2.4: Commercial BIA device specifications	89
Table 2.5: Accuracy of impedance measurements using AD5933 impedance analyser system.....	94
Table 2.6: Summary of research components and methods for unilateral BCRL diagnosis and monitoring	110
Table 3.1: Bioimpedance analyser module design specifications.....	116
Table 3.2: Resistors experimental parameters	132
Table 3.3: Capacitors experimental parameters	133
Table 3.4: Human upper arm model using different combinations of passive loads	133
Table 4.1: Electrode name and colour mapping.....	144
Table 4.2: Results of impedance measurement on passive loads at 5 kHz.....	173
Table 4.3: Results of impedance measurement on passive loads at 50 kHz.....	173
Table 4.4: Results of impedance measurement on passive loads at 100 kHz.....	173
Table 4.5: Results of impedance measurements on passive loads at 200 kHz	173
Table 4.6: Impedance measurement error for an impedance range of 100 Ω to 1 k Ω at 5 kHz, 50 kHz, 100 kHz, and 200 kHz	174
Table 4.7: Summary of impedance measurement validation results on passive loads (resistors).....	174
Table 4.8: Results of phase angle measurement on passive loads (capacitors) at 5 kHz	175
Table 4.9: Results of phase angle measurement on passive loads (capacitors) at 50 kHz	175

Table 4.10: Results of phase angle measurement on passive loads (capacitors) at 100 kHz	175
Table 4.11: Results of phase angle measurement on passive loads (capacitors) at 200 kHz	176
Table 4.12: Results of human upper arm model (Set 1)	179
Table 4.13: Results of human upper arm model (Set 2)	179
Table 4.14: Results of human upper arm model (Set 3)	180
Table 4.15: Bioimpedance analysers benchmarking.....	182
Table 4.16: Participant characteristics	189
Table 4.17: UBC participants clinical characteristics	189
Table 4.18: Statistical analysis of inter-arm R_0 ratios of healthy and UBC participants	191
Table 4.19: Descriptive Statistics and Confidence Intervals of Inter-arm R_0 ratios in Healthy and UBC participants with different stages of BCRL	191
Table 4.20: Comparison of normative R_0 ratios for the detection of lymphedema	194
Table 4.21: Cost analysis of the lymphedema diagnosis and monitoring system.....	195
Table 4.22: Comparison of Commercial BIA Analysers with Mobilymph.....	198

LIST OF SYMBOLS AND ABBREVIATIONS

%	:	Percentage
μ	:	Micro
A	:	Ampere
AC	:	Alternating current
ADC	:	Analog-to-digital converter
BCRL	:	Breast cancer-related lymphedema
BIA	:	Bioelectrical impedance analysis
BIS	:	Bioelectrical impedance spectroscopy
CDP	:	Complex decongestive therapy
DAC	:	Digital-to-analog converter
DC	:	Direct current
DFT	:	Digital Fourier transform
ECF	:	Extracellular fluid
ESD	:	Electrostatic discharge
FIFO	:	First In, First Out
HFOSC	:	High frequency internal oscillator
Hz	:	Hertz
ICC	:	Intraclass coefficient
LFOSC	:	Low frequency internal oscillator
LR	:	Likelihood ratio
LRs	:	Likelihood ratios
MFBI	:	Multiple frequency bioimpedance analysis
MISO	:	Master In Slave Out
MOSI	:	Master Out Slave In

MSB	:	Multi-segment bioimpedance
NLLS	:	Non-linear least squares
R	:	Resistance
R_0	:	Resistance to the current flow at zero frequency
R_∞	:	Resistance to the current flow at infinite frequency
R_{TIA}	:	Transimpedance amplifier gain resistor
RXD	:	Receive serial data
SD	:	Standard deviations
SPI	:	Serial peripheral interface
SSB	:	Single segment bioimpedance
TIA	:	Transimpedance amplifier
TXD	:	Transmit serial data
UI	:	User interface
V	:	Voltage
X_c	:	Reactance
Z	:	Impedance or bioimpedance
α	:	Exponent parameter
τ	:	Inverse of characteristic frequency
φ	:	Phase angle
ω	:	Frequency
Ω	:	Ohm
ω_c	:	Characteristic frequency

LIST OF APPENDICES

Appendix: Ethics Approval	226
---------------------------------	-----

Universiti Malaya

CHAPTER 1: INTRODUCTION

1.1 Overview

Breast cancer-related lymphedema (BCRL) is a chronic condition that can occur because of breast cancer treatments or metastatic breast cancer. It is estimated that between 8% and 56% of breast cancer survivors are at risk of developing lymphedema (Deutsch, Land, Begovic, & Sharif, 2008; Kilgore et al., 2018; Kopec et al., 2013; Zou et al., 2018). Lymphedema is characterized by the accumulation of protein-rich fluid in the tissue due to a disruption of the lymphatic system (Cheifetz & Haley, 2010). The accumulated fluid causes swelling in the upper extremity of the affected side. There are four stages of BCRL: Stage 0 (latency stage) is characterized by a damaged lymphatic system but shows no clinical signs of lymphedema. In Stage 1, early onset swelling is present and can be reduced with rehabilitation. Stage 2 is characterized by persistent swelling despite rehabilitation. As the disease progresses to Stage 3, lymphostatic elephantiasis, severe fibrosis, hypertrophic skin, and non-pitting oedema occur. At Stage 2 and 3, the disease becomes chronic and irreversible (Douglass & Kelly-Hope, 2019). Therefore, early detection and management of BCRL at Stage 0 and 1 is important because it is reversible and treatable (BORDEA, EL-BSAT, NODITI, & BORDEA; Soran et al., 2014; Whitworth & Cooper, 2018; Yildiz, Bakar, & Keser, 2022).

Post-operative breast cancer patients must regularly attend lymphedema rehabilitation clinics on a weekly to monthly cycle for 3 years as this is the prevalent timeframe for the onset of lymphedema (Koelmeyer et al., 2019; McLaughlin, Stout, & Schaverien, 2020). Previous studies have reported the association of BCRL patients with decreased quality of life, physical impairment, increased financial burden, elevated depression, and anxiety rates (Boyages et al., 2017; Chachaj et al., 2010; Clough-Gorr, Ganz, & Silliman, 2010; Cormier et al., 2009; Khan, Amatya, Pallant, & Rajapaksa, 2012; Shigaki, Madsen, Wanchai, Stewart, & Armer, 2013; Vassard et al., 2010).

There are several diagnostic and measuring tools that are used to identify and manage lymphedema. These include circumference measurement, water displacement, medical imaging techniques, and bioelectrical impedance analysis (BIA) (Armer & Stewart, 2005; DiSipio, Rye, Newman, & Hayes, 2013; S. Hayes, M. Janda, B. Cornish, D. Battistutta, & B. Newman, 2008; L. C. Ward, 2006). Circumference measurement is a common physical assessment in clinical settings because it is relatively inexpensive and easily accessible. However, it may not be reliable for identifying lymphedema at an early stage, and requires a trained healthcare provider to perform the measurement (Donahue, Crescenzi, Du, & Donahue, 2020; Johnson, Kennedy, & Henry, 2014). Water displacement is uncommonly used due to its unhygienic nature, cumbersome process, and potential for infection (Engin et al., 2019). Medical imaging can be sensitive and accurate for early lymphedema diagnosis, but it is not practical for regular lymphedema monitoring due to its cost and the use of radiation (Erdogan Iyigun et al., 2015).

BIA has been shown to be a reliable and sensitive tool for the diagnosis and monitoring of lymphedema. It is a quick, non-invasive procedure that can detect subtle changes in lymphatic fluid in at-risk breast cancer patients, allowing for early diagnosis and prevention of lymphedema progression (BH Cornish et al., 2001; E. Dylke et al., 2016; Kaufman, Shah, Vicini, & Rizzi, 2017; Seward et al., 2016; L Ward, Kilbreath, & Cornish, 2008). BIA works by transmitting a low-frequency current through the region of interest and measuring the bioimpedance in the extracellular space. In the case of unilateral BCRL, the bioimpedance values of the affected arm are compared to those of the non-affected arm to detect lymphedema. A normal, healthy population is used as a threshold for lymphedema detection, and a BCRL inter-arm ratio that exceeds this threshold indicates the presence of lymphedema (BH Cornish et al., 2001; LC Ward, Dylke, Czerniec, Isenring, & Kilbreath, 2011).

Some of the commercially available bioimpedance analysers for lymphedema measurement include the L-Dex U400 (E. S. Dylke & Ward, 2020), Quadscan 4000 (Mulasi, Kuchnia, Cole, & Earthman, 2015), and SOZO (Pfeiffer et al., 2021). While BIA is a useful technology for lymphedema management, the current commercially available bioimpedance analysers are expensive, bulky, and not suitable for remote monitoring or use in community settings such as homes or offices.

Therefore, the purpose of this study is to develop a low-cost and portable BCRL diagnosis and monitoring system using BIA technique. This BCRL system is a promising solution for addressing the challenges associated with current lymphedema diagnosis and management methods by aiding in early detection and treatment initiation. It is expected that this system will be able to significantly improve the quality of life for breast cancer survivors and reduce the economic burden associated with lymphedema treatment.

1.2 Objectives

The main objective of this project is to develop a portable unilateral BCRL (UBCRL) diagnosis and monitoring system using BIA technique. This involves the following sub – objectives:

- i. Development of a portable UBCRL bioimpedance analyser to measure upper limb lymphatic fluid of breast cancer patients.
- ii. Development of a smartphone application for diagnosis and monitoring of UBCRL patients.
- iii. To test and validate the developed UBCRL system with passive components with an LCR meter and on healthy participants using Quadscan 4000 bioimpedance analyser.

1.3 Scope of Work

The scope of this thesis work covers the development of a low-cost and portable bioimpedance analyser to measure upper limb lymphatic fluid in unilateral breast cancer patients. The device functionality will be tested against established impedance analyser (LCR meter) and commercial bioimpedance analyser (Quadscan 4000). Clinical validation of the device will be conducted on control group of 45 healthy participants as well as on a sample of 100 unilateral breast cancer patients from University of Malaya Medical Centre. The results of these studies will be used to evaluate the reliability of the developed bioimpedance analyser in detecting and discriminating upper limb lymphedema in breast cancer patients and healthy participants. The scope of the research work is to create a practical and cost-effective tool that can assist in the management of lymphedema in breast cancer patients and improve their quality of life.

1.4 Thesis Organisation

The thesis consists of five chapters and structured as follows. Chapter 1 provides an overview of the research topic and outlines the study's objectives. It also defines the scope of the work and introduces the organization of the thesis.

Chapter 2 presents an extensive literature review on breast anatomy and physiology, followed by an exploration of breast diseases, including breast cancer. Detailed discussions cover topics such as breast cancer symptoms, diagnosis methods, different types of breast cancer, and the various stages that it progresses through. The range of treatments available for breast cancer, along with their potential complications, is also examined. The chapter then shifts focus to breast cancer-related lymphedema (BCRL), delineating its stages and discussing the current clinical methods for diagnosis and monitoring. Specific diagnostic techniques such as water displacement, circumferential limb measurement, palpation, tonometry, perometry, lymphoscintigraphy, and

bioelectrical impedance analysis (BIA) are elaborated upon. The application of BIA for assessing lymphedema is explored, accompanied by an in-depth understanding of measurement protocols, electrode types, and the validity of BIA in lymphedema assessment. Additionally, the chapter delves into the design of BIA instrumentation, the analysis of bioimpedance data, sources of artifacts and noise in measurements, and the comparison of commercial bioelectrical impedance analysers. Lastly, this chapter provides insight into the development of bioelectrical impedance portable applications and the framework employed for smartphone applications, concluding with a comprehensive summary of the literature review.

Chapter 3 describes development and design of the hardware module, elaborating on the microcontroller and lymphedema detection components. The software module's development is similarly discussed, encompassing the smartphone application, firmware, cloud server components, and estimation of Cole parameters. Furthermore, the chapter elucidates the process of system integration and data acquisition, detailing the role of the microcontroller and Bluetooth functionality. The testing and validation phase is also covered extensively, including validation with passive loads, validation with healthy participants, and clinical validation, touching upon aspects like ethics applications, participant selection, study protocols, clinical measurements, and the determination of the unilateral upper limb lymphedema detection threshold.

Chapter 4 presents the results of hardware module development, including details about the microcontroller, lymphedema detection components, power supply unit, electrodes, and the 3D casing. The software module's results encompass the development of the smartphone application, firmware, cloud server components, and the estimation of Cole parameters. System integration and data acquisition are addressed in this chapter, with a focus on the microcontroller and Bluetooth functionality. The validation process

involving passive loads, healthy participants, and BCRL patients is meticulously documented, alongside an assessment of the estimation of Cole parameters. Clinical validation results, encompassing ethics applications, participant selection, measurements, and the determination of the lymphedema detection threshold, are also presented. The chapter concludes with a cost analysis and a comparative analysis between the developed system and commercial BIA analysers.

Chapter 5 concludes the thesis by summarizing the key findings and conclusions drawn from the study. It highlights the contributions of the research and acknowledges any limitations encountered. This chapter also offers insightful recommendations for future research directions, indicating potential areas of exploration and improvement for the developed system and methodology.

CHAPTER 2: LITERATURE REVIEW

2.1 Introduction

This chapter presents the review articles for the development of lymphedema diagnosis and monitoring system. It reviews the topics on breast anatomy and physiology, breast cancer, current clinical diagnosis and monitoring of breast cancer-related lymphedema (BCRL), bioimpedance analysis, and design of bioimpedance instrumentation and signal processing.

2.2 Breast Anatomy and Physiology

A breast is made up mainly of lobules, ducts, connective tissue, blood vessels, lymph vessels, and lymph nodes. The lobules are the glands that produce milk. The ducts transport milk to the nipple. The connective tissues consisting of fibrous and fatty tissues surrounds and holds everything together. The lymph nodes are part of lymphatic system in body. The lymph node and lymph vessel contain lymph fluid (yellow fluid) that flows through the lymphatic system. The lymphatic system collects and drains waste products into veins to eliminate waste products. The internal mammary chain is a chain of lymph nodes surrounding the centre of the chest and close to the breastbone. The closest lymph nodes to the internal mammary chain are the axillary lymph nodes, as shown in Figure 2.1.

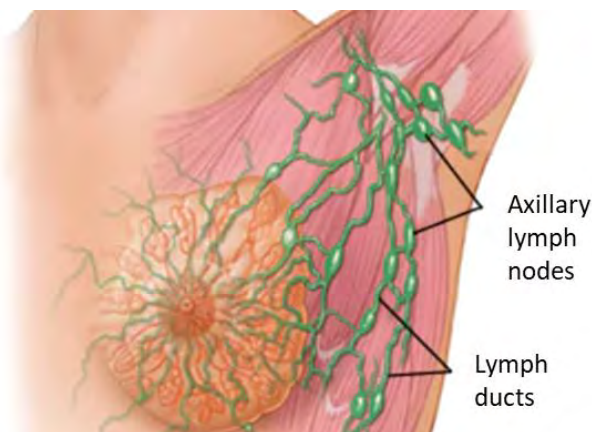


Figure 2.1: Breast anatomy and lymph nodes

2.3 Breast Diseases

Numerous breast diseases ranging from benign conditions such as fibrocystic changes and fibroadenomas to malignant diseases like breast cancer. Fibrocystic breast changes are characterized as benign lumps, tenderness, and discomfort. Fibrocystic are influenced by hormone fluctuations made in the ovaries during menstruation (Dang, Miles, Young, He, & Nguyen, 2023). On the other hand, fibroadenomas are benign tumours that manifest as solid breast lump. Typically, fibroadenomas is a painless mass (Ezike et al., 2023). One of the most prevalent malignancies impacting women globally, is breast cancer. Breast cancer is characterized by the uncontrolled proliferation of abnormal cells within breast tissue (Nayak et al., 2023). The female gender presents the most substantial risk factor for breast cancer. While the majority of those affected by breast cancer are female, approximately 0.5 – 1 % of cases occur in men (Anderson, 2023).

2.4 Breast Cancer

Breast cancer occurs when there is an uncontrolled growth of abnormal cells in breast. Breast cancer commonly occur in the lobules or ducts. The onset of breast cancer in the ducts is known as invasive ductal carcinoma in which the cancer cells grow outside the ducts and into other parts of breast tissue. Invasive lobular carcinoma is cancer cells that spread from the lobules to the other breast tissues. These invasive cancer cells are the two most common kinds of breast cancer. Invasive cancer cells can metastasize or spread to other parts of the body. Cancer cells that have metastasized can be carried by the lymph fluid to nearby lymph nodes.

2.4.1 Symptoms of Breast Cancer

The signs and symptoms of breast cancer as illustrated Figure 2.2 in may include:

- A distinct breast lump or thickness, distinguishable from nearby tissue
- Changes in breast's size, shape, or overall appearance

- Skin transformations on the breast, such as dimpling
- A recently inverted nipple
- Peeling, scaling, crusting, or flaking of the skin around the nipple (areola) of breast skin
- Skin redness or pitting of the skin like the texture of an orange peel over the breast
- Nipple discharge of thin or thick in colour from clear to milky to yellow, green, or red
- Lymph nodes swelling in the underarm lymph node region
- Breast or nipple pain

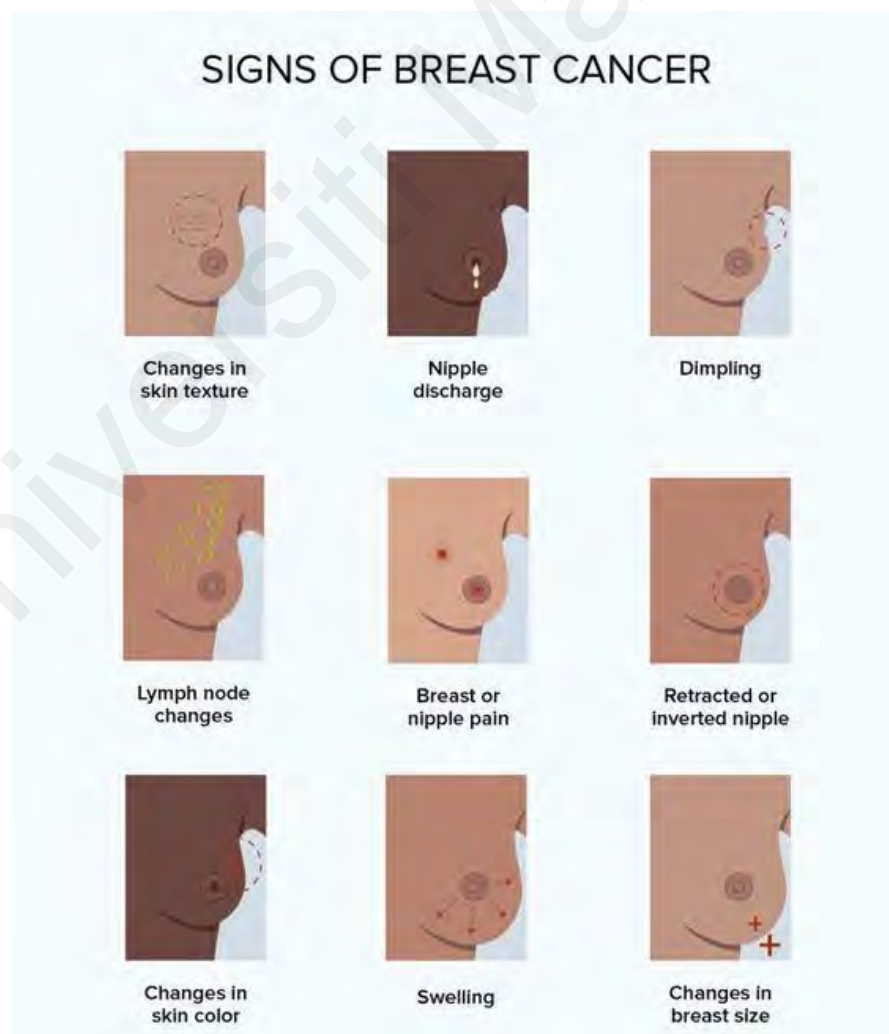


Figure 2.2: Signs and symptoms of breast cancer (Thomas, 2023)

2.4.2 Diagnosis of Breast Cancer

Breast cancer necessitates accurate and timely diagnosis for effective treatment and improved outcomes. The diagnostic approaches and techniques employed in the detection and assessment of breast cancer are as follows:

(a) *Clinical Examination and Self – Examination*

Clinical breast examination conducted by healthcare professionals involves palpation of the breasts and surrounding areas to identify any abnormalities or irregularities. Self – breast examination enables individuals to monitor changes in their breast tissue (Sayed et al., 2023).

(b) *Mammography*

Mammography is an established imaging technique that utilizes X – ray to capture detailed images of breast tissue. It is a tool for early detection, especially in asymptomatic individuals. Mammography aids in identifying abnormalities that may not be palpable during clinical examination (Nasser et al., 2023).

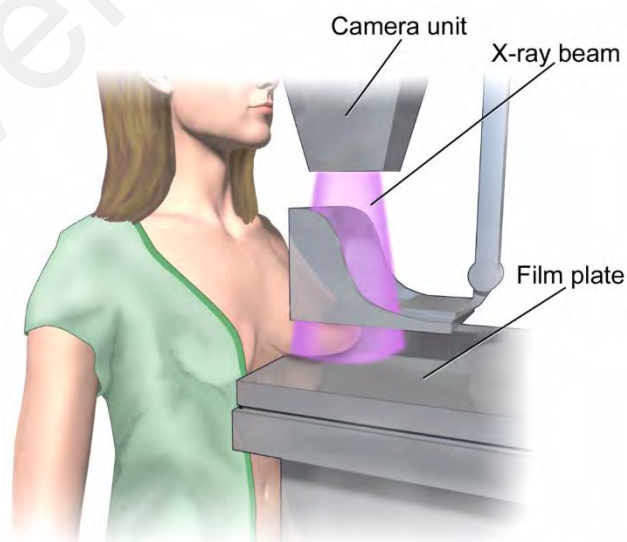


Figure 2.3: Breast mammography

(c) Ultrasonography

Breast ultrasonography employs sound waves (10 – 15 MHz) to create real – time images of breast tissue. It complements mammography by differentiating and characterizing the breast abnormalities between solid masses and fluid-filled cysts (Nasser et al., 2023).

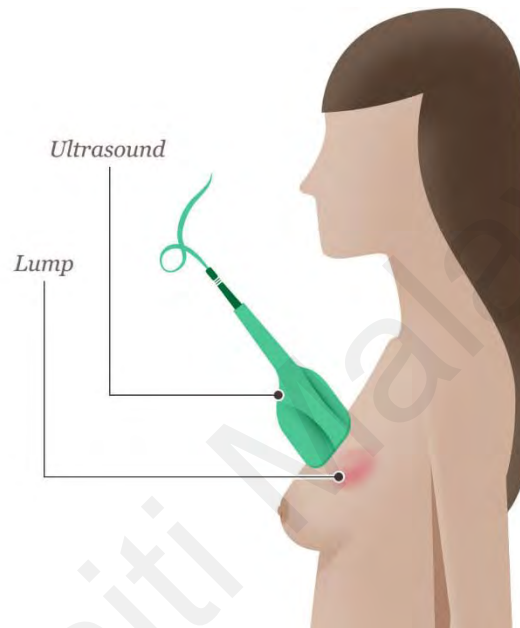


Figure 2.4: Breast ultrasound

(d) Magnetic Resonance Imaging (MRI)

Breast MRI uses powerful magnets and radio waves to generate detailed images of breast tissue. It functions to assess dense breast tissue and evaluate the extend of cancer in cases of diagnosed breast cancer. Figure 2.5 shows a normal MRI of the breast and an abnormal MRI of the breast, illustrating its capabilities in detecting variations in breast tissue composition and identifying abnormalities (Al Sharkawy, Sharkas, & Ragab, 2012).

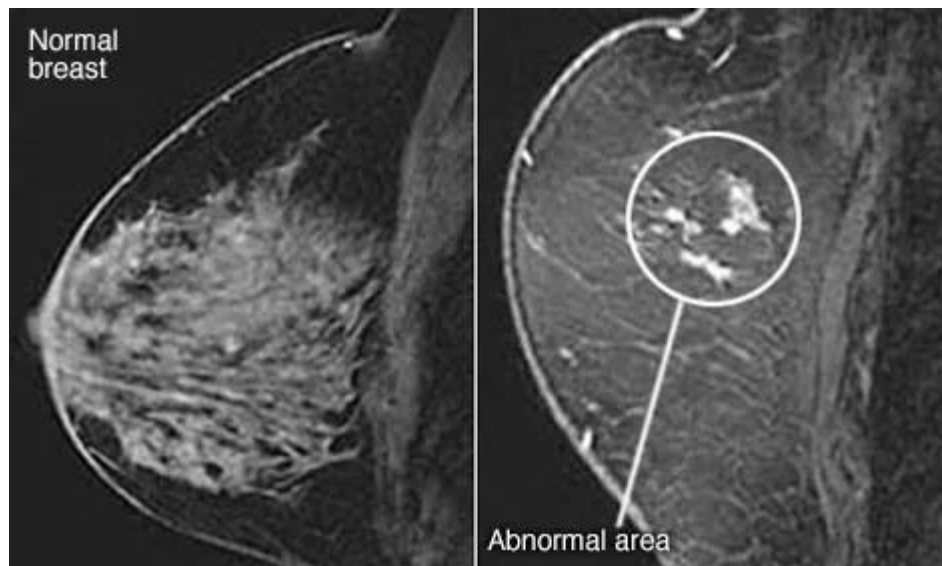


Figure 2.5: Comparison of normal and abnormal breast MRI images

(e) Biopsy

A biopsy involves the removal of a tissue sample from microscopic examination to determine whether cancer cells are present. Core needle biopsy and fine – needle aspiration are common techniques used to obtain breast tissue samples for analysis (Di Maria et al., 2023).

(f) Molecular biomarkers and genetic testing

Molecular biomarkers such as hormone receptors (ER, PR) and human epidermal growth factor receptor 2 (HER2), play a crucial role in determining the type of breast cancer and guiding treatment decisions. Genetic testing, including BCRA1 and BCRA2 gene testing, assesses the risk of hereditary breast cancer (Y. Choi et al., 2012).

2.4.3 Types of Breast Cancer

Breast cancer consists of various distinct types, each characterized by unique biological features, clinical behaviours, and treatment responses. The types of breast cancer are categorized into the following categories:

(a) ***Ductal Carcinoma in Situ (DCIS)***

DCIS is a non – invasive cancer where abnormal cells are confined to the lining of a breast milk duct and have not invaded nearby tissues. It can be detected through mammograms and is considered an early stage of breast cancer. DCIS is treatable, but if it is left untreated and undetected, it can spread into surrounding breast tissue (Abasher, Sidahmed, Abdelmoniem, & Ahmed, 2023).

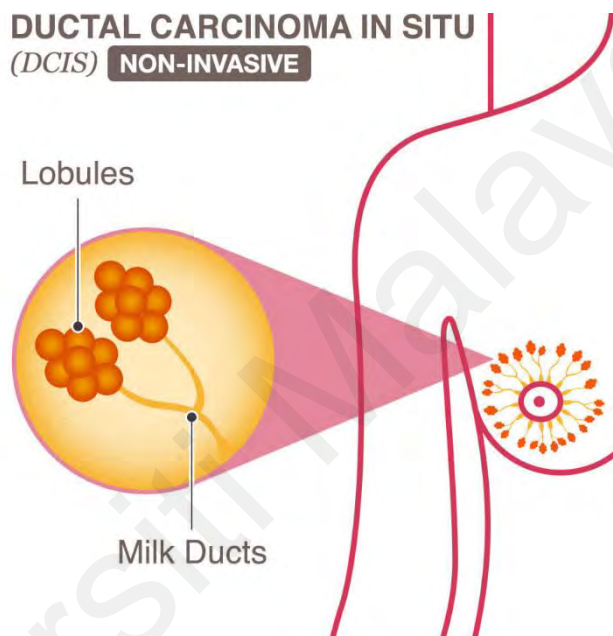


Figure 2.6: Ductal Carcinoma in Situ (DCIS)

(b) ***Invasive Ductal Carcinoma (IDC)***

IDC is the most common type of breast cancer making up to nearly 70 – 80% of all breast cancer diagnosis. IDC is characterized by cancer cells that invade the milk ducts and have spread beyond the ducts into other parts of the breast tissue (Roy, Biswas, & Datta, 2023).

(c) ***Invasive Lobular Carcinoma (ILC)***

ILC originates in the milk-producing glands (lobules) and tends to spread in a linear pattern within the breast tissue. It accounts for a smaller percentage of breast cancer cases compared to IDC (Roy et al., 2023).

(d) Triple-Negative Breast Cancer (TNBC)

TNBC lacks the receptors for oestrogen, progesterone, and HERS2. It is associated with aggressive tumour behaviour. Since the tumours cells lack the receptors, common treatments like hormone therapy and drugs are ineffective. However, using chemotherapy to treat TNBC is still an effective option (Azman et al., 2023).

(e) HER2-Positive Breast Cancer

HER2-positive breast cancer is characterized by overexpression of the HER2 protein. It tends to grow and spread faster, but targeted therapies such as HER2 inhibitors have improved treatment outcomes (Roy et al., 2023).

(f) Hormone Receptor-Positive (HR+) Breast Cancer

HR+ breast cancers have receptors for oestrogen and/or progesterone. They tend to respond well to hormone therapy, which blocks these hormones' effects on cancer growth (Mishra, Mishra, & Prajapati, 2023).

(g) Inflammatory Breast Cancer (IBC)

IBC is a rare and aggressive type of breast cancer presents with redness, swelling, and warmth in the breast. It can be mistaken for an infection due to its inflammatory nature.

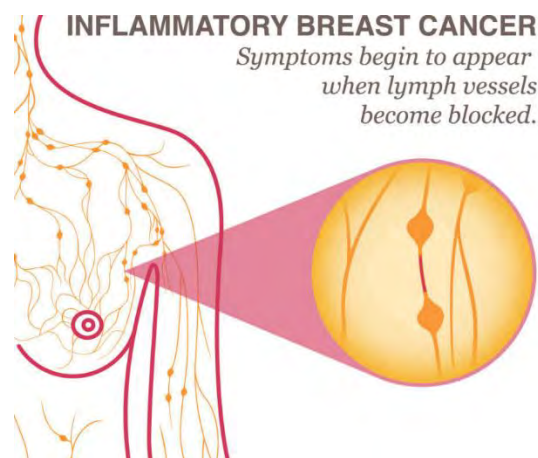


Figure 2.7: Inflammatory Breast Cancer (IBC)

(h) Metastatic Breast Cancer (MBC)

MBC is also classified as Stage 4 breast cancer occurs when cancer cells spread to other parts of the body, such as the bones, liver, lungs, or brain. It is considered an advanced stage of breast cancer (Roy et al., 2023).

(i) Phyllodes Tumour

Phyllodes tumours develop in the connective tissue of the breast and can be benign, borderline, or malignant. They are uncommon but may require surgical removal (Tan, 2023).

2.4.4 Stages of breast cancer

Breast cancer is staged to determine the extent of the disease and guide treatment decisions. The stages of breast cancer, classified using the TNM (Tumour, Node, Metastasis) system, provide a critical information about the size of the tumour, lymph node involvement and whether the cancer has spread to distant parts of the body (da Luz, Araujo, & de Araujo, 2022). The stages of breast cancer are as follows:

(a) Stage 0 (In Situ)

This stage represents non – invasive cancer where abnormal cells are confined to the ducts (DCIS) or lobules (LCIS) and have not invaded nearby tissues. These abnormal cells have the potential to become invasive over time if left untreated.

(b) Stage I

At Stage I, the tumour is small and confined to the breast. It has not spread to lymph nodes or other distant sites. Substage IA refers to a tumour less than 2 cm in size and substage IB refers to a tumour between 2 – 5 cm.

(c) Stage II

Stage II is divided into IIA and IIB. In IIA, the tumour small but may have spread to nearby lymph nodes. In IIB, the tumour is larger or may have spread to a few nearby lymph nodes.

(d) Stage III

Stage III also known as locally advanced breast cancer is divided into IIIA, IIIB, and IIIC. In IIIA, the tumour may be larger with limited spread to lymph nodes. In IIIB, the tumour may have invaded nearby structures like the chest wall or skin. In IIIC, cancer has spread to multiple nearby lymph nodes.

(e) Stage IV

Stage IV is metastatic breast cancer, where cancer has spread to distant parts of the body, such as the bones, liver, lungs, or brain. It is considered an advanced stage and requires systemic treatments to manage the disease.

Staging breast cancer helps oncologists determine the most appropriate treatment strategy. Early – stage breast cancer is often treated with surgery (lumpectomy or mastectomy), radiation therapy, and sometimes hormone therapy or targeted therapy. Advanced stages may involve a combination of surgery, chemotherapy, targeted therapy, hormone therapy, and radiation therapy.

2.4.5 Types of Breast Cancer Treatment

Breast cancer can be treated in several ways. The treatment depends on the kind of breast cancer and how far it has spread. Breast cancer patient's overall treatment often combines different types of treatment depending on the stage of tumour, the tumour's subtype, genomic markers, the presence of known mutations in inherited breast cancer genes and patient's physiological status.

2.4.5.1 Surgery

A breast surgery is the removal of the tumour and surrounding healthy tissue. The examination of axillary lymph nodes is often conducted during surgery. The two basic types of breast cancer surgery are lumpectomy and mastectomy.

(a) *Lumpectomy*

A lumpectomy or also known as breast-conserving surgery is a first treatment option for women with early-stage breast cancer. During lumpectomy surgery, the cancerous tissue is removed and a small amount of normal tissue around the lump. The normal tissue is taken to ensure all the cancerous tissue surrounding the lump is removed.

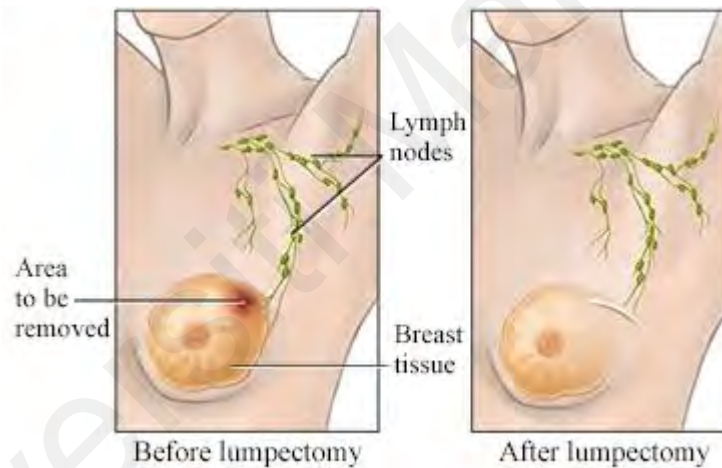


Figure 2.8: Lumpectomy

(b) Mastectomy

A mastectomy is a complete removal of breast tissues from a breast. It is a treatment option to treat and prevent breast cancer.



Figure 2.9: Mastectomy

2.4.5.2 Lymph Node Removal and Analysis

Breast cancer cells may have metastasized or spread to the axillary lymph nodes. Sentinel lymph node biopsy or axillary lymph node dissection near the breast cancer is performed to determine treatment and prognosis.

(a) Sentinel Lymph Node Biopsy

A sentinel (draining) lymph node is the first lymph node or group of nodes to receive lymphatic drainage from a cancer. Sentinel lymph node can be detected by injection of a blue dye or radioactive tracer around the nipple. The blue dye or radioactive tracer travels and identifies the first sentinel node. Biopsy of a sentinel lymph node is the removal of 1 to 3 lymph nodes. The examination of these lymph nodes reveal whether there are presence of cancer cells (McMasters et al., 1998). If the sentinel lymph node(s) are cancer-free, the remaining lymph nodes will also be free of cancer.

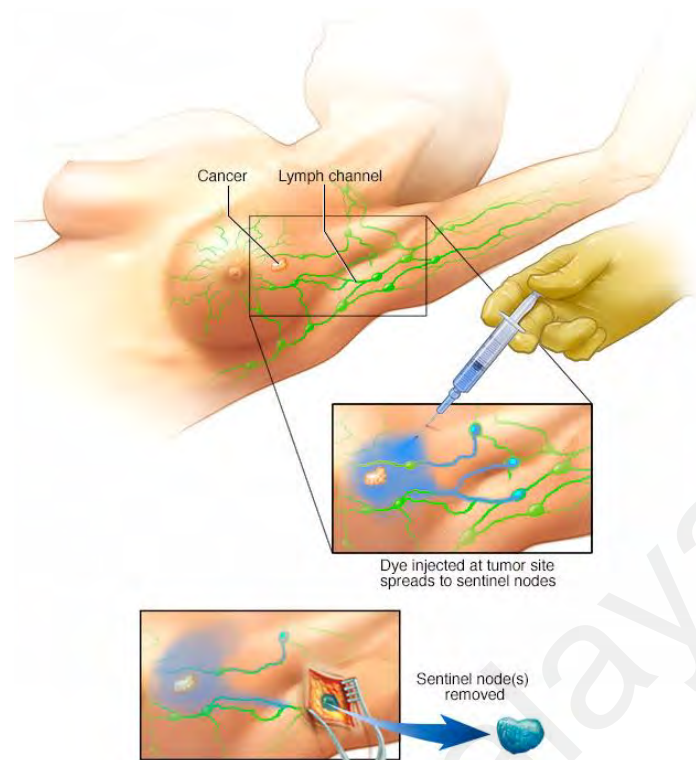


Figure 2.10: Sentinel lymph node biopsy

(b) Axillary Lymph Node Dissection

Axillary lymph node dissection is the standard procedure for determining the nodal stage and the need for adjuvant treatment (Schrenk, Rieger, Shamiyeh, & Wayand, 2000). The procedure involves the removal of many lymph nodes from under the tumour side arm. Substantial evidence has shown that axillary dissection provides local disease control and may translate into improved survival (McMasters et al., 1998).

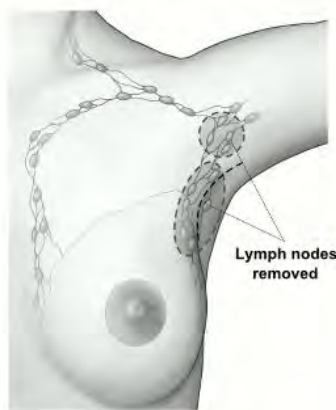


Figure 2.11: Axillary lymph node dissection

2.4.5.3 Radiation Therapy

Radiation therapy is the use of high-energy x-rays to destroy cancer cells. Radiation therapy helps to minimize the risk of breast cancer recurrence. The therapy can be given before (neoadjuvant radiation therapy) or after (adjuvant radiation therapy) surgery.

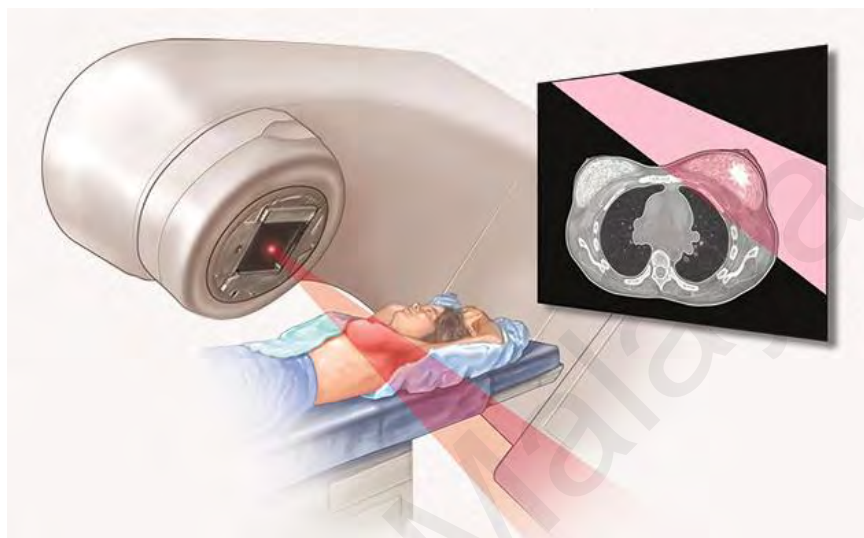


Figure 2.12: Radiation therapy

(a) Neoadjuvant Radiation Therapy

Neoadjuvant radiation therapy is radiation therapy given before surgery. It is to shrink large tumour to ease tumour removal during surgery. Neoadjuvant radiation therapy treatment is considered when a tumour cannot be removed with surgery.

(b) Adjuvant Radiation Therapy

Adjuvant radiation therapy is a breast cancer treatment after surgery and chemotherapy. It is recommended if a patient has large tumour, cancer in the lymph nodes or cancer cells outside of the capsule of the lymph node.

2.4.5.4 Systemic Therapy

Systemic therapy is a breast cancer treatment that uses medication to destroy cancer cells. Neoadjuvant systemic therapy is given before surgery to reduce tumour size. Adjuvant systemic therapy is administrated after surgery to minimize the risk of breast

cancer recurrence. The types of systemic therapies include chemotherapy, hormonal therapy, and immunotherapy.

(a) Chemotherapy

Chemotherapy uses drugs that may be given intravenously or by mouth. The anti-cancer drugs travel through bloodstream to destroy cancer cells and to stop cancer cell division.

(b) Hormonal therapy

Hormonal therapy is a treatment for cancer cells that test positive for either oestrogen or progesterone receptors. This type of cancer cells uses hormones to help its growth. Hormonal treatments block hormone actions and lower hormone levels in the body.

(c) Immunotherapy

Immunotherapy is designed to enhance the body's immune system to fight cancer cells. It uses materials made by the body or made in a laboratory to restore and improve immune system function.

2.4.6 Complications of Breast Cancer Treatment

Significant number of breast cancer women are at risk of developing treatment-related complications. Critical complications associated with breast cancer treatment include:

(a) Infertility

Breast cancer treatments, such as chemotherapy and hormonal therapies can have a negative impact on fertility in women of reproductive age (Fenton et al., 2022).

(b) Inflamed Lung Tissue

Breast cancer treatments like radiation therapy can lead to inflammation of lung tissue causing respiratory issues and discomfort (Siaravas, Katsouras, & Sioka, 2023).

(c) Osteoporosis

Hormonal therapies suppress oestrogen and increases the risk of developing osteoporosis, a condition characterized by weakened and brittle bones (Föger-Samwald, Dovjak, Azizi-Semrad, Kersch-Schindl, & Pietschmann, 2020).

(d) Cardiovascular Disease

Breast cancer survivors may face an increased risk of cardiovascular diseases due to the cardiotoxic effects of certain chemotherapy drugs and the overall impact of cancer treatments on the cardiovascular system (Yu, Xu, Yu, & Zheng, 2022).

(e) Lymphedema

Lymphedema is a common complication of breast cancer treatment. 56% of lymphedema occurred within two years after breast cancer treatment (Liao et al., 2013). Lymphedema occurs when lymphatic fluid builds up in the arms or legs, leading to swelling, discomfort, and a reduced range of motion (Heins et al., 2022).

The presence of these complications can have far-reaching consequences affecting survivors' physical, emotional, psychological, and quality of life.

2.5 Breast Cancer-related Lymphedema (BCRL)

Lymphedema is a continuous swelling (oedema) that occurs due to accumulation of protein-rich fluid in the subcutaneous space resulting from dysfunction of lymphatic system. It is a chronic condition that can be either primary or secondary lymphedema. Primary lymphedema is caused by genetic mutation and lymphatic vascular anomalies. Secondary lymphedema is acquired and can develop as a complication of surgical, traumatic, inflammatory, or neoplastic disruption or obstruction of lymphatic pathways (Rockson, 2001). Secondary lymphedema is more often reported compared to primary form.

The reported incidence of secondary lymphedema as a consequence of breast cancer treatment such as mastectomy ($p = 0.0012$), axillary lymph node dissection ($p = 0.0001$), chemotherapy ($p = 0.0001$) and radiation therapy ($p = 0.0003$) has been reported to be 25 to 38% (Armer, Radina, Porock, & Culbertson, 2003; Erdogan Iyigun et al., 2015; Farncombe, Daniels, & Cross, 1994; Kim et al., 2013; McLaughlin et al., 2017; Petrek & Heelan, 1998; Rockson, 2018; Sharkey et al., 2018; Soran et al., 2014; Tobin, Lacey, Meyer, & Mortimer, 1993; Vicini, Shah, Lyden, & Whitworth, 2012). Breast cancer treatment typically targets the breast and axilla on the treatment side. The treatment site for breast cancer puts the lymph nodes responsible for draining lymphatic fluid at the treatment site at risk for inflammation and lymphedema if the lymphatics are damaged, altered, or removed (Johnson et al., 2014).

The dysfunction of the lymphatic system leads to swelling of the affected upper body region (Rockson, Keeley, Kilbreath, Szuba, & Towers, 2019). Lymphedema of the upper limb commonly occurs in one limb and presents as enlargement and disfigurement of the limb, pain, reduced mobility, recurrent infection, and impaired function. The reported occurrence of lymphedema in the arm ranges from 2% to 83% (Clark, Sitzia, & Harlow, 2005; Deutsch et al., 2008; Hinrichs et al., 2004; Petrek & Heelan, 1998). Lymphedema may also affect head, neck, breast, or genitals (Grada & Phillips, 2017).

2.5.1 Stages of BCRL

Lymphedema severity is commonly classified into distinct stages, each characterized by specific clinical features. One common criterion for determining clinically significant lymphedema is a difference in circumference of more than 2 cm between the affected and unaffected limb (Erickson, Pearson, Ganz, Adams, & Kahn, 2001; Morrell et al., 2005; Petrek, Senie, Peters, & Rosen, 2001). Volume-based rating scales are often used in clinical trials to assess lymphedema. Other parameters used to determine lymphedema

stages include circumference, tissue texture, dermal changes, subjective sensations and tissue responses to gravity or pressure (Cheville et al., 2003). Subjective reporting based on patient questionnaires is also used. However, these assessments may be influenced by factors such as weight gain or inherent muscle differences between the limbs.

Figure 2.13 illustrates BCRL stages and the characteristics associated with each stage is summarized in Table 2.1.

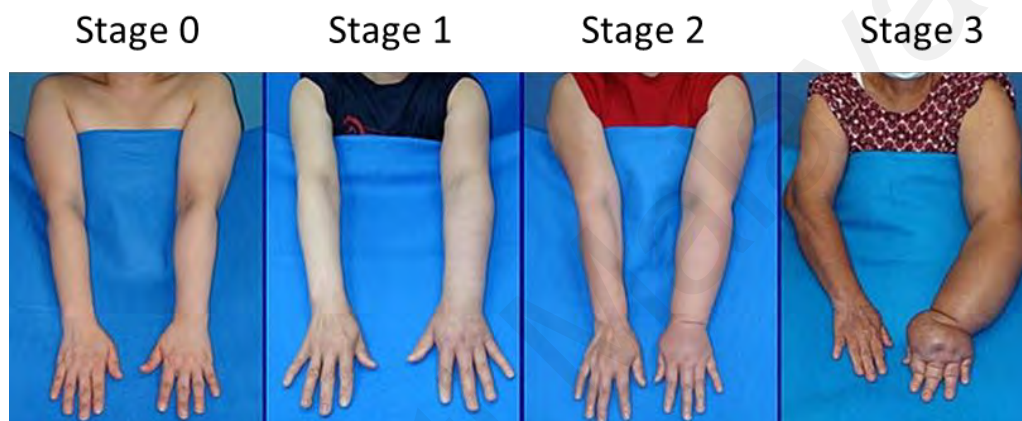


Figure 2.13: Stages of BCRL (Cheng, Chang, & Patel, 2021)

The four stages of BCRL are as follows:

(a) Stage 0

Stage 0 occurs after surgery or radiation when the lymphatic system is compromised. At this stage, BCRL is asymptomatic and show no clinical signs of lymphedema.

(b) Stage 1

Stage 1 displays swelling at the affected extremity. However, swelling can be reduced when the affected extremity is elevated. Pitting is observable and circumferential inter-arm volume differences range between 2 cm to 3 cm. In Stage 1, BCRL is mild and reversible.

(c) Stage 2

BCRL progresses to moderate, and it is irreversible at Stage 2. Stage 2 BCRL features no reduction in swelling with extremity elevation, and pitting is absent. Circumferential inter-arm volume differences increase to 3 cm to 5 cm, accompanied by intensified fibrous tissue and progressive skin hardening.

(d) Stage 3

Stage 3 is also known as lymphostatic elephantiasis. This advanced stage shows progressive fibrosclerosis and pronounced skin changes, including large hanging skin folds and papillomas. Stewart-Treves syndrome may also be observed.

Table 2.1 summarises the stages of BCRL, providing its description and characteristics of each stage.

Table 2.1: Description and characteristics of stages in BCRL

Stage	Description	Characteristics
0	Exists after surgery or radiation due to a damaged lymphatic system	Asymptomatic and show no clinical signs of lymphedema
1	Mild and reversible	<ul style="list-style-type: none">• Swelling reduced with elevation of the swollen extremity• Pitting• Circumferential inter-arm volume differences of 2 cm to 3 cm.
2	Moderate and irreversible	<ul style="list-style-type: none">• No reduction in swelling with elevation of the extremity• No pitting

		<ul style="list-style-type: none"> • Circumferential inter-arm volume differences of 3 cm to 5 cm • Increased fibrous tissue with progressive skin hardening
3	Lymphostatic elephantiasis	<ul style="list-style-type: none"> • Progressive fibrosclerosis • Skin changes (large hanging skin folds, papillomas) • Association with Stewart-Treves syndrome

2.5.2 Current BCRL Clinical Diagnosis and Monitoring

The clinical diagnosis and monitoring of breast cancer-related lymphedema (BCRL) is performed by a health professional that incorporates patient history, patient self-report of symptoms, and identification of the symptomatic characteristics. A complete medical assessment includes visual inspection of the affected body region, palpation of the affected body region to examine tissue changes, digital pressure to detect pitting oedema, and circumferential volume measurement of the affected limb. Several diagnosis methods to measure the extent of lymphedema include limb volume measurement by water displacement (Sukul, Den Hoed, Johannes, Van Dolder, & Benda, 1993), circumferential measurement of limbs (SITZIA, 1995), palpation (Lawenda, Mondry, & Johnstone, 2009; Romero, 1999), skin tonometry (Chen, Tsai, Hung, & Tsauo, 2008), perometry (Springer et al., 2010; L. C. Ward, Czerniec, & Kilbreath, 2009), bioelectrical impedance (BH Cornish, Bunce, Ward, Jones, & Thomas, 1996), and lymphoscintigraphy (Witte et al., 2000).

Overall, the incidence of lymphedema is unrecognized and under-reported due to inability to accurately diagnose lymphedema stages and lack of reliable diagnosis techniques to quantify lymphedema (Armer, 2005; S. Hayes et al., 2008; S. C. Hayes, M. Janda, B. Cornish, D. Battistutta, & B. Newman, 2008; S. C. Hayes et al., 2012; Johnson et al., 2014).

2.5.2.1 Water Displacement

Water displacement is an indirect extracellular measurement technique. Limb volume measurement by water displacement is considered the golden standard for volume measurements but not routinely used in the clinic (Sukul et al., 1993; Taylor, Jayasinghe, Koelmeyer, Ung, & Boyages, 2006). The volume measure of the arm is obtained by submerging the affected and unaffected limb in a cylinder filled to a known level of water as illustrated in Figure 2.14. The amount of water displaced by the submerged limbs is equivalent to its volume. Volume difference acquired between both limbs is compared to measure the extend of lymphedema.



Figure 2.14: Water displacement (Karlsson, Johansson, Nilsson-Wikmar, & Brogårdh, 2022)

Study conducted by Megens *et al.* (2001) and Sander *et al.* (2002) has found water displacement as a sensitive method for lymphedema assessment with intraclass correlation coefficient (ICC) of 0.99 for interrater reliability of water displacement volumes (Megens, Harris, Kim-Sing, & McKenzie, 2001; Sander, Hajer, Hemenway, & Miller, 2002). On the contrary in 2001, Cornish *et al.* concluded the volume of the extracellular sub-compartment is approximately 25% of the total volume in normal healthy person. Hence, total limb volume measurement by water displacement has a sensitivity four times less than any direct extracellular measurement technique.

Clinical practitioners and researches choose not to use water volume method because it is unhygienic, time-consuming (measurements take about 20 – 30 minutes) and not suitable for patients in the immediate postoperative period (Megens *et al.*, 2001; Sukul *et al.*, 1993).

2.5.2.2 Circumferential Limb Measurement

Circumferential upper limb volume measurement using measuring tape is one of the common techniques used to diagnose BCRL because of its practicality of usage in clinical settings. The circumferential measurements are recorded and compared with baseline (preoperative) measures of the same limb and with contralateral unaffected limb. The volume measuring technique uses measuring tape to measure multiple circumferential perimeters from axillary point to the fingers. There are two ways to determine the intervals for circumferential measurement points. The first technique takes circumferential readings from the wrist to axilla at a fix distance step (SITZIA, 1995). The second technique is based on the anatomic bony landmarks along the arm, such as the styloid, olecranon, and metacarpal phalangeal joints (Taylor *et al.*, 2006). The circumferential limb volume measurement is subsequently calculated using circular or elliptical truncated cone geometry to determine the extent of lymphedema (Casley-Smith,

1994). In 1995, Sitzia conducted a study to evaluate the accuracy of mathematic formula used to convert circumference to volume. The cylinder formulas overestimated volume by 1.5% compared to frustum volume calculation method. Although frustum formula demonstrated to be more accurate, the cylindrical formulas are convenient to use for calculation of lymphedema (SITZIA, 1995). These formulas presume the arm to be a truncated cone and neglect the swelling of the oedematous arm (Cau et al., 2016). Kaulesar Sukul *et al.* found the limits of agreement between volumetry and calculate volumetry to be too large (mean \pm 2 standard deviations = 521 \pm 238 mL) (Sukul et al., 1993).

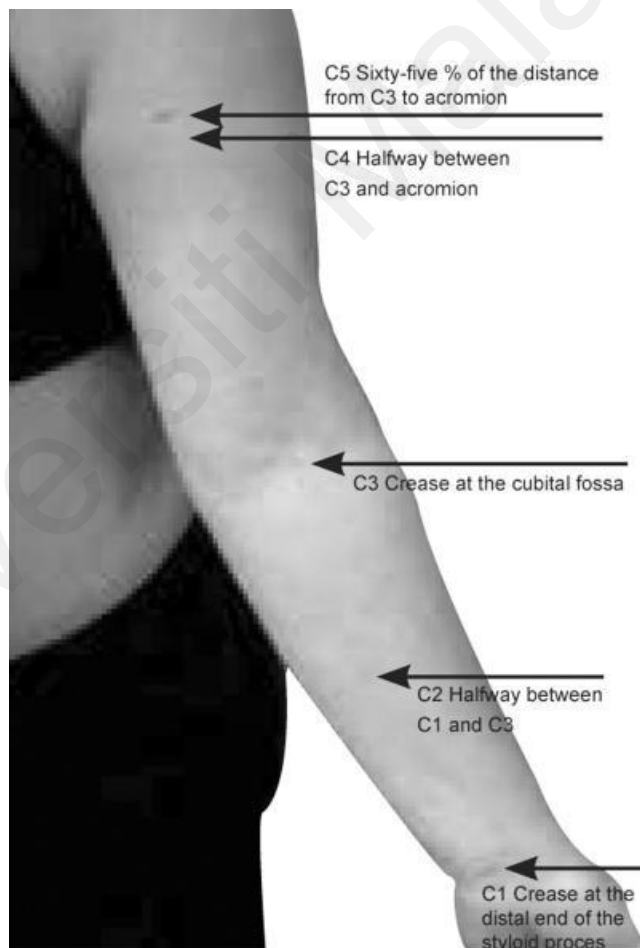


Figure 2.15: Five marks used by physiotherapists for circumference measurements (Gjorup, Zerahn, & Hendel, 2010)

Some researchers consider a maximum circumferential difference of greater than or equal to 2.0 cm or volume difference of greater than or equal to 200 mL between affected

and unaffected limb to indicate a positive diagnosis of lymphedema (Armer & Stewart, 2005). However, this method disregards patient's body size and physique (slim or obese). Other researchers use a 10% circumferential limb difference between affected and unaffected limb to determine presence of lymphedema (Lundgren, 1989). Circumferential limb measurements are highly biased by the tension placed on the limb by the tape measure, by variations of the degree of limb firmness and the contour of the limb (Bagheri, Ohlin, Olsson, & Brorson, 2005). The water displacement method is considered more reliable as it measures the arm oedema volume directly and is considered as the golden standard in limb volume measurement (Swedborg, 1977).

Study by Taylor *et al.* found circumferential volume measurement a reliable method to assess lymphedema but overestimated water volume by more than 110mL. The wide limit of agreement between water volume and circumferential measurement suggested circumferential volumes as an inaccurate technique for lymphedema diagnosis. Taylor *et al.* determined the minimal detectable change by considering a difference of 150mL as measurement error (Taylor et al., 2006). Circumferential volume measurement measures total limb volume which consists of bone, muscle fat, tissues, and extracellular fluid (ECF) that made up 25% of the total limb volume. It is possible individual with Stage 1 lymphedema with limb volume differences less than 100mL are being overlooked by current measurement and volume diagnostic standards. Thus, lymphedema diagnosis using volume measurement might be dismissing low grade edema group (Johnson et al., 2014). Circumferential limb measurement benefits from being a low cost lymphedema assessment and easily accessible, but it is time-consuming with inter- and intra-rater reliability (Sun et al., 2016).

2.5.2.3 Palpation

Palpation is most frequently employed technique subjective lymphedema assessment of patient's skin and subcutaneous texture by the clinician (Sierla, Dylke, Shaw, Poon, & Kilbreath, 2020b). Palpation techniques include a pinch or skin fold test, pitting test, tissue tension, skin crease and stemmers sign to estimate the presence of accumulated lymph fluid. Clinicians hypothesize the present of fluid in the superficial dermis using stemmers test, skin lift and skin crease. The pitting test and assessment of tissue tension are used to hypothesize the present of fluid in adipose tissue. (Sierla, Dylke, Shaw, Poon, & Kilbreath, 2020a). Clinicians determine the patient's skin mobility, tissue consistency, tissue fibrosis existence, and grade pitting oedema using palpation (Lawenda et al., 2009). Palpation is used over the affected region and unaffected region for comparison. The analysis of limbs palpated differences is a learned skill with time, requires practice and supportive learning. However, there is lack of clinical guidance for the interpretation of fibrosis palpation (Johnson et al., 2014).

Bentzen *et al.* (1993) investigation found limitations of the palpation scale. This method is insensitive to detect change and the ceiling effect, broad distance between different grades, and interobserver variability (Bentzen & Overgaard, 1993). Since lymphedema is a chronic condition that requires long-term surveillance, the reliability of recall by clinician on palpation change over duration of time is questionable. Wernicke *et al.* study showed that the accuracy and reliability of palpation to assess lymphedema fibrosis is not encouraging (Wernicke et al., 2009).

2.5.2.4 Tonometry

Tonometry is one of lymphedema assessment techniques used to quantify tissue tension and tissue resistance to compression objectively. As lymphedema progresses, patients will experience tissue fibrosis resulting in decreased tissue compressibility when

compared to a normal limb. The degree of tissue compressibility and depth of pitting oedema is measured using a tissue tonometer as shown in Figure 2.16. The degree of compressibility outcome is correlated with limb swelling (Bagheri et al., 2005; Moseley & Piller, 2008). Investigation has shown, the ability of a tonometer to differentiate if a lymphoedematous arm is softer or harder compared to a normal limb. Nevertheless, a tonometer could only register postoperative changes in the upper arm but not in the forearm (Bagheri et al., 2005).

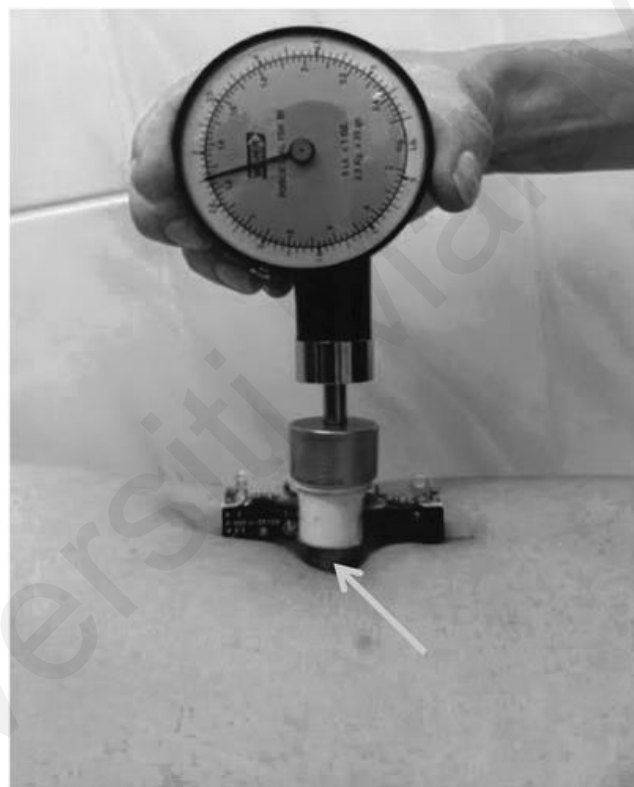


Figure 2.16: Tonometry (Zaleska, Olszewski, Durlik, Kaczmarek, & Freidenrich, 2018)

Instead of volume measurement, a tissue tonometer measures tissues resistance to determine the extent of tissue fibrosis (Oremus, Walker, Dayes, & Raina, 2015). Study by Chen *et al.* (2008) has shown good correlation of tonometry to limb volume measurement. However, lymphedema assessment using volume measurement has shown more precise measurement than tissue tonometry to manage lymphedema treatment (Chen et al., 2008).

Research conducted by Moseley and Piller has shown tonometry to have low covariance ranging from 1.29 to 3.25 %, consistent reproducibility and reliable technique to measure lymphedema (Moseley & Piller, 2008).

2.5.2.5 Perometry

A perometer is an optoelectronic device that uses arrays of infrared light and optoelectronic sensors to create a two-dimensional silhouette of the limb and derive limb volume by the disc model method (Tierney, Aslam, Rennie, & Grace, 1996) as shown in Figure 2.17. This technique is introduced in lymphedema assessment to help standardize limb volume measurement and overcome circumferential assessment method limitations such as the variations in anatomic landmarks and variations in tensions when assessing limb circumference (Bernas, Askew, Armer, & Cormier, 2010). Although it can calculate limb volume rapidly, hygienically, and accurately, the high cost of perometry limits its application (Bernas et al., 2010; Havens et al., 2021; Wanchai, Armer, Stewart, & Lasinski, 2016).



Figure 2.17: Perometry

2.5.2.6 Lymphoscintigraphy

The current imaging modality used to assess lymphedema quantitatively is by using lymphoscintigraphy. This method involves injection of a radioactive tracer into subdermal region of the affected limb. The injected tracer is monitored with a gamma camera to identify lymphatic drainage pathways, the amount of dermal backflow, number of lymph nodes, collateral lymph channels and clearance times of radiopharmaceutical agents (Morrell et al., 2005; Wanchai et al., 2016). Lymphoscintigraphy can help determine functional, morphological changes of the lymphatic system and to assess the results of therapeutic interventions (Bernas et al., 2010). This technique is reported to be from 73% to 97% with a specificity of 100% (Morrell et al., 2005; Ter, Alavi, Kim, & Merli, 1993; Tiwari, Cheng, Button, Myint, & Hamilton, 2003). It is proven to be the most useful and gold standard for diagnosing oedema in patients with no known risk factors. However, diagnostic results may vary among clinical centres since there is no specific protocol for lymphoscintigraphy such as type of radioactive tracer, injection site and imaging technique (Morrell et al., 2005).

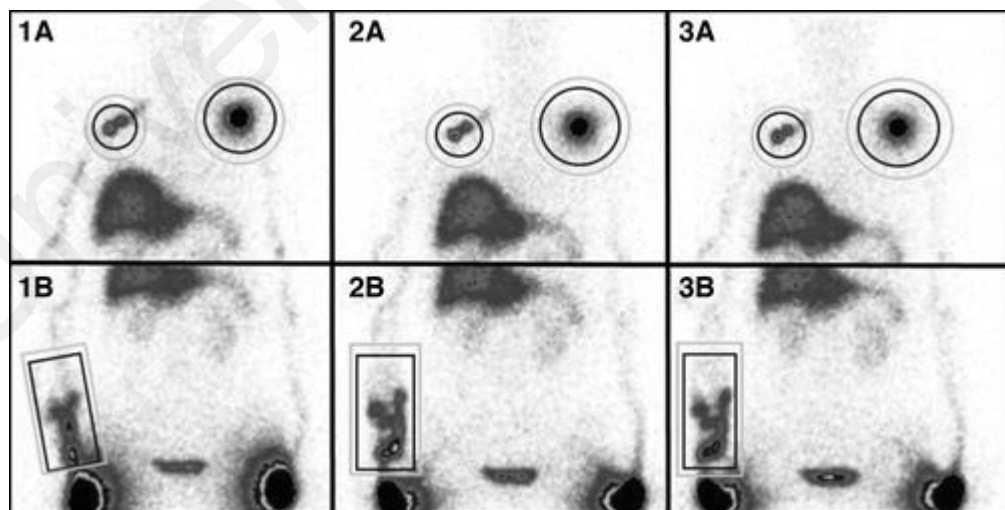


Figure 2.18: Lymphoscintigraphy of upper limb lymphedema (Barbieux et al., 2023)

2.5.2.7 Bioelectrical Impedance Analysis

Bioelectrical impedance analysis (BIA) is a non-invasive diagnostic method that measure fluid or water content in limbs by allowing alternating current to pass through the limb and measuring the impedance to the current flow (BH Cornish et al., 1996; BH Cornish et al., 2001). A prospective 3-year study by Cornish *et al.* (1996) has demonstrated the effectiveness and sensitivity BIA versus circumferential measurement in early detection of lymphedema and in monitoring lymphedema progression. BIA managed to predict the onset of lymphedema 10 months prior to clinical diagnosis from 20 out of 120 subjects at risk of developing lymphedema with 100% sensitivity and 98% specificity when compared with sequential circumference measurements (BH Cornish et al., 1996). Further studies have determined low sensitivity ranging from 42% to 100% and high specificity ranging from 64% to 100% (Barrio, Eaton, & Frazier, 2015; Berlit et al., 2012; Bilir, DeKoven, & Munakata, 2012; Box, Reul-Hirche, Bullock-Saxton, & Furnival, 2002; N. Bundred et al., 2020; N. J. Bundred et al., 2015; E. Dylke et al., 2016; Fu et al., 2013; Lahtinen, Seppälä, Viren, & Johansson, 2015; Lim, Han, Kim, & Park, 2019; Qin, Bowen, & Chen, 2018; Smoot, Wong, & Dodd, 2011). Study by Ward discovered impedance ratio of 20% higher from normal control, while volume ratio was indistinguishable over 28 days of lymphedema treatment. This findings indicates greater sensitivity of impedance in detecting lymphedema than circumferential measurement (L. C. Ward, 2006). In another study by Ward *et al.* to assess the agreement between bioimpedance and perometry for evaluation of unilateral arm lymphedema, the study found high correlation ($r = 0.926$) with the difference in arm volume between impedance and perometry measurements (L. C. Ward et al., 2009). BIA has been validated by many studies as an effective tool to measure fluid content in limbs (L. C. Ward et al., 2009; Warren, Janz, Slavin, & Borud, 2007). A retrospective study conducted by Coroneos *et al.*, concluded high correlation ($\rho = 0.71 - 0.94$, $p < 0.0001$) between BIA with limb

volume ratio using perometry, the degree of pitting oedema, evaluation of transport index using lymphoscintigraphy and staging using ICG lymphography (Coroneos, Wong, DeSnyder, Shaitelman, & Schaverien, 2019). BIA has the ability to measure or predict early stage lymphedema disease, however this diagnosis method is limited to limbs and fluid content measurement and is unable to measure fibrotic change (Johnson et al., 2014).

The comparison of BCRL advantages and disadvantages of the diagnosis methods is summarized in Table 2.2.

Table 2.2: Comparison of advantages and disadvantages of BCRL diagnosis methods

Diagnosis method	Advantages	Disadvantages
Water displacement	<ul style="list-style-type: none"> • Considered golden standard for volume measurements 	<ul style="list-style-type: none"> • Not routinely used in clinics • Unhygienic • Time-consuming • Requires trained healthcare providers to operate • Not suitable for patients in immediate postoperative period
Circumferential limb measurement	<ul style="list-style-type: none"> • Practicality in clinical settings • Low cost 	<ul style="list-style-type: none"> • Not reliable for identifying lymphedema at early stage • Requires trained healthcare providers to operate • Biased by tension placed on limb, variations in firmness and contour of limb
Palpation	<ul style="list-style-type: none"> • Low cost 	<ul style="list-style-type: none"> • Subjective and not reliable for identifying lymphedema at early stage • Requires trained healthcare providers to operate
Tonometry	<ul style="list-style-type: none"> • Consistent reproducibility and reliable technique 	<ul style="list-style-type: none"> • Requires trained healthcare providers to operate • High cost (~ RM 6, 500)

Perometry	<ul style="list-style-type: none"> • Can calculate limb volume rapidly, hygienically, and accurately 	<ul style="list-style-type: none"> • Not reliable for identifying lymphedema at early stage • High cost (~ RM 153,417) • Requires trained healthcare providers to operate
Lymphoscintigraphy	<ul style="list-style-type: none"> • Highly sensitive and accurate for early lymphedema diagnosis 	<ul style="list-style-type: none"> • Not practical for regular lymphedema monitoring • High cost, per scanning procedure is approximately RM 6,600 • Use of radiation
BIA	<ul style="list-style-type: none"> • Consistent reproducibility and reliable technique • Practical method for regular lymphedema monitoring 	<ul style="list-style-type: none"> • High cost (~ RM 40,000)

2.6 Bioelectrical Impedance Analysis and Breast Cancer-Related Lymphedema (BCRL)

Bioelectrical impedance analysis (BIA) has emerged as a valuable technique for assessing many physiological diseases such as diabetes (Sbrignadello, Göbl, & Tura, 2022), chronic kidney disease (Eyre et al., 2023), human immunodeficiency virus (HIV) (Freitas et al., 2011), dengue (F. Ibrahim, Faisal, Mohamad Salim, & Taib, 2010) including BCRL (L. C. Ward, Degnim, Dylke, & Kilbreath, 2020). BCRL is a common complication following breast cancer treatment. It can significantly impact the quality of life for affected individuals. As a non – invasive method, BIA offers a promising approach to diagnose and monitor BCRL to ensure early detection and effective management. In this section, BIA application in the context of BCRL will be reviewed to address its principles, methodologies, and data analysis.

2.6.1 Fundamental of Bioelectrical Impedance Analysis Technique

The human body tissue comprises of conductive and resistive materials. Water compartment or electrolyte solution in tissue act as a conductor and allows applied

electrical current to pass through. The opposition to the current flow in tissue is referred as bioelectrical impedance or bioimpedance (Z) and it is measured in ohm. Bioimpedance is a complex quantity composed of resistance (R) such as fat or bones and reactance (X_c) from tissue cell membranes (Kyle et al., 2004a). The resistance arises from extra- and intracellular fluid content and capacitance from cell membrane.

Bioelectrical impedance is a non – invasive technique that delivers a low amplitude alternating constant current (AC) through the surface electrodes and measures the voltage signal response from the body or body segment (Bera, 2014).

In bioimpedance measurement, AC is applied to avoid tissue damage. As AC flows in human body, tissue cell membranes cause phase difference or phase angle (φ) between voltage and current source. The relationships between bioimpedance, resistance and reactance are represented in Equation (2 - 1) to (2 - 3).

$$Z = R + jX_c \quad (2 - 1)$$

$$|Z| = \sqrt{R^2 + X_c^2} \quad (2 - 2)$$

$$\varphi = \tan^{-1} \left(\frac{X_c}{R} \right) \quad (2 - 3)$$

Bioimpedance and resistance are related to the conductive volume. To study the relationship between bioimpedance and resistance, the human body segment can be considered as a simple cylinder model. The impedance along the length (l) of cylinder is inversely proportional to its cross-sectional area (A) as illustrated in Figure 2.19 and is described in Equation (2 – 4) to (2 – 10).

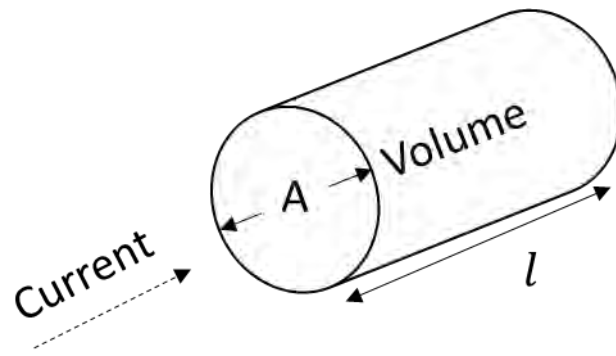


Figure 2.19: Cylinder model as a representation of human body

$$Z \propto \frac{1}{A} \quad (2 - 4)$$

Equation (2 – 4) may be rewritten as

$$Z = \rho \frac{1}{A} \quad (2 - 5)$$

where ρ is resistivity.

$$Z \propto l \quad (2 - 6)$$

Equation (2 – 6) can be rewritten as

$$Z = \rho l \quad (2 - 7)$$

Combining Equation (2 – 5) and (2 – 7) gives

$$A = \rho \frac{l}{Z} \quad (2 - 8)$$

The volume of the cylinder is

$$Volume = l \times A \quad (2 - 9)$$

Combining Equation (2 – 7) and (2 – 8) yields

$$Volume = \rho \frac{l^2}{Z} \quad (2 - 10)$$

Equation (2 – 10) represents the relationship between bioimpedance to volume and length of a conductive tissue volume. This relationship is important in the assessment of lymphedema. Equation (2 – 10) is applied in clinical practice to the body region at-risk of or affected by lymphedema, such as arm after breast cancer treatment. For these reasons, the measurement of lymph impedance at limb compartments are prominent for lymphedema disease diagnosis and management.

2.6.2 Frequency Analysis Methods for Breast Cancer-Related Lymphedema Assessment

Frequency analysis methods used in bioimpedance measurement provides valuable insights into biological tissues and fluid composition in the body region of interest. Biological tissues composed of both conductive fluids and capacitive membranes. One of the characteristics of biological tissues is current flow is frequency dependent. At a low frequency, current can only flow through extracellular fluid (ECF) compartment. Lymph fluid is located mainly in ECF compartment (Null & Agarwal, 2023; Santambrogio, 2018; Tokumoto et al., 2023). As opposed to low frequency, at high frequencies, current can penetrate cell membranes and flows through total body water. This behaviour is illustrated in Figure 2.20.

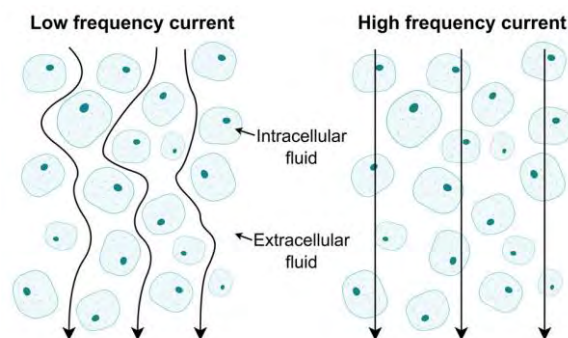


Figure 2.20: Current flow in biological tissue (Scagliusi et al., 2023)

2.6.2.1 Single Frequency Bioimpedance Analysis

Single frequency bioimpedance analysis (SFBIA) utilizes a specific frequency to measure the impedance of biological tissues. Typically, a SFBIA device uses 50 kHz to measure the bioimpedance of a human body. In 1992, study by LC Ward *et al.* (1992) found that impedance at 50 kHz is indicative of total fluid content and does not discriminate between tissue fluid compartments as compared with impedance at zero frequency (LC Ward *et al.*, 1992). Studies by Liu *et al.* (2021) and Jung *et al.* (2018) uses single frequency bioimpedance measurements at 1 and 5 kHz to measure both BCRL upper extremities (Jung *et al.*, 2018; Liu *et al.*, 2021). Both studies utilize SFBIA as an alternative simple and less expensive method compared to BIS to measure impedance at lowest frequency. Research to determine whether SFBIA is as accurate as BIS in measurement of ECF in lymphedema patients concluded high correlation between both frequencies analysis (York *et al.*, 2009).

2.6.2.2 Multiple Frequencies Bioimpedance Analysis

The commonly used method for bioimpedance analysis is the multiple frequencies bioimpedance analysis (MFBIA). MFBIA involves applying a low frequency of like 5 kHz and several higher frequencies such as 50, 100, 200 and 500 kHz. In theory, MFBIA is able to differentiate between the ECF and intracellular fluid (ICF) compartments. This is due to at lower frequencies, the impedance to the current flow allows for the evaluation of ECF. While at higher frequencies, the impedance can be used to determine the total body fluid (TBF). ICF is derived by subtracting ECF from TBF. MFBIA impedance parameters at 5 kHz to 200 kHz has the potential to indicate the nutrition status and fluid overload (Mulasi *et al.*, 2015). These parameters offer advantages to MFBIA over SFBIA when it comes to monitoring physiological conditions.

2.6.2.3 Bioelectrical Impedance Spectroscopy

Analysis of bioimpedance data obtained using a spectrum frequency of alternating current (AC) is known as bioimpedance spectroscopy (BIS). BIS generates wide spectrum frequency of AC to biological tissues.

BIS is a derivative of BIA. It can assess intracellular, extracellular, and total body water. Researchers have agreed BIS as reliable method for the assessment of lymphedema since accumulation of lymph represents an increase in extracellular water (E. S. Dylke & Ward, 2020).

Ideally, to determine the volume of ECF would be at zero frequency. However, this is impossible due to technical and safety reasons (Naranjo-Hernández, Reina-Tosina, & Min, 2019). To overcome this obstacle, BIS devices make impedance measurements over a practicable range of frequencies and extrapolate these data to zero frequency by using Fricke's equivalent electrical circuit model and Cole modelling approach as represented in Figure 2.21 and Figure 2.22 respectively.

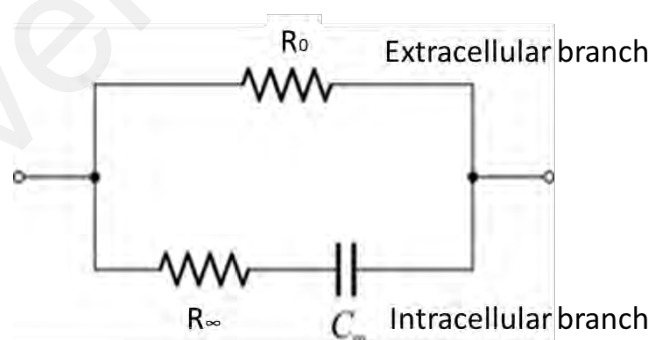


Figure 2.21: Fricke's equivalent electrical circuit model

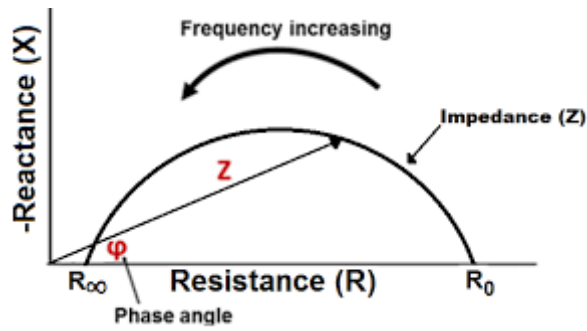


Figure 2.22: Cole plot (T. Cole, 2018)

The resistance to the current flow at zero frequency (R_0) is the measure of ECF volume. Taking this into consideration, Equation (2 – 10) becomes

$$Volume_{ECF} = \rho \frac{l}{R_0} \quad (2 - 11)$$

In theory, increment of ECF volume due to lymph accumulation is reflected by a decrease in R_0 with the assumption length and resistivity are constant. Equation (2 – 11) can be solved to determine a volumetric measure in mL if the length and resistivity are known. However, resistivity has unknown certainty and length may be indeterminate. Thus, the lymph volume in mL is therefore rarely used or reported in practical usage.

(a) Bioimpedance Spectroscopy Data Analysis

BIS measured data is analysed by fitting the data to Cole equation for data visualization through Cole plot (Figure 2.22) and for data analysis through Cole parameters (Gudivaka, Schoeller, Kushner, & Bolt, 1999).

i Cole Equation

In 1940, Cole established mathematical equation that could fit BIS measured data (K. S. Cole, 1940). The Cole equation is commonly used to represent and analyse BIS data. The analysis is based on four parameters contained in the Cole equation (2 - 12). The

Cole parameters are R_0 , resistance to current flow at infinite frequency (R_∞), exponent parameter (α) and the inverse of characteristic frequency (τ).

$$Z(\omega) = R_\infty + \frac{R_0 - R_\infty}{1 + (j\omega\tau)^\alpha} \quad (2 - 12)$$

Cole equation exhibits non – linear relation between complex impedance value and frequency. It is represented as a suppressed semi – circle in the impedance plane (Figure 2.22). The Cole equation parameter Z can be decomposed into resistance (R) (2 - 14) and reactance (X_c) (2 - 15) using mathematical equation in (2 – 13).

$$j^\alpha = \cos\left(\frac{\alpha\pi}{2}\right) + j \sin\left(\frac{\alpha\pi}{2}\right) \quad (2 - 13)$$

$$R(\omega) = R_\infty + \frac{(R_0 - R_\infty) \left(1 + (\omega\tau)^\alpha \cos\left(\frac{\alpha\pi}{2}\right)\right)}{1 + 2(\omega\tau)^\alpha \cos\left(\frac{\alpha\pi}{2}\right) + (\omega\tau)^{2\alpha}} \quad (2 - 14)$$

$$X(\omega) = -j \frac{(R_0 - R_\infty) \left(1 + (\omega\tau)^\alpha \cos\left(\frac{\alpha\pi}{2}\right)\right)}{1 + 2(\omega\tau)^\alpha \cos\left(\frac{\alpha\pi}{2}\right) + (\omega\tau)^{2\alpha}} \quad (2 - 15)$$

ii Cole Parameters Estimation

Practically, it is impossible to determine R_0 , R_∞ and other Cole parameters directly due to technical and safety reasons. Therefore, the Cole parameters are determined through estimations by extrapolating and fitting curve BIS measured data with Cole model over a practicable frequencies range (L. C. Ward, 2018). Recently, study by L.C. Ward *et al.* (2020) has developed a protocol for the assessment of breast oedema. In this study, R_0 was determined by using polynomial curve fitting instead of Cole modelling. L.C. Ward *et al.* (2020) found Cole modelling parameters estimation is prone to error in the breast oedema assessment (L. C. Ward et al., 2020).

i Impedance Plane Fitting

Impedance plane fitting or Cole modelling is conventionally used method to estimate the Cole parameters is by fitting BIS data to the Cole plot in the impedance plane (BH Cornish, Thomas, & Ward, 1993). A Cole plot as represented in Figure 2.22 is a perfect semicircle with its centre depressed below the resistance axis. In a Cole plot, the resistive component of impedance is plotted against the reactive component (R - X_c plot) (BH Cornish et al., 1993). The accuracy of R₀ estimation depends on the quality of raw BIS impedance measurement and of Cole model curve fitting.

BIS is particularly applicable for impedance measurement in arms and legs due to theoretical assumption of body parts as a conductive volume cylinder (Bruce Cornish, 2006). However, this is not true for impedance measurement of the breast. BIS measured data at both highest and lowest measurement frequencies are compromised by errors in reactance measurement. This minimizes Cole modelling accuracy (BH Cornish & Ward, 1998).

ii Non-linear Least Squares Curve Fitting

Non-linear least squares (NLLS) is a commonly utilized method to fit the Cole model to BIS data (Kun & Peura, 1999). NLLS approximate the best coefficients for a given model that fits the experimental data through successive iterations. This method applied Equation (2 – 16) to minimize the summed squared of the error between measured data points and the fitted model.

$$\min \sum_{i=1}^N e_i^2 = \min \sum_{i=1}^N (y_i - \bar{y}_i)^2 \quad (2 - 16)$$

where N is the number of data points, *e* is the error, *y* is the data and \bar{y} is the model.

BIS measured data can be evaluated with three different models, $R(\omega)$ (Equation (2 – 14)), $jX(\omega)$ (Equation (2 -15)) and $R(\omega) + jX(\omega)$ using natural frequency (ω) as independent variable for Cole parameters estimation. Each of the Cole parameters can be computed from the change of raw impedance data with frequency (Siconolfi, Gretebeck, Wong, Pietrzyk, & Suire, 1997; Leigh Ward, Fuller, Cornish, Elia, & Thomas, 1999).

The conventional Cole modelling method is primarily affected by reactive component of impedance measurement. However, research investigations have shown the resistive component is immune to such errors (Buendía, Seoane, Harris, Caffarel, & Gil, 2010; Scharfetter, Hartinger, Hinghofer-Szalkay, & Hutten, 1998). A comparative study by Ayllon *et al.* (2009) demonstrated the best fitting with minimal Standard Error of Estimate is the fitting obtained from resistance only. The results support the possibility of analysing only resistive component of the impedance to accurately fit Cole equation and to estimate Cole parameters (Ayllon, Seoane, & Gil-Pita, 2009). Resistance-based modelling was correlated with lower error rates than impedance plane fitting and was able to analyse raw impedance data regardless of its quality (L. C. Ward *et al.*, 2020).

iii Polynomial Curve Fitting

Polynomial curve fitting is an alternative method for Cole parameters estimation introduced to overcome error associated with reactance measurement by impedance plane curve fitting (Cole plot).

Research conducted by L.C. Ward *et al.* (2020) applied a sixth-order polynomial curve fitting to the resistance against frequency data. The study concluded BIS data analysis and R_0 estimation using polynomial curve fitting as a robust alternative approach to conventional Cole modelling in the case of breast oedema assessment (L. C. Ward *et al.*, 2020).

2.6.3 Measurement Protocol

The measurement protocol in BIS is essential for obtaining accurate and reliable results. It involves preliminary preparations, such as electrode placement and skin cleaning to optimize conditions. The measurement posture should be chosen carefully to minimize the effects of body fluid distribution and muscle contraction. Additionally, the protocol considers whether to perform whole-body or segmental body bioimpedance measurements based on the specific research or clinical objectives. By following a standardized protocol, consistency and accuracy can be achieved, enhancing the validity and reproducibility of BIS measurements.

2.6.3.1 Preliminary Measurement Preparations

In bioimpedance measurements the implementation of standardized and accurate procedure is crucial for obtaining reliable results. To achieve this, researchers have adhered to a set of preliminary measurement guidelines (Mialich, Sicchieri, & Junior, 2014; Naranjo-Hernández et al., 2019). These involve instructing study participants to abstain from engaging in physical exercise, consuming alcohol or caffeine, and eating for a period of four hours prior to measurements (Androutsos, Gerasimidis, Karanikolou, Reilly, & Edwards, 2015). Additionally, to optimize the quality of skin contact and minimize the impedance resulting from skin-electrode contact, it is recommended that all jewelry be removed, and the skin at the electrode placements be cleaned using alcohol wipes (B. Svensson, Dylke, Ward, & Kilbreath, 2015).

2.6.3.2 Measurement Posture

Measurement can be performed with the subject in supine, sitting or standing position. Ag-AgCl electrodes are placed on the hands and feet in supine or sitting position. Arms and legs are slightly abducted with palms facing down in supine position. In standing position, measurement is performed with subject standing on stainless steel electrode

plates with hands in contact with electrodes on the handles (Van Zanten, Piller, & Ward, 2016). Several studies have reported standing position standardizes anatomical positioning for obtaining accurate, repetitive, and precise measurements (Koelmeyer, Ward, Dean, & Boyages, 2020; Thurlow, Taylor-Covill, Sahota, Oldroyd, & Hind, 2018).

The body impedance measurements are affected by body posture due to the redistribution of body fluids. Researches have recommended approximately 5 to 10 minutes equilibrium time before body impedance measurements to minimize the effect of posture change (Gibson, Beam, Alencar, Zuhl, & Mermier, 2015; Medrano, Eitner, Walter, & Leonhardt, 2010). However, study by Koelmeyer *et al.* on 100 women discovered no significant difference in impedance ratios between two devices (tetrapolar gel Ag-AgCl and stand-on BIA device), irrespective of different measurement postures (sitting or standing) or clinical condition (control or lymphedema) (Koelmeyer *et al.*, 2020).

2.6.3.3 Whole-body Versus Segmental Body Bioimpedance Measurement

Two approaches commonly employed in bioimpedance measurement are whole-body and segmental bioimpedance measurement. Whole-body bioimpedance measurement involves the placement of electrodes on hands and feet. The electrical current is passed through the entire body in this configuration. On the other hand, segmental bioimpedance involves the placement of electrodes on specific segments of the body, such as the arm, trunk, or leg. Figure 2.23 describe the two approaches of bioimpedance measurement.

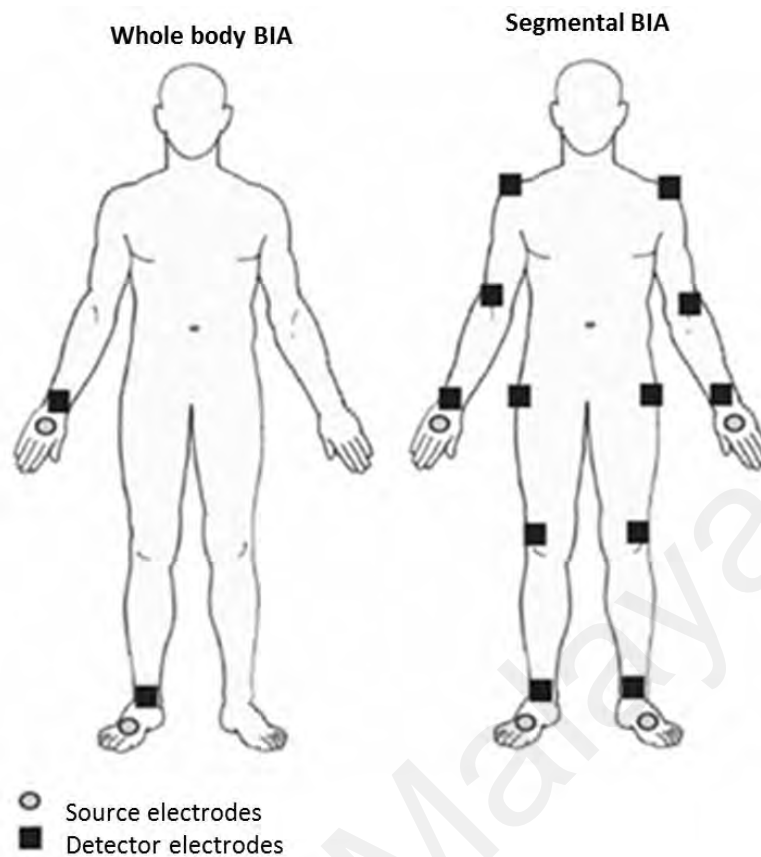


Figure 2.23: Whole-body and segmental bioimpedance measurement (Mialich et al., 2014)

Whole-body bioimpedance measurement employ three different approaches: the hand-to-foot method, the foot-to-foot method and the hand-to-hand method. Among these, the hand-to-foot method is the most utilized. The hand-to-foot method was validated by Lukaski *et al.* (1986) in 140 normal adults. The study established the measurement approach reliable for use in assessment of body composition in healthy human (Lukaski, Bolonchuk, Hall, & Siders, 1986). Deurenberg *et al.* validated the hand-to-hand method on 298 Singaporean, reporting that readings obtained using handheld impedance were significantly acceptable (Deurenberg & Deurenberg-Yap, 2002).

The concept of whole-body bioimpedance assumes that the human body can be treated as a single cylinder to estimate TBW. This approach while convenient has its limitations. Specifically, the contribution of the trunk to the overall resistance is relatively small, accounting for approximately 10% of the total resistance. However, in reality, the trunk

constitutes a significant portion of the conductor volume, representing around 50% (Mulasi et al., 2015). This assumption indicates that the alterations in fluid or fat content within the trunk region would not significantly impact the overall measurements of TBW (Sardinha et al., 2023). Whole-body bioimpedance approach may be compromised the accuracy of conditions such as obesity or cases of fluid overload due to the said assumption.

On the other hand, segmental bioimpedance measurements present an alternative approach. This method views the human body as comprising five distinct segments or cylinders, each with its own resistance characteristics. Unlike the whole-body approach, segmental analysis provides a detailed assessment of impedance by considering individual body segments separately (Catapano et al., 2023). This consideration is relevant to enhance the accuracy of TBW estimation.

Thus, segmental bioimpedance measurement approach has emerged as a valuable alternative, particularly for evaluating diseases that affect the balance of body fluids. Several studies have highlighted the advantage of segmental bioimpedance measurement over whole-body. Tanaka *et al.* (2007) confirmed the reliability and accuracy of segmental bioimpedance measurement in total muscle volume assessment compared to whole-body measurement (Tanaka, Miyatani, Masuo, Fukunaga, & Kanehisa, 2007). Another study by Cornish *et al.* focused on the placement of electrodes at either end of the arm for early diagnosis of lymphedema in breast cancer patients. Their findings suggested that segmental approach enables the detection of lymphedema at its initial stages (BH Cornish et al., 2000). Svensson *et al.* study on impedance measurement for the hand and segmented arm measurement confirmed the high reliability of segmental measurement for early detection of upper limb swelling (B. Svensson et al., 2015; B. J. Svensson, Dylke, Ward, & Kilbreath, 2017).

2.6.4 Electrodes

Electrode is one of key elements in electrical sensing. An electrode is a conductor that functions to perform electrical contact with non-metallic part of a circuit. Electron transfer or current flow occurs at electrode. It transduces signals between electronics and living tissues or cells. In bioelectrical impedance application, electrode acts as a medium between circuit and living tissues. Electrodes are used to stimulate cells with electrical signals and measure the impedance of target tissue to infer cell physiology. Types, shapes and placement of electrodes have different impact on measurement values (Dey, Ashour, Fong, & Bhatt, 2019). There are two types of electrodes, non-invasive and invasive electrodes (Grayson, Shawgo, Li, & Cima, 2004). Non-invasive electrodes are surface electrodes applied to the skin of subject. Invasive electrodes are intrusive and implanted within nerves or muscle.

2.6.4.1 Types of Surface Electrodes

Bioimpedance measurements on the human body uses surface electrodes that consists of a metal electrode or electrolytic gel. The most common type of electrodes used in bioimpedance application is silver/silver chloride (Ag/AgCl) gel electrode with an electrolyte based on Cl^- (Hafid et al., 2017; Karamehmetoglu, Ugur, Arslan, & Palamar, 2009; Uchiyama, Ishigame, Niitsuma, Aikawa, & Ohta, 2008; White, Orazem, & Bunge, 2013; Winterhalter et al., 2008). It is reported the use of Ag/AgCl electrodes for measurement frequency range 0.1 Hz to 10 kHz (Uchiyama et al., 2008) and 1 Hz to 100 kHz (White et al., 2013). Study by Nguyen *et al.* demonstrated Ag/AgCl to have high contact impedance from 1 kHz to 10 kHz due to the epidermis layer that affects the lower frequency signal (Nguyen et al., 2013).

An alternative to gel electrodes is dry electrodes. There are different materials used for dry electrodes such as stainless steel (Fasano & Hinderliter, 2004; Vosika, Lazovic,

Misevic, & Simic-Krstic, 2013), gold (Dudzinski et al., 2017; Fasano & Hinderliter, 2004; Vosika et al., 2013), and graphite-epoxy resin composite (Pauliukaite, Ghica, Fatibello-Filho, & Brett, 2010). Solid gel dry electrodes exhibit faster reaction time compared to hydrogel gel electrodes (Winterhalter et al., 2008). Kusche, Kaufman, & Ryschka investigated the characteristics of different kinds of dry electrodes under variation of frequency, contact duration, contact pressure, placement position and subjects. The Ag/AgCl gel and dry electrodes have the highest electrodes impedance among all the electrodes. However, Ag/AgCl gel and dry electrodes show the lowest contact skin-electrode impedance under all experimented conditions. The investigation concluded metal electrodes and carbon rubber electrodes can be used to acquire the bioimpedance measurement under appropriate parameters such as contact pressure of 5N, attachment of electrodes 5 minutes before measurement, and using high (Kusche, Kaufmann, & Ryschka, 2018).

Recent investigation was conducted to compare and assess BIS measurement using Ag/AgCl electrode and stainless-steel dry electrode. The research findings supports reliable BIS measurement from both Ag/AgCl gel and stainless steel dry electrodes with a standard deviation of less than 0.6% (Koelmeyer et al., 2020).

Capacitive electrodes have been proposed as a non-contact impedance measurement between electrodes and skin. The impedance measurement results were unreliable as compared with conventional bioimpedance method. Capacitive electrodes have high electrodes impedance and are susceptible to motion artifacts (Eilebrecht, Willkomm, Pohl, Wartzek, & Leonhardt, 2013; Naranjo-Hernández et al., 2019).

At present, textile electrodes were introduced in bioimpedance measurement continuous and wearable application. A custom-made silver-based electrode garment were used to measure impedance between wrist and ankle in a tetrapolar electrodes

configuration (Atwa, Hassan, & Ahmed, 2019; Ferreira, Pau, Lindecrantz, & Seoane, 2016).

2.6.4.2 Electrode Design and Configuration

In bioimpedance analysis, the electrodes design and configuration have a strong influence on the bioimpedance data. Kyle *et al.* recommended the electrode contact area to be more than 4 cm² for clinical application of bioimpedance analysis (Kyle *et al.*, 2004b). Bioimpedance measurement requires minimum of two electrodes. The electrodes comprise of current or driving electrodes (red colour in Figure 2.24 and Figure 2.25) and voltage or sensing electrodes (black colour in Figure 2.24 and Figure 2.25). Bioimpedance measurement can be conducted in either two-electrode or four-electrode (tetrapolar) or eight-electrode (octopolar) configuration.

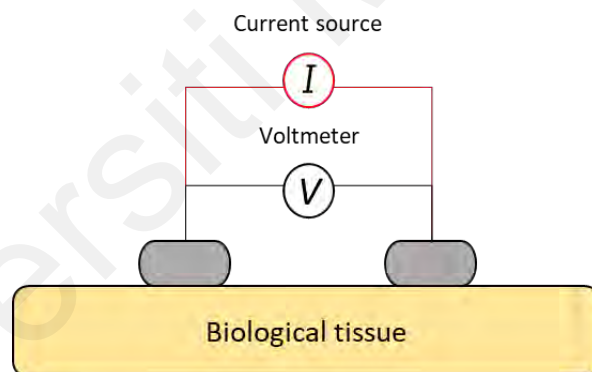


Figure 2.24: Two-electrode bioimpedance measurement

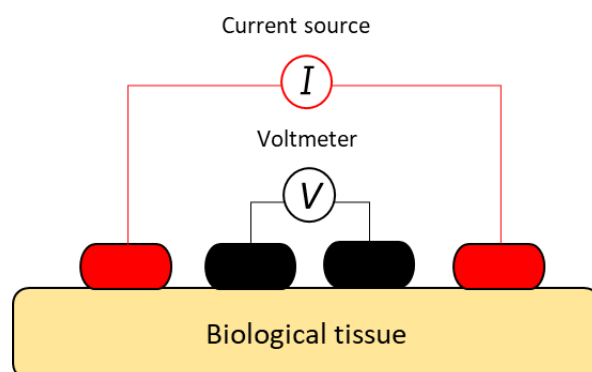


Figure 2.25: Four-electrode bioimpedance measurement

The two-electrode method (Figure 2.24) uses two electrodes for impedance measurement. The current electrode and voltage electrode are conducted using the same electrodes. The two-electrode method suffers voltage drop in its measurement data due to contact impedance problem. Subsequently, the tetrapolar and octopolar electrodes configuration become widely used for bioimpedance measurements because of the current distribution uniformity (Grimnes & Martinsen, 2000; Khalil, Mohktar, & Ibrahim, 2014).

A four-electrode or tetrapolar electrode arrangement is commonly used to measure bioimpedance directly between electrodes placed on the skin surface. The tetrapolar electrode consists of a pair of *sense* or voltage electrodes spanning the body region of interest and another pair of *drive* or current electrodes located distally to the voltage electrodes which function to inject current into the body. Separation between current electrodes from voltage electrodes circuitry helps to eliminate the large skin surface-electrode resistance (BH Cornish, Ward, Thomas, & Bunce, 1998). The tetrapolar electrodes configuration is the most applied because it minimizes the influence of electrodes in the measurement process. However, this configuration can be affected by the anisotropy of the tissue such as muscle, blood vessels or nerve fibres (Naranjo-Hernández et al., 2019).

In the beginning, electrodes were placed spanning the region of interest. Example of placing tetrapolar electrode at limb is by locating one sense electrode at wrist and another set typically 40 cm proximal on the arm (BH Cornish et al., 2001; LC Ward et al., 1992). The current electrodes were located distally at the base of fingers and at the acromion. Kyle *et al.* recommended separation of minimum 5 cm the between electrodes for clinical application of bioimpedance analysis (Kyle et al., 2004b). Cornish *et al.* has found an equipotential electrode placement produces greater precision of measurement. The

principle of equipotential can be applied by placing second set of voltage electrode on ulnar styloid of the contralateral limb for the upper limb and in between malleoli for the lower limbs (BH Cornish, Jacobs, Thomas, & Ward, 1999). Equipotential electrode placement ensures bioimpedance measurement consistency and reduces measurement variability in individual and application.

Recent study by Qin *et al.* investigated the difference between single segment bioimpedance (SSB) and multi-segment bioimpedance (MSB) in evaluating lymphedema. The study reported SSB more sensitive (0.9) compared to MSB (0.75) for unilateral lymphedema. MSB was found more useful in bilateral lymphedema assessment with sensitivity of 0.56 and specificity of 0.60. MSB provides quantified differential extents of edema (Qin, Bowen, James, & Chen, 2020).

2.6.5 Sources of Artifacts and Noise in Bioimpedance Measurements

A major source of errors in bioimpedance measurements is contributed by electrodes. This is due to the stray capacitance and electrode polarization, the high contact impedance, interface noise, and the artifacts due to movement, fluctuations, and contact problems (Callejón, Del Campo, Reina-Tosina, & Roa, 2017; Fernandez, Lebiga, Koklu, Sabuncu, & Beskok, 2015; Naranjo-Hernández et al., 2019). Several researchers recommend the use of contact Ag/AgCl electrodes with low intrinsic impedance, low electrode to skin contact impedance, appropriate selection of type of gel, attentive placement of electrodes and avoidance of expired electrodes to minimize measurement errors (Bogonez-Franco, Nescolarde, Bragos, Rosell-Ferrer, & Yandiola, 2009; Bolton et al., 1998; McAdams, Henry, Anderson, & Jossinet, 1992; McAdams, Lackermeier, McLaughlin, Macken, & Jossinet, 1995).

The impedance of electrodes is influenced by the frequency and the characteristics of the electrodes (Taji, Shirmohammadi, Groza, & Batkin, 2013). Maximizing the surface of the electrodes can minimize this effect (Fernandez et al., 2015).

2.6.6 Quantitative Evaluation of Lymphedema Using BIA

Early study by Yamazaki *et al.* (1988) inferred increment of resistance as swelling reduction after pneumatic massage therapy for patients with pre-existing lymphedema before and after lymphedema treatment (Yamazaki, Idezuki, Nemoto, & Togawa, 1988). Later Watanabe *et al.* (1989) suggested sensitive indicators to evaluate local oedema quantitatively by utilizing R_0 and the ratio of extracellular resistance and intracellular resistance ($R_0: R_i$) in group of control (no oedema) patients with group of patients with lower limb lymphedema (Watanabe et al., 1989). Ward *et al.* (1992) compared differences in R_0 values between affected and unaffected limbs to differentiate women with and without lymphedema (LC Ward et al., 1992). This measurement approach has been shown to be significantly more sensitive than circumferential measurement both in the early diagnosis and in monitoring lymphedema progression by Cornish *et al.* (1996) to monitor treatment response in BCRL women (BH Cornish et al., 1996). Past studies have proven by measuring the increment of lymph volume in ECF as indicator of BCRL early stage (E. S. Dylke & Ward, 2020).

The measurement protocol was then improvised to equipotential measurement with impedance outcomes utilized as inter-limb ratios rather than inter-limb differences. The evaluation of lymphedema using ratios helped to minimise inter-patient variability because of the wide range of absolute R_0 observed between patients (LC Ward et al., 1992). The R_0 ratios (Equation 2 - 17) protocol was effectively applied by Cornish *et al.* in 2000 and 2001 for early detection of lymphedema. The studies established ratio thresholds to identify patients with unilateral upper limb lymphedema.

$$R_0 \text{ ratios} = \frac{\text{Non - affected limb } R_0}{\text{Affected limb } R_0} \quad (2 - 17)$$

The early lymphedema detection threshold was set at three standard deviations (SD) above the mean ratio in a healthy control population (BH Cornish et al., 2001; BH Cornish et al., 2000). The mean and standard deviation of 60 healthy female Australian population published by Cornish *et al.* was 0.964 ± 0.034 . Study by Ridner *et al.* determined the normative inter-limb mean and standard deviation ratios to be 0.965 ± 0.027 (Ridner, Dietrich, Deng, Bonner, & Kidd, 2009). In 2011, LC Ward *et al.* established mean and standard deviations of 0.986 ± 0.040 in 127 healthy population using current model impedance device (LC Ward et al., 2011). In a study conducted by Jung *et al.* (2018), 643 healthy female Korean participants were recruited to establish the normalise upper limb ratio. The study investigated two parameters: resistance at 1 kHz and 5 kHz. The results indicated that for SFBIA ratios at 1 kHz, the values were 1.011 ± 0.029 for the dominant affected arms and 0.990 ± 0.028 for the non – dominant affected arms. Additionally, the study found that the SBIA ratios at 5 kHz were 1.013 ± 0.030 for the dominant affected arms and 0.998 ± 0.029 for the non – dominant affected arms (Jung et al., 2018). In a recent study conducted by Liu *et al.* (2021), upper limb bioimpedance measurements were carried out on 1305 healthy women from China. The aim of the study was to differentiate between patients with lymphedema and healthy individuals. The study established +2SD and mean +3SD values for both dominant and non – dominant affected arms. The finding of the study revealed ratios of 1.012 ± 0.028 for dominant affect arm and 0.989 ± 0.027 for non – dominant affected arm (Liu et al., 2021). Table 2.3 summarises the normative inter-limb mean and standard deviation ratios and lymphedema detection threshold for each study.

Table 2.3: Normative inter-limb ratios and lymphedema detection threshold

Authors	Healthy female population						Lymphedema detection threshold			
	Mean		Standard Deviation	Age	Number of subjects	Country	Dominant affected		Non-dominant affected	
	Dominant	Non-dominant					2SD	3SD	2SD	3SD
Cornish (2001)	1.037	0.964	0.034	27 - 84	60	Australian	1.105	1.139	1.032	1.066
Ridner <i>et al.</i> (2009)	1.024	0.986	0.027	> 18	60	United States	1.078	1.105	1.040	1.067
L.C. Ward (2011)	1.014	0.966	0.041	18 - 86	172	Australian	1.117	1.134	1.048	1.106
Jung <i>et al.</i> (2018)										
Resistance at 1 kHz	1.011	0.990	0.029	49.6 ± 9.0	643	Korea	1.069	1.098	1.046	1.077
Resistance at 5 kHz	1.013	0.998	0.030				1.073	1.103	1.056	1.085
Liu <i>et al.</i> (2021)	1.012	0.989	0.028	53.7 ± 12.8	1305	China	1.068	1.096	1.043	1.070

The differences in R_0 due to limb dominance and whether the at-risk or affected limb was dominant or non-dominant were considered to establish the ratio thresholds. At present, this measurement protocol is used for early detection of lymphedema. Nevertheless, recent studies have suggested that 3 SD might be too conservative and that 2 SD provides better sensitivity (Fu et al., 2013; Qin et al., 2018).

However, the R_0 ratios assessment protocol was only suitable for unilateral lymphedema usage and was not applicable in bilateral lymphedema. In cases of bilateral lymphedema, swelling and change in R_0 occurs in both limbs. To overcome bilateral lymphedema impedance issue, Cornish *et al.* applied Watanabe *et al.* approach using $R_0: R_i$ ratios. Comparison of $R_0: R_i$ ratio between affected lower limbs and unaffected upper limbs was proven useful indicator to detect lymphedema in bilateral cases (B. H. Cornish, Thomas, Ward, Hirst, & Bunce, 2002).

The present lymphedema assessment method uses Lymphedema index or L-Dex score that came from commercial research and development by a leading BIS devices manufacturer, Impedimed (Impedimed, 2019; L. C. Ward et al., 2009). Although comparison of a patient's R_0 ratio to the normative mean + 3 SD threshold allows lymphedema classification in cross-section studies, the same method could not be applied to monitor lymphedema progression for the same patient in longitudinal studies. Hence, the L-Dex score was introduced.

Individual patient's inter-arm R_0 ratio (unaffected: affected) is scaled and linearized to the healthy population mean + 3 SD threshold using L-Dex score. An L-Dex score more than 10 units to the ratio of the mean + 3 SD threshold indicates presence of lymphedema as illustrated in Figure 2.26.

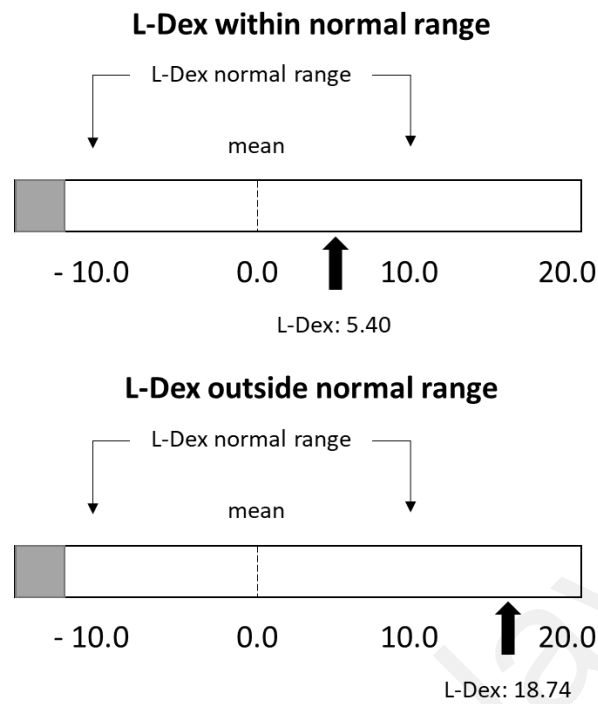


Figure 2.26: Interpretation of L-Dex scores

2.6.7 Validity of BIA in Lymphedema Assessment

Numerous studies on the accordance between populations and reliability of BIA upper limb lymphedema assessment have been conducted. In cases of unilateral lymphedema affecting dominant limb, strong concordance has been shown for the normative inter-limb (unaffected: affected; nondominant: dominant) mean and SD between differing healthy populations in Australia (LC Ward et al., 2011), United States (Ridner et al., 2014; Ridner et al., 2018) and China (Wang et al., 2017). The inter and intra-reliability of BIS measurement of the upper limb has been found to be excellent by various studies (S. Czerniec et al., 2010; Ferro et al., 2018; Fu et al., 2013). Likewise, high reliability was shown for BIS assessment of the hand [intraclass correlation (ICC) = 0.900 – 0.967] (E. Dylke et al., 2014) and the lower limb (concordance correlation coefficient = 0.88) (Gordon, Melrose, Warner, Buttner, & Ward, 2011).

Determination of validity, sensitivity, specificity and predictive performance of BIS is complicated due to lack of agreement on a gold standard and definitive reference method

for the diagnosis and assessment of lymphedema (Enøe, Georgiadis, & Johnson, 2000; Van Stralen et al., 2009). However, much studies have suggested lymphoscintigraphy (Coroneos et al., 2019; E. Dylke et al., 2016) and perometry (N. Bundred et al., 2020; N. J. Bundred et al., 2015) as a gold standard lymphedema diagnosis and assessment (Smoot et al., 2011). The performance of BIS has been compared against multiple reference standards such as imaging (Coroneos et al., 2019; E. Dylke et al., 2016; Unno et al., 2008), perometry (N. Bundred et al., 2020; B. H. Cornish et al., 2002), water displacement (Belgrado et al., 2010), circumferential measurement (Berk *et al.*, 2008; Labs, Tschoepl, Gamba, Aschwanden, & Jaeger, 2000; Spitz *et al.*, 2019), subjective assessment of symptoms (Armer et al., 2003) and clinical diagnosis (Smoot et al., 2011). There is no consensus on the definitive assessment tools for the availability of lymphedema in these studies. Consequently, this has led to a numerous finding of sensitivity and specificity for BIS.

B. Cornish *et al.* found the 100% sensitivity and 98% specificity for the assessment of upper limb lymphedema by BIS using normative mean + 3 SD threshold in comparison to sequential circumference measurements. No recent BIS analysis has achieved 100% sensitivity (BH Cornish et al., 2001). Further studies have found high specificity 64% to 100% with low sensitivity from 42% to 100%. The vast range of sensitivity and specificity may relate to differences in measurement protocol, different BIS thresholds and reference measurements chosen across the literature. For example, B. Cornish *et al.* determined present of lymphedema after two consecutive BIS measurement in 1-week apart. Meanwhile, recent studies have relied on single measurement despite the fact fluctuating lymphedema values in patients (S. A. Czerniec, Ward, & Kilbreath, 2016). In terms of detection thresholds, some researcher agree that a volume difference of 5% between arms is an indicator of lymphedema onset (Lahtinen et al., 2015), whereas other studies adopt a 10% inter-limb volume difference (Barrio et al., 2015; N. J. Bundred et al., 2015). The

same goes to BIS criteria, L-Dex score of 10 (Bloomquist et al., 2016), 7.5 (N. Bundred et al., 2020), 7.1 (Fu et al., 2013) or 6.5 (Ridner et al., 2020) with the latter three using an inter-limb ratio of normative mean + 2 SD. Fu *et al.* determined the impact of differing detection threshold on sensitivity of BIS. L-Dex of 10 has a 66% sensitivity while L-Dex of 7.1 shows increment of sensitivity to 80% (Fu et al., 2013). Hayes *et al.* investigation has obtained a 65% sensitivity of circumferential limb measurement with reference to BIS measurement (S. Hayes, Cornish, & Newman, 2005), whereas Berlit *et al.* obtained a 75% BIS sensitivity compared with circumferential measurement (Berlit et al., 2012).

The variety of reference tools and thresholds have led to misinterpretation or over-interpretation of accuracy for BIS (L. C. Ward, Kilbreath, & Dylke, 2015). Since there is no definitive reference protocol available, maximum likelihood estimation is recommended as an alternative method of analysis (Enøe et al., 2000). At present, this method has not been applied to determine the predictive performance of BIS. Furthermore, the number of research studies on BIS sensitivity and specificity is small. Thus, it is not possible to conclude BIS is more or less accurate than as assumed gold standard since the absolute reference accuracy is unknown.

Sensitivity and specificity can be mathematically combined to determine positive and negative likelihood ratios (LRs). LRs are one of the best methods to determine diagnostic accuracy (McGee, 2002). Some research studies have implemented LRs to determine the presence of lymphedema and obtained positive likelihood ratio (LR) (9 – 13) and negative LR (0.3 – 0.6) (E. Dylke et al., 2016; Smoot et al., 2011). The LRs method can increase certainty in BIS diagnosis. For instance, a patient had undergone sentinel node biopsy is considered to have low chance of having BCRL. A single patient's increment of inter-limb circumference difference provides a 50% probability of getting BCRL. This

contributes to a predictive probability of 90% when combined with a positive BIS inter-arm ratio.

Impedance measurement at low frequency reflects mostly interstitial fluid of which lymph fluid is a principal component. Thus, even though BIS measure lymph fluid indirectly, BIS is highly correlated to lymph volume and is sensitive to changes in fluid levels. Studies have shown BIS capability of detecting a miniscule change of 35mL lymph volume in whole arm impedance measurement (L. C. Ward, 2015). This is similar to change of approximately 0.04 units in inter-arm impedance ratio in BCRL patients (L. C. Ward, 2018).

BIS has been utilized repeatedly in prospective BCRL study to initiate early treatment with the aim to reduce lymphedema occurrence and progression (Koelmeyer et al., 2019; Ridner et al., 2018; Ridner et al., 2020). Koelmeyer *et al.* investigation has revealed women assigned in early surveillance group were less likely to develop lymphedema and the lymphedema progression was less severe (Koelmeyer et al., 2019; Ridner et al., 2019). Considerable evidence suggests immediate intervention after BIS measurement of 10 L-Dex points can impede and reduce lymphedema progression rates (Kaufman et al., 2017; Kilgore et al., 2018; Ridner et al., 2018; Whitworth & Cooper, 2018; Whitworth, Shah, Vicini, & Cooper, 2018).

The use of BIS to determine lymphedema for the whole arm and segmented parts of the arm are expanding. Measurement protocols, normative data and diagnostics thresholds for segmented parts of the upper limb and breast have been studied and published (E. Dylke et al., 2014; B. J. Svensson et al., 2017; LC Ward, Dylke, & Kilbreath, 2012; L. C. Ward et al., 2020).

2.6.8 Commercial Bioelectrical Impedance Analyser

The commercially available BIA devices for lymphedema measurement are Quadscan 4000, InBody 720, SFB7, L-Dex U400, Inbody 720 and SOZO from Impedimed Limited. Study by Jane Wigg (2013) uses Quadscan 4000 to measure limb and body fluid shifts. The study concluded Quadscan 4000 ability to provide accurate ECF and TBW for the assessment of BCRL (Jane Wigg, 2013). Research conducted by Jung *et al.* (2018) and Liu *et al.* (2021) utilized InBody 720 to determine the normal range, detection threshold, and standard deviation of ECF for the diagnosis of lymphedema (Jung *et al.*, 2018; Liu *et al.*, 2021).

SFB7 and L-Dex U400 measure impedance from 3 kHz and 1000 kHz. Both devices use tetrapolar electrode arrangements to measure body impedance according to equipotential electrode placement on the wrists and ankles. Research by E. Dylke *et al.* (2016) established BCRL diagnostic thresholds using SFB7 as compared to lymphoscintigraphy (E. Dylke *et al.*, 2016). Recent study by Keeley (2021) uses L-Dex U400 to compare the performance of limb measurement or BIS for the early detection of BCRL (Keeley, 2021). Ridner *et al.* (2022) conducted 3-years postoperative surveillance using L-Dex U400 and concluded that BIS screening should be a standard approach for prospective BCRL surveillance (Ridner *et al.*, 2022).

SOZO is the latest commercially available BIS device for lymphedema measurement. SOZO measures impedance at 256 frequencies up to 1000 kHz with subject in upright standing position. Donahue *et al.* (2020) compares the performance of two analysers using L-Dex U400 and SOZO for the assessment of BCRL and found that both analysers measurements are statistically interchangeable (Donahue *et al.*, 2020). A prospective surveillance study conducted by Koelmeyer *et al.* (2021) using SOZO to assess the feasibility of monitoring BCRL over 6 months for women at high risk of developing

lymphedema. The study found that home monitoring has increased self – management awareness in BCRL patients (Koelmeyer, Moloney, Boyages, Sherman, & Dean, 2021).

All BIS devices apply the lymphedema index (L-Dex) method in the clinical assessment of unilateral lymphedema of the limb. The usage settings of the BIA device are in hospital, outpatient clinic, and physician office. Unlike other BIA device, SOZO stores subject’s body impedance results in cloud database. The comparisons of BIA devices in terms of its functionality are summarized in Table 2.4.

Universiti Malaya

Table 2.4: Commercial BIA device specifications

BIA Device	Frequency Scan	Measurement Position	Number of electrodes	Measurement Speed	Dimensions (length x width x height) cm	Cloud Platform	Price
Quadscan 4000	5, 50, 100, 200 kHz	Supine	4	Less than 30 seconds	24 x 15 x 3.5	Absent	RM 14,183.23
InBody 720	1, 5, 50, 250, 500 kHz and 1 MHz	Stand-On	8	Less than 30 seconds	87 x 52 x 120	Absent	RM 9,305.00
SOZO	3 kHz to 1000 kHz	Stand-On	8	Less than 30 seconds	64.8 x 44.5 x 129.8	Present	RM 44,130.89
SFB7	4 kHz to 1000 kHz	Supine	4	Less than 1 second	19 x 13 x 11	Absent	RM 31,432.50
L-Dex U400	3 kHz to 1000 kHz	Supine	4	Less than 1 second	19 x 13 x 11	Absent	RM 41,372.71

2.7 Design of Bioelectrical Impedance Instrumentation

Bioimpedance devices are based on the injection of current at one or more frequencies into a biological medium. The voltage is measured based on the circulation of that current (Tucker, Fox, & Sadleir, 2012). In accordance with IEC60601, a current must be less than 1mA when applied to human body to avoid any potentially adverse effects (Anusha, Preejith, Joseph, & Sivaprakasam, 2017).

The frequency of the injected current can be generated by using oscillator or digital-to-analog-converter (DAC). The frequency or signal generator allows a biological medium to be stimulated with a known frequency. A voltage-controlled current source (VCCS) changes this oscillating signal into a current that can be injected into the biological medium (Hersek, Töreyn, & Inan, 2015; Sanders et al., 2015).

It is possible to monitor the injected current to prevent it from exceeding the established limits (Hersek et al., 2016), but the most frequent way is to inject a current with a fixed amplitude (Harder et al., 2016). Although many current source topologies have been adopted for the VCCS, the majority are based on the modified Howland current pump, implemented using discrete operational amplifier-based designs (OPAM). This design is impractical for integrated circuits (IC) due to the need for precision resistors with high values. In this instance, designs based on transconductors and complementary metal-oxide semiconductor (CMOS) technology-fabricated integrated current drivers (Constantinou, Bayford, & Demosthenous, 2015) have been presented. For the design of the VCCS, a constant current for varying loads and a high output impedance, especially in the case of EIT (Chitturi & Farrukh, 2019), are desirable properties.

The response signal from the impedance is sampled by ADC and discrete Fourier transform (DFT) is processed by digital signal processing (DSP). The DFT algorithm provides a real and imaginary data at each output frequency.

Santoso *et al.* (2020) introduced a low-cost BIS instrumentation system consisting of three main units: AC current source, data acquisition and software module as depicted in the system block diagram presented in Figure 2.27.

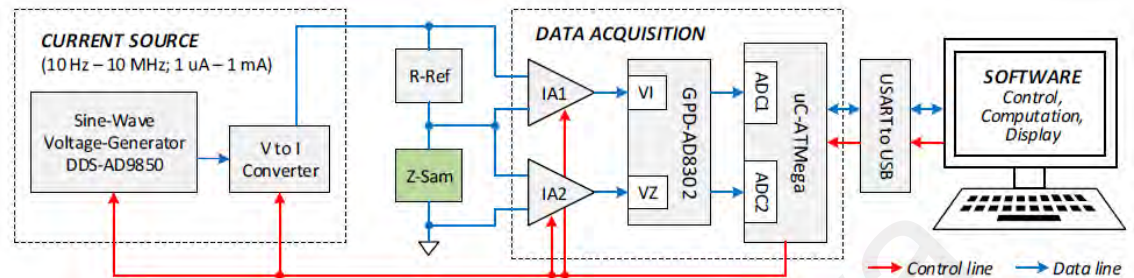


Figure 2.27: Block diagram of the BIS instrumentation system by Santoso *et al.* (2020)

The AC current source comprises of a sine wave voltage generator (AD9850) and voltage to current converter. The voltage generator is set to produce a frequency range of 10 Hz to 10 MHz, with amplitudes of 1-volt peak to peak in amplitude. The voltage to current convertor utilized the Howland current source. The data acquisition system encompasses two main components: the signal conditioning circuit and gain phase detector. The signal conditioning performs high impedance buffering, filtering, and signal amplification before transmitting the signals to the gain phase detector module (AD8302). The AD8302 measures gain and phase difference between two signals and generates two output voltage signals: magnitude and phase. These signals undergo an internal process within the AD8302 to determine gain and phase differences. The ATmega microcontroller converts these two signals into digital data via an ADC before transmitting the data to a computer (PC). On the PC, the data is further processed to compute impedance values. This process is repeated for various frequencies until one full frequency cycle is completed. The developed BIS instrumentation system impedance measurement performance was tested on four parallel RC circuits, with R value fixed at 5.6 k Ω and the C values set at different values of 1 nF, 10 nF, 33 nF, and 47 nF. The

measured impedance values were compared with those obtained from LCR meter. The comparison revealed a maximum error of 1.5% in the impedance measurements (Santoso, Pitaloka, Widodo, & Juswono, 2020).

Ain *et al.* (2021) implemented a similar BIS instrumentation system to the one described by Santoso *et al.* (2020). In their study, they utilized the AD9850 function generator module, DC cancellation circuits comprises of R (1 k Ω) and C (100 μ F) components, buffer and VCCS (OPA2134 Ammeters). Additionally, the setup included voltmeter built from the AD620 differential amplifier as well as the phase-gain detection module accomplished using the AD8302. The block diagram of the developed system is represented in Figure 2.28. The developed system is carried out by testing on beef, chicken, and mutton to determine the type and quality of the meat. The study concluded the ability of the system to distinguish the three types of meat and provides information on changes in the characteristics of meat from day to day from the impedance value (Ain *et al.*, 2021).

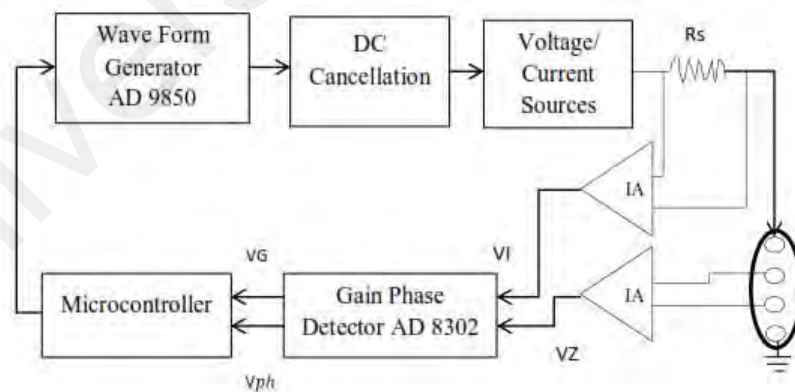


Figure 2.28: Block diagram of the BIS instrumentation system by Ain *et al.* (2021)

Zompanti *et al.* (2023) also utilized similar BIS instrumentation system, with a notable variation being the substitution of the signal with AD9833. To assess the effectiveness of their prototype, they conducted an evaluation using a known impedance Z. This

impedance was examined using the developed device, and its theoretical behaviour was simulated using EIS Spectrum Analyzer software to enable a comparison of the obtained results. The evaluation procedure involved testing the impedance against an equivalent circuit of a biological tissue ($R = 995 \Omega$ and $C = 14.6 \text{ nF}$), spanning a frequency range 10 – 125 kHz, in increments of 5 kHz. The outcomes of this evaluation revealed that the device achieved a maximum relative error of approximately 10% for measuring the magnitude of sample impedance and about 4% for measuring the phase of the sample impedance (Zompanti, Cicco, Ciarrocchi, Santonico, & Pennazza, 2023).

Simic *et al.* (2013) developed an impedance analyser system utilizing the AD5933. Their approach incorporates a signal conditioning circuit employing AD8606 to prevent electrolysis from occurring. Additionally, the study includes self – calibration system using two analogue multiplexers 74HTC4051 to enhance accuracy (Simic, 2013). Figure 2.29 shows the circuit diagram implemented in the system. The researchers conducted measurements on various passive components to assess its accuracy. The findings of the study reported the following maximum errors for magnitude and phase measurements (Table 2.5).

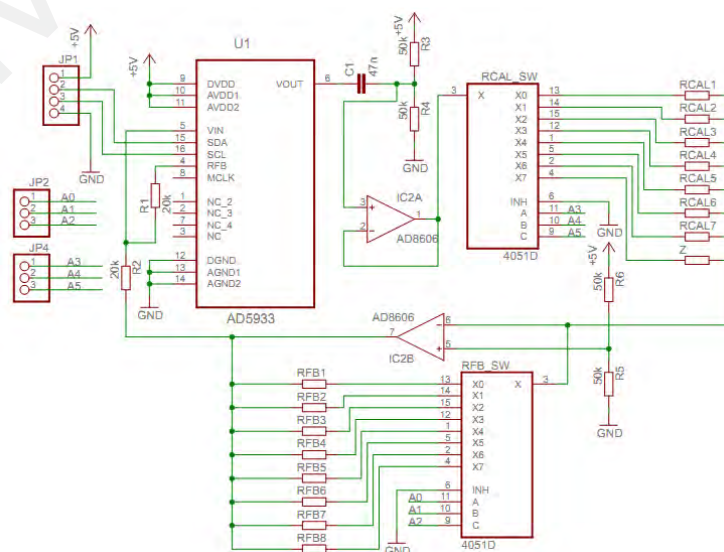


Figure 2.29: AD5933 impedance analyser system by Simic *et al.* (2013)

Table 2.5: Accuracy of impedance measurements using AD5933 impedance analyser system

Component	Magnitude error (%)	Phase Error (%)
Resistors (15 kΩ)	0.3	0.7
Capacitor (1nF)	2	3.5
Series RC (R = 15 kΩ, C = 1nF)	0.3	5.5
Parallel RC (R = 15 kΩ, C = 1nF)	3	5.5

Noveletto *et al.* (2016) developed a bioimpedance measurements device using the AD5933. The AD5933 employed a sinusoidal voltage in a bipolar configuration which is not a recommended method in IEC-60601. To overcome this, the researchers in this study, devised two distinct analogue front-end (AFE) circuits to establish four-electrode configuration. This is to eliminate the electrode contact impedance and load dependency. Thus, their study aimed to identify and compare the optimal AFE circuits, focusing on different Voltage Controlled Current Source (VCCS) configurations. AFE-1 depicted in Figure 2.30 uses a Load-in-the-loop VCCS, while AFE-2 shown in Figure 2.31 uses a mirrored modified Howland VCCS. The AFEs impedance performance results were evaluated on parallel RC configurations at 5, 50 and 100 kHz. The findings revealed that AFE-2 exhibited better performance especially for frequencies higher than 50 kHz, presenting a magnitude error of (0.5 – 3%) and phase error of (3 – 6%). In contrast, AFE-1 demonstrated a magnitude error of (0.5 – 7%) and phase error of (2 – 13%) (Noveletto, Bertemes-Filho, & Dutra, 2016).

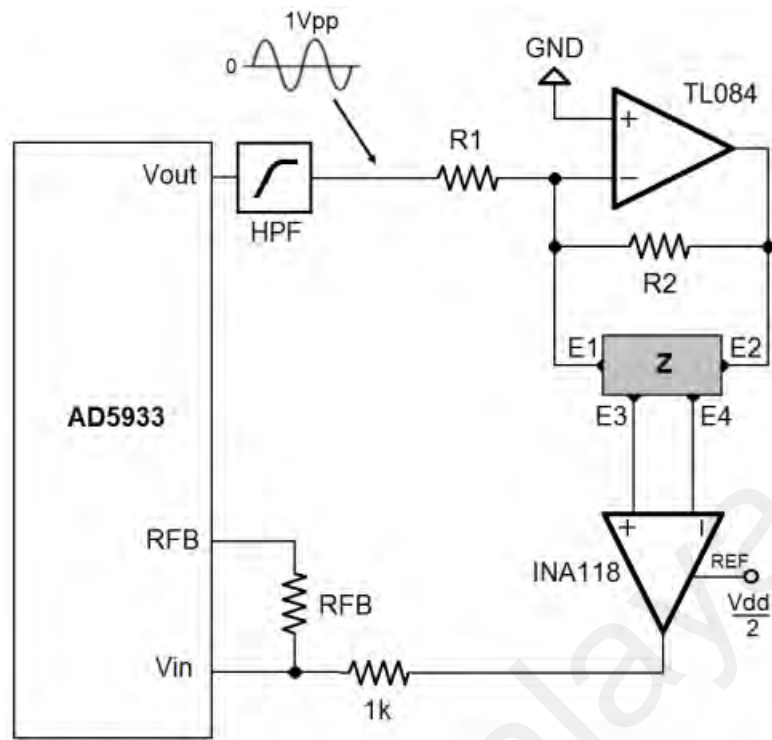


Figure 2.30: Schematic of the Load-in-the-Loop current source (AFE-1) (Noveletto et al., 2016)

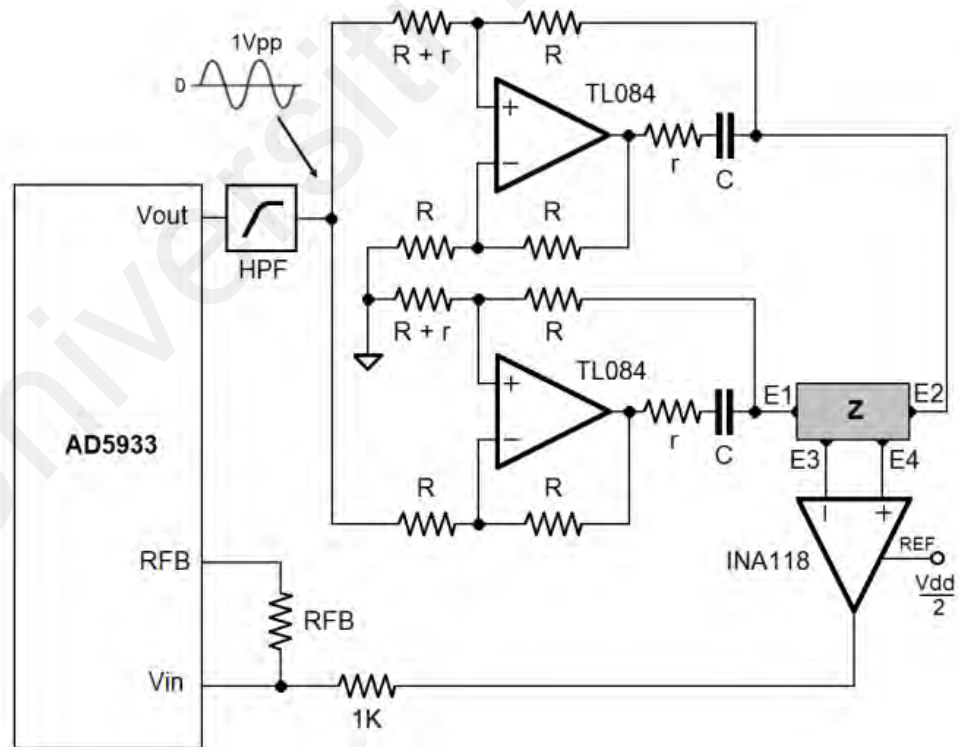


Figure 2.31: Schematic of the Mirrored Howland-Modified current source (AFE-2) (Noveletto et al., 2016)

One of the most commonly used chips for bioimpedance measurements in previous research is the AD5933 (Ferreira, Seoane, Ansedo, & Bragos, 2010; Seoane, Ferreira, Sanchez, & Bragós, 2008). However, implementation of AD5933 requires an additional AFE to enable four-electrode measurements and to make the impedance range suitable for body segment measurements. To address these limitations, Analog Devices developed AD5941 integrated circuit. It combines a constant voltage source to stimulate the tissue, a current meter and voltmeter to perform bioimpedance measurements directly with four electrodes without the need for additional circuitry. The AD5941 bioimpedance instrumentation block diagram is shown in Figure 2.32. Figure 2.32 shows discrete isolation capacitors (C_{ISO1} , C_{ISO2} , C_{ISO3} , and C_{ISO4}) that ensure there is no DC voltage across the body. R_{LIMIT} limits the current supplied to the sensor to comply with the IEC 60601 standard. The resistances of the electrodes connected to the unknown impedance are represented by $R_{ACCESSx}$.

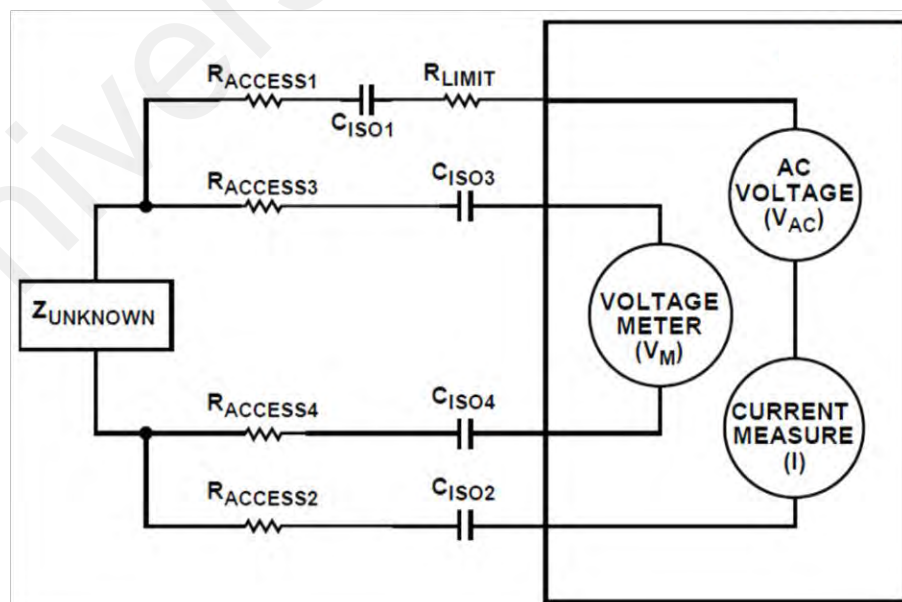


Figure 2.32: AD5941 bioimpedance instrumentation block diagram

Tonello *et al.* (2023) conducted a body hydration monitoring study using BIA instrumentation systems. The system uses limiting series resistor and isolation capacitors to comply with IEC60601. The resistor permits a controlled amount of current to flow through the body, while the capacitor functions to prevent any direct current (DC) from entering the human body. The hardware configuration of the system is presented in Figure 2.33. The operation of AD5941 involves applying an AC voltage source to stimulate the tissue with a known AC voltage. This signal generates a current through the body and is subsequently detected by transimpedance amplifier (TIA). The unknown bioimpedance of the tissue is determined by analysing the known excitation voltage signal and the measured voltage output from the TIA. The initial validation of the system aimed to detect various hydration conditions by focusing on the resistive component of the impedance. The preliminary tests performed on two subjects have shown significant differences thus confirming the possibility of the proposed system to discriminate different levels of hydration (Tonello *et al.*, 2023).

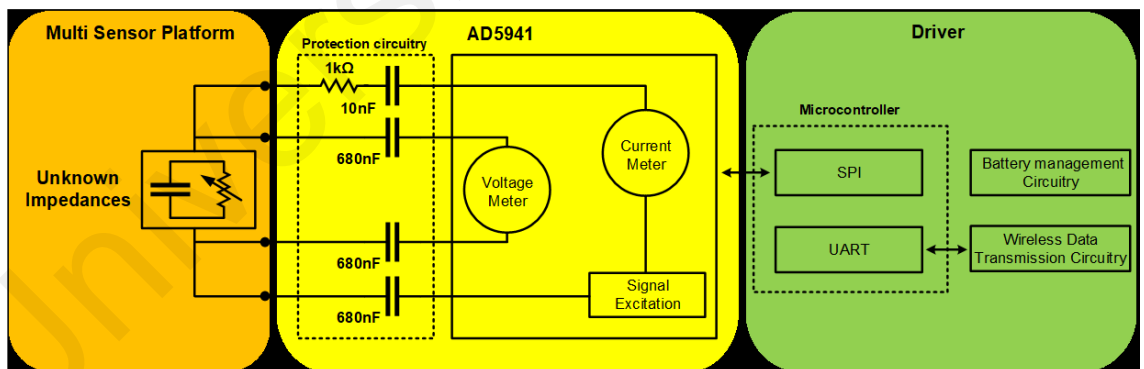


Figure 2.33: BIA instrumentation hardware block diagram by Tonello *et al.* (2023)

Scagliusi *et al.* (2023) uses the AD5941 in the development of bioimpedance measurement system to monitor heart failure. The AD5941 sensor is utilized for bioimpedance spectroscopy from 1 to 200 kHz. This setup involves a four-electrode configuration integrated with isolating capacitors and limiting resistors to adhere to the

IEC60601 standard. The magnitude and phase angle of the bioimpedance measurement are transmitted to the microcontroller using the SPI protocol. A comparison was made with the commercial SFB7 to evaluate the precision of the prototype system's bioimpedance measurements. A 100-point logarithmic frequency sweep was conducted from 3 kHz to 200 kHz. The results demonstrated similar bioimpedance measurement with average offset of only 10 Ω in the resistance value (Scagliusi et al., 2023).

2.7.1 Testing and Validation

Bioimpedance spectroscopy system designs performance have been tested and validated using passive loads as a model for human tissue and biological phantom prior direct measurement on human body. Designs malfunction and artifacts can cause high risk and considered unsafe for users (Khalil, Dali, Mohktar, & Ibrahim, 2014).

Passive loads utilities resistor-capacitor (R-C) mesh modules in various configurations to depict the electrical properties of biological tissues. Lee *et al.* conducted bioimpedance spectroscopy design validation on 49 different combinations of passive loads values in the range of 22 to 43 Ω for resistors and 22 to 49 nF for capacitor. The results are fitted to a Cole – Cole plot and compared with reference system (Lee et al., 2013).

Study by Santoso *et al.* verified the performance of the developed BIS system using a parallel RC circuits and liquid solution. The parallel RC circuit represents electrical model of biological tissues with resistor value fixed at 5.6k Ω and the capacitors values set at different values (1 nF, 10 nF, 33nF, and 47 nF). Results of the parallel RC experiment is compared with Precision LCR meter ST2830. The second experiment uses mixture of mineral water and milk in different combination of concentrations. Mixture of liquid solutions were used to illustrate human body composition. The results are presented in Nyquist plot (Santoso et al., 2020).

Another biological phantom to validate bioimpedance analyser reliability was proposed by Khalil *et al.* This investigation verifies the ability of a multiple frequency bioimpedance analyser to measure the change in fat and fluid content in a phantom model. The biological phantom was constructed using fresh cucumbers filled with a mixture of varying percentages of oil and saline fluid (Khalil, Dali, et al., 2014).

2.8 Bioelectrical Impedance Portable Application

At present, BIA portable devices are being used extensively for early detection and monitoring of diseases (B. Ibrahim, Hall, & Jafari, 2017). The advancements in micro-electronics and chip design have enabled the development of portable BIA monitoring systems. Miniaturized BIS systems are able to produce similar frequency range for current injection as commercially available benchtop devices (Lindeboom et al., 2021).

Yang *et al.* (2006) developed a portable BIA systems weighted 0.5 kg and size of portable multimeter with frequency range from 20 kHz to 1MHz and impedance magnitude resolution of 0.36Ω (Yang, Wang, Yu, Niu, & He, 2006). Lee *et al.* (2013) presented a low-power, wireless and compact size (4.8 cm x 3 cm x 2 cm) wearable BIS system for continuous monitoring applications (Lee et al., 2013). Ibrahim *et al.* (2017) demonstrated a wearable BIS device for continuous monitoring of physiological signals. The system is able to measure small bioimpedance in the range of 1 – 120 Ω at the upper arm with RMSE of 0.07Ω using frequencies from 4 kHz to 120 kHz (B. Ibrahim et al., 2017).

Hegarty-Craver *et al.* has designed a wearable BIA system (Figure 2.34) for continuous monitoring of fluid distribution in lower limbs. The system applied frequencies ranging from 10 – 100 kHz (Hegarty-Craver, Grant, & Reid, 2015). In 2019, Mabrouk *et al.* (2019) developed a portable BIA system to assess ankle oedema in acute ankle injuries throughout the course of rehabilitation. The developed BIA system

provides extra information regarding ankle readiness to perform activities and personalized rehabilitation course (Mabrouk et al., 2019).

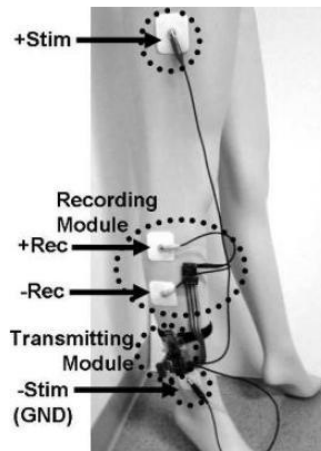


Figure 2.34: Prototype of the portable and wearable BIA system (Hegarty-Craver et al., 2015)

2.9 Smartphone Application

In a study conducted by Krzesinski *et al.* (2021), a novel integration of BIA system with smartphone application was introduced for the remote monitoring of heart failure patients in a home-based setting. The proposed system is shown in Figure 2.35. The developed system represents a significant contribution to the complex system of care for patient with heart failure (Krzesinski et al., 2021).

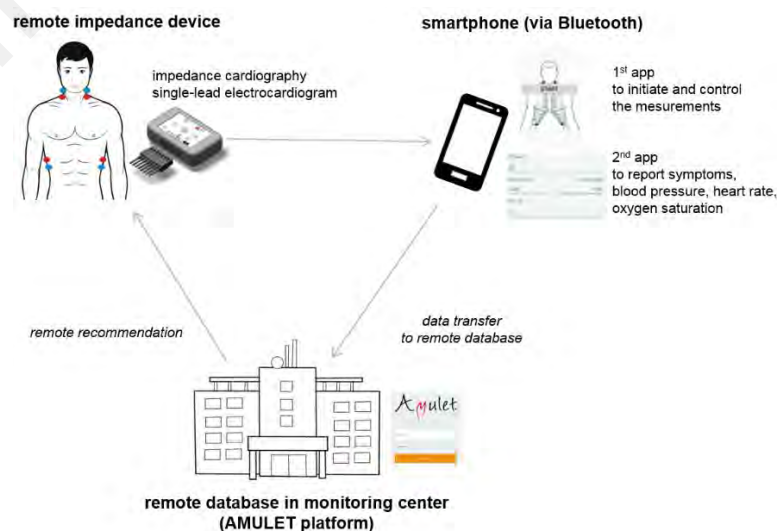


Figure 2.35: BIA system and smartphone application by Krzesinski *et al.* (2021)

A similar approach was implemented by Scagliusi *et al.* (2023) to monitor changes in body volume due to oedema in heart disease patients combining BIA with a smartphone application. The objective was to enhance remote patient monitoring at home to ensure rapid intervention in cases of worsening conditions. The BIA device collects measurements through four electrodes and transmitted the data to Android device via Bluetooth. The key components of the measurement prototype are depicted in the Figure 2.36 (Scagliusi et al., 2023).

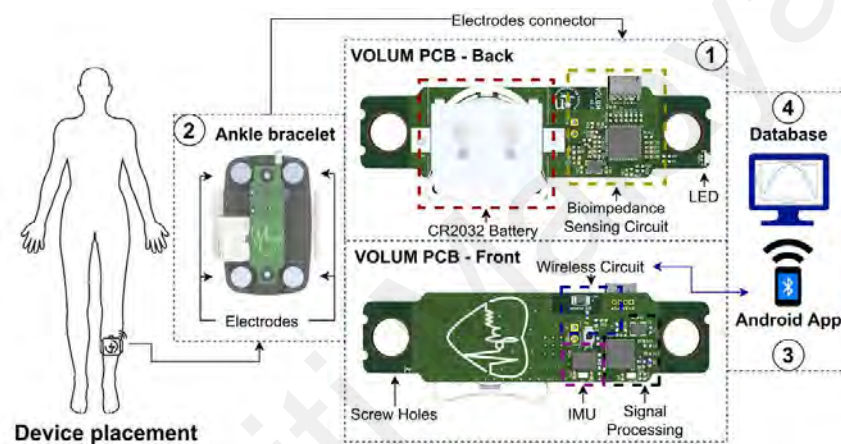


Figure 2.36: Elements of the measurement prototype for monitoring changes in body volume due to oedema by Scagliusi *et al.* (2023)

A user tongue electronic system (UTES) that comprises of BIA and user tongue smartphone application (UTAP) was developed by Luo *et al.* (2021) to assess the volume conduction properties of the tongue in neurological disorders affecting bulbar function. The UTAP connects to the UTES via Bluetooth. The functionality of UTAP as shown in Figure 2.37 is to perform tongue volume conduction properties, transfer and plot the data and transmit data to the cloud server. UTES has the potential to be performed in clinic or at home. The system aims to reduce patients visiting a study centre on a regular basis and to allow at-home measurements (Luo, Pulido, Rutkove, & Sanchez, 2021).

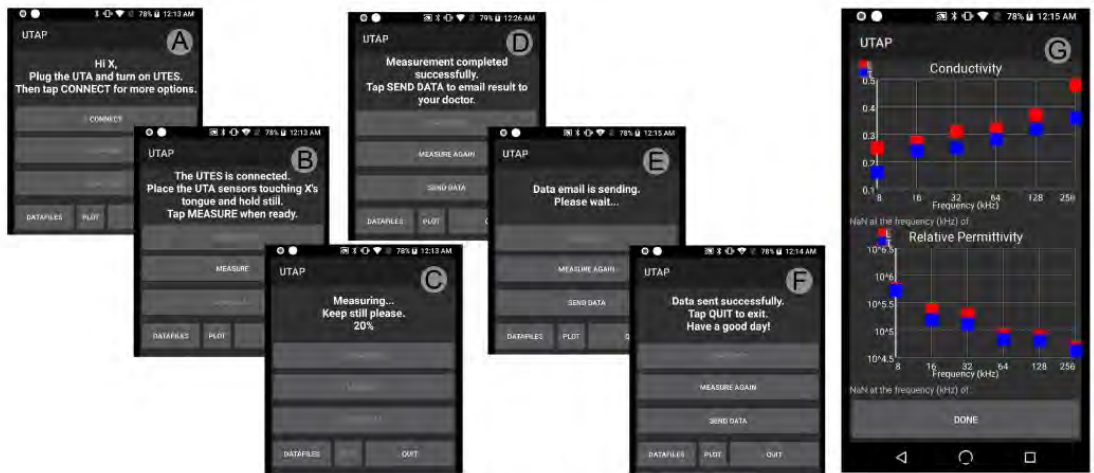


Figure 2.37: User tongue application (UTAP) developed by Luo *et al.* (2021)

Research by A. Choi *et al.* (2015) incorporates BIA system and mobile application to facilitate daily obesity management. This research focused on monitoring body fat and skeletal muscle mass. The overall process flow is shown in Figure 2.38 (A. Choi *et al.*, 2015).

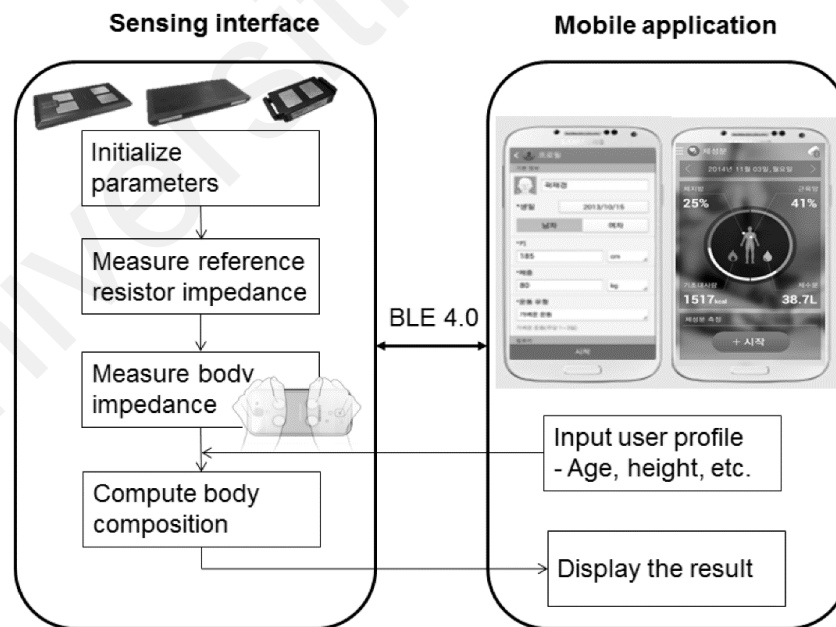


Figure 2.38: Daily obesity management system proposed by A. Choi *et al.* (2015)

2.9.1 Frameworks

Smartphone applications have become an integral part of modern life, offering a wide range of functionalities and services to users. With the increasing demand for mobile apps, developers have explored various frameworks and technologies to create applications that are both efficient and user-friendly. Two prominent frameworks for developing smartphone applications (iOS and Android) are Flutter and React Native.

Flutter is an open-source user interface (UI) software development toolkit developed by Google. It enables developers to create natively compiled applications for mobile, web, and desktop from a single codebase. Flutter uses the Dart programming language and provides a rich set of customizable widgets for building user interfaces. One of its key features is its “hot reload” capability, allowing developers to instantly see changes in the app as they code, which speeds up the development process. Flutter’s performance is noteworthy as it compiles code to native ARM code, resulting in fast execution and smooth animations. Its visually appealing and consistent UI across platform make it an attractive choice for developers.

React Native, on the other hand, is an open-source framework developed by Facebook for building native mobile applications using the React JavaScript library. It allows developers to create applications for multiple platforms using a single codebase. React Native components are directly mapped to native iOS and Android components, resulting in a native-like performance and user experience. Its "hot reloading" feature also aids in quick development iterations. React Native has a large and active community, which means extensive third-party libraries and modules are available for adding additional functionalities to applications.

The choice between Flutter and React Native depends on factors such as the target audience, project requirements, developer familiarity with programming languages, and

desired performance. Both frameworks have their advantages and drawbacks. Flutter provides a consistent UI experience and offers high-performance applications, while React Native leverages existing web development skills and has a larger community.

In recent years, smartphone applications developed using both Flutter and React Native have gained popularity due to their cross-platform capabilities and efficient development processes. These frameworks have enabled developers to create feature-rich applications that cater to various user needs and preferences.

2.10 Medical Device Standards

The development of medical devices, including both hardware and software components, is subject to regulatory standards to ensure their safety, efficacy, and quality. These standards are designed to mitigate risk associated with medical devices and ensure that they meet the necessary performance criteria. The key medical device standards applicable to the bioimpedance analyser and smartphone application developed for the diagnosis and monitoring of unilateral breast cancer-related lymphedema are reviewed in this section.

2.10.1 Medical Device Standards for Bioimpedance Analyser

2.10.1.1 ISO 13485

ISO 13485 specifies the requirements for a quality management system specifically tailored to the medical device industry. Compliance with this standard is essential for ensuring that the bioimpedance analyser is designed, manufactured, and maintained in a manner that meets regulatory requirements and ensure consistent quality.

2.10.1.2 IEC 60601

The International Electrotechnical Commission (IEC) standard IEC 60601 establishes general requirements for the safety and essential performance of medical electrical

equipment. Compliance with this standard ensures that the bioimpedance analyser is designed and manufactured to mitigate risks to patients and operators. This section focuses on two key principles related to current delivered to the human body.

(a) Current Limitation

IEC 60601-1 mandates that the patient leakage current, the current unintentionally flowing through the patient during normal operation must be less than 1 mA under normal conditions and less than 10 mA under single fault conditions. This limit prevents harmful effects like tissue stimulation and burns. For BIA devices specifically, IEC 60601-2-27: Particular requirements for the safety of medical electrical equipment for bioimpedance analysis specifies even stricter limits. Under normal operation, the patient leakage current should be less than 50 μA for frequencies below 1 kHz and less than 100 μA for frequencies above 1 kHz. This further minimizes potential risks associated with BIA measurements.

(b) Absence of Direct Current (DC)

IEC 60601-1 prohibits the presence of DC components in the patient leakage current. DC can lead to undesirable effects like polarization of tissue and accumulation of charges, potentially causing discomfort or injury. IEC 60601-2-27 emphasizes that DC component of the measurement current should be less than 10 μA under normal operation and less than 50 μA under single fault conditions.

2.10.2 Medical Device Standards for Smartphone Application

2.10.2.1 ISO 14971

ISO 14971 specifies a process for identifying and mitigating risks associated with medical devices. Compliance with this standard is essential that the smartphone application is designed and developed to minimize risks to patients and users.

2.10.2.2 IEC 62366-1

IEC 62366-1 specifies the application of usability engineering to medical devices. Compliance with this standard ensures that the smartphone application is designed with the end-user in mind, making it intuitive and easy to use.

2.10.2.3 ISO 9241-210

ISO 9241-210 provides guidance on human-centred design principles for interactive systems. Compliance with this standard ensures that the smartphone application is designed to be user-friendly and accessible to a wide range of users.

2.11 Statistical Analysis

The review section on statistical analysis within the thesis presents an in-depth exploration of various statistical methods employed for data analysis in diverse research contexts. Some of the prominent statistical methods applied are:

(a) *Student's t-test*

The Student's t-test, a foundational statistical technique, is utilized to compare means between two groups. In research, it can be harnessed to compare characteristics or measurements between distinct cohorts. The t-test unfurls the statistical significance of observed distinctions, proffering insights into potential influences on diverse parameters.

(b) *Paired t-test*

A variant of the t-test, the paired t-test, serves to evaluate means within related groups. It aids in assessing pre- and post-intervention shifts within the same entities. This methodology facilitates discerning transformations in variables such as size, levels, or other attributes before and after interventions, thereby revealing the efficacy of interventions.

(c) Analysis of Variance (ANOVA)

ANOVA, a robust statistical technique, assumes its role in comparing means across three or more groups. Applied in research, it unveils variations in characteristics or measurements across diverse stages or methods. This method discerns the statistical significance of differences and provides insights into the factors influencing those variations.

(d) Correlation Analysis

Correlation analysis probes the interrelation between multiple variables. Within research, it navigates the correlation amidst factors like age, size, and involvement. This exploration exposes potential risk factors and guides decisions.

(e) Regression Analysis

Regression analysis deciphers the interplay between a dependent variable and independent variables. In research, it forecasts outcomes grounded in variables like genetics, aiding in quantifying their influences and predicting trends.

(f) Chi-Square Test

The Chi-Square test deciphers the association between categorical variables. Within research, it dissects relationships between stages and responses. This method scrutinizes whether observed ties are statistically substantial.

(g) Logistic Regression

Logistic regression, tailored for binary dependent variables, uncovers factors impacting likelihood. In research, it identifies associations with occurrences and assembles predictive models.

(h) R-Squared (Coefficient of Determination)

R-squared quantifies the variance in a dependent variable explained by independent variables. In research, it gauges the explanatory power of selected variables, such as size, on outcomes.

By utilizing statistical methods, researchers can effectively analyse data and discover meaningful insights that push the boundaries of knowledge. The choice of method should be based on the study's design and the characteristics of the data.

2.12 Summary

Current BCRL diagnosis and monitoring tools reveals a significant gap in practicality and accessibility. Various diagnosis methods such as circumference measurement, water displacement, lymphoscintigraphy and BIA has its own advantages and limitations. Circumference measurement while practical in clinical settings, lacks reliability for early-stage detection and requires trained professionals. Water displacement method is hindered by its cumbersome process. Lymphoscintigraphy though sensitive and accurate, is impractical for regular monitoring due to high operation and the use of radiation. BIA is a reliable and sensitive tool, but existing commercial analysers are expensive and bulky limiting their use for remote monitoring settings. This review identified no specific BCRL detection threshold for the Malaysian population unlike Korea, China, United States of America and Australia.

From the literature review, BIA has been chosen as the method for diagnosing and monitoring unilateral BCRL driven by its non-invasive characteristics, along with high sensitivity and accuracy in evaluating fluid imbalances and tissue composition. BIA serves as a valuable tool in providing essential data for the early detection of unilateral BCRL, thereby facilitating timely interventions and personalized treatment plans.

The choice of utilizing BIS for frequency analysis aims to achieve a more comprehensive assessment of tissue characteristics. This frequency-based approach is well-suited for BCRL assessment, as it can provide detailed insights into the underlying changes in tissue properties.

The adoption of a segmental measurement protocol is driven by its capability to offer localized insights into fluid imbalances. Concentrating the measurements on the affected limb facilitates the identification of fluid discrepancies in the limb. This targeted approach enhances the precision and accuracy of BCRL assessment, contributing to a deeper and more comprehensive understanding of the condition.

For the development of a smartphone application, Flutter framework will be used. Flutter offers a modern and user-friendly way to interface with the bioimpedance measurement system. Through this application, patients can conveniently track and monitor changes in their condition, fostering engagement and adherence to the recommended monitoring routines. The integration of smartphone technology into the solution enhances its accessibility and usability, promoting patient empowerment and involvement in their own care.

Testing and validation of the system includes the use of passive RC components, in conjunction with an LCR meter (RS Pro LCR-6100), serves as a benchmark for validating the accuracy and reliability of the developed bioimpedance measurement system. Additionally, the comparison with the Quadscan 4000 provides a means to assess the system's performance against an established commercial solution, ensuring its capability to deliver consistent and dependable results.

Table 2.6: Summary of research components and methods for unilateral BCRL diagnosis and monitoring

Research component	Method
Unilateral BCRL diagnosis and monitoring method	BIA with BIS as frequency analysis
Measurement protocol	Segmental measurement
Smartphone application development platform	Flutter
Cole parameters estimation	Non-linear Least Squares Curve Fitting
Testing and validation	LCR meter (RS Pro LCR-6100) and Quadscan 4000

In summary, the development of a portable unilateral BCRL management system involves the strategic integration of BIA, frequency analysis using BIS, segmental measurement, smartphone application development, and testing and validation. This holistic approach aims to address the unique challenges of BCRL and provide patients with a comprehensive and effective tool for monitoring and managing their condition, ultimately improving their quality of life and healthcare outcomes.

CHAPTER 3: METHODOLOGY

3.1 Introduction

This chapter presents the research methodology that were used to develop the unilateral BCRL diagnosis and monitoring system. The chapter is divided into several sections, each of which discusses a specific aspect of the system's development. These sections include the design and development of the hardware module, the data acquisition and transmission module, the smartphone application module, the cloud server module, the firmware module, the estimation of Cole parameters and to determine unilateral upper limb lymphedema detection threshold in Malaysia women population.

The verification of device functionality is also discussed, including validation with passive loads and healthy participants, as well as statistical analysis. Finally, the clinical validation of the device is presented, including the ethics application, selection of participants, study protocol, clinical measurements, and statistical analysis.

The research methodology flowchart of this project is summarized in Figure 3.1. It provides an overview of the research process and illustrates the different stages of development for the BCRL diagnosis and monitoring system.

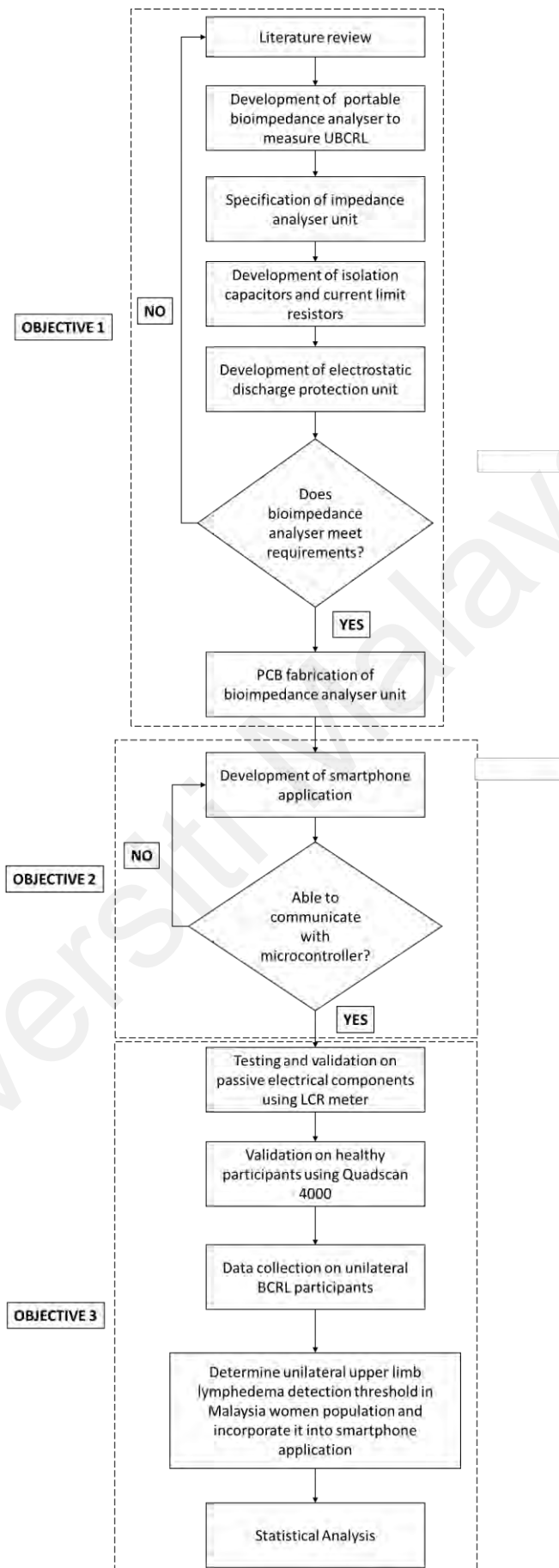


Figure 3.1: Research methodology flowchart

The system architecture as depicted in Figure 3.2 comprises several components to achieve accurate and efficient BCRL diagnosis and monitoring. The main components of the system are BCRL bioimpedance measuring device, smartphone application for control and data transfer via Bluetooth, evaluation of BCRL in Google Cloud Platform, storage of lymphedema results in Firestore database and display of results on smartphone application.



Figure 3.2: Unilateral BCRL diagnosis and monitoring system

In this research project, bioelectrical impedance analysis (BIA) is selected as a method to diagnose and monitor the extent of lymphedema. Bioimpedance analyser device development requires an impedance analyser unit, isolation capacitors, current limit and calibration resistors, calculation of high-speed TIA gain resistor, low pass filter unit, ESD protection unit, and power supply unit. A microcontroller is used to control the impedance analyser unit and for data transmission. The acquired bioimpedance value is transmitted to the smartphone via Bluetooth. The smartphone application is designed to enable the users to initiate measurement and monitor their daily lymphedema progression. BIA measurement of R_0 or extracellular fluid (ECF) volume is utilized to quantify lymphedema in BCRL patients. The estimation of Cole parameters is applied using the Non-linear Least Squares Curve Fitting method. The block diagram for the development of UBCRL diagnosis and monitoring system are represented in Figure 3.3.

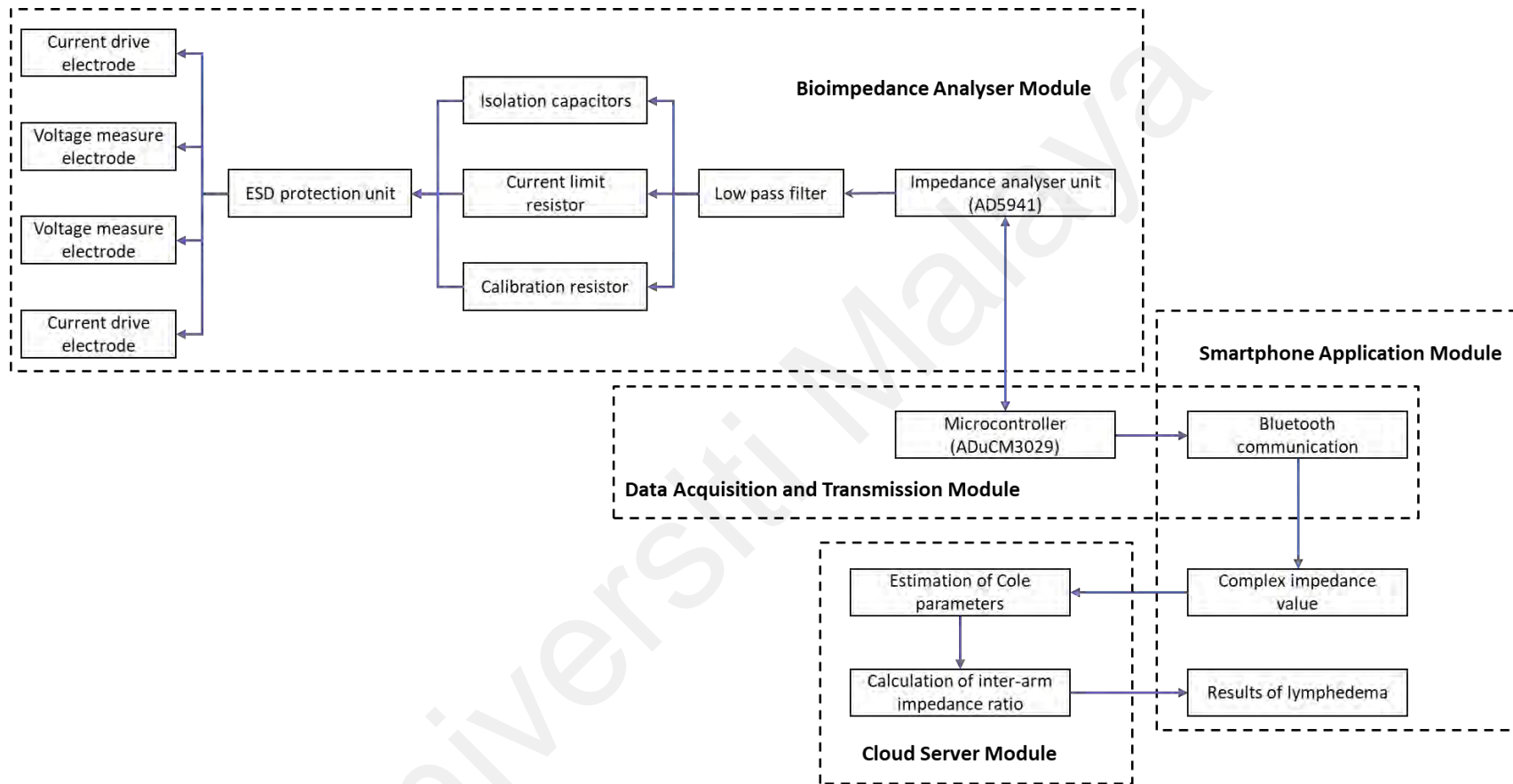


Figure 3.3: Unilateral BCRL diagnosis and monitoring system block diagram

3.2 Development of Hardware Module

The development of the hardware module for the BCRL diagnosis and monitoring system required the integration of several key components, including a microcontroller, bioimpedance analyser module, electrodes, power supply, and a 3D printed casing. These components were carefully selected and configured to ensure the accurate and reliable acquisition of bioimpedance data, which is critical for the diagnosis and ongoing monitoring of BCRL.

3.2.1 Microcontroller

The microcontroller chosen for the hardware module of the BCRL diagnosis and monitoring system was the ADuCM3029, Analog Devices, U.S.A. The firmware for the microcontroller was designed to control the bioimpedance analyser, acquire, and transmit bioimpedance data, and communicate with the smartphone application. The microcontroller was also responsible for managing the power supply.

3.2.2 Bioimpedance Analyser

Bioimpedance analyser module requires impedance analyser unit (AD5941, Analog Devices, U.S.A), isolation capacitors, current limit, and calibration resistors, and ESD protection unit. The bioimpedance analyser module block diagram is illustrated in Figure 3.4.

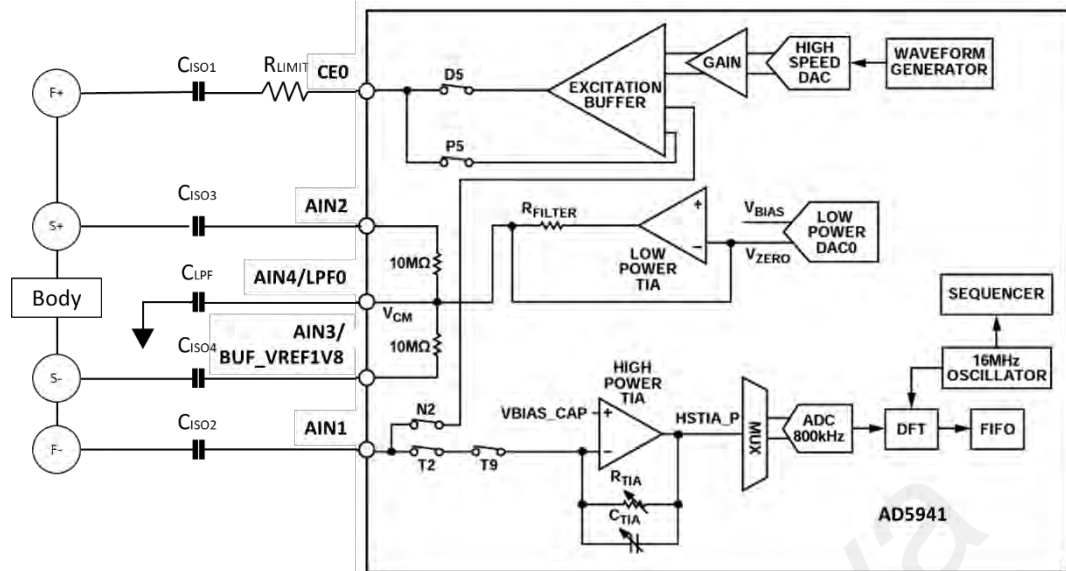


Figure 3.4: Bioimpedance analyser module block diagram

The microcontroller functions to control the impedance analyser unit and analyse the complex impedance measurement through serial peripheral interface (SPI) communication. The impedance analyser will generate current at spectrum of frequencies (5 to 200kHz) and senses bioimpedance values of 100 to 1k Ω . Isolation capacitors, current limit resistors and ESD protection are included to restrict the amount of DC and AC delivered to the human body. The electrodes act as a medium between the circuit and the human skin. The design specification for the bioimpedance analyser is represented in Table 3.1. The bioimpedance analyser schematic diagram is shown in Figure 3.5 and Figure 3.6.

Table 3.1: Bioimpedance analyser module design specifications

Parameters	Design specification
Impedance range (Ω)	100 to 1k
Frequency range (kHz)	5 to 200
Impedance percentage error (%)	0.5
Phase error (Degree)	1
Power supply (V)	3
Number of electrodes	4

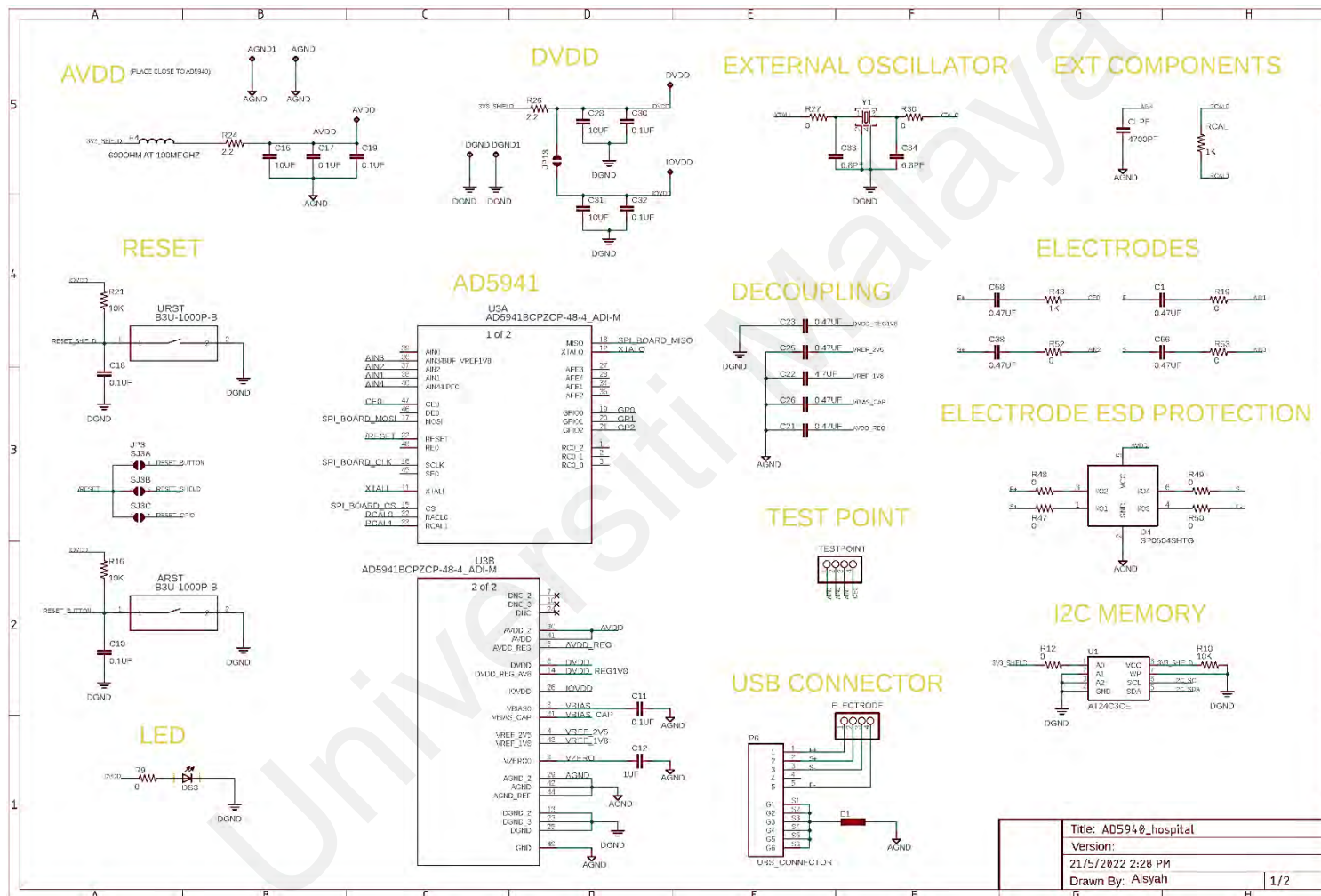


Figure 3.5: Schematic diagram of the developed bioimpedance analyser (Part 1)

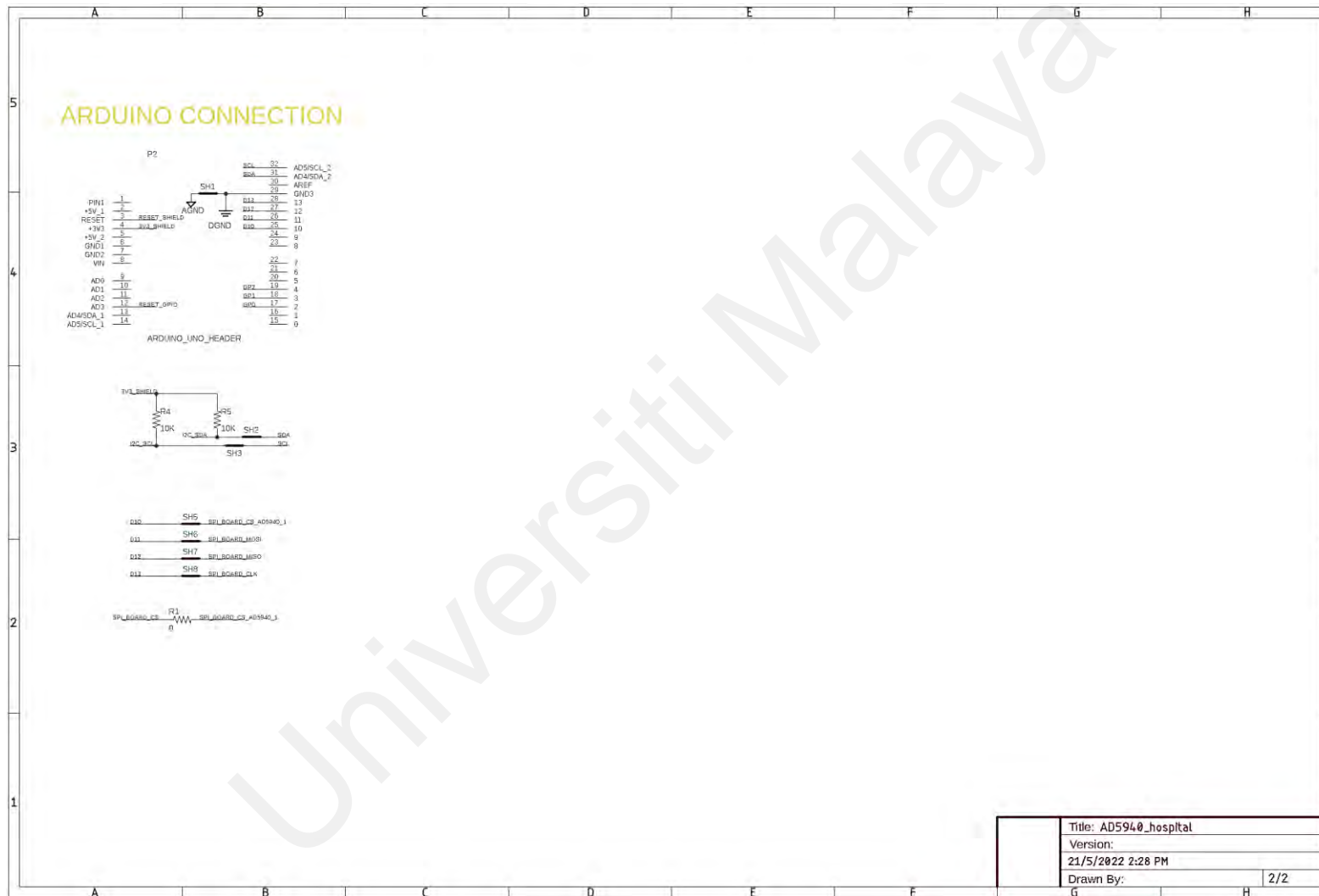


Figure 3.6: Schematic diagram of the developed bioimpedance analyser (Part 2)

3.2.2.1 Impedance Analyser Unit

The impedance analyser unit selected in this project is AD5941 by Analog Device Inc. Figure 3.7 show pin configuration of AD5941. AD5941 was used to generate current at spectrum of frequencies ranging from 5 kHz to 200 kHz. A 4-wire BIA measurement configuration was selected in this study. The impedance analyser unit was designed to measure impedance from 10 Ω to 1 k Ω .

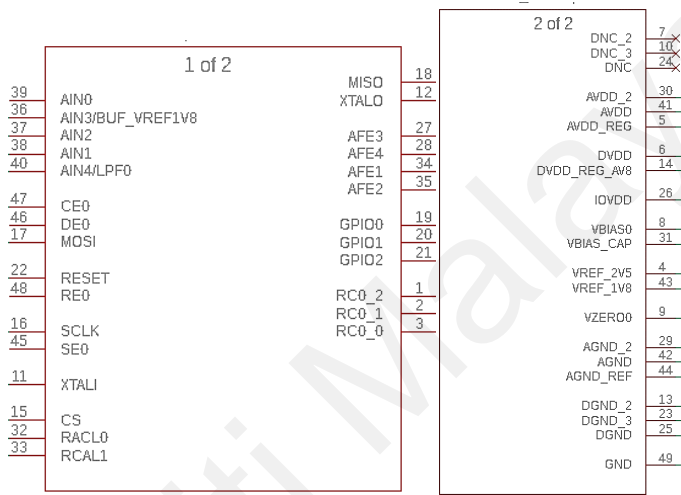


Figure 3.7: AD5941 pin configuration

(a) Excitation Signal

A sine wave excitation voltage signal of 5 kHz to 200 kHz was generated from analog output supplies (CE0 and AIN1). Programmable switch D5 in AD5941 was closed to connect the output of the excitation loop to the CE0 pin. CE0 and AIN1 pins were selected as drive electrodes (F+ and F-) to deliver electrical signals to the human body. Internal differential sense was configured by closing programmable switches P5 and N2 to connect CE0 and AIN1 back to the excitation buffer. This is to ensure the accuracy of the voltage source. The voltage amplitude (DACV_{oltp}) was set to peak to peak voltage of 800mV_{pp} with DAC gain of 1 to ensure the signal is within the ADC input range of +- 1.5V.

$$DACV_{oltp} = Voltage * Gain \quad (3-1)$$

(b) Measuring Voltage

The response current was measured and converted to voltage by a high power transimpedance amplifier (HSTIA_P) and was biased by the internal 1.11V source. The converted signal was transmitted to ADC at an 800 kSPS speed. Next, DFT was performed on ADC data at 8192 points where the real and imaginary parts of the unknown impedance are calculated and stored in the data first-in, first out (FIFO).

(c) Differential Voltage Meter

The differential voltage meter operation was designed to amplify the difference signal while rejecting common signal at the two inputs. AIN2 and AIN3/BUF_VREF1V8 were selected as sense electrodes (S+ and S-). The V_{BIAS} (1.1V) output of DAC was connected to the positive input of TIA. The output of TIA obtained was common-mode voltage (V_{CM}). V_{CM} was connected to the AIN4/LPF0 pin. A low-pass filter was created by connecting AIN4/LP0 pin to capacitor and to ground (GND).

3.2.2.2 Isolation Capacitors

Isolation capacitors were included in the development of lymphedema measurement module to ensure no DC current to flow through the human body. The isolation capacitors (C_{ISO1} , C_{ISO2} , C_{ISO3} , C_{ISO4}) selected have a capacitance value of 0.47 μ F. Such value was selected due to the sufficient capacitance value to eliminate the DC current and is also readily accessible in compact sizes that are ideal for wearable and portable electronics application. The isolation capacitors were connected to the analogue inputs (CE0, AIN1, AIN2 and AIN3) of AD5941.

3.2.2.3 Current Limit Resistor

The maximum allowable AC current entering the human body is 500 μ A at 50 kHz and 600 μ A at 60 kHz. In this design, the AC current was set at 80% of maximum allowable AC current which was 400 μ A rms. The maximum output voltage from

AD5941 is 1.2 Vp-p (0.4242 V rms). Therefore, the current limit resistor (R_{LIMIT}) was calculated based on the Equation (3 – 2).

$$R_{LIMIT}(\Omega) = \frac{\text{Maximum voltage}(V)}{\text{Maximum current}(A)} \quad (3-2)$$

$$R_{LIMIT} = \frac{0.4242 \text{ V rms}}{400 \mu A} = 1060.66 \Omega$$

As such, 1 k Ω was selected as R_{LIMIT} and was connected to CE0 in series with C_{ISO1} . The C_{ISO1} value was omitted in this calculation due to its insignificant value.

3.2.2.4 Transimpedance Amplifier Gain Resistor

The transimpedance amplifier gain resistor (R_{TIA}) was determined by calculating the minimum impedance (Z_{MIN}) and maximum current (I_{MAX}) into the transimpedance amplifier. Figure 3.8 illustrates the current flow in TIA.

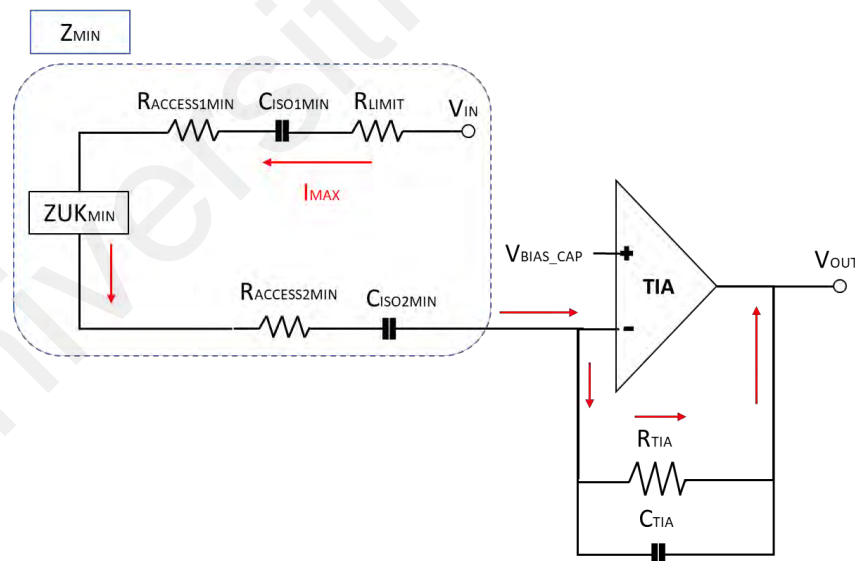


Figure 3.8: Overall current flow in transimpedance amplifier

Equation 3 - 3 was used to calculate Z_{MIN} .

$$Z_{MIN} = \sqrt{r^2 + i^2} \quad (3-3)$$

$$Z_{MIN} = \sqrt{(R_{LIMIT} + R_{ACCESS1MIN} + ZUK_{MIN} + R_{ACCESS2MIN})^2 + (XC_{ISO1MIN} + XC_{ISO2MIN})^2}$$

Where,

Z_{MIN} is the minimum impedance,

$R_{ACCESS1MIN}$ and $R_{ACCESS2MIN}$ represent resistances in lead connecting the sensor and are assumed to be 0 Ω ,

ZUK_{MIN} is the minimum unknown impedance. Assumed to be 50 Ω in this equation and

$XC_{ISO1MIN}$ and $XC_{ISO2MIN}$ are 1.693 Ω at 200 kHz.

Solving the equation equates Z_{MIN} to 1.05 k Ω .

The maximum output voltage from the DAC is 600 mV peak. Thus, Equation 3 - 4 was utilized to calculate I_{MAX} into the transimpedance amplifier.

$$I_{MAX}(A) = \frac{Max_{DAC}(V)}{Z_{MIN}} \quad (3-4)$$

Solving the equation gives I_{MAX} value of 571 μA .

The maximum peak voltage that is within ADC range is 900 mV peak. Therefore, R_{TIA} obtained is

$$R_{TIA} = \frac{900 \text{ mV}}{571 \mu A} = 1.58 \text{ k}\Omega$$

Since there is no 1.58 k Ω R_{TIA} on AD5941, 1 k Ω was selected as R_{TIA} .

3.2.2.5 Calibration Resistor

Calibration resistor (R_{CAL}) was used in conjunction with the high-speed DAC and excitation amplifier to generate accurate currents. R_{CAL} functions to calibrate the TIA gain resistor. The R_{CAL} value was selected to a value that was approximately equivalent to R_{TIA} to achieve optimum condition. Therefore, R_{CAL} selected was 1 k Ω with 0.1 % tolerance. R_{CAL} was connected between R_{CAL0} and R_{CAL1} pin of the AD5941 chip.

3.2.2.6 Electrostatic Discharge Protection Unit

Electrostatic discharge protection unit was included in this design to protect user and product from the effects of an accidental discharge. SP0504S chip was selected to protect drive and sense electrodes channels. The 4 channels input, and output were connected to F^+ , F^- , S^+ and S^- .

3.2.3 Power Supply Unit

The bioimpedance detection module was designed to be operated by 3V battery. The 3V battery was connected to two units of Step-Up DC/DC converters (LTC3528) to produce 3.3V and 5V. 3V was used to power AD5941 analog supply (AVDD), digital supply (DVDD) and input output supply (IOVDD). To supply AVDD, the 3.3V was connected to bead ferrites (600 Ω at 100MHz) to prevent electromagnetic interference. All AD5941 power supplies were connected with decoupling capacitors to prevent voltage spikes and ensure only DC signal passed through.

3.2.4 Electrodes

Tetrapolar electrodes configuration was applied in this study to measure bioimpedance. Silver/silver chloride (Ag/AgCl) gel electrode was selected as an interface between the hardware module and human body.

3.3 Development of Software Module

The development of the software module involved several key components to create a comprehensive and functional system. This section outlines the step-by-step process for each component: development of a smartphone application, design of a firmware module, creation of a cloud server module, and the estimation of Cole parameters.

3.3.1 Development of Smartphone Application Module

The development of smartphone application module involves the design of user interface (UI) to communicate with lymphedema sensor via Bluetooth, to diagnose and monitor the lymphedema progression and to communicate with cloud server for signal processing through application programming interfaces (APIs).

Flutter open-source software framework was selected to develop cross-platform smartphone application for Android and iOS. The mobile software framework was developed in Android Studio integrated development environment (IDE).

The smartphone application was designed to initiate bioimpedance measurement and to receive bioimpedance data from the sensor. Next, the bioimpedance data were sent to the cloud server for analysis. The analysed data were then sent to smartphone application to diagnose and monitor the lymphedema progression. The smartphone application operation flowchart is illustrated in Figure 3.9.

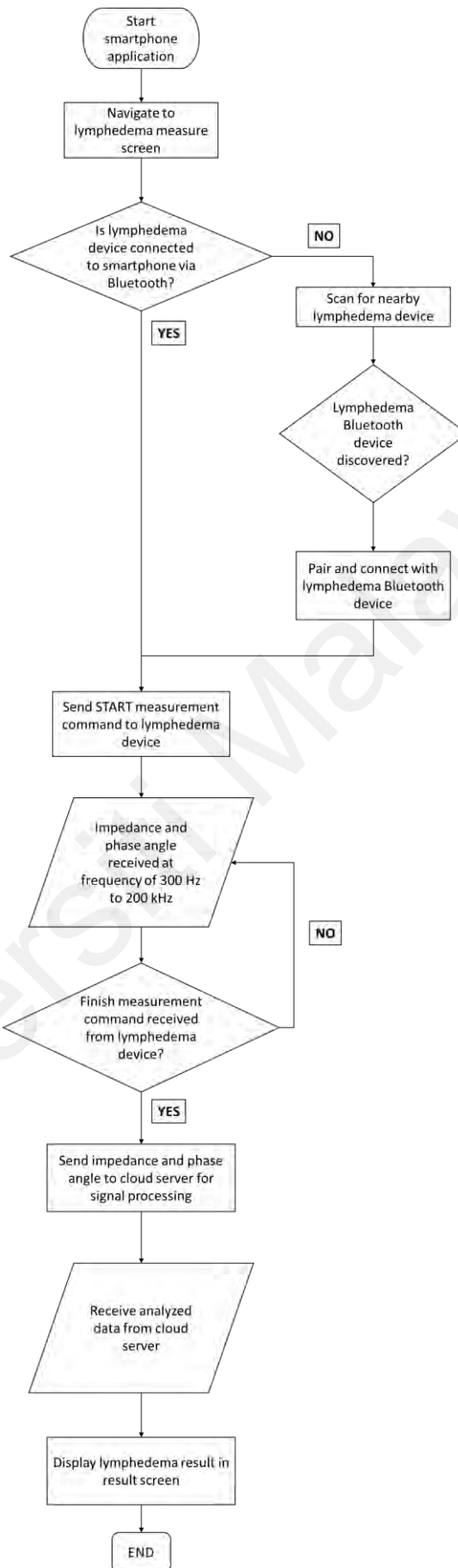


Figure 3.9: Smartphone application operation flowchart

3.3.2 Development of Firmware Module

ADuCM3029 and AD591 firmware were developed in Keil μ Vision IDE. First, initialization of ADuCM3029 and AD5941 resources and configuration. Next, UART communication was set to a baud rate of 230400. This UART communication was established to transmit and receive message between firmware and smartphone application. Then, the system waited for the start measurement command from the smartphone application. Frequency sweeps start after the measurement command is received. The DFT data were processed to obtain the magnitude and phase of the impedance at each frequency or bioimpedance spectroscopy. The bioimpedance spectroscopy data obtained were sent to smartphone application for signal processing. ADuCM3029 sent a message to the smartphone application after the frequency sweep had finished. The ADuCM3029 and AD5941 firmware flowchart is illustrated in Figure 3.10.

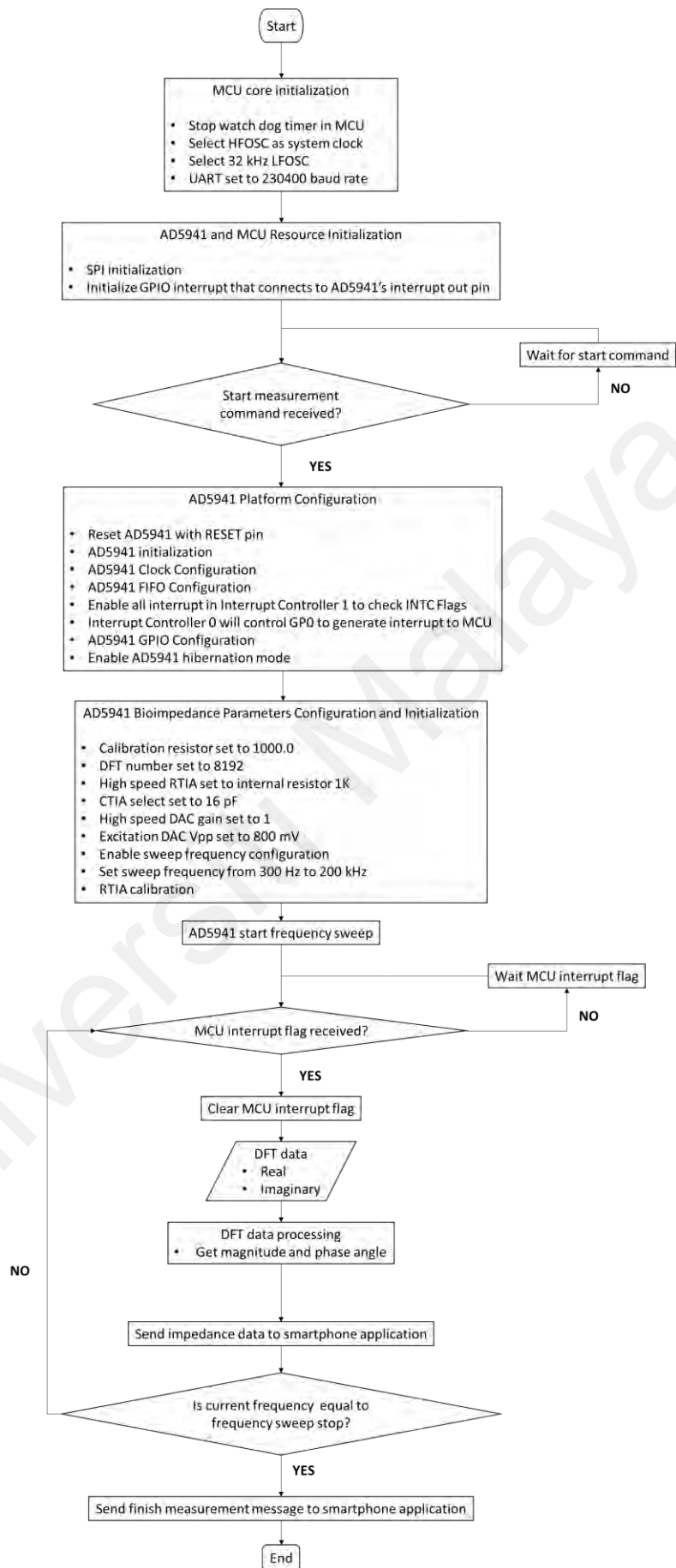


Figure 3.10: ADuCM3029 and AD5941 firmware flowchart

3.3.3 Development of Cloud Server Module

In this study, cloud server was applied to store user data and to perform signal processing. Firebase cloud platform was applied due to its functionalities which are Firestore Database and Cloud Functions.

User's lymphedema measurements were stored in Firestore Database. The HTTP Cloud Functions was selected. The programming language runtime applied in this function was Python 3.10. The signal processing function was deployed to the server once completed. The deployed function was triggered through an HTTPS requests sent from mobile application.

3.3.4 Estimation of Cole Parameters

In this study, the bioimpedance spectroscopy (BIS) measured data were processed to obtain resistance to the current flow at zero frequency (R_0) and infinite frequency (R_∞). BIS measured data were fitted based on Cole modelling using Non-linear Least Squares (NLLS) fitting. The NLLS fit method was performed on Cole resistance model according to Equation 2 – 14, using the frequency as independent variable for estimating the Cole parameters (R_0 , R_∞ , α , τ) as the model coefficients. Figure 3.11 illustrates the BIS data processing flowchart to obtain the Cole parameters.

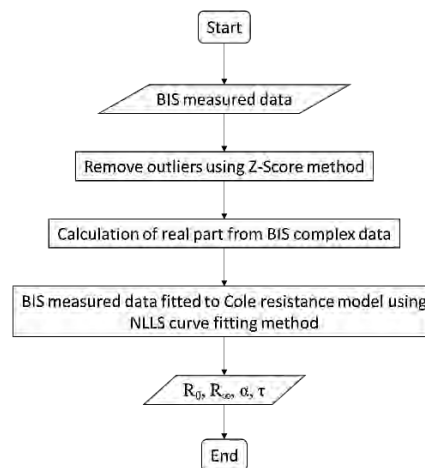


Figure 3.11: Bioimpedance spectroscopy data processing flowchart

3.4 System Integration and Data Acquisition

The development of lymphedema data acquisition and transmission module involved microcontroller and Bluetooth module. Microcontroller was used to control and acquire bioimpedance data from AD5941 through SPI interface. Bluetooth module was applied to wirelessly transmit the acquired bioimpedance data to smartphones.

3.4.1 Microcontroller

ADuCM3029 microcontroller (master) was used to control AD5941 (slave). Communication protocol between AD5941 and ADuCM3029 was established using the SPI. Master In Slave Out (MISO) (pin 18) and Master Out Slave In (MOSI) (pin 17) of AD5941 was connected to MOSI_A and MISO_A of ADuCM3029 respectively. The AD5941 measurement blocks was controlled via direct register writes through the SPI interface. Measurement commands were stored in the command FIFO and the measurement results were stored in the data FIFO.

The measured bioimpedance data were transmitted via universal asynchronous receiver-transmitter (UART) interface at baud rate of 230400. The ADuCM3029 transmit serial data (TXD) and receive serial data (RXD) lines were connected to RXD and TXD of the Bluetooth module respectively.

3.4.2 Bluetooth

nRF52840 Bluetooth Low Energy (BLE) module was used in this project as a wireless data transmission medium between the microcontroller and smartphone. 5V power and AGND of the ADuCM3029 were connected to VCC and GND of nRF52840 accordingly. Transmitter (TXD) and receiver (RXD) pins of nRF52840 was connected to RXD and TXD of ADuCM3029 respectively for serial communication.

The process of initializing the nRF52840 Bluetooth module and establishing a connection between the module and the target smartphone device was performed. This was done by scanning for nearby devices and identifying the target smartphone device. Once the smartphone device was identified, a connection between the nRF52840 Bluetooth and the target device was established.

After the devices are connected, the serial data transmitted and received at the nRF52840 was sent to and received from the smartphone application using nRF52840 BLEUART. The process flowchart for the Bluetooth module is presented in Figure 3.12.

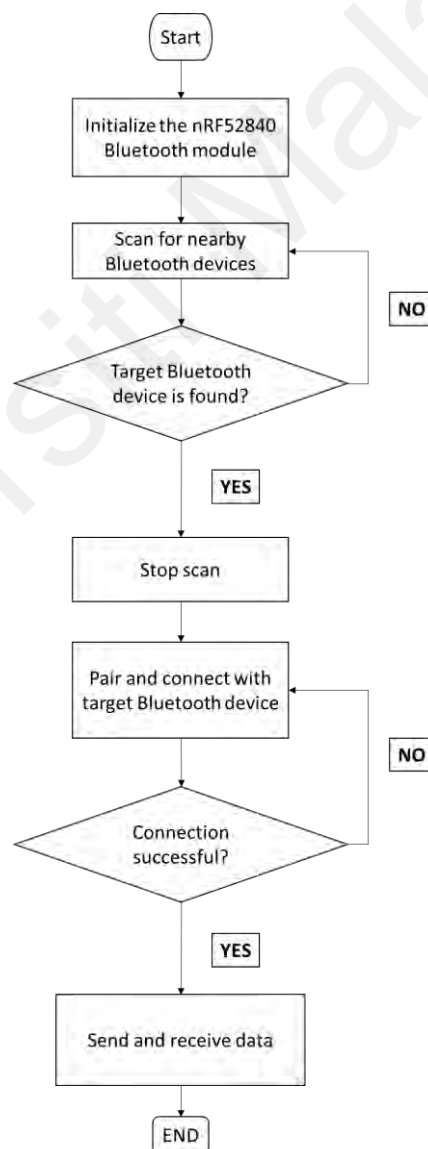


Figure 3.12: Bluetooth process flowchart

3.5 Testing and Validation of the Unilateral BCRL System

In this study, the device functionality was verified using passive loads. This involved measuring the device to various passive loads and comparing the resulting performance to LCR meter (RS Pro LCR-6100) as a reference value.

In addition to passive load testing, the device's bioimpedance measurement performance was also evaluated against commercial bioimpedance analyser, Quadscan 4000. This is to determine the relative performance of the device with existing bioimpedance analyser.

3.5.1 Testing and Validation with Passive Loads

There were two methods conducted to validate the device with passive loads. The device impedance measurement performance was verified with LCR meter as a reference device. The first method was to verify impedance and phase angle measurement performance on resistors and capacitors. This involved applying known resistive and capacitive loads to device and measuring the resulting performance to ensure that it was able to accurately measure these values and comparable with existing impedance analyser.

The second method involved using resistors and capacitors as a model for human tissue. This method involved the creation of a model for human tissue using combination of passive loads. The device was then used to measure the impedance of this model to verify its performance in measuring values that mimic those found in the human body.

The drive (F^+) and sense (S^+) electrode was connected to one side of impedance point and F^- and S^- to the opposite side of the point. Figure 3.13 shows the connection of electrodes to the impedance under measure (Z_{uk}).

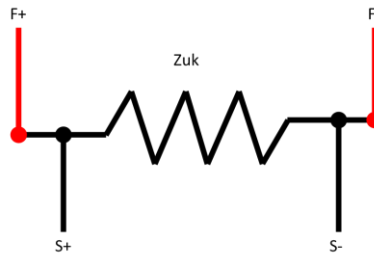


Figure 3.13: Electrodes connection to the impedance under measure

3.5.1.1 Resistors

A set of resistors were measured using LCR meter to check the accuracy for all impedance and frequency range. The impedance measured were taken as a reference value and compared with the developed device. The impedance measurements were repeated 10 times to obtain the device's precision and standard deviation. In this experimental study, the parameters listed Table 3.2 in were used.

Table 3.2: Resistors experimental parameters

Parameters	Value
Device	Developed device, LCR meter
Voltage (V)	800 mVpp
Frequency (kHz)	5, 50, 100, 200
Resistors (Ω)	100, 300, 500, 700, 1 k Ω

3.5.1.2 Capacitors

A set of capacitors were measured using LCR meter to check the accuracy for all phase angles and frequency range. The phase angles measured were taken as reference value and compared with the developed device. The phase angle measurements were repeated 10 times to obtain the device's precision and standard deviation. In this experimental study, the parameters listed in Table 3.3 were used to perform these measurements on capacitors.

Table 3.3: Capacitors experimental parameters

Parameters	Value
Device	Developed device, LCR meter
Voltage (V)	800 mVpp
Frequency (kHz)	5, 50, 100, 200
Capacitors (uF)	0.01, 0.001

3.5.1.3 Electrical Circuit Model of Human Upper Arm

The combination of passive loads was connected according to Figure 2.21. In this validation test, 3 different combinations of resistors and capacitors values in the range of 150 to 500 Ω for R_0 and R_∞ and 0.01 μF for membrane capacitance (C_m) were chosen. The values of R_0 , R_∞ , and C_m were chosen to represent the bioimpedance values of the upper limb tissue in healthy and lymphedema-affected individuals. The model tissues passive load values were chosen based on studies by Santoso *et al.* and Zhuang *et al.* (Santoso et al., 2020; Zhuang et al., 2022). The impedance measurements were repeated 3 times to obtain the device's precision and standard deviation. The combinations of load values were listed in Table 3.4.

Table 3.4: Human upper arm model using different combinations of passive loads

Human Tissue model	R_0 (Ω)	R_∞ (Ω)	C_m (μF)
1	150	100	0.01
2	300	100	0.01
3	500	100	0.01

The human tissue model was measured using LCR meter at 800 mVpp, frequency of 20 Hz, 100 Hz, 300 Hz, 500 Hz, 1 kHz, 3 kHz, 5kHz, 10 kHz, 50 kHz, 100 kHz, 150 kHz, 200 kHz, 300 kHz, 500 kHz and 1 MHz. The resulting impedance measurements were set as a reference value. Next, the developed device was used to measure the human tissue

model at frequency sweep of 300 Hz to 200 kHz. The results were processed and analysed to extract R_0 and R_∞ parameters. The parameters were then compared with those from the reference value using Root Mean Square (RMSE). R – squared statistical analysis was employed to determine the ability of NLLS to fit the resistance estimation model. The Impedance plane or Cole – Cole plot was plotted to evaluate the frequencies response on the human tissue models.

3.5.2 Validation with Healthy Participants

The bioimpedance measurement of the developed device was validated against the commercial bioimpedance analyser Quadscan 4000. The bioimpedance of the healthy participants' arms was measured at the frequency of 5 kHz, 50 kHz, 100 kHz, and 200 kHz. The measurements were collected first using Quadscan 4000. Participants were then measured using the developed device after an interval of 5 minutes. The values of bioimpedance measurements taken from healthy arms using the Quadscan 4000 and the developed device were compared using a paired *t*-test.

3.5.3 Clinical Validation

There were several steps involved in the clinical validation process, including ethics application, selection of a participant, establishment of study protocols, and statistical analysis.

3.5.3.1 Ethics Application

Ethics was applied at Medical Research Ethics Committee, University of Malaya Medical Centre (UMMC) to perform clinical validation on UMMC breast cancer patients.

3.5.3.2 Selection of Participant

Two groups of volunteered women were recruited in this study. Healthy group ($n = 45$) and unilateral breast cancer (UBC) patients ($n = 100$) who were receiving

lymphedema treatment at the outpatient clinic of the UMMC. The criteria below were followed in the selection process.

(a) Healthy Participants Selection Criteria

Healthy participants will be recruited according to the following selection criteria:

i Inclusion Criteria

- Participants aged 18 years and above

ii Exclusion Criteria

- Participants with upper limb abnormality
- Participants diagnosed with breast cancer or lymphedema
- Participants that have water retention in any parts of upper limb
- Participants with implantable device (cardiac implantable electronic device such as cardiac pacemaker or defibrillator; artificial joints, pins, plates, or other types of metal objects in their body)

(b) Unilateral Breast Cancer Participants Selection Criteria

UBC participants will be recruited according to the following selection criteria:

i Inclusion criteria

- Participants aged 18 years and above
- Participants diagnosed with breast cancer and Stage 0, 1 and 2 unilateral BCRL.

ii Exclusion criteria

- Participants diagnosed with bilateral BCRL.

- Participants with implantable device (cardiac implantable electronic device such as cardiac pacemaker or defibrillator; artificial joints, pins, plates, or other types of metal objects in their body)

3.5.3.3 Study Protocol

In order to obtain a standardized bioimpedance assessment, participants were asked to abstain from exercise, caffeine, alcohol, and meals 4 hours prior to the measurement. All jewellery was removed and the skin at the electrode sites was cleaned with an alcohol wipe before Ag-AgCl electrodes placement.

The measurement electrodes were placed at the mid-wrist of the ulnar styloid and the head of the humerus. The drive electrodes were positioned 5 cm distal to the measurement electrodes (Kyle et al., 2004b). The electrodes placement was chosen in preference to the standard shoulder to wrist sites (BH Cornish et al., 2000). The shoulder of the participants was flexed to 90 degrees with forearm pronated, wrist in neutral, and fingers extended as shown in Figure 3.14.



Figure 3.14: Electrode placement on the participant

3.5.3.4 Clinical Measurements

Clinical lymphedema measurements were conducted on UBC participants using a measuring tape and the developed device. Clinical assessments and classification of lymphedema were performed by trained UMMC physiotherapists. The classification of lymphedema is based on the physical examination and comparison of the circumferential upper limb volume. The classification of lymphedema stages was based on Section 0.

Stage 0 exists after surgery or radiation due to a damaged lymphatic system. Stage 1 UBC participants was characterized with circumferential inter-arm volume differences of 2 cm to 3 cm. In Stage 2, UBC participants was presented with circumferential inter-arm volume differences of 3 cm to 5 cm.

The developed device was used to measure the bioimpedance of healthy and UBC participants' arms. The inter-arm bioimpedance ratios were evaluated and statistically analysed.

Independent *t*-test was applied to determine the significant difference of inter-arm ratios between participants in healthy and Stage 0, healthy and Stage 1, Stage 0 and Stage 1, and Stage 1 and Stage 2.

3.5.4 Determination of Unilateral Upper Limb Lymphedema Detection Threshold

The diagnosis and monitoring of lymphedema in the upper limb were developed by quantifying R_0 ratio. R_0 ratio was calculated by comparing R_0 measured from the unaffected and affected upper limbs using Equation 2 -17. The lymphedema detection threshold was set at 2 standard deviations (SD) above the mean ratio in a healthy population.

The normative upper limbs ratio was established by comparing R_0 measured from non – dominant and dominant limbs. The diagnosis of lymphedema is made by comparing the R_0 ratio against normative inter-limb ratio using non - dominant arm as the numerator when dominant limb is at risk and dominant arm as the numerator when non – dominant arm is at risk.

Lymphedema progression can be monitored by measuring R_0 ratio value pre–surgery and during ongoing post-surgery breast cancer treatment. The pre-surgery R_0 ratio was

used a reference value. A R_0 ratio value greater than 2 SD (as determined from healthy population) from the reference value was deemed predictive of the onset of lymphedema.

Universiti Malaya

CHAPTER 4: RESULTS & DISCUSSION

4.1 Introduction

This chapter presents the result of the development and verification of a unilateral breast cancer-related lymphedema (BCRL) diagnosis and monitoring system. The hardware module, data acquisition and transmission module, smartphone application module, cloud server module, firmware module, and bioimpedance spectroscopy data processing results are presented. The functionality of the device is verified through validation with passive loads and healthy participants, and the clinical validation of the device is presented, including the ethics application, selection of participants. The results of clinical measurements and the development of the lymphedema detection thresholds are also explained and discussed.

In this section, the development of the hardware, software, and data processing components of the unilateral BCRL diagnosis and monitoring system is described. This includes the design and development of the hardware module, data acquisition and transmission module, smartphone application module, cloud server module, firmware module, and estimation of Cole parameters.

4.2 Development of Hardware Module

The design and development of the hardware module of the BCRL diagnosis and monitoring system involved microcontroller, bioimpedance analyser, electrodes, and 3D printed casing.

4.2.1 Microcontroller

The ADuCM3029 is a low-power, high-performance device that combines an Arm Cortex-M3 processor with a variety of analogue and digital peripherals. It was selected for its data processing ability, as well as its compact size and low power consumption, which are important considerations for a portable device. The ADuCM3029 was

programmed using C++ and the accompanying software development kit (SDK) provided by Analog Devices. Overall, the ADuCM3029 played a central role in the hardware module, providing the necessary powering power and control for the BCRL diagnosis and monitoring system.

4.2.2 Bioimpedance analyser

Bioimpedance analyser module involved the design of a schematic circuit diagram in EAGLE software and the subsequent fabrication of a printed circuit board (PCB). The board diagram is as shown in **Error! Reference source not found..** The schematic design diagram was then fabricated as shown in Figure 4.2.

The PCB size is 66.4 x 55.9 mm and has a thickness of 1.6 mm. The PCB is a two-layer board and was fabricated using standard PCB manufacturing techniques. The cost per board was approximately RM 150. The layout of the PCB was carefully designed to ensure that the module was compact, lightweight, and easy to use.

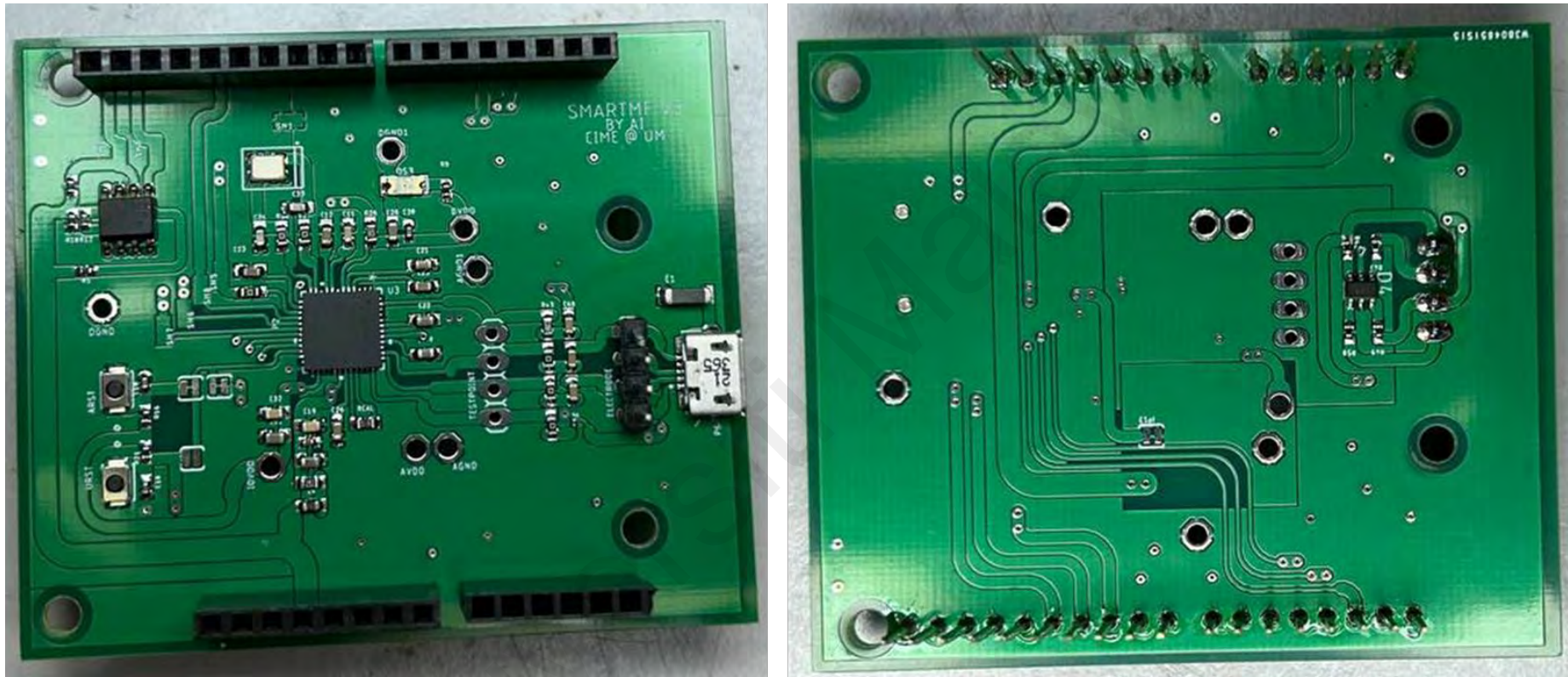


Figure 4.2: Hardware module PCB

4.2.3 Power Supply Unit

The power supply unit of the BCRL diagnosis and monitoring system is an integral part of the hardware module and is responsible for providing stable and reliable power to the other components of the system. To achieve this, an alkaline battery was used as the primary power source, which was able to provide a stable voltage of 3V.

The design of the power supply unit was carefully considered to ensure that it was able to meet the power requirements of the system, while also being compact and portable. The use of an alkaline battery allowed for a simple and cost-effective solution, while also providing a long lifespan and consistent performance.

4.2.4 Electrodes

The electrodes of the BCRL diagnosis and monitoring system are an essential component of the hardware module. To ensure reliable and accurate measurements, Ag/AgCl gel electrodes were used, which are well-suited for bioimpedance measurement applications due to their low contact skin-electrode impedance and high stability (Kusche et al., 2018).

The electrodes were connected to the rest of the hardware module using snap connectors as shown in Figure 4.3. Table 4.1 details the name and colour mapping for the bioimpedance electrodes cables. The use of snap connectors allowed for a quick and easy connection, while also ensuring a secure and reliable connection.



Figure 4.3: Bioimpedance electrodes cables

Table 4.1: Electrode name and colour mapping

Electrode Name	Colour
Drive positive (F+)	Red
Sense positive (S+)	Green
Sense negative (S-)	Blue
Drive negative (F-)	Black

4.2.5 3D Casing

The 3D casing was designed using AutoDesk Inventor and was then 3D printed using PLA filament. The design of the casing is as shown in Figure 4.4 and Figure 4.5. The 3D printed casing is shown in Figure 4.6.

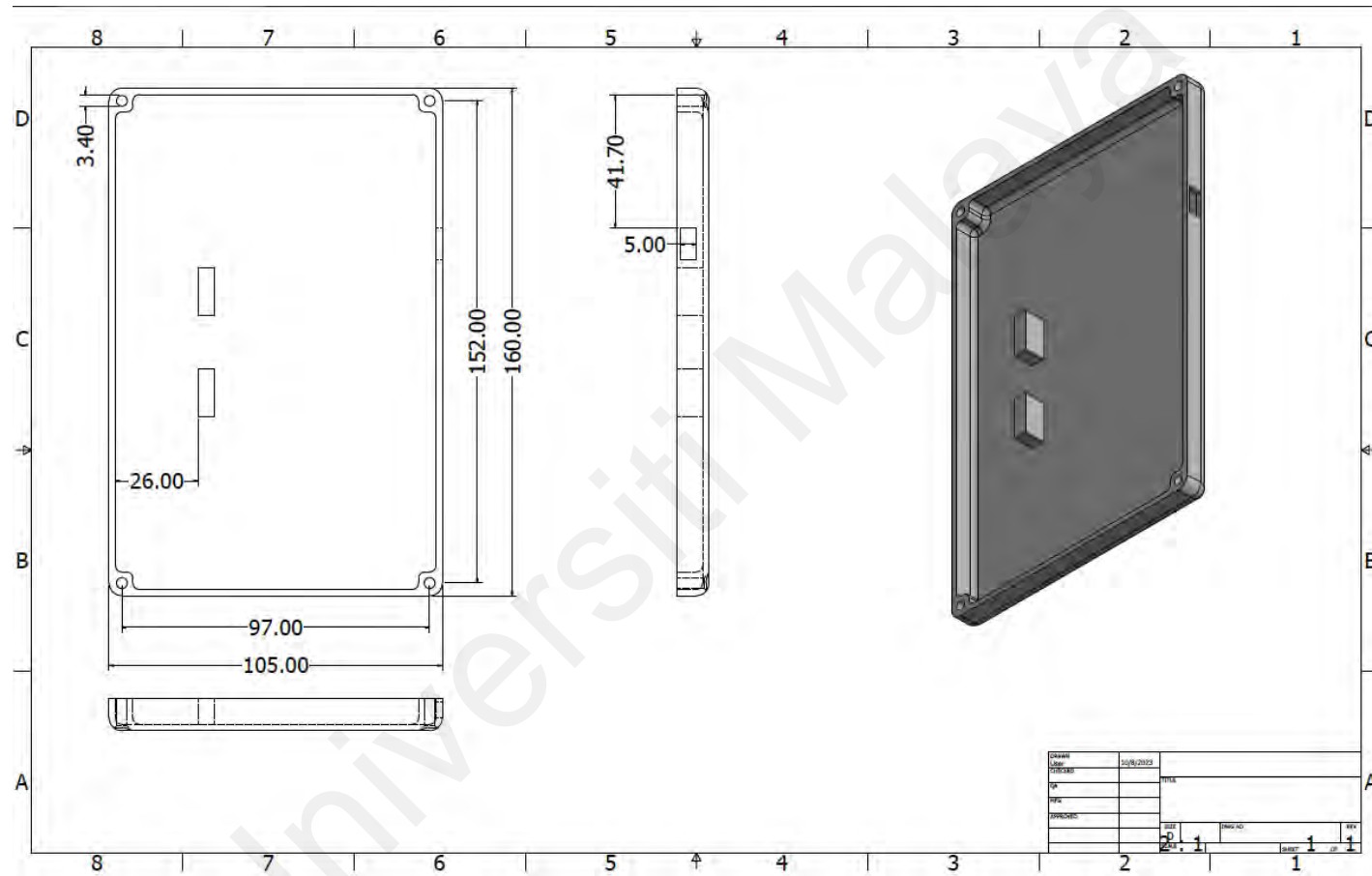


Figure 4.4: Mobilymph bottom part drawing and dimension (mm)

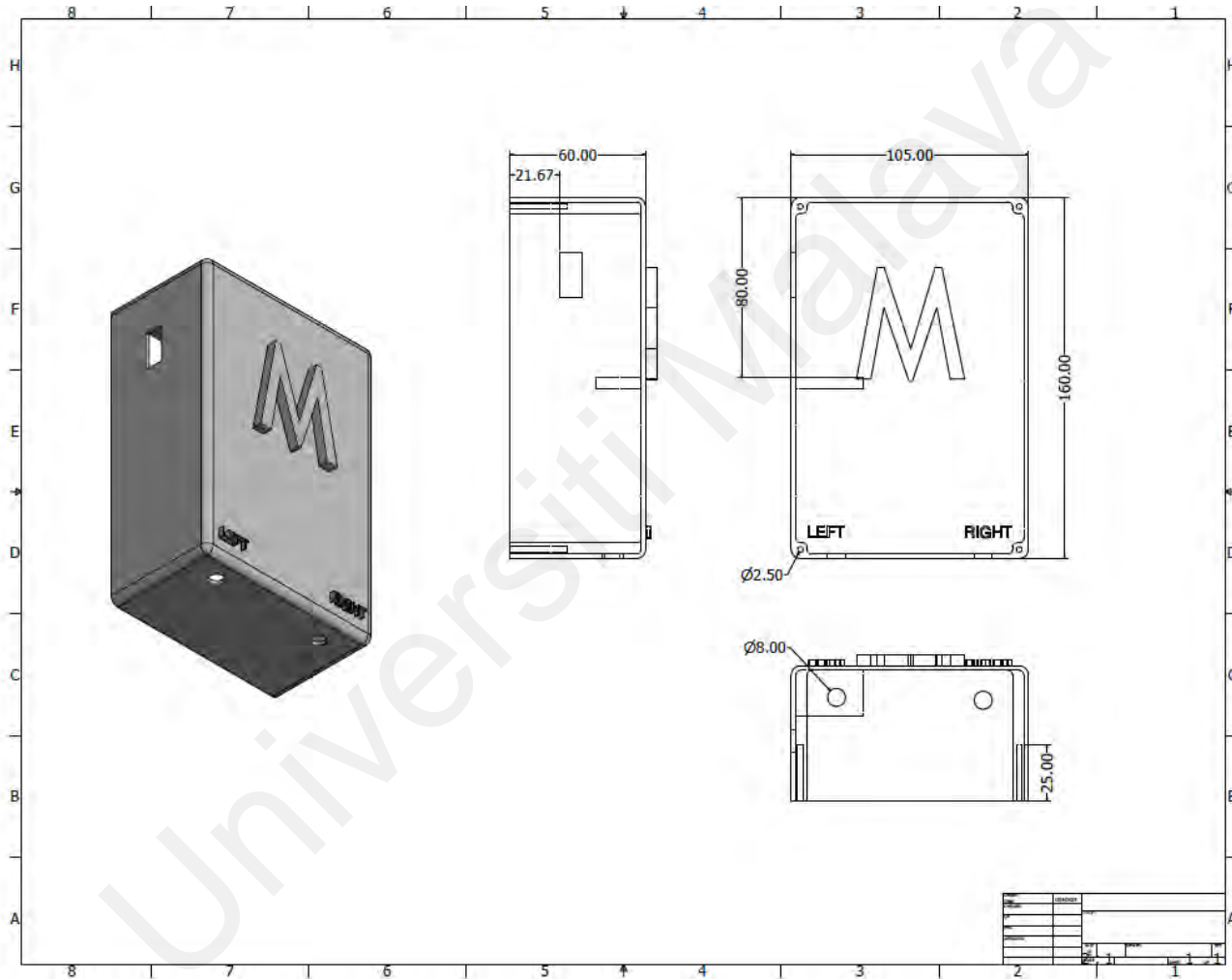


Figure 4.5: Mobilymph top part drawing and dimension (mm)



Figure 4.6: Mobilymph enclosure

The overall size of the 3D casing for the hardware module is 16 (length) x 10.5 (width) x 6 (height) cm, which is significantly smaller than other devices used for lymphedema diagnosis and monitoring, such as the SOZO (44.5 x 46.8 x 105.3 cm) and the Quadscan 4000 (24 x 15.5 x 3 cm). The compact size of the BCRL diagnosis and monitoring system makes it highly portable and easy to use in a variety of settings.

Overall, the 3D casing was able to provide a compact and lightweight form factor that is convenient for users.

4.3 Development of Software Module

In this section, the results of the comprehensive software module development for the unilateral BCRL diagnosis and monitoring system are presented. The software module includes the development of a smartphone application, design of a firmware module, creation of a cloud server module and the estimation of Cole parameters. These integrated components form a robust system that enables efficient data collection, storage, and analysis for the diagnosis and monitoring of unilateral BCRL.

4.3.1 Development of Smartphone Application Module

This section focuses on the development of the smartphone application module, known as Mobilymph, which plays a crucial role in facilitating lymphedema measurements. The module consists of various smartphone application screens, including Home screen, Progress screen, Ready to Measure screen, Measure screen, Results screen, and Profile screen. Additionally, a navigation flowchart illustrating the seamless navigation between these screens is presented. The following subsections provide an overview and insights into the design and functionality of each smartphone application screen, as well as the overall navigation flowchart.

4.3.1.1 Smartphone Application Screens

(a) Home Screen

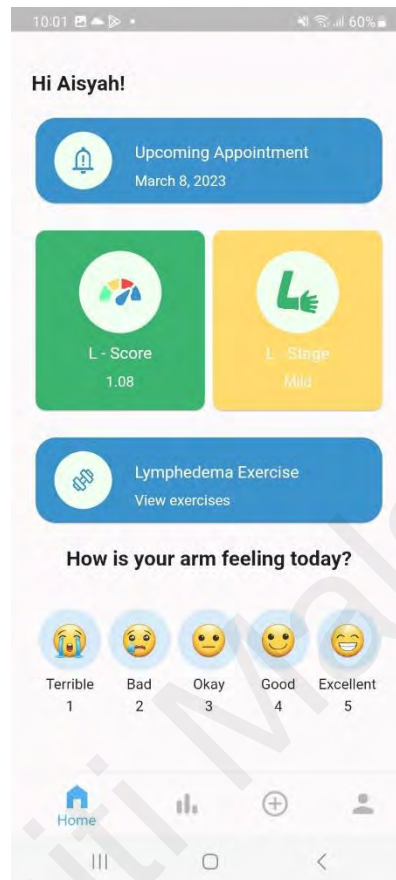


Figure 4.7: The Home screen of the Mobilymph smartphone application

The Home screen of the Mobilymph smartphone application serves as the central hub for users to access key information and features related to lymphedema management. It provides a comprehensive overview of the user's upcoming appointments, along with their current lymphedema score and stage. This allows users to stay informed about their progress and monitor changes in their condition.

In addition, the lymphedema-related information, the Home screen also offers a section dedicated to exercise for lymphedema rehabilitation. Users can easily access and follow exercises to aid in their rehabilitation process.

Furthermore, the Home screen includes a feature that allows users to record their emotional or quality of life (QoL) score for the day. Researchers have emphasized the need to evaluate QoL in lymphedema management. A study by Kayali *et al.* highlighted that QoL scores worsened as the severity of lymphedema increased (Kayali Vatansever, Yavuzşen, & Karadibak, 2020).

Overall, the Home screen offers a user-friendly interface that combines essential lymphedema-related information, rehabilitation exercises, and QoL tracking, empowering users to actively participate in their lymphedema management journey.

Universiti Malaysia

(b) *Progress Screen*

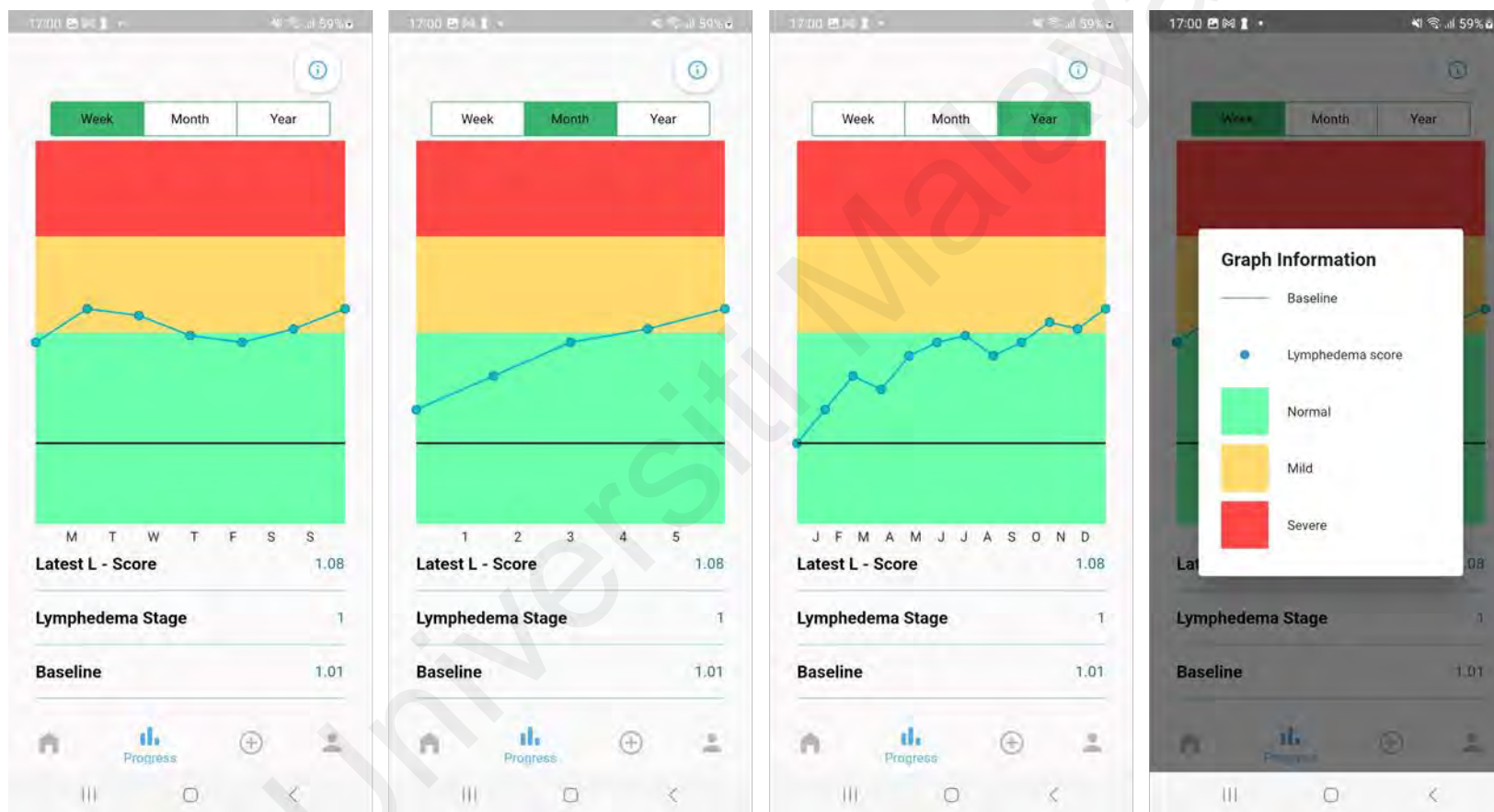


Figure 4.8: The Progress screen of the Mobilymph smartphone application

In the Progress screen of the Mobilymph smartphone application, users have access to comprehensive tracking system that allows them to monitor their progression over different time periods – weekly, monthly, and yearly. This features enables users to gain insights into the changes in their lymphedema score and assess the effectiveness of their management strategies.

The Progress screen includes information button that provides detailed explanations of the displayed graph. This helps users understand the visual representation of their lymphedema score and its significance.

The graph on the Progress screen illustrates the lymphedema score using blue dots. A blue dots in a green container indicates a normal lymphedema score, while a yellow container represents mild lymphedema and a red container indicates severe lymphedema. To provide additional context, a black line is used to depict the baseline value, which represents the user's lymphedema score before initiating breast cancer treatment. This baseline allows users to track the deviation of their lymphedema score from the initial value, providing a valuable reference point for monitoring their progress.

The Progress screen serves as a visual tool that empowers users to actively track and understand their lymphedema progression, supporting them in making informed decisions about their treatment and management strategies.

(c) *Ready to Measure Screen*

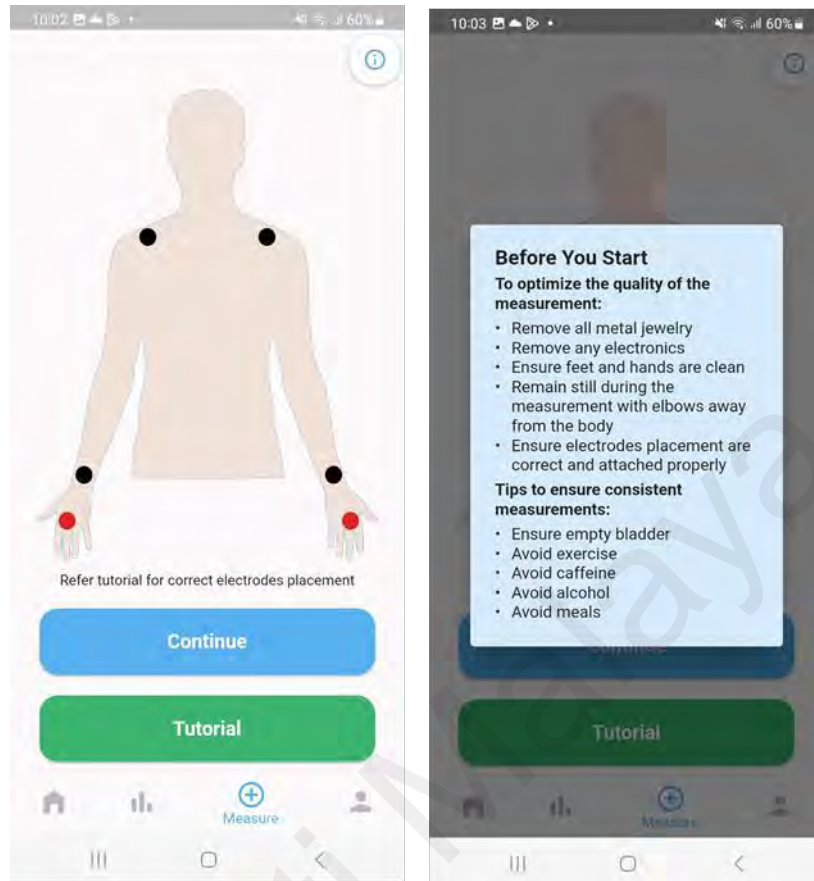


Figure 4.9: The Ready to Measure screen of Mobilymph smartphone application

In the Ready to Measure screen of the Mobilymph smartphone application, users are provided with essential information and resources to ensure optimal and consistent measurements.

The screen features an information button that displays instructions on how to optimize the quality of measurements and achieve consistent results. This information helps users understand the key factors that can impact the accuracy of their measurements and guides them in taking the necessary steps to ensure reliable data.

To assist users in correctly placing the electrodes, the Ready to Measure screen also includes the Tutorial button. This tutorial demonstrates proper placement of the electrodes. A visual guide is also represented to guide users. The electrode placement

image is color-coded, with red representing the current electrode and black representing the voltage measurement electrode.

Once users are prepared and ready to proceed with the measurement, the Ready to Measure screen includes the Continue button. Users can simply tap the Continue button to move forward and begin the measurement process.

By providing clear instructions and visual guidance users can perform accurate and reliable bioimpedance measurements for effective lymphedema assessment.

Universiti Malaysia

(d) *Measure Screen*

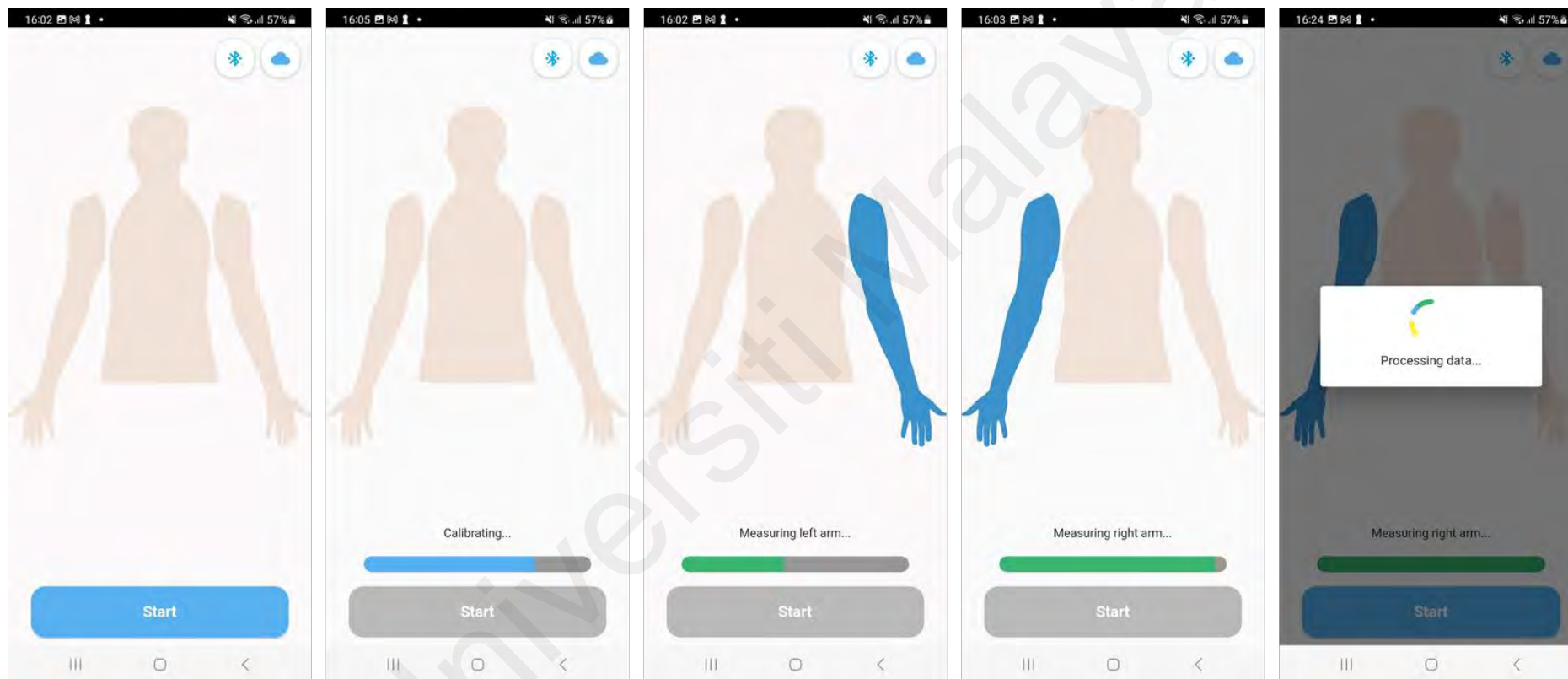


Figure 4.10: The Measure screen of Mobilymph smartphone application

In the Measure screen of the Mobilymph smartphone application, users have access to key features necessary for the lymphedema measurement process. The screen includes a Bluetooth button, which enables users to establish and terminate a connection with the Mobilymph measuring device. The Bluetooth button also serves as an indicator, displaying a blue connected Bluetooth icon when connected and grey disconnected Bluetooth icon when disconnected. This button is essential for the measurement process as it enables the smartphone to send and receive data from the peripheral Mobilymph device.

Additionally, the Measure screen includes a Cloud button that indicates the smartphone's internet connectivity status. This button facilitates the transmission of measurement data to the Google Cloud Platform for further processing and retrieval of lymphedema results.

To initiate the measurement process, users can press the Start button, which sends a START command to the Mobilymph measuring device. During the measurement process, the screen displays a calibration indicator, notifying users of the calibration progress. Once the calibration is complete, the system proceeds to measure left arm, visually represented by highlighting the left arm in blue on the accompanying human image. After measuring the left arm, the image switches to highlight the right arm blue, indicating that the measurement process has moved on to the right arm. Throughout the measurement process, users can track the progress through a green linear progression bar, which visually represents the advancement from the start to the end of the measurement. Upon completing the measurement, a Processing Data dialog appears, indicating that the received data is being sent to the cloud for further processing.

(e) *Results Screen*

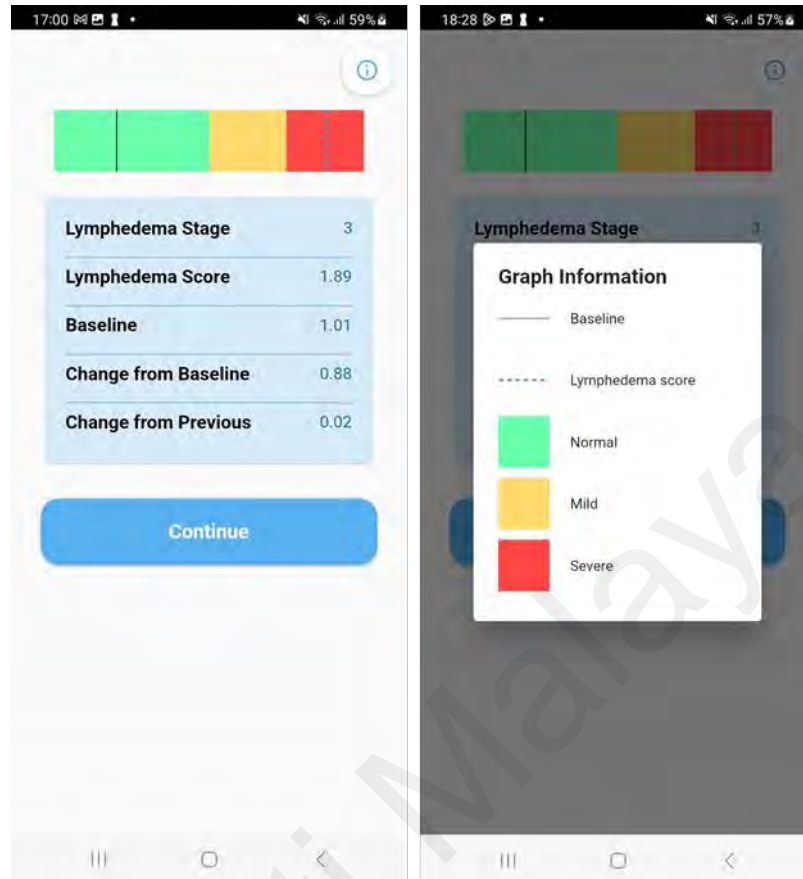


Figure 4.11: The Results screen of Mobilymph smartphone application

After receiving the lymphedema results from the Google Cloud Platform, the Results screen displays the pertinent information. This includes the lymphedema stage, which categorizes the severity of lymphedema, the lymphedema score itself, the baseline value for reference, the value of lymphedema score changes from the baseline, and the value of lymphedema score change from the previous measurement. This metric allows users to track their progress and observe any fluctuations in their lymphedema score, providing valuable insights for managing and monitoring their condition effectively.

In the Results screen of the Mobilymph smartphone application, users can access a horizontal graph that provides a visual representation of their lymphedema assessment results. The graph includes several elements to aid in interpretation and understanding.

Firstly, a black line represents the baseline, which signifies the initial lymphedema score before any treatment or intervention. This baseline serves as a reference point for tracking changes in the lymphedema score over time.

The lymphedema score is depicted by a blue dashed line on the graph. Depending on the stage acquired from the lymphedema assessment, the blue dashed line falls into different color-coded regions. A green region indicates a normal lymphedema score, a yellow region represents mild lymphedema, and a red region signifies severe lymphedema. This color-coded representation helps users quickly assess the severity of their lymphedema based on their obtained score. An information button is available to provide users with more detailed information about the graph.

(f) *Profile Screen*

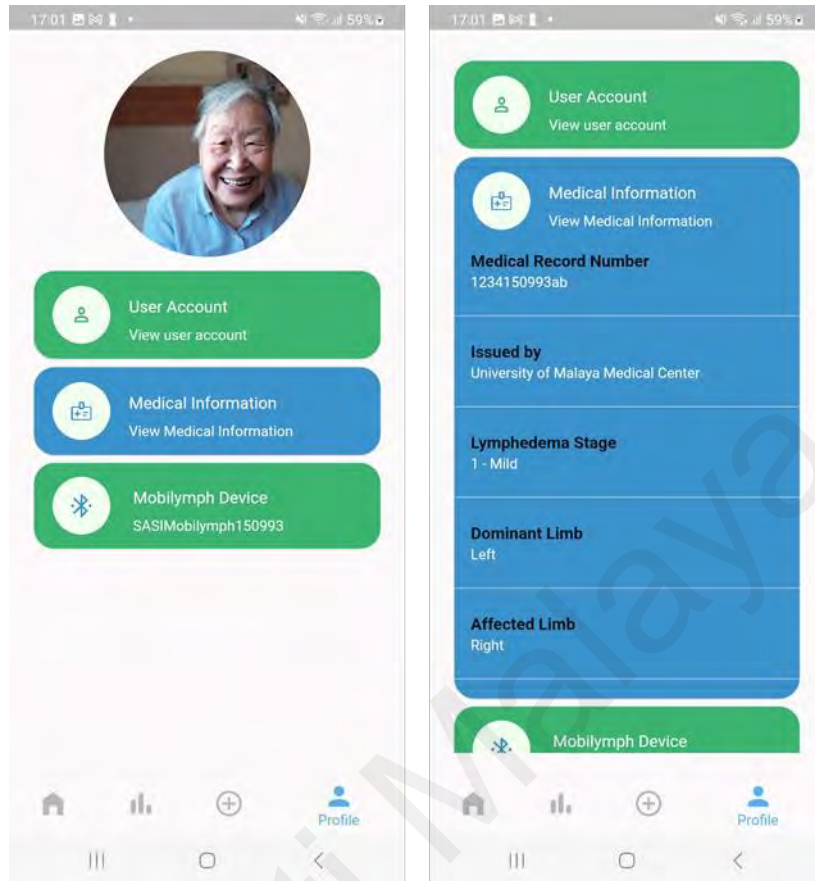


Figure 4.12: The Profile screen of Mobilymph smartphone application

In the Profile screen of the Mobilymph smartphone application, users can access their personal and medical information, as well as details related to their Mobilymph device. The user account section displays general information about the user, such as their name and contact details. Under the Medical Information section, users can find specific details related to their medical history and lymphedema condition such as dominant and affected limbs. This includes the user's medical record number, which serves as a unique identifier for their medical records number, which serves as a unique identifier for their medical records. Additionally, the assigned rehabilitation clinic is indicated, providing users with information about their designated healthcare facility.

4.3.1.2 Smartphone Application Screens and Navigation Flowchart for Lymphedema Measurement

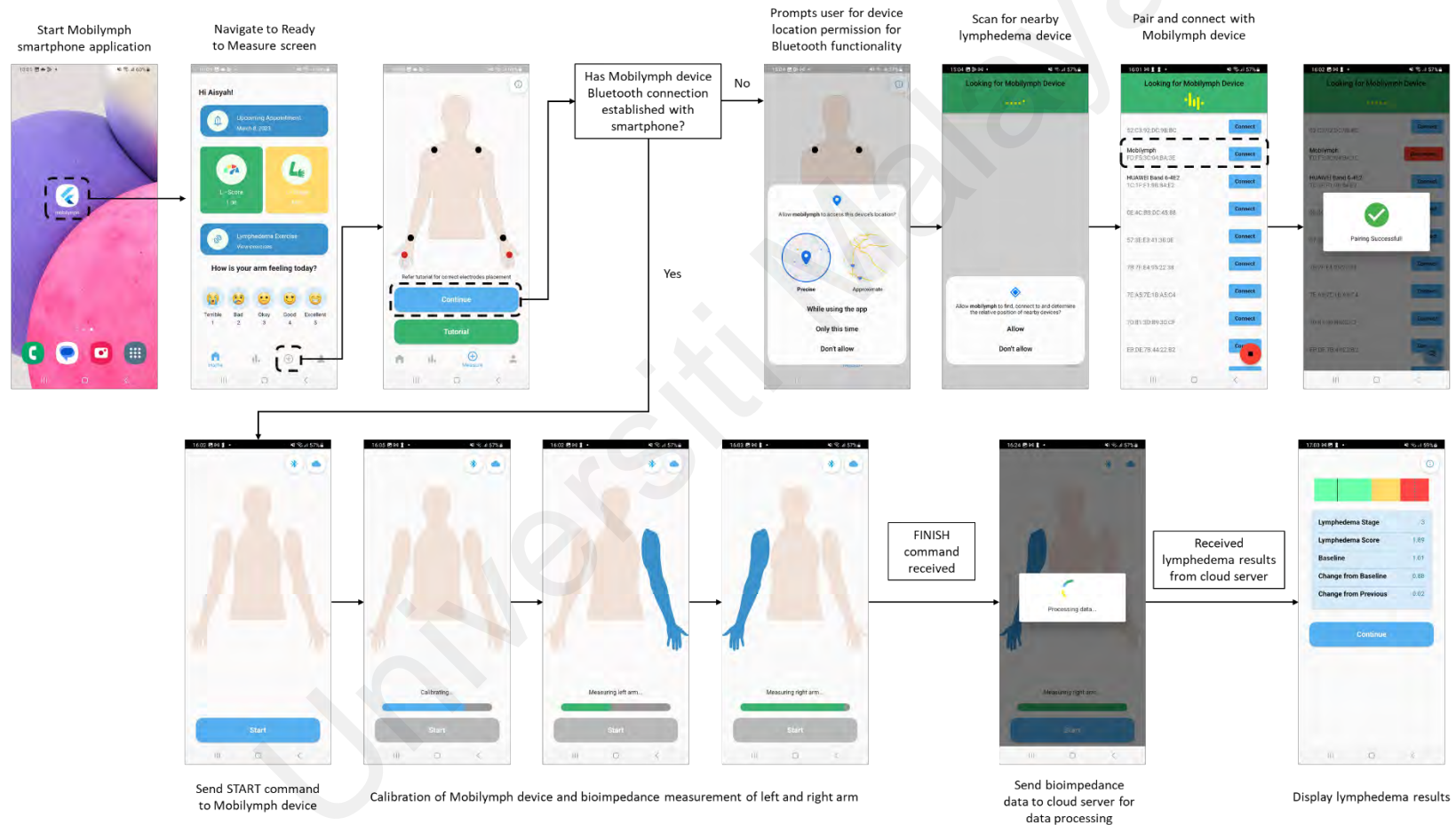


Figure 4.13: Smartphone application screens and navigation flowchart to start lymphedema measurement

The flow of the smartphone application screens and navigation for lymphedema measurement begins with starting the Mobilymph smartphone application. From the Home screen, the user navigates to the Ready to Measure screen. In this screen, the user presses the Continue button. At this point, the backend of the application checks if the Mobilymph device has established a Bluetooth connection with the smartphone. If the connection is already established, the application proceeds to the Measure screen. However, if there is no established connection, the user is prompted to grant device location permission and the application scans for nearby Mobilymph measuring device, and then proceed to the Measure screen.

In the Measure screen, the user presses the Start button to initiate the measurement process. Once the finish command is received, the bioimpedance data captured by the Mobilymph device is sent to cloud server for further data processing and analysis. The lymphedema results obtained from the cloud server are then displayed in the Results screen.

4.3.2 Development of Firmware Module

The firmware module plays a crucial role in facilitating the bioimpedance measurement process using the ADuCM3029 and AD5941. Upon start up, the resources of the microcontrollers were initialized and UART communication was established.

Once the microcontroller received the start command 'm' from the smartphone application, it performed the RTIA calibration to ensure accurate impedance measurements. Subsequently, the firmware processed the impedance data using the Discrete Fourier Transform (DFT) technique. This processing allowed for the extraction of magnitude and phase angle at each frequency point, resulting in the generation of bioimpedance spectroscopy data.

The firmware transmitted data to smartphone application via Bluetooth in the following format: [Frequency\tMagnitude\tPhase]. The ‘\t’ represents tab and ‘x’ character served as an indicator of the end of a data entry, and the firmware moved on to the next frequency. Once the frequency sweep was completed, the ADuCM3029 microcontroller sent a finish command ‘f’ to the smartphone application, indicating a successful completion of the measurement process.

```

COM3 - Tera Term V1
File Edit Setup Control Window Help
0.120864x347.47 10.081528 0.001423x394.95 10.051680 -0.016962x442.42 10.082276 -0.078498x489.90
10.077270 -0.072750x584.85 10.119567 -0.177434x632.32 10.097225 -0.020861x679.80 10.088663 -0.130010x727.2
.75 10.091645 -0.052723x822.22 10.102225 -0.046637x869.70 10.072177 -0.018581x917.17 10.097357 -0.0017
971x1012.12 10.078895 0.004983x1059.60 10.081963 -0.059759x1107.07 10.092826 0.071808x1154.55 10.088961
0.004842x1249.49 10.082700 -0.002293x1296.97 10.080022 0.018792x1344.44 10.087519 0.005468x1391.92 10.0851
2920 0.044621x1486.87 10.081116 0.013139x1534.34 10.078662 0.022948x1581.82 10.081367 0.059684x1629.29 10.0851
10.082988 0.047826x1724.24 10.083966 -0.006859x1771.72 10.082375 0.030254x1819.19 10.078751 0.089624x1866.6
.14 10.085979 -0.009705x1961.62 10.082795 0.007912x2009.09 10.083947 0.053454x2056.57 10.082829 0.032651
429x2151.52 10.082744 0.044054x2198.99 10.082745 0.055289x2246.46 10.078171 0.059876x2293.94 10.081154
0.037012x2388.89 10.085443 0.059174x2436.36 10.081783 0.034102x2483.84 10.075001 0.060214x2531.31 10.0767
1741 0.088218x2626.26 10.076184 0.067611x2679.74 10.078401 0.080914x2721.21 10.083078 0.046323x2768.69
10.076372 0.102142x2863.64 10.083986 0.085514x2911.11 10.073721 0.100885x2958.59 10.085031 0.102085x3006.0
.54 10.076315 0.102202x3101.01 10.083525 0.072446x3148.48 10.076028 0.084427x3195.96 10.083418 0.10443
998x3290.91 10.076350 0.080197x3338.38 10.084342 0.101761x3385.86 10.077821 0.091510x3433.33 10.084405
0.112427x3528.28 10.078486 0.102865x3575.76 10.085405 0.101275x3623.23 10.081102 0.132163x3670.71 10.07851
2764 0.125239x3765.66 10.078191 0.143214x3819.13 10.078444 0.109731x3860.61 10.078693 0.131667x3908.00
10.078585 0.128542x4003.03 10.080372 0.137779x4050.51 10.080470 0.127151x4097.98 10.078247 0.128064x4145.4
.93 10.081755 0.141242x4240.40 10.081204 0.135788x4287.88 10.080036 0.135583x4335.35 10.082455 0.13364
427x4430.30 10.084262 0.172737x4477.78 10.079774 0.134763x4525.25 10.079360 0.147190x4572.73 10.080315
0.134955x4667.68 10.078317 0.166177x4715.15 10.080571 0.157007x4762.63 10.080152 0.156324x4810.10 10.0812
0126 0.142228x4905.05 10.083630 0.166535x4952.53 10.081115 0.152451x5000.00 10.079431 0.152163x5000.00
10.086570 0.215427x8937.37 10.089017 0.273117x10906.06 10.090634 0.318953x12874.75 10.096311 0.371282x14843.
2.12 10.098452 0.448295x18780.81 10.101634 0.481029x20749.43 10.100180 0.522859x22718.18 10.106788 0.548515
116x26655.55 10.105274 0.635260x28624.24 10.107405 0.662395x30592.93 10.109022 0.710841x32561.62 10.110296
0.782647x36498.99 10.108416 0.806781x38467.68 10.112145 0.835950x40436.36 10.114348 0.885497x42405.05 10.1138
1997 0.968082x46342.43 10.116051 0.987579x48311.11 10.113784 1.020088x50279.80 10.117641 1.055294x52248.48
10.120568 1.119795x56185.86 10.123849 1.162586x58154.55 10.117235 1.201786x60123.23 10.119417 1.258962x62091.
0.61 10.122733 1.315094x66029.29 10.123579 1.349702x67997.98 10.125323 1.365575x69966.66 10.124022 1.40977
285x79904.04 10.123362 1.471014x75872.73 10.120043 1.526188x77841.41 10.123390 1.558300x79810.10 10.123734
1.646319x83747.48 10.128765 1.663252x85716.16 10.125693 1.708936x87684.85 10.124075 1.728958x89653.54 10.12644
8888 1.834087x93590.91 10.127892 1.852231x95559.59 10.123604 1.887033x97528.28 10.122929 1.920903x99496.97
10.126248 1.996181x103434.34 10.125825 2.014371x105403.03 10.128000 2.076122x107371.72 10.125100 2.084130x109340
09.09 10.128336 2.190092x113277.78 10.126627 2.193304x115246.46 10.126274 2.253708x117215.15 10.124595 2.30502
907x121152.52 10.127887 2.337711x123121.21 10.127811 2.418618x125089.90 10.128534 2.441244x127058.59 10.127327
2.518660x130995.96 10.126637 2.553626x132964.64 10.124142 2.573367x134933.33 10.124272 2.643759x136902.02 10.1266
5066 2.694059x140839.39 10.125613 2.755587x142808.08 10.123666 2.765339x144776.77 10.131124 2.810902x146745.45
10.122391 2.866153x150682.83 10.129756 2.957574x152651.52 10.121965 2.973699x154620.20 10.129333 2.985226x156588
57.58 10.125200 -356.921875x160526.27 10.124721 3.120741x162496.95 10.124076 3.187452x164463.64 10.125805 3.21595
042x168401.02 10.125463 3.270890x170369.70 10.117518 3.306158x172338.39 10.120206 3.327085x174307.08 10.126189
3.446464x178244.44 10.120403 3.473480x180213.13 10.125833 3.494428x182181.81 10.122364 3.569501x184150.50 10.1211
2387 3.594100x188087.88 10.128877 3.647104x190056.56 10.124364 3.696773x192025.25 10.121305 3.698821x193993.94
10.126443 3.930454x197931.31 10.121591 3.887342x199900.00 10.113511 3.92835xf

```

Figure 4.14: Firmware development progress in Tera Term

Showcases the successful development of the firmware module from the initial start command (‘m’) to the data being formatted and finish command (‘f’). The progress is displayed in the Tera Term application, demonstrating the step-by-step execution of the firmware code.

4.3.3 Development of Cloud Server Module

The Firebase cloud server module in this study incorporates two essential components: Cloud Functions and Firestore database. Cloud Functions handle the server-side processing and computations, while Firestore database serves as the data storage and retrieval system. This section presents the results to the integration and utilization of the

Firebase cloud server components. The performance, functionality, and effectiveness of Cloud Functions and Firestore database within the system architecture will be discussed in detail.

4.3.3.1 Cloud Functions

The cloud function was successfully implemented to perform the bioimpedance spectroscopy signal processing, specifically computing the Cole parameters. The computation includes obtaining the R_0 value for each arm. The cloud function then proceeded to evaluate the R_0 ratio which serve as a quantitative measure for lymphedema assessment.

For the configuration of the cloud function, the trigger type was set as HTTP with the trigger URL defined as <https://asia-southeast1-mobilymph.cloudfunctions.net/mobilymph-results>. The runtime chosen for the cloud function was Python 3.11, and the region selected for deployment was Singapore.

The function execution commenced upon triggering the function URL from the developed smartphone application. The received data was processed by the cloud function, and the results were returned to the smartphone application and Firestore Database. The entire execution process of the function took approximately 265 milliseconds, with a successful completion indicated by the status code of 200.

Figure 4.15 shows the cloud function logs of a successful deployment and execution of the cloud function. The low execution time indicates the efficiency and responsiveness of the cloud function in processing the received data and generating the required results. This cloud-based approach enables seamless integration with smartphone applications and facilitates efficient analysis of bioimpedance spectroscopy for lymphedema assessment.

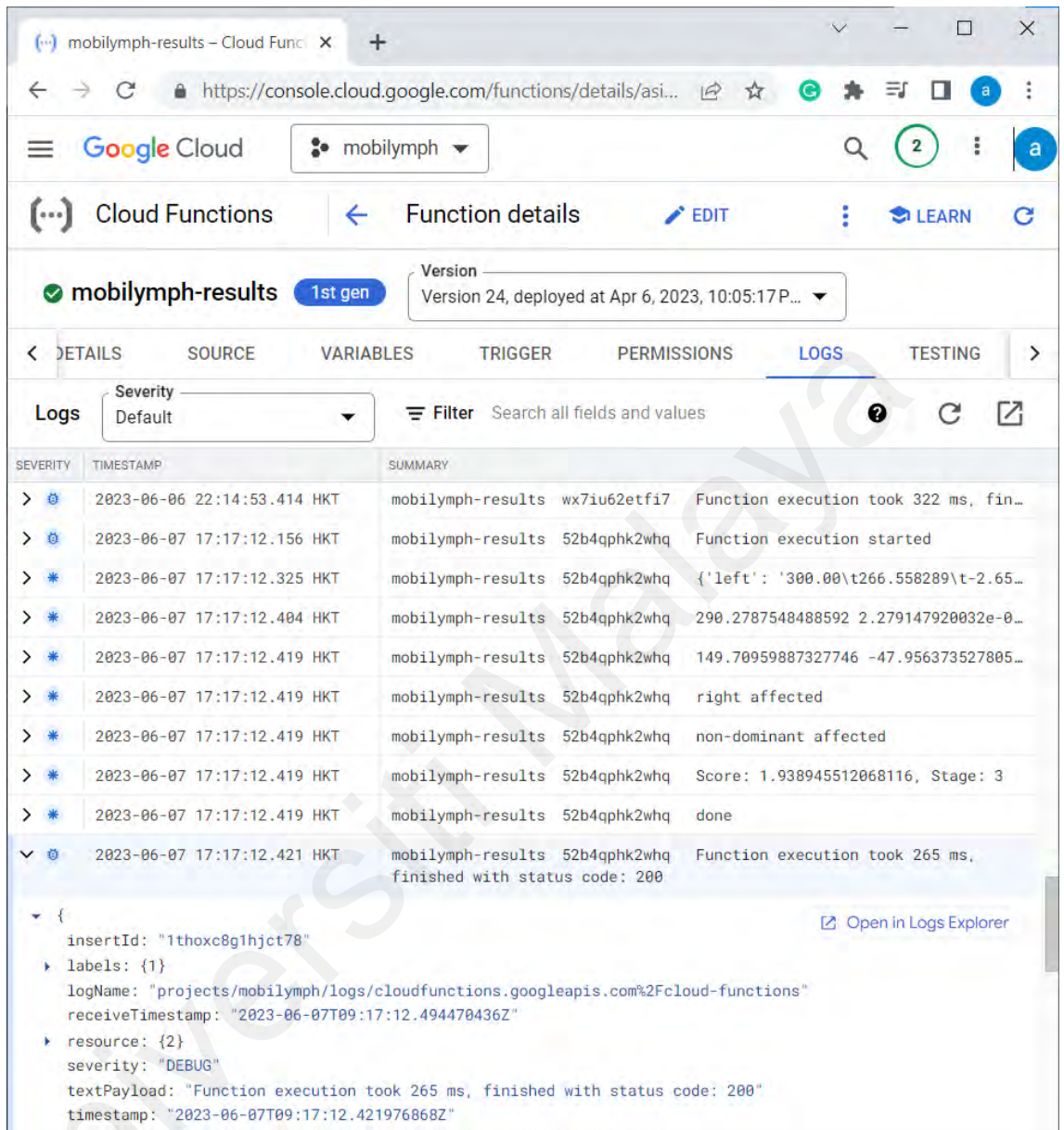


Figure 4.15: Cloud function logs

4.3.3.2 Firestore Database

The development of the Firestore Database module within the cloud server architecture enables efficient storage and retrieval of lymphedema measurement data. The database is organized into collections based on users' medical record numbers. Within each collection, documents are created to hold the lymphedema results, with each document

corresponding to a specific time point when the data was collected. These documents store the lymphedema results received from the Cloud Functions.

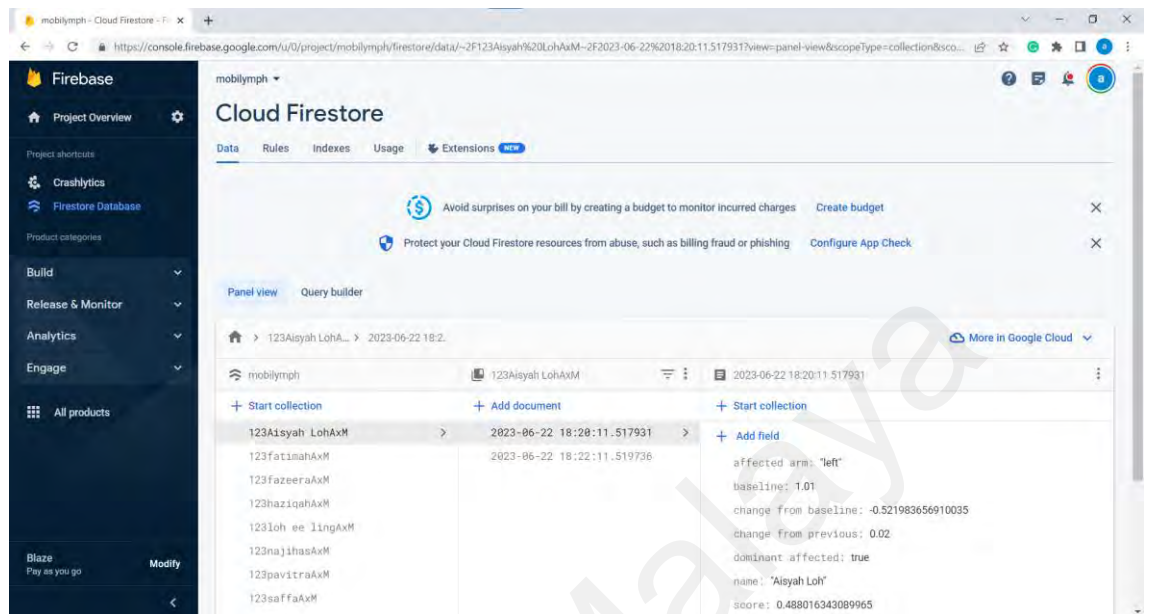


Figure 4.16: Organization of Firestore Database for lymphedema measurement data

Within each document, essential user medical information such as dominant and affected arm, lymphedema score and stage, baseline value, and changes in the lymphedema score from both the baseline and previous measurements are recorded. This comprehensive data enables medical practitioners to remotely monitor the progression of users' lymphedema over time by selecting the appropriate collection or medical record number.

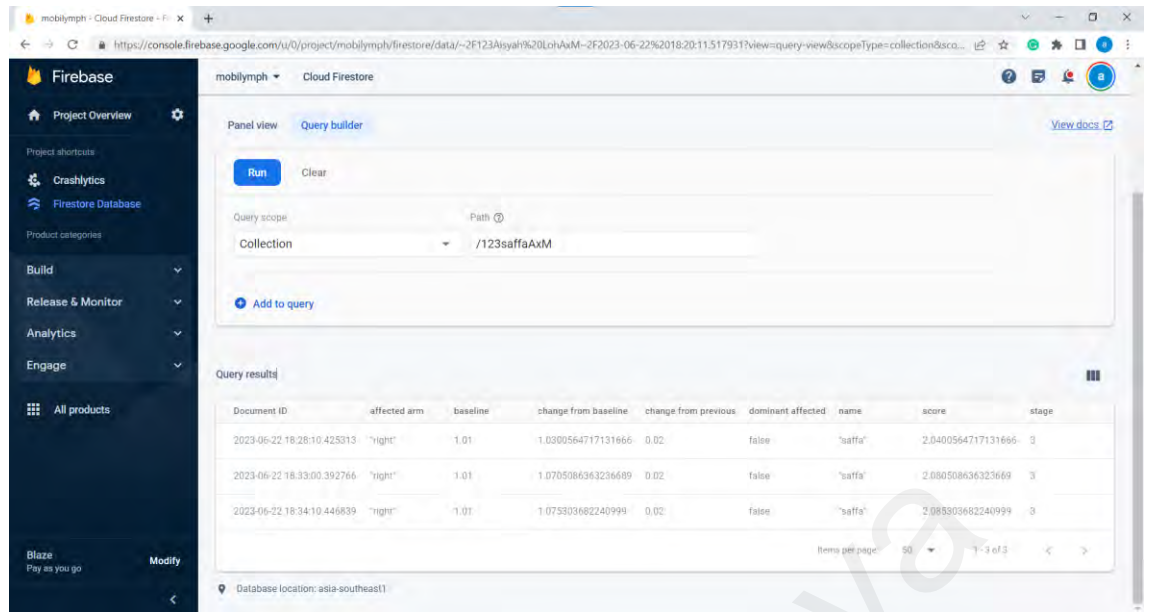


Figure 4.17: Query builder in Firestore Database

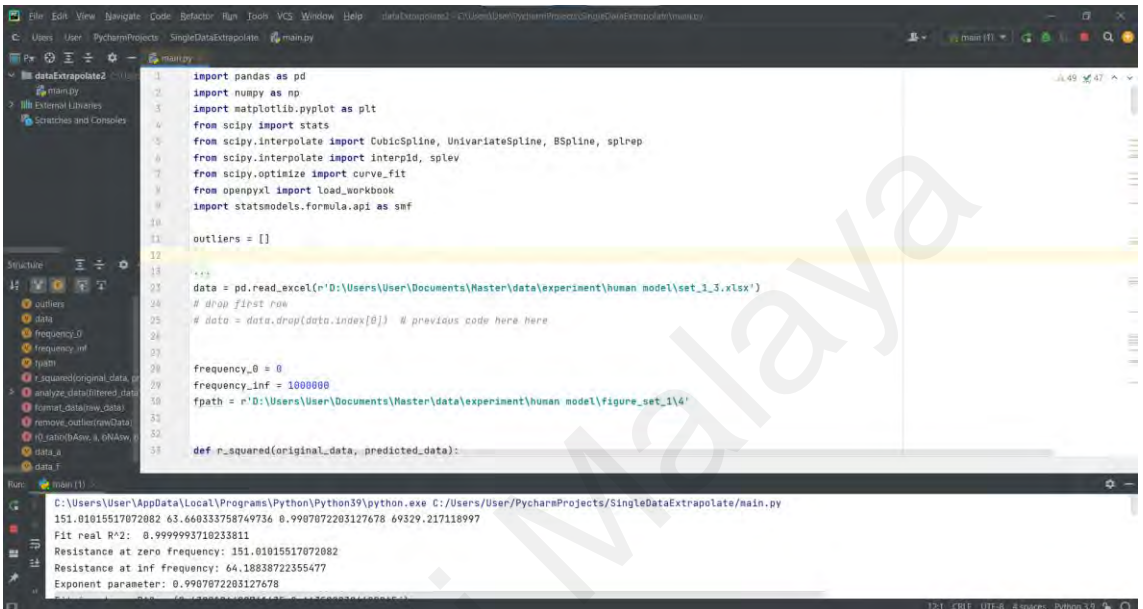
Figure 4.17 showcases the query builder, demonstrating how a specific collection can be selected to display its contents. In this case, the lymphedema measurements collected throughout the specified time frame are shown. This feature enables efficient data exploration and analysis for monitoring lymphedema progression.

4.3.4 Estimation of Cole Parameters

In this study, the estimation of Cole parameters was performed UBCRL hardware module measured on the equivalent electrical circuit model of human upper arm or parallel RC circuit ($R_0 = 150 \Omega$, $R_\infty = 100 \Omega$, $C_m = 0.01 \mu\text{F}$). The data were processed to obtain the resistance to the current flow at zero frequency (R_0) and infinite frequency (R_∞). The measured data were then fitted based on the Cole modelling using the Non-linear Least Squares (NLLS) fitting method. The NLLS fit method involved performing a curve fitting on the Cole resistance model, with the frequency as the independent variable. The model coefficients (R_0 , R_∞ , α , τ) were estimated through the fitting process.

The NLLS fitting was performed in PyCharm using Python. The code successfully estimated the R_0 , R_∞ , α , and τ . The coefficient of determination (R-squared) was

calculated to determine the relationship between the estimated and real values to assess the accuracy of the estimation. The obtained R-squared value was 0.9999, indicating a strong correlation between estimated and real values. This high R-squared value suggests that the NLLS fitting method accurately captured the underlying trends in the data.



```
1 import pandas as pd
2 import numpy as np
3 import matplotlib.pyplot as plt
4 from scipy import stats
5 from scipy.interpolate import CubicSpline, UnivariateSpline, BSpline, splrep
6 from scipy.interpolate import interpfd, splev
7 from scipy.optimize import curve_fit
8 from openpyxl import load_workbook
9 import statsmodels.formula.api as smf
10
11 outliers = []
12
13 ...
14 data = pd.read_excel(r'D:\Users\User\Documents\Master\data\experiment\human model\set_1_3.xlsx')
15 # drop first row
16 # data = data.drop(data.index[0]) # previous code here here
17
18 frequency_0 = 0
19 frequency_inf = 1000000
20 fpath = r'D:\Users\User\Documents\Master\data\experiment\human model\figure_set_1\4'
21
22 def r_squared(original_data, predicted_data):
23
24
25
26
27
28
29
30
31
32
33
34
35
36
37
38
39
40
41
42
43
44
45
46
47
48
49
50
51
52
53
54
55
56
57
58
59
60
61
62
63
64
65
66
67
68
69
70
71
72
73
74
75
76
77
78
79
80
81
82
83
84
85
86
87
88
89
90
91
92
93
94
95
96
97
98
99
100
```

```
151.01015517072082 63.660333758749736 0.9907072203127678 69329.217118997
Fit real R^2: 0.99999993710233811
Resistance at zero frequency: 151.01015517072082
Resistance at inf frequency: 64.18838722355477
Exponent parameter: 0.9907072203127678
```

Figure 4.18: NLLS results and R-squared value in PyCharm

Figure 4.18 shows a screenshot of the PyCharm IDE displaying the results of the resistance estimation. The values of R_0 , R_∞ , α , and τ obtained from the NLLS fitting, are shown in the terminal output. Additionally, the terminal displays the calculated R-squared value, which quantifies the goodness of fit between the estimated and real values.

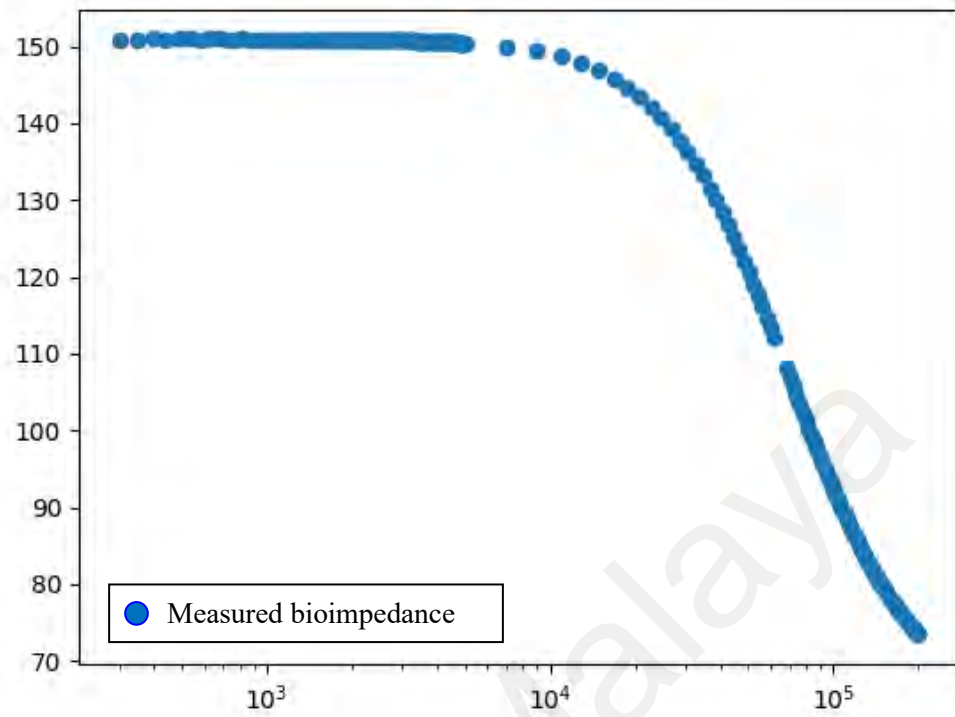


Figure 4.19: Resistance versus frequency of a parallel RC circuit

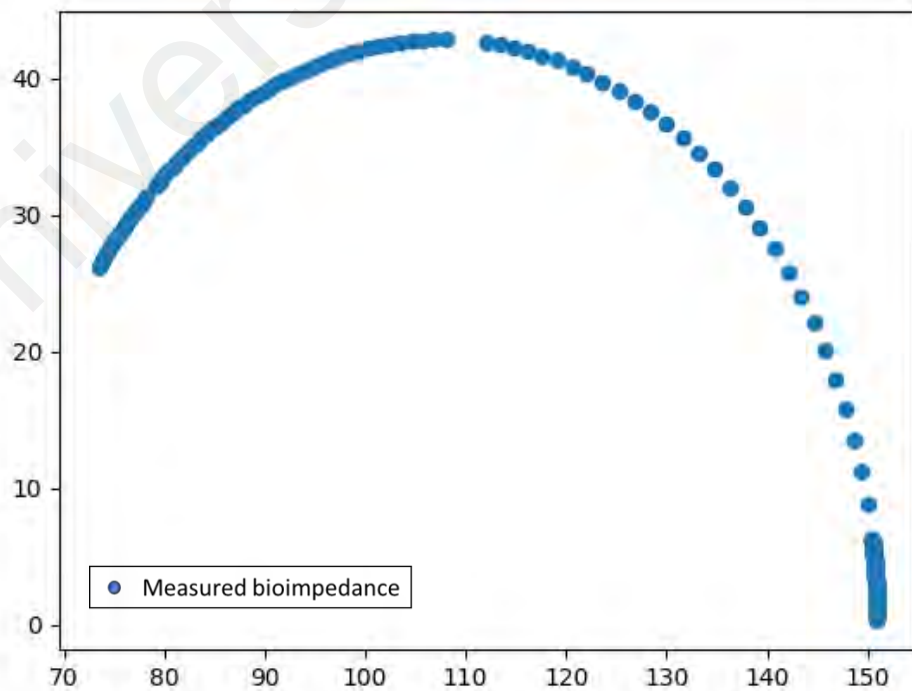


Figure 4.20: Resistance versus imaginary of a parallel RC circuit

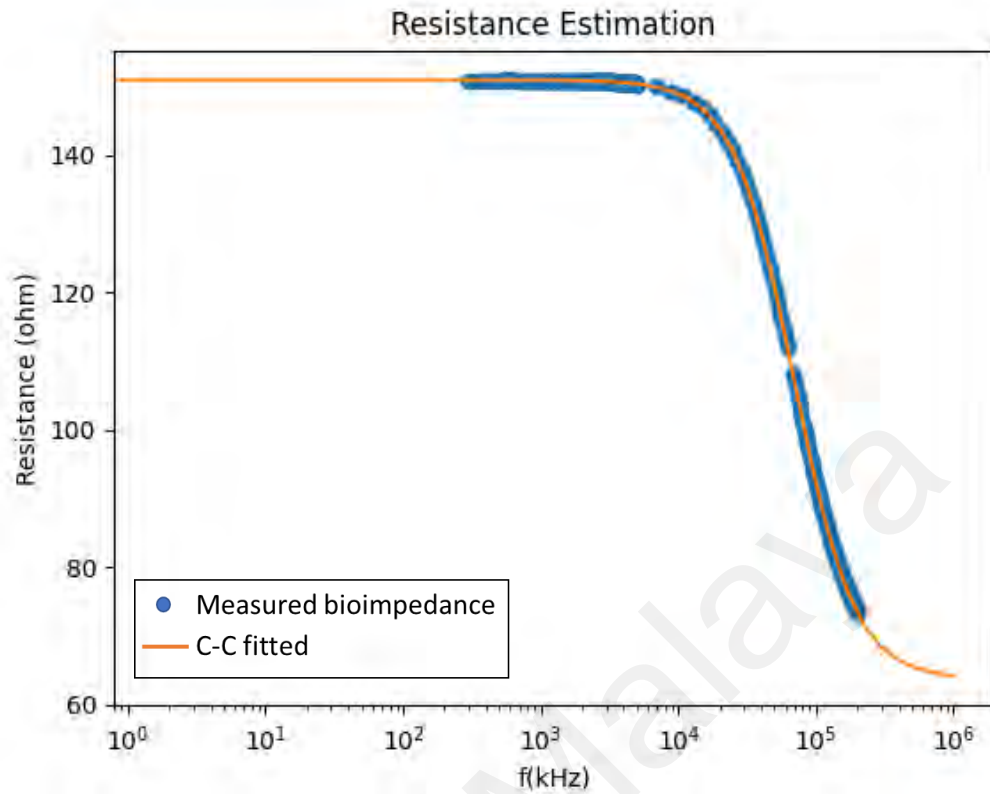


Figure 4.21: Estimated resistance (R_0 and R_∞) of a parallel RC circuit

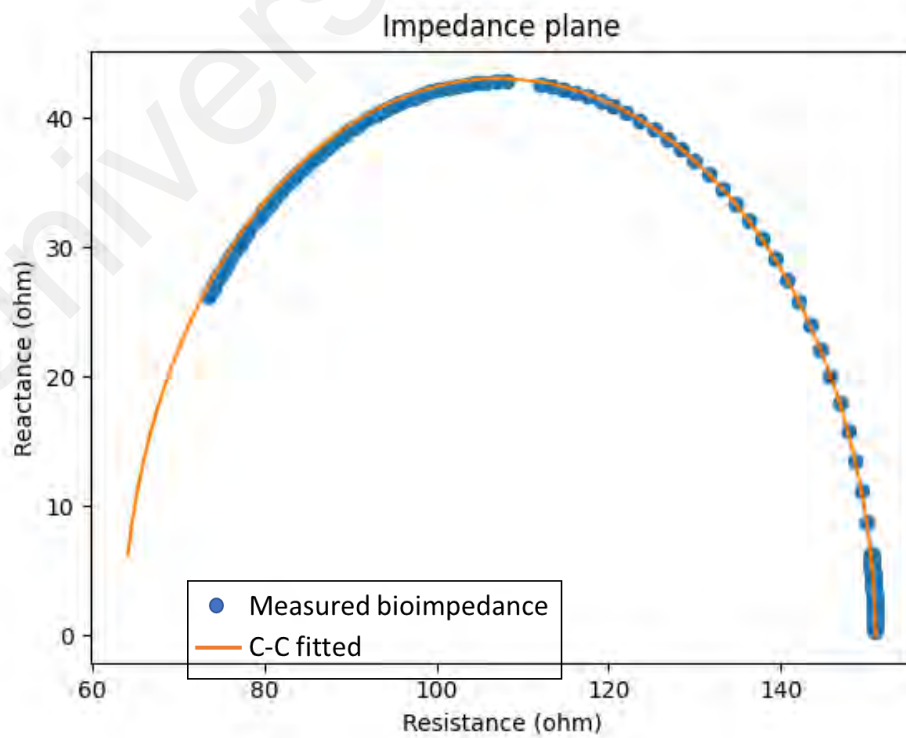


Figure 4.22: Cole – Cole plot of a parallel RC circuit

Figure 4.19 and Figure 4.20 displays the raw BIS measured data obtained in the study. The data points represent the measured resistance values at different frequencies. The orange line in Figure 4.21 and Figure 4.22 represents the estimated resistance value and the Cole – Cole plot obtained using the NLLS fitting method. The estimated values are plotted alongside the raw measured data, showing the fit of the model to the data.

4.4 System Integration and Data Acquisition

In this section, we present the results of the data acquisition and transmission module of the lymphedema diagnosis and monitoring system. The module is responsible for collecting and transmitting bioimpedance data from the device to the smartphone application. The module consists of a microcontroller and Bluetooth module, which are used to facilitate communication between the device and the smartphone. In this section, the results of the data transmission tests conducted to ensure the successful communication between the device and the smartphone application is presented.

4.4.1 Microcontroller

The data acquisition and transmission module in the ADuCM3029 microcontroller was successful in establishing UART communication with the computer using a terminal interface. The communication was conducted using Tera Term and serial port speed of 230400. The result of the UART communication test is shown in Figure 4.23.



Figure 4.23: UART communication test using Tera Term

4.4.2 Bluetooth

The nRF52840 was able to scan nearby devices, form a connection, and transmit and receive data. The wireless transmission was tested using the BluefruitConnect smartphone application. The nRF52840 received a character 'm' from the smartphone application, and in response, the ADuCM3029 transmitted "Hello from ADuCM3029". This test was repeated by sending characters 't' and 'c' to confirm that the ADuCM3029 was able to receive and transmit the correct command. When 'c' was received, ADuCM3029 returned "Helloo from ADuCM3029" and for 't', it returned "HelloOo from ADuCM3029". The screenshot from the smartphone application of the received and transmitted command is presented in Figure 4.24. Overall, the Bluetooth communication between the smartphone application and the system was successful.



Figure 4.24: Bluetooth communication between smartphone application and nRF52840

4.5 Testing and Validation of the Unilateral BCRL System

In this section, the results of the device functionality tests are presented. These results provide an overview of the device's performance in terms of its impedance measurement and bioimpedance measurement capabilities which include information on accuracy, error, precision, and standard deviation of the developed device. The results are based on validation tests conducted on passive loads and healthy participants. This provides insight into the reliability and effectiveness of the developed device.

4.5.1 Testing and Validation with Passive Loads

The device's impedance measurement performance is evaluated by validating it using resistors, capacitors, and model of human tissue created from combination of passive loads against LCR meter (RS Pro LCR-6100) as reference device. The section presents the results of the validation in terms of accuracy, error, precision, and standard deviation of the device's impedance measurements. The information is crucial to ensure that the device is reliable and accurate before proceeding to test with healthy participants where measurements are required to be precise.

4.5.1.1 Resistors

In this section, the performance of the developed device in impedance measurement was evaluated by validating it against an LCR meter on a set of resistors over a range of frequencies (5 kHz, 50 kHz, 100 kHz, 200 kHz). The performance of the developed device is evaluated by analysing the error percentage, standard deviation, and precision of the device's impedance measurements. Additionally, linearity of the measurements is also evaluated to determine how well the measurements conform to a range of impedance measured. Tables and figures below present a comparison between the LCR meter and the developed device impedance measurement for various resistance values.

Table 4.2: Results of impedance measurement on passive loads at 5 kHz

Passive Loads (Ω)	LCR Meter (Ω)	Developed Device (Ω)	Error (%)	Standard Deviation	Precision (%)
100	99.52	99.99	0.47	0.002	0.002
300	306.20	306.95	0.25	0.009	0.003
500	500.90	503.00	0.42	0.009	0.002
700	722.60	725.35	0.38	0.009	0.001
1k	995.10	999.81	0.47	0.016	0.002

Table 4.3: Results of impedance measurement on passive loads at 50 kHz

Passive Loads (Ω)	LCR Meter (Ω)	Developed Device (Ω)	Error (%)	Standard Deviation	Precision (%)
100	99.51	99.93	0.42	0.001	0.001
300	306.20	306.82	0.20	0.009	0.003
500	501.00	502.78	0.36	0.010	0.002
700	722.60	725.04	0.34	0.020	0.003
1k	995.10	999.45	0.44	0.031	0.003

Table 4.4: Results of impedance measurement on passive loads at 100 kHz

Passive Loads (Ω)	LCR Meter (Ω)	Developed Device (Ω)	Error (%)	Standard Deviation	Precision (%)
100	99.51	99.88	0.37	0.012	0.012
300	306.20	306.67	0.16	0.013	0.004
500	500.90	502.57	0.33	0.039	0.008
700	722.60	724.66	0.29	0.049	0.007
1k	995.04	998.96	0.39	0.056	0.006

Table 4.5: Results of impedance measurements on passive loads at 200 kHz

Passive Loads (Ω)	LCR Meter (Ω)	Developed Device (Ω)	Error (%)	Standard Deviation	Precision (%)
100	99.50	99.55	0.05	0.058	0.058
300	306.10	305.83	0.09	0.198	0.066
500	500.90	501.23	0.07	0.218	0.043
700	722.50	722.78	0.04	0.289	0.041
1k	994.90	996.29	0.14	0.763	0.076

Table 4.6: Impedance measurement error for an impedance range of 100 Ω to 1 k Ω at 5 kHz, 50 kHz, 100 kHz, and 200 kHz

	5 kHz	50 kHz	100 kHz	200 kHz
100 Ω	0.47 %	0.42 %	0.37 %	0.05 %
300 Ω	0.25 %	0.20 %	0.16 %	0.09 %
500 Ω	0.42 %	0.36 %	0.33 %	0.07 %
700 Ω	0.38 %	0.34 %	0.29 %	0.04 %
1 k Ω	0.47 %	0.44 %	0.39 %	0.14 %

From Table 4.6, the impedance measurement error percentage is highest at 5 kHz compared to other frequencies. The error percentage decreases with increasing frequencies. This is due to the influence of BIS system resolution on smaller impedance (Jiang et al., 2019).

In summary, the results of the validation show that the error percentage of the developed device's impedance measurements is less than 0.5% for all resistors tested over the range of frequencies, indicating that the device is highly accurate in its impedance measurements. Additionally, the standard deviation of the measurements is less than 0.5% which indicates that the measurements are consistent and reliable. The precision of the measurements is also found to be less than 0.08%. Table 4.7 shows the summary of impedance measurement validation results on passive loads (resistors).

Table 4.7: Summary of impedance measurement validation results on passive loads (resistors)

Frequency (kHz)	Error (%)	Standard Deviation	Precision (%)
5	0.40	0.009	0.002
50	0.35	0.014	0.002
100	0.31	0.034	0.007
200	0.08	0.305	0.057

Table 4.7 demonstrates that the developed device is reliable and accurate in impedance measurements over the range of frequencies and can be used with confidence for intended

applications. The accuracy and precision of the device in measuring impedance of resistors is crucial as it will be used as a reference to measure bioimpedance of the human in the next step, which will give more accurate results of the tissue properties.

4.5.1.2 Capacitors

In this section, the performance of the developed device in phase angle measurement was evaluated by validating it against an LCR meter on capacitors over a range of frequencies (5 kHz, 50 kHz, 100 kHz, 200 kHz). The performance of the developed device is evaluated by analyzing the error percentage, standard deviation, and precision of the device's phase angle measurements. Tables below present a comparison between the LCR meter and the developed device phase angle measurement for selected capacitance values.

Table 4.8: Results of phase angle measurement on passive loads (capacitors) at 5 kHz

Passive Loads (uF)	LCR Meter (°)	Developed Device (°)	Error (%)	Standard Deviation	Precision (%)
0.01	- 89.00	- 89.08	0.09	0.002	0.002
0.001	- 89.49	- 89.55	0.07	0.010	0.011

Table 4.9: Results of phase angle measurement on passive loads (capacitors) at 50 kHz

Passive Loads (uF)	LCR Meter (°)	Developed Device (°)	Error (%)	Standard Deviation	Precision (%)
0.01	- 88.78	- 88.91	0.15	0.002	0.002
0.001	- 89.38	- 89.47	0.10	0.002	0.002

Table 4.10: Results of phase angle measurement on passive loads (capacitors) at 100 kHz

Passive Loads (uF)	LCR Meter (°)	Developed Device (°)	Error (%)	Standard Deviation	Precision (%)
0.01	- 88.68	- 88.79	0.12	0.009	0.010
0.001	- 89.33	- 89.42	0.10	0.003	0.003

Table 4.11: Results of phase angle measurement on passive loads (capacitors) at 200 kHz

Passive Loads (uF)	LCR Meter (°)	Developed Device (°)	Error (%)	Standard Deviation	Precision (%)
0.01	- 88.53	- 88.60	0.08	0.009	0.011
0.001	- 89.24	- 89.22	0.03	0.010	0.011

In conclusion, the results of the phase angle measurement on capacitors using the developed device have shown high level of accuracy and precision with error percentage less than 0.15 %, standard deviation of less than 0.01 and precision of less than 0.01 %. These results indicate that the developed device is reliable and accurate tool for measuring phase angle of capacitors over a range of frequencies. The comparison between the LCR meter and the developed device phase angle measurement for various capacitance values further support this.

4.5.1.3 Electrical Circuit Model of Human Upper Arm

In BIS, the electrical current travelling through the huma body can be modelled as a single-dispersion RC circuit model or the Fricke's equivalent electrical circuit model (Songkakul et al., 2021). R_0 represents the extracellular fluid in parallel with R_∞ and C_m that represents intracellular fluid and cell membrane capacitance as shown in Figure 2.21. The impedance of the electrical circuit model can be expressed as Equation 2 – 12.

The purpose of this validation study was to evaluate the accuracy and reliability of the bioimpedance measurements obtained using the developed device on electrical models of the human upper arm. The results of the validation study including a comparison of the

bioimpedance measurements and estimated resistances (R_0 and R_∞) obtained using the developed device and LCR meters are presented in this section. 3 different models of the human upper arm were created by using a range of resistor and capacitor values, specifically 150 to 500 Ω for R_0 and R_∞ and 0.01 μF for membrane capacitance (C_m) to represent the bioimpedance values of both healthy and lymphedema-affected upper limb tissue as shown in Table 3.4. These values were chosen based on previous study by Santoso *et al.* and Zhuang *et al.* (Santoso *et al.*, 2020; Zhuang *et al.*, 2022).

The human tissue model was measured using an LCR meter at 800 mVpp and at frequency of 20 Hz, 100 Hz, 300 Hz, 500 Hz, 1 kHz, 3 kHz, 5kHz, 10 kHz, 50 kHz, 100 kHz, 150 kHz, 200 kHz, 300 kHz, 500 kHz, and 1 MHz. The impedance measurements at each frequency were set as a reference value. The developed device was then used to measure the human tissue model at a frequency sweep from 300 Hz to 200 kHz. The measurements were repeated 3 times to obtain the device's precision and standard deviation.

In this study, the Impedance plane or Cole – Cole plot was utilized to evaluate the electrical response of developed device on the human tissue models at different frequencies. The Cole plot is a graphical representation of complex impedance data and is used to analyse bioimpedance measurements. The plot is created by plotting the real part of the impedance (Z') against the imaginary part of the impedance (Z'') at different frequencies. The shape of the plot can be used to identify the type of tissue being measured and is useful for detecting changes in the tissue over time.

Practically, determining the Cole parameters of R_0 and R_∞ directly is impossible due to technical and safety limitations. Instead, the Cole parameters are estimated by extrapolating and fitting the BIS measured data with the Cole resistance mathematical model (Equation 2 – 14) over a practical frequency range. The BIS measured data is fitted

using Non-linear Least Squares (NLLS) fitting. The frequency values were used as independent variable for estimating the Cole parameters. The BIS measured data were analysed to extract the R_0 and R_∞ parameter according to Section 3.3.3.

In order to evaluate the performance of the developed device in estimating the resistances (R_0 and R_∞) in the human tissue model, R-squared and Root Mean Square Error (RMSE) statistical measures were used. R-squared is a measure of how well the NLLS regression model approximates the real data points. The R-squared value ranges from 0 to 1, with 0 indicating that the model explains none of the data points and 1 indicating that the model is a perfect fit. RMSE is a measure of the difference between the estimated values and reference values and is expressed in the same units as the measurements. A lower RMSE value indicated a better fit. Both statistical techniques were used to determine how well the developed device's measurements matched the reference values obtained from LCR meter, providing an assessment of the device's accuracy and reliability in estimating R_0 and R_∞ . The findings of the study are presented through graphical and tabular representations in the following figures and tables.

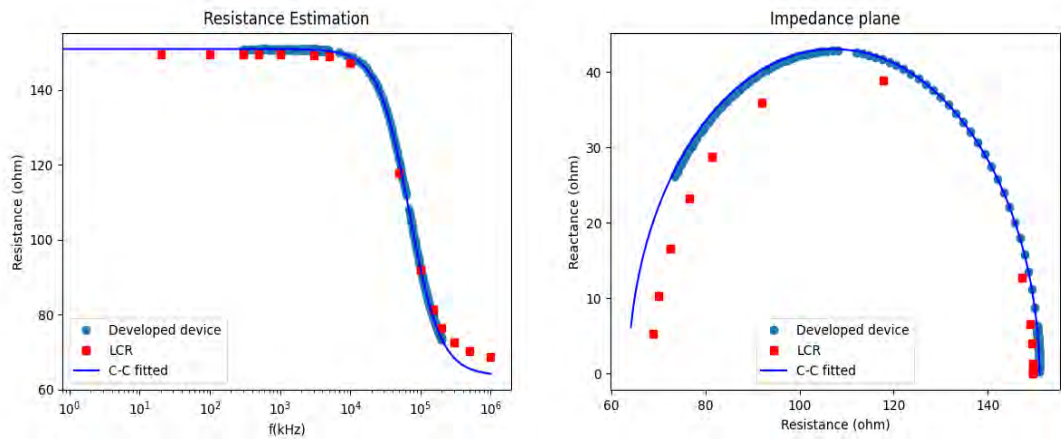


Figure 4.25: Resistance estimation and Impedance plane (Cole – Cole plot) of Set 1

Table 4.12: Results of human upper arm model (Set 1)

Parameter	LCR Meter (Ω)	Developed Device (Ω)	Error (%)	RMSE (Ω)	R-squared	Standard Deviation	Precision (%)
R_0	149.64	151.005	0.92	1.809	0.999	0.004	0.003
R_∞	68.47	63.66	7.02			0.005	0.007

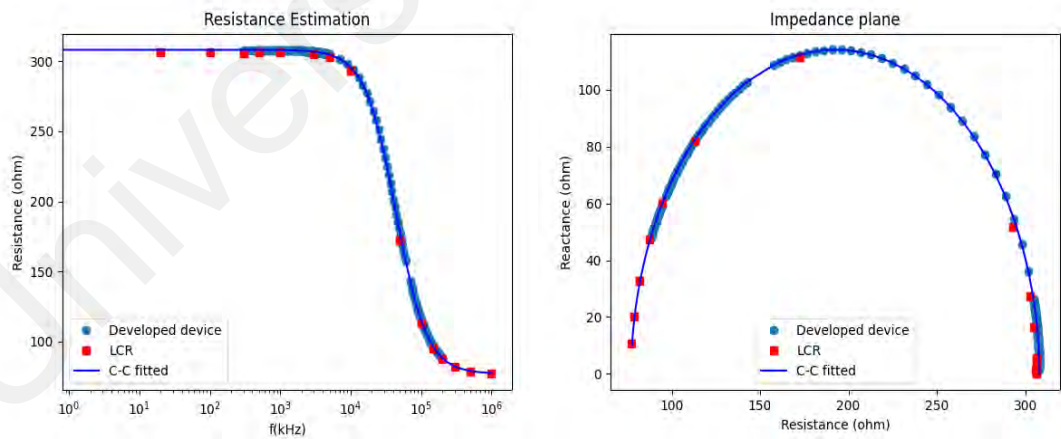


Figure 4.26: Resistance estimation and Impedance plane (Cole – Cole plot) of Set 2

Table 4.13: Results of human upper arm model (Set 2)

Parameter	LCR Meter (Ω)	Developed Device (Ω)	Error (%)	RMSE (Ω)	R-squared	Standard Deviation	Precision (%)
-----------	------------------------	-------------------------------	-----------	-------------------	-----------	--------------------	---------------

R_0	306.35	308.13	0.58	2.553	0.9999	0.004	0.001
R_∞	76.55	76.91	0.47			0.014	0.018

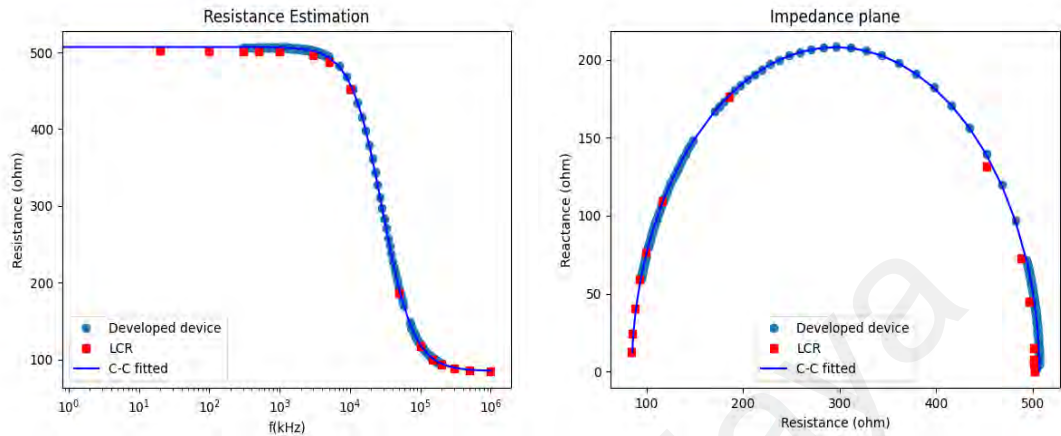


Figure 4.27: Resistance estimation and Impedance plane (Cole – Cole plot) of Set 3

Table 4.14: Results of human upper arm model (Set 3)

Parameter	LCR Meter (Ω)	Developed Device (Ω)	Error (%)	RMSE (Ω)	R-squared	Standard Deviation	Precision (%)
R_0	501.74	507.10	1.07	5.032	0.99995	0.034	0.007
R_∞	83.90	84.83	1.11			0.070	0.082

The graphical interpretation of the results indicated that the obtained electrical response of the electrical circuit model is accurate and consistent with the Cole – Cole plot expected electrical behavior (Powles, 1993). The shape of the plot indicates that the measured values are in agreement with the standard values with the lowest RMSE value of 1.809 Ω in Set 1 and highest RMSE value of 5.032 Ω in Set 3. The overall mean resistances estimation error percentage for R_0 is 0.85% and R_∞ is 2.87%. These results are in line with the findings of Santoso *et al.* reported a mean resistance estimation error of 1.06% for R_0 in their study (Santoso *et al.*, 2020). The BIS system developed by Songkakul *et al.* to monitor hydration status obtained a mean resistance RMSE of 0.971

Ω tested on the Fricke's equivalent circuit model at frequencies of 5 kHz to 195 kHz. However, unlike this study, their research did not estimate resistance for R_0 and R_∞ (Songkakul et al., 2021). The highest estimated resistance error percentage for R_∞ was found to be 7.02% in Set 1, which is attributed to the limited ability of the developed BIS system to measure lower impedances. Despite this limitation, this study primarily focused on the measurement of R_0 to assess the lymphatic fluid.

The results of this study have revealed a strong correlation between the measured data and the predicted data, as evidence by the high R-squared value of 0.999 for all three sets. This suggests a reliable and accurate fit between the two data sets, with a low standard deviation of less than 0.07 and a high precision of less than 0.08.

In conclusion, the impedance spectrum measurements on the electrical circuit model of the human upper arm obtained were accurate and consistent with the expected electrical behavior, as demonstrated by the graphical interpretation of the results. The mean resistances estimation error percentage for R_0 was found to be comparable with previous studies. The high R-squared value indicates a strong curve fit between the measured data and the predicted data. Although the developed BIS system showed limitations in measuring lower impedances, it was still able to provide meaningful results for the estimation of R_0 using practicable range of frequencies of 300 Hz to 200 kHz. These results collectively demonstrate that the developed device is a reliable and accurate tool for estimating R_0 .

4.5.2 Validation with Healthy Participants

The developed device was benchmarked with the commercial bioimpedance analyser Quadscan 4000 by measuring the bioimpedance of the arms of 45 healthy participants. The measurements were collected at frequencies of 5 kHz, 50 kHz, 100 kHz, and 200 kHz

using both Quadscan 4000 and the developed device. The measurements were collected in two rounds with an interval of 5 minutes between each round.

The results were analysed using paired t-test and the bioimpedance mean differences between both analysers were calculated. The significance values and bioimpedance mean differences between the two analysers are presented in Table 4.15.

Table 4.15: Bioimpedance analysers benchmarking

Frequency	p – value	Bioimpedance means difference (Ω)
5 kHz	0.074	1.215
50 kHz	0.091	1.408
100 kHz	0.880	-0.119
200 kHz	0.091	-0.398

These results imply that the bioimpedance measurement obtained from the developed device is equivalent to those obtained from the commercial Quadscan 4000 bioimpedance analyser. These results are consistent with the findings of Cannon *et al.*, who developed a segmental BIS analyser for body composition measurement and found that the bioimpedance values from their device were within 10% of the reference device, BodyStat Multiscan 5000 and Impedimed SFB7 (Cannon & Choi, 2019).

Overall, these validation study suggest that the developed device provides reliable and accurate bioimpedance measurements, comparable to those obtained by Quadscan 4000. This demonstrates the validity and reliability of the developed device for measuring bioimpedance in human body.

4.5.3 Estimation of Cole Parameters on Healthy Participant and UBCRL patient

The estimation of Cole parameters based on bioimpedance measurements was conducted on both healthy participant and UBCRL patient in their upper limbs. The R_0

obtained for healthy participant is 346Ω while the R_0 obtained for the UBCRL patient's upper limb is 414Ω . The coefficient of determination (R-squared) was calculated to determine the relationship between the estimated and real values to assess the accuracy of the estimation. The obtained R-squared value was 0.9999, indicating a strong correlation between estimated and real values. This high R-squared value suggests that the NLLS fitting method accurately captured the underlying trends in the data.

The raw BIS measured data collected during the study are represented in Figure 4.28, Figure 4.29, Figure 4.32, and Figure 4.33. Each data points in the figures corresponds to a measured impedance value at different frequencies. The orange line in , Figure 4.30, Figure 4.31, Figure 4.34, and Figure 4.35 represents the estimated resistance value and the Cole – Cole plot obtained using the NLLS fitting method. The estimated values are plotted alongside the raw measured data, showing the fit of the model to the data.

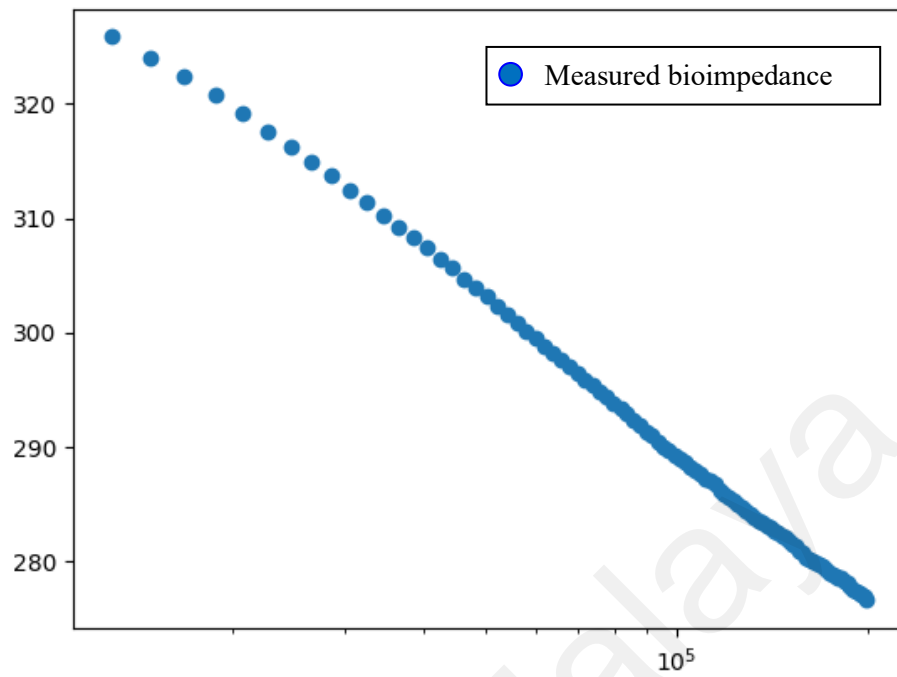


Figure 4.28: Resistance versus frequency of a healthy participant (Subject 45) upper limb

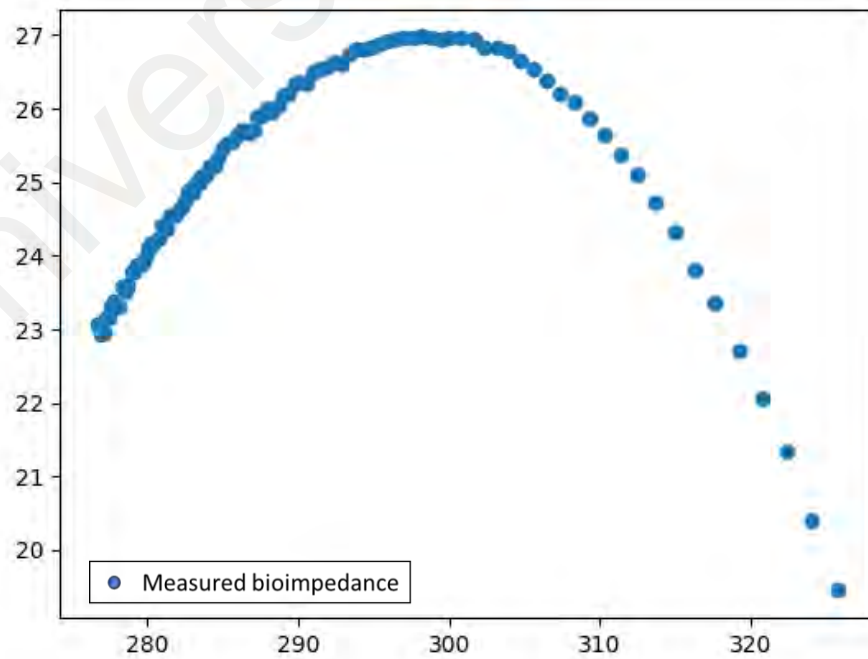


Figure 4.29: Resistance versus imaginary of a healthy participant (Subject 45) upper limb

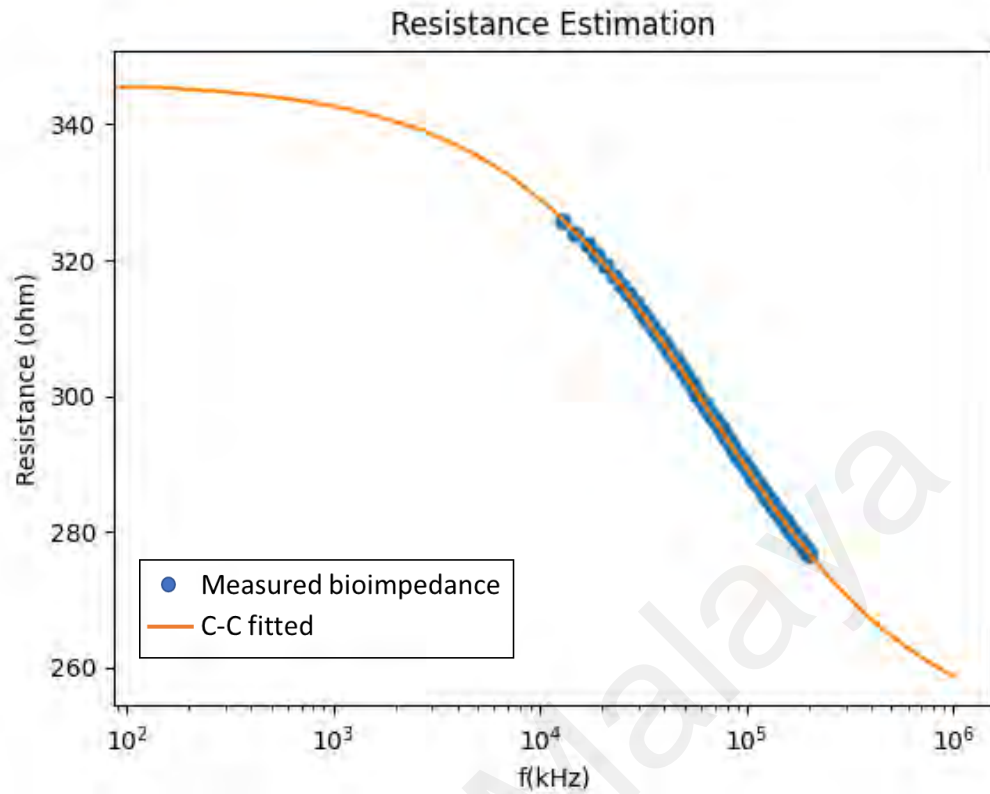


Figure 4.30: Estimated resistance (R_0 and R_∞) of a healthy participant (Subject 45) upper limb

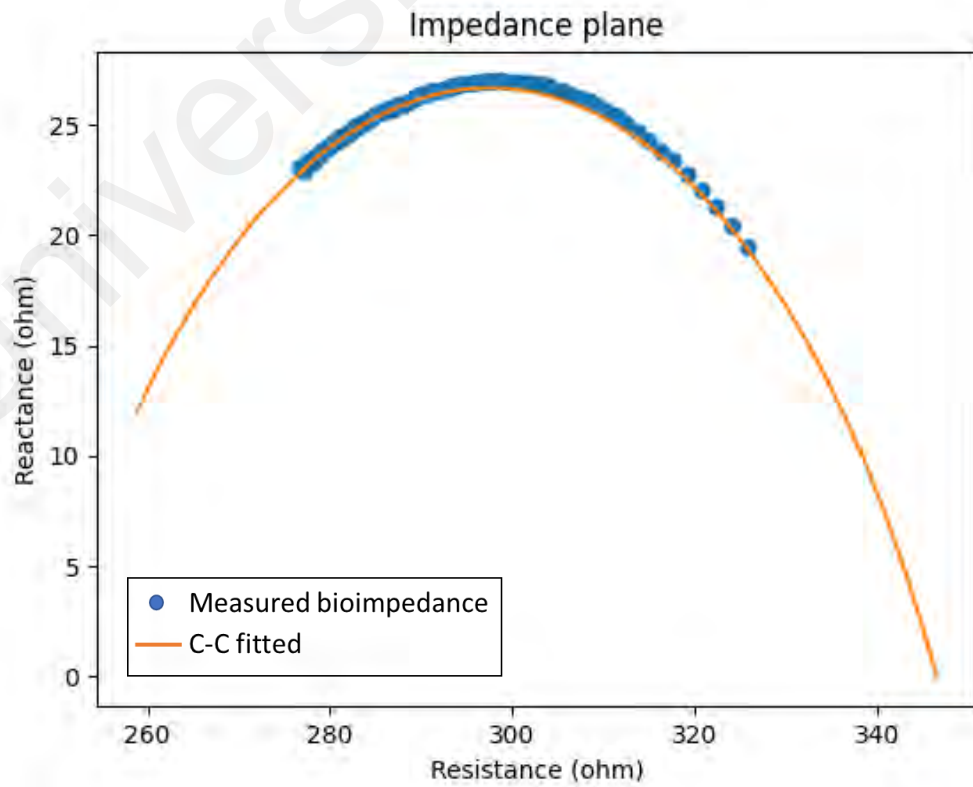


Figure 4.31: Cole – Cole plot of a healthy participant (Subject 45) upper limb

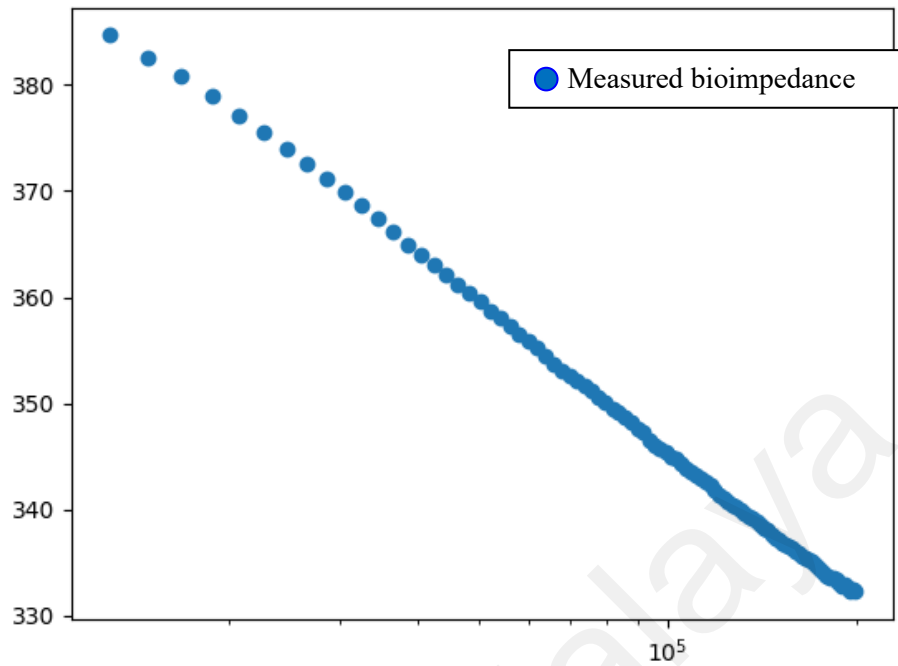


Figure 4.32: Resistance versus frequency of a UBCRL Stage 1 patient (Subject 98) upper limb

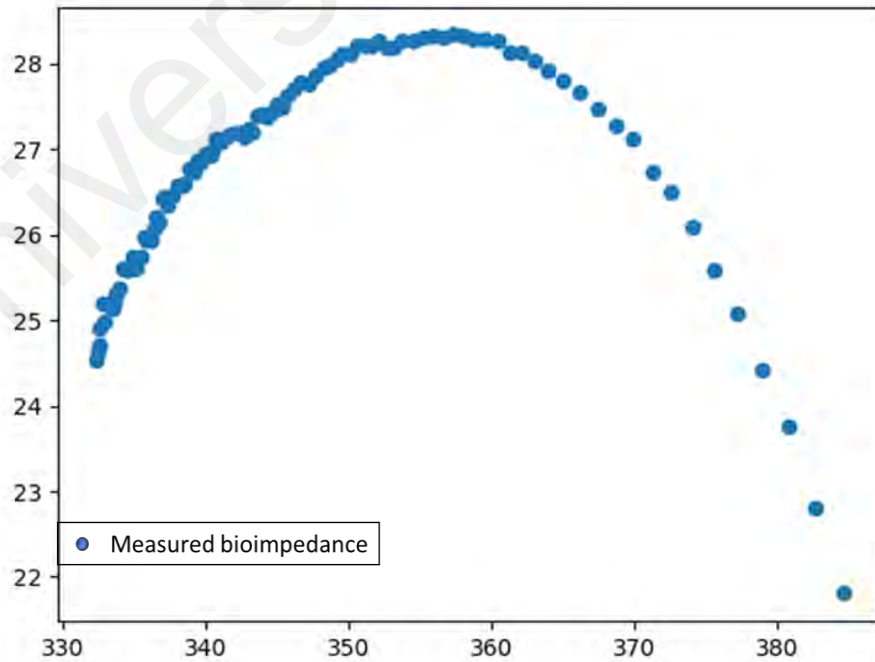


Figure 4.33: Resistance versus imaginary of a UBCRL Stage 1 (Subject 98) upper limb

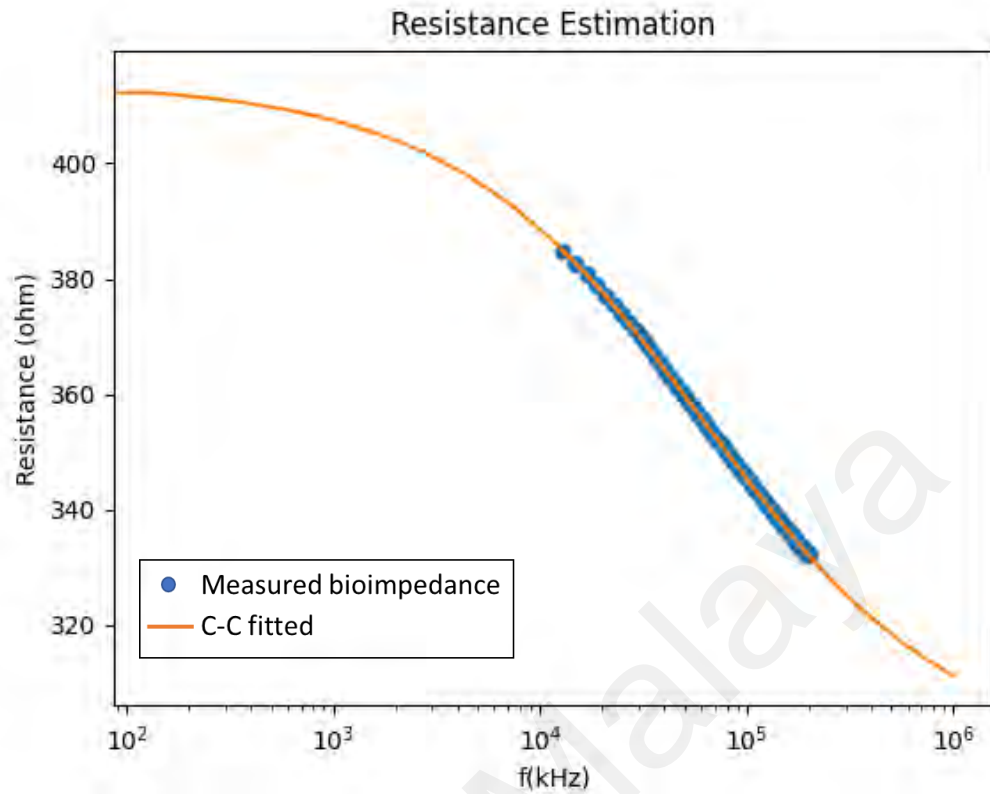


Figure 4.34: Estimated resistance (R_0 and R_∞) of a UBCRL Stage 1 (Subject 98) upper limb

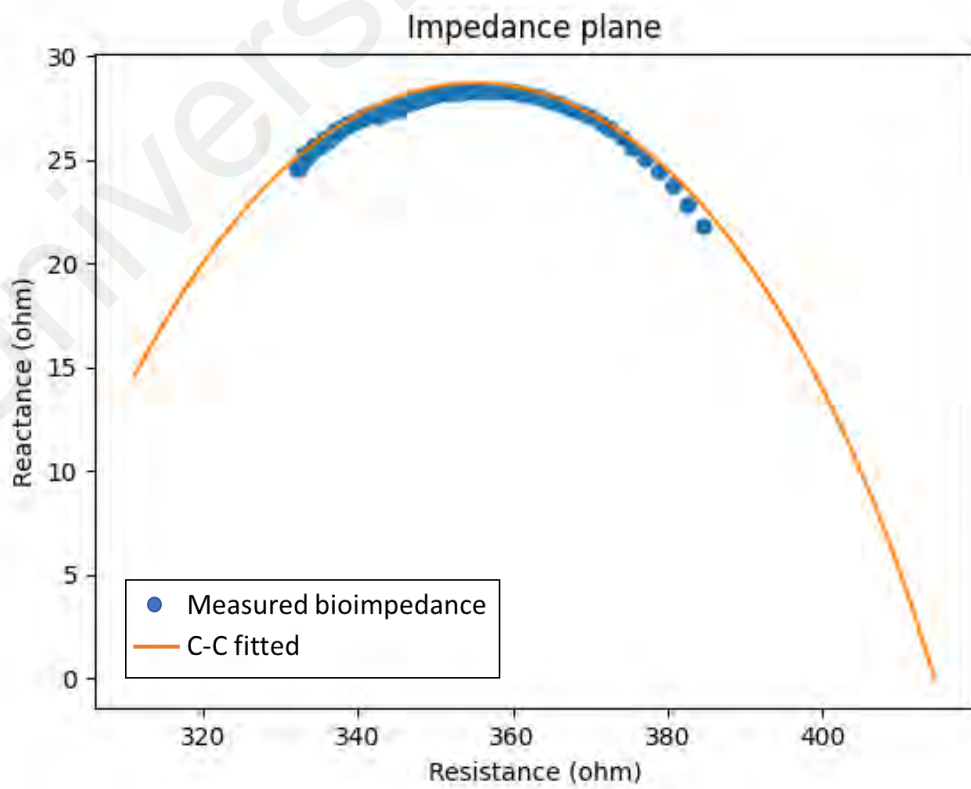


Figure 4.35: Cole – Cole plot of a UBCRL Stage 1 (Subject 98) upper limb

Overall, this investigation demonstrates the successful estimation of Cole parameters through bioimpedance measurements on both healthy participant and UBCRL patient. The strong correlation between the estimated and real values, as well as the effective model fit, underscore the reliability and potential utility of the NLLS fitting method in characterizing tissue impedance behaviour in these individuals.

4.5.4 Clinical Validation

The clinical validation process involved several key steps to ensure the validity and reliability of the results. These steps included obtaining ethical approval, selecting participants, establishing study protocols, and conducting statistical analysis. The participants in this study consisted of both healthy individuals and unilateral breast cancer (UBC) patients who were recruited from the University of Malaya Medical Center (UMMC). The aim of the clinical validation was to evaluate the performance of the developed device in measuring the arm bioimpedance of different populations.

4.5.4.1 Ethics Application

Ethical approval for this study was obtained from the Medical Research Ethics Committee, UMMC (MREC ID No.:2020316-8181). All participants provided written informed consent prior to participating in the study.

4.5.4.2 Selection of Participants

This study recruited two groups of volunteered women. Healthy ($n = 45$) and UBC ($n = 100$) who were referred to the outpatient clinic at UMMC for lymphedema treatment. The UBC participants comprised of three different stages of BCRL, including Stage 0 ($n = 55$), Stage 1 ($n = 27$), and Stage 2 ($n = 18$).

The criteria in the selection of participants process are as in Section 3.5.3.2(a) and 3.5.3.2(b). This study included participants over 18 years of age. Participants who were

pregnant or had cardiac or metal implants in the upper limbs were excluded from the study. Specifically, the exclusion criteria for healthy participants are women with history of breast cancer, BCRL and any medical conditions that could influence upper limb volume. For the UBC participants, women who are diagnosed with bilateral BCRL were excluded. Detailed information regarding the participants characteristics and UBC clinical characteristics are presented in Table 4.16 and Table 4.17.

Table 4.16: Participant characteristics

Characteristic	Healthy group (n = 45)	UBC group (n = 100)
Age	45.5 ± 18.2	59.3 ± 10.2
Dominant arm (Right: Left)	42: 3	81: 9
Affected limb (Dominant: Non-dominant)	-	54: 46

Table 4.17: UBC participants clinical characteristics

Clinical characteristic	Stage 0 (Subclinical)	Stage 1 (Mild)	Stage 2 (Moderate)
Dominant limb affected	30	16	8
Non-dominant limb affected	25	11	10
Surgery			
Mastectomy	42	17	11
Breast conservation	9	8	1
Mastectomy	42	17	11
Breast conservation	9	8	1

4.5.4.3 Clinical Measurements

Clinical assessments and classification of lymphedema were performed by trained UMMC physiotherapists. The classification of lymphedema is based on the physical examination and comparison of the circumferential upper limb volume. Stage 0 exists

after surgery or radiation due to a damaged lymphatic system. In this stage, UBC participants are asymptomatic and show no clinical signs of lymphedema. Stage 1 UBC participant is characterized with mild lymphedema and circumferential inter–arm volume differences of 2 cm to 3 cm. In Stage 2, UBC participant is presented with moderate lymphedema with circumferential inter–arm volume differences of 3 cm to 5 cm (Ayre & Parker, 2019).

The developed device was used to measure the bioimpedance of healthy and UBC participants' arms. The inter-arm R_0 ratio for UBC participants were determined by dividing the R_0 values of the unaffected and affected arms. As for healthy participants, the inter-arm R_0 ratio were evaluated by dividing R_0 values of non-dominant and dominant arms.

The results of the bioimpedance measurements were analysed using independent *t*-test to determine the significant difference of inter-arm ratios between participants in healthy and Stage 0 (Category 1), healthy and Stage 1 (Category 2), Stage 0 and Stage 1 (Category 3), and Stage 1 and Stage 2 (Category 4). The significant values of the different categories are summarized in Table 4.18.

The boxplots were used to further visualize the distribution of the data as illustrated in Figure 4.36. A confidence intervals (CI) table was generated based on the boxplots to observe different R_0 ratio values in healthy and different stages of BCRL. Summarizes the mean, standard deviation, minimum and maximum R_0 values within 95% level of confidence, providing an estimate of the range within which the true population value is likely to fall.

Table 4.18: Statistical analysis of inter-arm R_0 ratios of healthy and UBC participants

Category	Group comparison	Dominant Affected (p – value)	Non-dominant Affected (p – value)
1	Healthy and Stage 0	0.63	0.63
2	Healthy and Stage 1	0.001	0.001
3	Stage 0 and Stage 1	0.001	0.001
4	Stage 1 and Stage 2	0.001	0.001

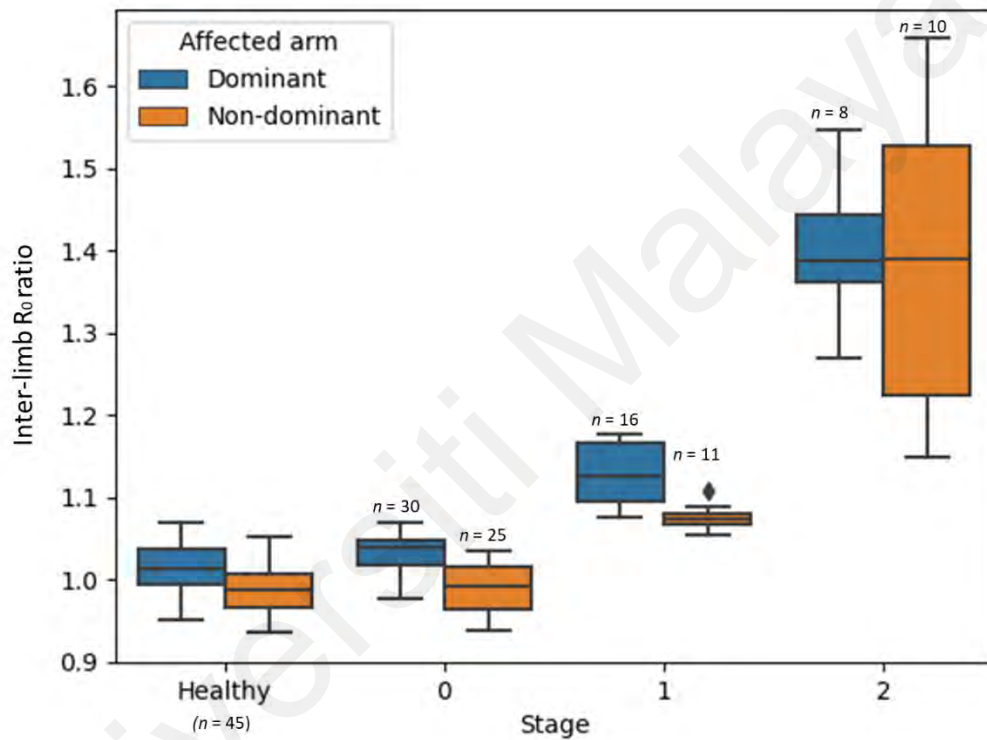


Figure 4.36: Inter-arm R_0 ratios in healthy and UBC participants with different stages of BCRL

Table 4.19: Descriptive Statistics and Confidence Intervals of Inter-arm R_0 ratios in Healthy and UBC participants with different stages of BCRL

Group	Dominant Affected			Non-dominant Affected		
	Mean	Standard Deviation	95% CI	Mean	Standard Deviation	95% CI
Healthy	1.015	0.031	(0.953, 1.077)	0.985	0.031	(0.923, 1.047)
Stage 0	1.034	0.021	(0.992, 1.076)	0.989	0.029	(0.932, 1.048)
Stage 1	1.145	0.035	(1.075, 1.215)	1.076	0.014	(1.048, 1.104)
Stage 2	1.394	0.090	(1.214, 1.574)	1.447	0.172	(1.104, 1.791)

The developed device demonstrated the ability to distinguish between healthy individuals and different stages of BCRL. The inter-arm R_0 ratios measured have shown significant difference in Category 2 ($p < 0.001$), Category 3 ($p < 0.001$), and Category 4 ($p < 0.001$). The inter-arm R_0 ratios in Category 1 were comparable ($p = 0.63$) with overlapping confidence intervals as shown in Figure 4.36. However, for Stage 1 and Stage 2, the median inter-arm R_0 ratios are clearly different, and the ranges do not overlap.

The inter-arm bioimpedance ratios in Stage 1 and Stage 2 UBC participants were found to be significantly different from those in healthy and Stage 0 participants. This difference can be attributed to the accumulation of lymph fluid in the affected arm, leading to a smaller bioimpedance value. Thus, the greater the lymph fluid accumulation in the affected arm, the larger the inter-arm R_0 ratio (L. C. Ward, 2015). On the other hand, the inter-arm R_0 ratios between healthy and Stage 0 participants were comparable, as lymphedema in Stage 0 is latent and only causes heavy sensations or numbness in the affected arm, but does not cause visible swelling (Yildiz et al., 2022). The results of the bioimpedance measurements demonstrated that the inter-limb R_0 ratio increases with the progression of BCRL stages. This finding provides evidence that the inter-limb R_0 ratio has the potential to be used for BCRL classification. However, it is important to note that additional data and research is needed to further validate these results and determine the optimal thresholds for BCRL classification using the developed device.

The results obtained in this study represents a clinically significant outcome, offering clinicians and patients the ability to use this approach for early lymphedema detection and treatment intervention.

4.5.5 Determination of Unilateral Upper Limb Lymphedema Detection Threshold

In this study, the R_0 ratios for the assessment of unilateral BCRL patients were determined using the developed system on a sample of 45 healthy Malaysian women. The

lymphedema detection was determined based on 2 standard deviations (SD) above the normative mean, as recommended by a study by Dylke *et al.* The findings of this study suggest that using 2SD threshold rather than a 3SD threshold has a higher sensitivity and specificity for identifying women with mild to moderate lymphatic changes as determined by lymphoscintigraphy (E. Dylke *et al.*, 2016). Furthermore, 2SD threshold has been widely adopted by other studies (Ridner *et al.*, 2009; LC Ward *et al.*, 2011).

The mean and standard deviation for the inter-arm R₀ ratio (non-dominant: dominant) was 1.015 ± 0.031 . The standard deviation in this study is lower than that observed by Cornish *et al.* (0.034) and Ridner *et al.* (0.041). The R₀ratio mean values are closer to unity compared to those of Cornish *et al.* (1.037) (BH Cornish *et al.*, 2001). The normative inter-arm R₀ ratio value is approximately similar to LC Ward *et al.* (1.014).

In this study, the presence of lymphedema is indicated when the R₀ ratio exceeded 1.077 when the dominant limb is at risk and 1.047 when the non-dominant limb is at risk. The detection threshold was found to be comparable to Ridner *et al.* which was 1.078 and 1.040, respectively. A comparison of normative R₀ ratios for the detection of lymphedema is presented in Table 4.20.

In conclusion, the new lymphedema detection threshold for the assessment of unilateral BCRL by the developed system in the Malaysian population has been determined. It is concluded that in accord with the observations of Ridner *et al.* and LC Ward *et al.* findings. The results suggest that the threshold may be used with confidence as markers for lymphedema and may offer a new approach for the early detection and treatment of BCRL in Malaysian population.

Table 4.20: Comparison of normative R_0 ratios for the detection of lymphedema

Researchers	Healthy women population						Lymphedema detection threshold	
	Mean		Standard Deviation	Age	Number of subjects	Country	Dominant affected	Non-dominant affected
	Dominant	Non-dominant						
(BH Cornish et al., 2001)	1.037	0.964	0.034	27 – 84	60	Australia	1.105	1.032
(Ridner et al., 2009)	1.024	0.986	0.027	> 18	60	United States	1.078	1.040
(LC Ward et al., 2011)	1.014	0.986	0.041	18 – 86	172	Australia	1.117	1.048
Jung <i>et al.</i> (2018)								
Resistance at 1 kHz	1.011	0.990	0.029	49.6 ± 9.0	643	Korea	1.050	1.046
Resistance at 5 kHz	1.013	0.998	0.030				1.070	1.030
Liu <i>et al.</i> (2021)	1.012	0.989	0.028	53.7 ± 12.8	1305	China	1.068	1.047
Developed system	1.015	0.985	0.031	27 – 63	45	Malaysia	1.077	1.047

4.6 Cost Analysis

In this section, a cost analysis is conducted to estimate the pricing of various components and modules involved in the project. The analysis aims to provide an overview of the cost implications and help determine the price of one system based on production quantity of 100 units. The table below summarizes the modules and components with their respective prices.

Table 4.21: Cost analysis of the lymphedema diagnosis and monitoring system

Module/Components	Material/Platform	Price per unit (RM)
Microcontroller	EVAL-ADICUP3029	251.60
Bioimpedance analyser module	PCB	159.40
Battery	AAA	1.40
Electrodes	Ag/AgCl gel	3.30
3D Casing	PLA	3.50
Bluetooth	Adafruit Feather nRF52840	91.00
Cloud Server	Firebase	1.00
Total (RM)		511.20

The cost of each module and component is based on market prices and estimates. The microcontroller, ADuCM3029, provides the main processing unit for the system. The bioimpedance analyser module costs RM160 per board. The power supply consists of two AAA batteries. Six Ag/AgCl gel electrodes are used for one lymphedema measurement. The 3D casing is made using PLA filament. The Bluetooth module is the Adafruit Feather nRF52840. The cloud server module is implemented using Firebase and are set up under the Blaze plan. The Blaze plan provide flexible and scalable options for developers and businesses. It offers a pay-as-you-go model, allowing users to pay for the resources and services they consume. It should be noted that the prices provided are estimates and vary depending on factors such as supplier, location, and production volume.

4.7 Comparison with Commercial BIA Analysers

In comparison to other commercial BIA analysers currently available in the market, the developed system (Mobilymph) offers significant advantages in terms of costing while remaining comparable in terms of other specifications. Table 4.22 provides a clear comparison between Mobilymph system and selected commercial BIS analysers.

Examining Mobilymph in relation to other BIS analysers, several critical factors can be observed. Firstly, in terms of frequency range, the other analysers cover a range of 3 kHz to 1000 kHz. In contrast with Mobilymph that covers a narrower range of 5 kHz to 200 kHz. Despite this difference, Mobilymph addresses the limitation by utilizing the estimation of Cole parameters, providing a comprehensive spectrum for lymphedema assessment.

Secondly, Mobilymph distinguishes itself with its compact dimensions of 14 x 5 x 8 cm, making it highly portable and user-friendly. This smaller size enables easy transportation and usage in various settings, such as homes, hospitals, outpatient clinics and physician offices. In contrast, the larger dimensions of the other devices may limit their portability and practicality in different environments.

Furthermore, the measurement position is another important aspect to consider. While the commercial analysers offer measurements in supine and standing position, Mobilymph allows measurements to be taken in sitting position.

While Mobilymph has a measurement speed of less than 30 seconds, which is slightly slower than the other analysers' measurement speeds of less than 1 second, it still offers a reasonable speed that meets practical requirements.

In terms of lymphedema management, Mobilymph provides a comprehensive solution with its smartphone application and cloud platform integration. These features facilitate

early diagnosis and enable healthcare professionals to monitor patients remotely. The smartphone application allows users to visualize and analyse their lymphedema data conveniently, empowering them to take an active role in their own management. The cloud platform integration ensures secure storage and easy access to data, promoting seamless collaboration between patients and healthcare providers. This combination of smartphone application, cloud platform, and remote monitoring capabilities sets Mobilymph apart from the other devices in terms of supporting effective lymphedema and early diagnosis.

Lastly, cost is a significant consideration. Mobilymph offers a much more affordable option compared to the other commercial BIS analysers, with a price of only RM511.20. In comparison, the other devices have significantly higher prices, ranging from RM 31,432.50 to RM 44,130.89.

In summary, Mobilymph stands out as a cost-effective solution that provides a comprehensive frequency range, smartphone application integration, cloud platform and remote monitoring capabilities, and the flexibility for use in various healthcare settings. This versatility empowers users to monitor their lymphedema condition conveniently within their own homes. These advantages make Mobilymph a favourable choice for lymphedema assessment compared to the other commercial BIS analysers.

Table 4.22: Comparison of Commercial BIA Analysers with Mobilymph

BIA Device	SOZO	SFB7	L-Dex U400	Quadscan 4000	Mobilymph
Frequency Scan	3 kHz to 1000 kHz	4 kHz to 1000 kHz	3 kHz to 1000 kHz	5, 50, 100, 200 kHz	5 kHz to 200 kHz
Dimensions (length x width x height) cm	64.8 x 44.5 x 129.8	19 x 13 x 11	19 x 13 x 11	24 x 15 x 3.5	14 x 5 x 8
Measurement Position	Stand-On	Supine	Supine	Supine	Sitting
Number of electrodes	8	4	4	4	4
Measurement speed	Less than 30 seconds	Less than 1 second	Less than 1 second	Less than 30 seconds	Less than 30 seconds
Smartphone Application	Present	Absent	Absent	Absent	Present
Cloud Platform	Present	Absent	Absent	Absent	Present
Remote monitoring	Absent	Absent	Absent	Absent	Present
Price	RM 44130.89	RM 31,432.50	RM 41,372.71	RM 14,183.23	RM 511.20

4.8 Summary

In this chapter, the development and evaluation of the unilateral BCRL diagnosis and monitoring system were presented. The hardware module, consisting of the microcontroller, bioimpedance analyser module, power supply unit, electrodes and 3D casing was developed and described in detail. The data acquisition and transmission module, including the microcontroller and Bluetooth, was also developed to enable data communication. Additionally, the smartphone application module, with its various screens and navigation flowchart, was created to provide a user-friendly interface for lymphedema measurement. The cloud server module, incorporating cloud functions and the Firestore database, was developed to enable data storage and remote monitoring. The firmware module and the estimation of Cole parameters were also discussed. The estimation of Cole parameters on BIS measured data showed a high level of accuracy and reliability with an R-squared value of 0.999.

The functionality of the device was verified through validation experiments with passive loads, including resistors and capacitors, as well as through validation with healthy participants. The results of the validation demonstrated that the developed device exhibited highly accurate impedance measurements with an error percentage and standard deviation of less than 0.5%. The precision of the measurements was also found to be less than 0.08%. The phase angle measurement on capacitors showed high accuracy and precision, with an error percentage of less than 0.15%, a standard deviation and precision of less than 0.01%. The measurements obtained from electrical circuit model of human upper arm showed agreement with the standard values, with low RMSE values. The overall mean resistances estimation error percentage for R_0 and R_∞ was found to be 0.85% and 2.87% respectively. The results indicated a reliable fit between the measured and predicted data, with a high R-squared value of 0.999 and low standard deviation and precision values.

Validation with healthy participants demonstrated that the bioimpedance measurements obtained from the developed device were equivalent to those obtained from the commercial Quadscan 4000 bioimpedance analyser, with negligible bioimpedance means and statistical differences.

The device was also clinically validated, involving ethics applications, participant selection, and clinical measurements. The developed device demonstrated the ability to distinguish between healthy individuals and different stages of BCRL. The inter-arm R_0 ratios measured have shown significant difference in Healthy and Stage 1 ($p < 0.001$), Stage 0 and Stage 1 ($p < 0.001$), and Stage 1 and Stage 2 ($p < 0.001$). The inter-arm R_0 ratios in Healthy and Stage 0 were comparable ($p = 0.63$).

The unilateral upper limb lymphedema detection threshold in Malaysian women population was determined with the R_0 ratio exceeded 1.077 when the dominant limb is at risk and 1.047 when the non-dominant limb is at risk.

The developed system cost is RM511.20 which is more affordable compared to the commercial BIS analysers. A comparison with commercial BIS analysers highlighted the advantages of developed system in terms of costing, frequency range, dimensions measurement position, measurement speed, and advanced lymphedema management capabilities facilitated by smartphone application and cloud platform integration. These features set the developed system apart, providing a cost-effective and comprehensive solution for lymphedema assessment and management. In addition, current commercial bioimpedance analysers do not have a custom made for UBCRL diagnosis and monitoring system embedded in it.

In summary, this chapter presented the results and evaluation of the Unilateral BCRL diagnosis and monitoring system. The findings are significant in the field of lymphedema

diagnosis and monitoring as they suggest the potential for early diagnosis using the developed system. This early detection capability has important implications for time intervention and management of lymphedema.

Universiti Malaya

CHAPTER 5: CONCLUSIONS AND RECOMMENDATION FOR FUTURE

WORK

5.1 Conclusion

A unilateral breast cancer-related lymphedema diagnosis and monitoring system using bioimpedance analysis and smartphone application (Mobilymph) has been successfully developed.

This thesis has made major contributions to UBCRL diagnosis and monitoring. To our knowledge, this is the first UBCRL system that is a non-invasive, portable, and cost-effective system that can accurately diagnose and monitor UBCRL patients. The developed system is sensitive and can differentiate between healthy and lymphatic arms ($p < 0.001$). Patients suffering from UBCRL can now obtain precise assessments of their lymphatic changes at their convenience.

Furthermore, the integration of a smartphone application makes it a highly effective approach to patient care, promoting remote UBCRL monitoring. This application allows patients to monitor their lymphedema status at home, allowing for early intervention in worsening conditions.

This research also contributes to identifying the UBCRL detection threshold specific for the UBCRL Malaysian patients (1.077 for dominant affected arm and 1.047 for non-dominant affected arm). This contribution enhances the accuracy and applicability of BCRL assessment in this demographic group.

In conclusion, the contribution of this thesis includes the development of a portable and low-cost UBCRL diagnosis and monitoring system, the determination of BCRL detection thresholds in UBCRL Malaysian patients, and the remote monitoring system

for UBCRL. This enhances patient care, early intervention, and provides a better understanding of UBCRL management.

5.2 Limitation and Recommendation for Future Work

The limitation of this study is the small sample size of the patients which may impact the generalisability of the findings. Additionally, the BCRL diagnosis and monitoring system developed in this study focused only on unilateral cases, potentially limiting its applicability to bilateral BCRL cases.

To address these limitations and further enhance the scope and impact of future research, several improvements can be considered. Conducting longitudinal studies involving a larger sample size and longer follow-up periods would provide valuable insights into long-term monitoring and management of lymphedema.

Beyond the diagnosis and monitoring of lymphedema, the developed system may have potential applications in other areas of healthcare. One such area could be monitoring the effectiveness of lymphedema rehabilitation programs. By tracking changes in lymphatic fluid levels over time, the system could provide valuable insights into the efficacy of different treatment approaches and help optimize patient care.

In addition, the future study should expand the BCRL diagnosis and monitoring system to cover both unilateral and bilateral cases can provide a more comprehensive solution for a wider range of patients. These improvements can contribute to the overall effectiveness and relevance of BCRL diagnosis and management strategies.

REFERENCES

- Abasher, M. M., Sidahmed, A. A., Abdelmoniem, A., & Ahmed, H. O. M. (2023). Breast Cancer in Elderly Females. *American Journal of Medical Science and Innovation*, 2(2), 16-25.
- Ain, K., Chandra, F., Zaka, Q., Fahrani, B., Amelia, A., Enggar, A. F., . . . Ariwanto, B. (2021). *Design of Bioimpedance Spectroscopy to Characterize Meat Based on Gain and Phase Detector (AD8302)*. Paper presented at the 2021 International Conference on Instrumentation, Control, and Automation (ICA).
- Al Sharkawy, M., Sharkas, M., & Ragab, D. (2012). Breast cancer detection using support vector machine technique applied on extracted electromagnetic waves. *The Applied Computational Electromagnetics Society Journal (ACES)*, 292-301.
- Anderson, B. (2023). Breast Cancer. Retrieved from <https://www.who.int/news-room/fact-sheets/detail/breast-cancer>
- Androutsos, O., Gerasimidis, K., Karanikolou, A., Reilly, J., & Edwards, C. (2015). Impact of eating and drinking on body composition measurements by bioelectrical impedance. *Journal of human nutrition and dietetics*, 28(2), 165-171.
- Anusha, A., Preejith, S., Joseph, J., & Sivaprakasam, M. (2017). *Design and implementation of a hand-to-hand multifrequency bioimpedance measurement scheme for Total Body Water estimation*. Paper presented at the 2017 IEEE International Instrumentation and Measurement Technology Conference (I2MTC).
- Armer, J. M. (2005). The problem of post-breast cancer lymphedema: impact and measurement issues. *Cancer investigation*, 23(1), 76-83.
- Armer, J. M., Radina, M. E., Porock, D., & Culbertson, S. D. (2003). Predicting breast cancer-related lymphedema using self-reported symptoms. *Nursing research*, 52(6), 370-379.
- Armer, J. M., & Stewart, B. R. (2005). A comparison of four diagnostic criteria for lymphedema in a post-breast cancer population. *Lymphatic research and biology*, 3(4), 208-217.
- Atwa, A. M. E., Hassan, H. E., & Ahmed, S. I. (2019). The impact of a hospital-based awareness program on the knowledge of patients about breast cancer and cancer cervix. *International Journal of Studies in Nursing*, 4(1), 20.
- Ayllon, D., Seoane, F., & Gil-Pita, R. (2009). *Cole equation and parameter estimation from electrical bioimpedance spectroscopy measurements-a comparative study*. Paper presented at the 2009 Annual International Conference of the IEEE Engineering in Medicine and Biology Society.
- Ayre, K., & Parker, C. (2019). Lymphedema after treatment of breast cancer: a comprehensive review. *Journal of Unexplored Medical Data*, 4, 5.

- Azman, A. A., Siok-Fong, C., Rajab, N. F., Md Zin, R. R., Ahmad Daud, N. N., & Mohamad Hanif, E. A. (2023). The potential roles of lncRNA TINCR in triple negative breast cancer. *Molecular biology reports*, 1-9.
- Bagheri, S., Ohlin, K., Olsson, G., & Brorson, H. (2005). Tissue tonometry before and after liposuction of arm lymphedema following breast cancer. *Lymphatic research and biology*, 3(2), 66-80.
- Barbieux, R., Doyenard, S., Pluska, A., Enciso, K., Roman, M. M., Leduc, O., . . . Probyn, S. (2023). Lymphoscintigraphy as a Therapeutic Guidance Tool Can Improve Manual Lymphatic Drainage for the Physical Treatment of Patients with Upper Limb Lymphedema: Randomized Clinical Trial. *Lymphatic research and biology*.
- Barrio, A. V., Eaton, A., & Frazier, T. G. (2015). A prospective validation study of bioimpedance with volume displacement in early-stage breast cancer patients at risk for lymphedema. *Annals of surgical oncology*, 22(3), 370-375.
- Belgrado, J.-P., Bracale, P., Bates, J., Röh, N., Rosiello, R., Cangiano, A., & Moraine, J. (2010). Lymphoedema: What can be measured and how... overview. *European Journal of Lymphology and Related Problems*, 21(61), 3.
- Bentzen, S., & Overgaard, M. (1993). Early and late normal tissue injury after postmastectomy radiotherapy. *Acute and long-term side-effects of radiotherapy*, 59-78.
- Bera, T. K. (2014). Bioelectrical impedance methods for noninvasive health monitoring: a review. *Journal of medical engineering*, 2014.
- Berlit, S., Brade, J., Tuschy, B., Hornemann, A., Leweling, H., Eghardt, V., & Suetterlin, M. (2012). Comparing bioelectrical impedance values in assessing early upper limb lymphedema after breast cancer surgery. *in vivo*, 26(5), 863-867.
- Bernas, M. J., Askew, R. L., Armer, J. M., & Cormier, J. N. (2010). Lymphedema: how do we diagnose and reduce the risk of this dreaded complication of breast cancer treatment? *Current Breast Cancer Reports*, 2(1), 53-58.
- Bilir, S. P., DeKoven, M. P., & Munakata, J. (2012). Economic benefits of BIS-aided assessment of post-BC lymphedema in the United States. *The American journal of managed care*, 18(5), 234-241.
- Bloomquist, K., Hayes, S., Adamsen, L., Møller, T., Christensen, K. B., Ejlersten, B., & Oturai, P. (2016). A randomized cross-over trial to detect differences in arm volume after low-and heavy-load resistance exercise among patients receiving adjuvant chemotherapy for breast cancer at risk for arm lymphedema: study protocol. *BMC cancer*, 16(1), 1-8.
- Bogonez-Franco, P., Nescolarde, L., Bragos, R., Rosell-Ferrer, J., & Yandiola, I. (2009). Measurement errors in multifrequency bioelectrical impedance analyzers with and without impedance electrode mismatch. *Physiological measurement*, 30(7), 573.

- Bolton, M., Ward, L., Khan, A., Campbell, I., Nightingale, P., Dewit, O., & Elia, M. (1998). Sources of error in bioimpedance spectroscopy. *Physiological measurement*, 19(2), 235.
- BORDEA, M. P., EL-BSAT, R., NODITI, A., & BORDEA, C. THE ROLE OF PHYSIOTHERAPY TREATMENT IN ARM LYMPHOEDEMA ASSOCIATED WITH BREAST CANCER.
- Box, R. C., Reul-Hirche, H. M., Bullock-Saxton, J. E., & Furnival, C. M. (2002). Physiotherapy after breast cancer surgery: results of a randomised controlled study to minimise lymphoedema. *Breast cancer research and treatment*, 75(1), 51-64.
- Boyages, J., Xu, Y., Kalfa, S., Koelmeyer, L., Parkinson, B., Mackie, H., . . . Taksa, L. (2017). Financial cost of lymphedema borne by women with breast cancer. *Psycho-oncology*, 26(6), 849-855.
- Buendía, R., Seoane, F., Harris, M., Caffarel, J., & Gil, R. (2010). *Hook Effect correction & resistance-based Cole fitting prior Cole model-based analysis: Experimental validation*. Paper presented at the 2010 Annual International Conference of the IEEE Engineering in Medicine and Biology.
- Bundred, N., Foden, P., Todd, C., Morris, J., Watterson, D., Purushotham, A., . . . Evans, A. (2020). Increases in arm volume predict lymphoedema and quality of life deficits after axillary surgery: a prospective cohort study. *British journal of cancer*, 123(1), 17-25.
- Bundred, N. J., Stockton, C., Keeley, V., Riches, K., Ashcroft, L., Evans, A., . . . Hodgkiss, T. (2015). Comparison of multi-frequency bioimpedance with perometry for the early detection and intervention of lymphoedema after axillary node clearance for breast cancer. *Breast cancer research and treatment*, 151(1), 121-129.
- Callejón, M. A., Del Campo, P., Reina-Tosina, J., & Roa, L. M. (2017). A parametric computational analysis into galvanic coupling intrabody communication. *IEEE journal of biomedical and health informatics*, 22(4), 1087-1096.
- Cannon, T., & Choi, J. (2019). Development of a segmental bioelectrical impedance spectroscopy device for body composition measurement. *Sensors*, 19(22), 4825.
- Casley-Smith, J. (1994). Measuring and representing peripheral oedema and its alterations. *Lymphology*, 27(2), 56-70.
- Catapano, A., Trinchese, G., Cimmino, F., Petrella, L., D'Angelo, M., Di Maio, G., . . . Mollica, M. P. (2023). Impedance Analysis to Evaluate Nutritional Status in Physiological and Pathological Conditions. *Nutrients*, 15(10), 2264.
- Cau, N., Galli, M., Cimolin, V., Aranci, M., Caraceni, A., & Balzarini, A. (2016). Comparative study between circumferential method and laser scanner 3D method for the evaluation of arm volume in healthy subjects. *Journal of Vascular Surgery: Venous and Lymphatic Disorders*, 4(1), 64-72.

- Chachaj, A., Małyszczak, K., Pyszel, K., Lukas, J., Tarkowski, R., Pudelko, M., . . . Szuba, A. (2010). Physical and psychological impairments of women with upper limb lymphedema following breast cancer treatment. *Psycho-Oncology: Journal of the Psychological, Social and Behavioral Dimensions of Cancer*, 19(3), 299-305.
- Cheifetz, O., & Haley, L. (2010). Management of secondary lymphedema related to breast cancer. *Canadian Family Physician*, 56(12), 1277-1284.
- Chen, Y.-W., Tsai, H.-J., Hung, H.-C., & Tsauo, J.-Y. (2008). Reliability study of measurements for lymphedema in breast cancer patients. *American journal of physical medicine & rehabilitation*, 87(1), 33-38.
- Cheng, M.-H., Chang, D. W., & Patel, K. M. (2021). *Principles and practice of lymphedema surgery*: Elsevier Health Sciences.
- Cheville, A. L., McGarvey, C. L., Petrek, J. A., Russo, S. A., Thiadens, S. R., & Taylor, M. E. (2003). *The grading of lymphedema in oncology clinical trials*. Paper presented at the Seminars in radiation oncology.
- Chitturi, V., & Farrukh, N. (2019). An alternate voltage-controlled current source for electrical impedance tomography applications. In *Data Analytics and Learning* (pp. 93-102): Springer.
- Choi, A., Kim, J. Y., Jo, S., Jee, J. H., Heymsfield, S. B., Bhagat, Y. A., . . . Cho, J. (2015). Smartphone-based bioelectrical impedance analysis devices for daily obesity management. *Sensors*, 15(9), 22151-22166.
- Choi, Y., Kim, E. J., Seol, H., Lee, H. E., Jang, M. J., Kim, S. M., . . . Park, S. Y. (2012). The hormone receptor, human epidermal growth factor receptor 2, and molecular subtype status of individual tumor foci in multifocal/multicentric invasive ductal carcinoma of breast. *Human pathology*, 43(1), 48-55.
- Clark, B., Sitzia, J., & Harlow, W. (2005). Incidence and risk of arm oedema following treatment for breast cancer: a three-year follow-up study. *Qjm*, 98(5), 343-348.
- Clough-Gorr, K. M., Ganz, P. A., & Silliman, R. A. (2010). Older breast cancer survivors: Factors associated with self-reported symptoms of persistent lymphedema over 7 years of follow-up. *The breast journal*, 16(2), 147-155.
- Cole, K. S. (1940). *Permeability and impermeability of cell membranes for ions*. Paper presented at the Cold Spring Harbor Symposia on Quantitative Biology.
- Cole, T. (2018). *Development of a Novel Device for Non-invasive Leg Fluid Volume Measurements*. University of Toronto (Canada),
- Constantinou, L., Bayford, R., & Demosthenous, A. (2015). A wideband low-distortion CMOS current driver for tissue impedance analysis. *IEEE Transactions on Circuits and Systems II: Express Briefs*, 62(2), 154-158.

- Cormier, J. N., Xing, Y., Zaniletti, I., Askew, R., Stewart, B., & Armer, J. (2009). Minimal limb volume change has a significant impact on breast cancer survivors. *Lymphology*, 42(4), 161.
- Cornish, B. (2006). Bioimpedance analysis: scientific background. *Lymphatic research and biology*, 4(1), 47-50.
- Cornish, B., Bunce, I., Ward, L., Jones, L., & Thomas, B. (1996). Bioelectrical impedance for monitoring the efficacy of lymphoedema treatment programmes. *Breast cancer research and treatment*, 38(2), 169-176.
- Cornish, B., Chapman, M., Hirst, C., Mirolo, B., Bunce, I., Ward, L., & Thomas, B. (2001). Early diagnosis of lymphedema using multiple frequency bioimpedance. *Lymphology*, 34(1), 2-11.
- Cornish, B., Chapman, M., Thomas, B., Ward, L., Bunce, I., & Hirst, C. (2000). Early diagnosis of lymphedema in postsurgery breast cancer patients. *Annals of the New York Academy of Sciences*, 904(1), 571-575.
- Cornish, B., Jacobs, A., Thomas, B., & Ward, L. (1999). Optimizing electrode sites for segmental bioimpedance measurements. *Physiological measurement*, 20(3), 241.
- Cornish, B., Thomas, B., & Ward, L. (1993). Improved prediction of extracellular and total body water using impedance loci generated by multiple frequency bioelectrical impedance analysis. *Physics in Medicine & Biology*, 38(3), 337.
- Cornish, B., & Ward, L. (1998). Data analysis in multiple-frequency bioelectrical impedance analysis. *Physiological measurement*, 19(2), 275.
- Cornish, B., Ward, L., Thomas, B., & Bunce, I. (1998). Quantification of lymphoedema using multi-frequency bioimpedance. *Applied radiation and isotopes: including data, instrumentation and methods for use in agriculture, industry and medicine*, 49(5-6), 651-652.
- Cornish, B. H., Thomas, B. J., Ward, L. C., Hirst, C., & Bunce, I. H. (2002). A new technique for the quantification of peripheral edema with application in both unilateral and bilateral cases. *Angiology*, 53(1), 41-47.
- Coroneos, C. J., Wong, F. C., DeSnyder, S. M., Shaitelman, S. F., & Schaverien, M. V. (2019). Correlation of L-Dex bioimpedance spectroscopy with limb volume and lymphatic function in lymphedema. *Lymphatic research and biology*, 17(3), 301-307.
- Czerniec, S., Ward, L., Refshauge, K., Beith, J., Lee, M., York, S., & Kilbreath, S. (2010). Assessment of breast cancer-related arm lymphedema—comparison of physical measurement methods and self-report. *Cancer investigation*, 28(1), 54-62.
- Czerniec, S. A., Ward, L. C., & Kilbreath, S. L. (2016). Breast cancer-related arm lymphedema: fluctuation over six months and the effect of the weather. *Lymphatic research and biology*, 14(3), 148-155.

- da Luz, F. A. C., Araujo, B. J., & de Araujo, R. A. (2022). The current staging and classification systems of breast cancer and their pitfalls: Is it possible to integrate the complexity of this neoplasm into a unified staging system? *Critical Reviews in Oncology/Hematology*, 103781.
- Dang, B. Q., Miles, B., Young, P., He, J., & Nguyen, Q. D. (2023). An Interesting Imaging Presentation of a Common Benign Entity: Fibrocystic Changes in a Postmenopausal Patient. *Cureus*, 15(3).
- Deurenberg, P., & Deurenberg-Yap, M. (2002). Validation of skinfold thickness and hand-held impedance measurements for estimation of body fat percentage among singaporean chinese, malay and indian subjects. *Asia Pacific Journal of Clinical Nutrition*, 11(1), 1-7.
- Deutsch, M., Land, S., Begovic, M., & Sharif, S. (2008). The incidence of arm edema in women with breast cancer randomized on the National Surgical Adjuvant Breast and Bowel Project study B-04 to radical mastectomy versus total mastectomy and radiotherapy versus total mastectomy alone. *International Journal of Radiation Oncology* Biology* Physics*, 70(4), 1020-1024.
- Dey, N., Ashour, A., Fong, S. J., & Bhatt, C. (2019). *Wearable and Implantable Medical Devices: Applications and Challenges*: Academic Press.
- Di Maria, A., Barone, G., Ferraro, V., Tredici, C., Manara, S., De Carlo, C., . . . Confalonieri, F. (2023). Recurrence of Basal Cell Carcinoma Treated with Surgical Excision and Histopathological Analysis with Frozen Section Technique with Complete Margin Control (CMC-FS): A 15-Year Experience of a Reference Center. *Cancers*, 15(15), 3840.
- DiSipio, T., Rye, S., Newman, B., & Hayes, S. (2013). Incidence of unilateral arm lymphoedema after breast cancer: a systematic review and meta-analysis. *The lancet oncology*, 14(6), 500-515.
- Donahue, P. M., Crescenzi, R., Du, L., & Donahue, M. J. (2020). Implementation of single-tab electrodes for bioimpedance spectroscopy measures. *Lymphatic research and biology*, 18(3), 277-283.
- Douglass, J., & Kelly-Hope, L. (2019). Comparison of staging systems to assess lymphedema caused by cancer therapies, lymphatic filariasis, and podoconiosis. *Lymphatic research and biology*, 17(5), 550-556.
- Dudzinski, K., Dawgul, M., Pluta, K. D., Wawro, B., Torbicz, W., & Pijanowska, D. G. (2017). Spiral concentric two electrode sensor fabricated by direct writing for skin impedance measurements. *IEEE Sensors Journal*, 17(16), 5306-5314.
- Dylke, E., Alsobayel, H., Ward, L., Liu, M., Webb, E., & Kilbreath, S. (2014). Use of impedance ratios to assess hand swelling in lymphoedema. *Phlebology*, 29(2), 83-89.
- Dylke, E., Schembri, G., Bailey, D., Bailey, E., Ward, L., Refshauge, K., . . . Kilbreath, S. (2016). Diagnosis of upper limb lymphedema: development of an evidence-based approach. *Acta Oncologica*, 55(12), 1477-1483.

- Dylke, E. S., & Ward, L. C. (2020). Three Decades of Bioelectrical Impedance Spectroscopy in Lymphedema Assessment: An Historical Perspective. *Lymphatic research and biology*.
- Eilebrecht, B., Willkomm, J., Pohl, A., Wartzek, T., & Leonhardt, S. (2013). Impedance measurement system for determination of capacitive electrode coupling. *IEEE transactions on biomedical circuits and systems*, 7(5), 682-689.
- Engin, O., Akalın, E., Sarıbay, E., Aslan, C., Şahin, E., & Alper, S. (2019). Easy volumeter in detection of breast cancer-related lymphedema: A validity study. *Lymphatic research and biology*, 17(5), 543-549.
- Enøe, C., Georgiadis, M. P., & Johnson, W. O. (2000). Estimation of sensitivity and specificity of diagnostic tests and disease prevalence when the true disease state is unknown. *Preventive veterinary medicine*, 45(1-2), 61-81.
- Erdogan Iyigun, Z., Selamoglu, D., Alco, G., Pilancı, K. N., Ordu, C., Agacayak, F., . . . Guler Uysal, F. (2015). Bioelectrical impedance for detecting and monitoring lymphedema in patients with breast cancer. Preliminary results of the florence nightingale breast study group. *Lymphatic research and biology*, 13(1), 40-45.
- Erickson, V. S., Pearson, M. L., Ganz, P. A., Adams, J., & Kahn, K. L. (2001). Arm edema in breast cancer patients. *Journal of the National Cancer Institute*, 93(2), 96-111.
- Eyre, S., Stenberg, J., Wallengren, O., Keane, D., Avesani, C. M., Bosaeus, I., . . . Johansson, A. C. (2023). Bioimpedance analysis in patients with chronic kidney disease. In (Vol. 49, pp. 147-157): Wiley Online Library.
- Ezike, K. N., Okwudire-Ejeh, I. A., Dallang, B. C., Ndaiya, R., EZIKE, K. N., OKWUDIRE-EJEH, I. A., . . . NDAIYA, R. (2023). Cysticercosis Mimicking Fibroadenoma of the Breast in a Young Female: A Case Report From North Central Nigeria. *Cureus*, 15(4).
- Farncombe, M., Daniels, G., & Cross, L. (1994). Lymphedema: the seemingly forgotten complication. *Journal of pain and symptom management*, 9(4), 269-276.
- Fasano, W., & Hinderliter, P. (2004). The Tinsley LCR Databridge Model 6401 and electrical impedance measurements to evaluate skin integrity in vitro. *Toxicology in vitro*, 18(5), 725-729.
- Fenton, A., Downes, N., Mendiola, A., Cordova, A., Lukity, K., & Imani, J. (2022). Multidisciplinary Management of Breast Cancer and Role of the Patient Navigator. *Obstetrics and Gynecology Clinics*, 49(1), 167-179.
- Fernandez, R. E., Lebiga, E., Koklu, A., Sabuncu, A. C., & Beskok, A. (2015). Flexible bioimpedance sensor for label-free detection of cell viability and biomass. *IEEE transactions on nanobioscience*, 14(7), 700-706.
- Ferreira, J., Pau, I., Lindcrantz, K., & Seoane, F. (2016). A handheld and textile-enabled bioimpedance system for ubiquitous body composition analysis. An initial

functional validation. *IEEE journal of biomedical and health informatics*, 21(5), 1224-1232.

Ferreira, J., Seoane, F., Ansele, A., & Bragos, R. (2010). *AD5933-based spectrometer for electrical bioimpedance applications*. Paper presented at the Journal of Physics: Conference Series.

Ferro, A. P., Ferreira, V. T. K., Rezende, M. S., de Souza, T. R., Almeida, A. M. d., Guirro, R. R. d. J., & Guirro, E. C. d. O. (2018). Intra-and inter-rater reliability of bioimpedance in the evaluation of lymphedema secondary to treatment of breast cancer. *Lymphatic research and biology*, 16(3), 282-286.

Föger-Samwald, U., Dovjak, P., Azizi-Semrad, U., Kersch-Schindl, K., & Pietschmann, P. (2020). Osteoporosis: Pathophysiology and therapeutic options. *EXCLI journal*, 19, 1017.

Freitas, P., Carvalho, D., Santos, A., Mesquita, J., Correia, F., Xerinda, S., . . . Medina, J. (2011). Assessment of body fat composition disturbances by bioimpedance analysis in HIV-infected adults. *Journal of Endocrinological Investigation*, 34, e321-e329.

Fu, M. R., Cleland, C. M., Guth, A. A., Kayal, M., Haber, J., Cartwright, F., . . . Axelrod, D. (2013). L-dex ratio in detecting breast cancer-related lymphedema: reliability, sensitivity, and specificity. *Lymphology*, 46(2), 85.

Gibson, A., Beam, J., Alencar, M., Zuhl, M., & Mermier, C. (2015). Time course of supine and standing shifts in total body, intracellular and extracellular water for a sample of healthy adults. *European journal of clinical nutrition*, 69(1), 14-19.

Gjorup, C., Zerahn, B., & Hendel, H. W. (2010). Assessment of volume measurement of breast cancer-related lymphedema by three methods: circumference measurement, water displacement, and dual energy X-ray absorptiometry. *Lymphatic research and biology*, 8(2), 111-119.

Gordon, S., Melrose, W., Warner, J., Buttner, P., & Ward, L. (2011). Lymphatic filariasis: a method to identify subclinical lower limb change in PNG adolescents. *PLoS Negl Trop Dis*, 5(7), e1242.

Grada, A. A., & Phillips, T. J. (2017). Lymphedema: pathophysiology and clinical manifestations. *Journal of the American Academy of Dermatology*, 77(6), 1009-1020.

Grayson, A. C. R., Shawgo, R. S., Li, Y., & Cima, M. J. (2004). Electronic MEMS for triggered delivery. *Advanced drug delivery reviews*, 56(2), 173-184.

Grimnes, S., & Martinsen, O. (2000). Bioimpedance and bioelectricity basics academic press. *New York*.

Gudivaka, R., Schoeller, D., Kushner, R., & Bolt, M. (1999). Single-and multifrequency models for bioelectrical impedance analysis of body water compartments. *Journal of Applied Physiology*, 87(3), 1087-1096.

- Hafid, A., Benouar, S., Kedir-Talha, M., Abtahi, F., Attari, M., & Seoane, F. (2017). Full impedance cardiography measurement device using raspberry PI3 and system-on-chip biomedical instrumentation solutions. *IEEE journal of biomedical and health informatics*, 22(6), 1883-1894.
- Harder, R., Diedrich, A., Whitfield, J. S., Buchowski, M. S., Pietsch, J. B., & Baudenbacher, F. J. (2016). Smart multi-frequency bioelectrical impedance spectrometer for BIA and BIVA applications. *IEEE transactions on biomedical circuits and systems*, 10(4), 912-919.
- Havens, L. M., Brunelle, C. L., Gillespie, T. C., Bernstein, M., Bucci, L. K., Kassamani, Y. W., & Taghian, A. G. (2021). Use of technology to facilitate a prospective surveillance program for breast cancer-related lymphedema at the Massachusetts General Hospital. *Mhealth*, 7.
- Hayes, S., Cornish, B., & Newman, B. (2005). Comparison of methods to diagnose lymphoedema among breast cancer survivors: 6-month follow-up. *Breast cancer research and treatment*, 89(3), 221-226.
- Hayes, S., Janda, M., Cornish, B., Battistutta, D., & Newman, B. (2008). Lymphedema secondary to breast cancer: how choice of measure influences diagnosis, prevalence, and identifiable risk factors. *Lymphology*, 41(1), 18-28.
- Hayes, S. C., Janda, M., Cornish, B., Battistutta, D., & Newman, B. (2008). Lymphedema after breast cancer: incidence, risk factors, and effect on upper body function. *Journal of clinical oncology*, 26(21), 3536-3542.
- Hayes, S. C., Johansson, K., Stout, N. L., Prosnitz, R., Armer, J. M., Gabram, S., & Schmitz, K. H. (2012). Upper-body morbidity after breast cancer: incidence and evidence for evaluation, prevention, and management within a prospective surveillance model of care. *Cancer*, 118(S8), 2237-2249.
- Hegarty-Craver, M., Grant, E., & Reid, L. (2015). *A wearable bioimpedance spectroscopy system for characterizing fluid distribution in the lower limbs*. Paper presented at the 2015 IEEE International Conference on Multisensor Fusion and Integration for Intelligent Systems (MFI).
- Heins, M. J., de Ligt, K. M., Verloop, J., Siesling, S., Korevaar, J. C., Berendsen, A., . . . Hugtenburg, J. (2022). Adverse health effects after breast cancer up to 14 years after diagnosis. *The Breast*, 61, 22-28.
- Hersek, S., Töreyn, H., & Inan, O. T. (2015). A robust system for longitudinal knee joint edema and blood flow assessment based on vector bioimpedance measurements. *IEEE transactions on biomedical circuits and systems*, 10(3), 545-555.
- Hersek, S., Töreyn, H., Teague, C. N., Millard-Stafford, M. L., Jeong, H.-K., Bavare, M. M., . . . Inan, O. T. (2016). Wearable vector electrical bioimpedance system to assess knee joint health. *IEEE Transactions on Biomedical Engineering*, 64(10), 2353-2360.

- Hinrichs, C. S., Watroba, N. L., Rezaishiraz, H., Giese, W., Hurd, T., Fassl, K. A., & Edge, S. B. (2004). Lymphedema secondary to postmastectomy radiation: incidence and risk factors. *Annals of surgical oncology*, 11(6), 573-580.
- Ibrahim, B., Hall, D. A., & Jafari, R. (2017). *Bio-impedance spectroscopy (BIS) measurement system for wearable devices*. Paper presented at the 2017 IEEE Biomedical Circuits and Systems Conference (BioCAS).
- Ibrahim, F., Faisal, T., Mohamad Salim, M., & Taib, M. N. (2010). Non-invasive diagnosis of risk in dengue patients using bioelectrical impedance analysis and artificial neural network. *Medical & biological engineering & computing*, 48, 1141-1148.
- Impedimed. (2019). L-dex score. Retrieved from <https://www.impedimed.com/healthcare/l-dex-score/>
- Jane Wigg, N. L. (2013). Redefining essential care in lymphoedema. *Clinical Focus*.
- Jiang, Z., Yao, J., Wang, L., Wu, H., Huang, J., Zhao, T., & Takei, M. (2019). Development of a portable electrochemical impedance spectroscopy system for bio-detection. *IEEE Sensors Journal*, 19(15), 5979-5987.
- Johnson, K. C., Kennedy, A. G., & Henry, S. M. (2014). Clinical measurements of lymphedema. *Lymphatic research and biology*, 12(4), 216-221.
- Jung, M., Jeon, J. Y., Yun, G. J., Yang, S., Kwon, S., & Seo, Y. J. (2018). Reference values of bioelectrical impedance analysis for detecting breast cancer-related lymphedema. *Medicine*, 97(44).
- Karamehmetoglu, S. S., Ugur, M., Arslan, Y. Z., & Palamar, D. (2009). A quantitative skin impedance test to diagnose spinal cord injury. *European Spine Journal*, 18(7), 972-977.
- Karlsson, K., Johansson, K., Nilsson-Wikmar, L., & Brogårdh, C. (2022). Tissue dielectric constant and water displacement method can detect changes of mild breast cancer-related arm lymphedema. *Lymphatic research and biology*, 20(3), 325-334.
- Kaufman, D. I., Shah, C., Vicini, F. A., & Rizzi, M. (2017). Utilization of bioimpedance spectroscopy in the prevention of chronic breast cancer-related lymphedema. *Breast cancer research and treatment*, 166(3), 809-815.
- Kayali Vatansever, A., Yavuzşen, T., & Karadibak, D. (2020). The reliability and validity of quality of life questionnaire upper limb lymphedema (ULL-27) Turkish patient with breast cancer related lymphedema. *Frontiers in oncology*, 10, 455.
- Keeley, V. (2021). The early detection of breast cancer treatment-related lymphedema of the arm. *Lymphatic research and biology*, 19(1), 51-55.
- Khalil, S. F., Dali, N. S. M., Mohktar, M. S., & Ibrahim, F. (2014). *Validation of multiple frequency bioimpedance analyzer using biological phantom*. Paper presented at the 2014 IEEE Conference on Biomedical Engineering and Sciences (IECBES).

- Khalil, S. F., Mohktar, M. S., & Ibrahim, F. (2014). The theory and fundamentals of bioimpedance analysis in clinical status monitoring and diagnosis of diseases. *Sensors*, *14*(6), 10895-10928.
- Khan, F., Amatya, B., Pallant, J. F., & Rajapaksa, I. (2012). Factors associated with long-term functional outcomes and psychological sequelae in women after breast cancer. *The Breast*, *21*(3), 314-320.
- Kilgore, L. J., Korentager, S. S., Hangge, A. N., Amin, A. L., Balanoff, C. R., Larson, K. E., . . . Khan, Q. J. (2018). Reducing breast cancer-related lymphedema (BCRL) through prospective surveillance monitoring using bioimpedance spectroscopy (BIS) and patient directed self-interventions. *Annals of surgical oncology*, *25*(10), 2948-2952.
- Kim, M., Kim, S. W., Lee, S. U., Lee, N. K., Jung, S.-Y., Kim, T. H., . . . Shin, K. H. (2013). A model to estimate the risk of breast cancer-related lymphedema: combinations of treatment-related factors of the number of dissected axillary nodes, adjuvant chemotherapy, and radiation therapy. *International Journal of Radiation Oncology* Biology* Physics*, *86*(3), 498-503.
- Koelmeyer, L. A., Borotkanics, R. J., Alcorso, J., Prah, P., Winch, C. J., Nakhel, K., . . . Boyages, J. (2019). Early surveillance is associated with less incidence and severity of breast cancer-related lymphedema compared with a traditional referral model of care. *Cancer*, *125*(6), 854-862.
- Koelmeyer, L. A., Moloney, E., Boyages, J., Sherman, K. A., & Dean, C. M. (2021). Prospective surveillance model in the home for breast cancer-related lymphoedema: a feasibility study. *Breast cancer research and treatment*, *185*, 401-412.
- Koelmeyer, L. A., Ward, L. C., Dean, C., & Boyages, J. (2020). Body positional effects on bioimpedance spectroscopy measurements for lymphedema assessment of the arm. *Lymphatic research and biology*, *18*(5), 464-473.
- Kopec, J. A., Colangelo, L. H., Land, S. R., Julian, T. B., Brown, A. M., Anderson, S. J., . . . Wolmark, N. (2013). Relationship between arm morbidity and patient-reported outcomes following surgery in women with node-negative breast cancer: NSABP protocol B-32. *The journal of supportive oncology*, *11*(1), 22.
- Krzesinski, P., Sobotnicki, A., Gacek, A., Siebert, J., Walczak, A., Murawski, P., & Gielerak, G. (2021). Noninvasive bioimpedance methods from the viewpoint of remote monitoring in heart failure. *JMIR mHealth and uHealth*, *9*(5), e25937.
- Kun, S., & Peura, R. A. (1999). Selection of measurement frequencies for optimal extraction of tissue impedance model parameters. *Medical & biological engineering & computing*, *37*(6), 699-703.
- Kusche, R., Kaufmann, S., & Ryschka, M. (2018). Dry electrodes for bioimpedance measurements—design, characterization and comparison. *Biomedical Physics & Engineering Express*, *5*(1), 015001.

- Kyle, U. G., Bosaeus, I., De Lorenzo, A. D., Deurenberg, P., Elia, M., Gómez, J. M., . . . Pirlich, M. (2004a). Bioelectrical impedance analysis—part I: review of principles and methods. *Clinical nutrition*, 23(5), 1226-1243.
- Kyle, U. G., Bosaeus, I., De Lorenzo, A. D., Deurenberg, P., Elia, M., Gómez, J. M., . . . Pirlich, M. (2004b). Bioelectrical impedance analysis—part II: utilization in clinical practice. *Clinical nutrition*, 23(6), 1430-1453.
- Lahtinen, T., Seppälä, J., Viren, T., & Johansson, K. (2015). Experimental and analytical comparisons of tissue dielectric constant (TDC) and bioimpedance spectroscopy (BIS) in assessment of early arm lymphedema in breast cancer patients after axillary surgery and radiotherapy. *Lymphatic research and biology*, 13(3), 176-185.
- Lawenda, B. D., Mondry, T. E., & Johnstone, P. A. (2009). Lymphedema: a primer on the identification and management of a chronic condition in oncologic treatment. *CA: a cancer journal for clinicians*, 59(1), 8-24.
- Lee, S., Polito, S., Agell, C., Mitra, S., Yazicioglu, R. F., Riistama, J., . . . Penders, J. (2013). *A low-power and compact-sized wearable bio-impedance monitor with wireless connectivity*. Paper presented at the Journal of Physics: Conference Series.
- Liao, S.-F., Li, S.-H., Huang, H.-Y., Chen, S.-T., Kuo, S.-J., Chen, D.-R., & Wei, T.-S. (2013). The efficacy of complex decongestive physiotherapy (CDP) and predictive factors of lymphedema severity and response to CDP in breast cancer-related lymphedema (BCRL). *The Breast*, 22(5), 703-706.
- Lim, S. M., Han, Y., Kim, S. I., & Park, H. S. (2019). Utilization of bioelectrical impedance analysis for detection of lymphedema in breast Cancer survivors: a prospective cross sectional study. *BMC cancer*, 19(1), 1-8.
- Lindeboom, L., Lee, S., Wieringa, F., Groenendaal, W., Basile, C., van der Sande, F., & Kooman, J. (2021). On the potential of wearable bioimpedance for longitudinal fluid monitoring in end-stage kidney disease. *Nephrology Dialysis Transplantation*.
- Liu, S., Zhao, Q., Ren, X., Cui, Y., Yang, H., Wang, S., . . . Wang, S. (2021). Determination of bioelectrical impedance thresholds for early detection of breast cancer-related lymphedema. *International Journal of Medical Sciences*, 18(13), 2990.
- Lukaski, H. C., Bolonchuk, W. W., Hall, C. B., & Siders, W. A. (1986). Validation of tetrapolar bioelectrical impedance method to assess human body composition. *Journal of Applied Physiology*, 60(4), 1327-1332.
- Lundgren, E. (1989). Sequelae of axillary dissection vs. axillary sampling with or without irradiation for breast cancer. A randomized trial. *Acta Chirurgica Scandinavica*, 155(10), 515-519.
- Luo, X., Pulido, H. V. G., Rutkove, S. B., & Sanchez, B. (2021). A Bioimpedance-Based Device to Assess the Volume Conduction Properties of the Tongue in

Neurological Disorders Affecting Bulbar Function. *IEEE Open Journal of Engineering in Medicine and Biology*, 2, 278-285.

- Mabrouk, S., Hersek, S., Jeong, H. K., Whittingslow, D., Ganti, V. G., Wolkoff, P., & Inan, O. T. (2019). Robust longitudinal ankle edema assessment using wearable bioimpedance spectroscopy. *IEEE Transactions on Biomedical Engineering*, 67(4), 1019-1029.
- McAdams, E., Henry, P., Anderson, J. M., & Jossinet, J. (1992). Optimal electrolytic chloriding of silver ink electrodes for use in electrical impedance tomography. *Clinical Physics and Physiological Measurement*, 13(A), 19.
- McAdams, E., Lackermeier, A., McLaughlin, J., Macken, D., & Jossinet, J. (1995). The linear and non-linear electrical properties of the electrode-electrolyte interface. *Biosensors and bioelectronics*, 10(1-2), 67-74.
- McGee, S. (2002). Simplifying likelihood ratios. *Journal of general internal medicine*, 17(8), 647-650.
- McLaughlin, S. A., Staley, A. C., Vicini, F., Thiruchelvam, P., Hutchison, N. A., Mendez, J., . . . Klimberg, S. (2017). Considerations for clinicians in the diagnosis, prevention, and treatment of breast cancer-related lymphedema: Recommendations from a multidisciplinary expert ASBrS panel. *Annals of surgical oncology*, 24(10), 2818-2826.
- McLaughlin, S. A., Stout, N. L., & Schaverien, M. V. (2020). Avoiding the swell: advances in lymphedema prevention, detection, and management. *American Society of Clinical Oncology Educational Book*, 40, e17-e26.
- McMasters, K. M., Giuliano, A. E., Ross, M. I., Reintgen, D. S., Hunt, K. K., Byrd, D. R., . . . Edwards, M. J. (1998). Sentinel-lymph-node biopsy for breast cancer—not yet the standard of care. In: Mass Medical Soc.
- Medrano, G., Eitner, F., Walter, M., & Leonhardt, S. (2010). Model-based correction of the influence of body position on continuous segmental and hand-to-foot bioimpedance measurements. *Medical & biological engineering & computing*, 48(6), 531-541.
- Megens, A. M., Harris, S. R., Kim-Sing, C., & McKenzie, D. C. (2001). Measurement of upper extremity volume in women after axillary dissection for breast cancer. *Archives of physical medicine and rehabilitation*, 82(12), 1639-1644.
- Mialich, M. S., Sicchieri, J. F., & Junior, A. J. (2014). Analysis of body composition: a critical review of the use of bioelectrical impedance analysis. *Int J Clin Nutr*, 2(1), 1-10.
- Mishra, P., Mishra, S., & Prajapati, K. K. (2023). Breast cancer in women: Its risk factors and prevention. *Breast (Female--Male)*, 246(2,600), 40,450-440.
- Morrell, R. M., Halyard, M. Y., Schild, S. E., Ali, M. S., Gunderson, L. L., & Pockaj, B. A. (2005). *Breast cancer-related lymphedema*. Paper presented at the Mayo Clinic Proceedings.

- Moseley, A., & Piller, N. (2008). Reliability of bioimpedance spectroscopy and tonometry after breast conserving cancer treatment. *Lymphatic research and biology*, 6(2), 85-87.
- Mulasi, U., Kuchnia, A. J., Cole, A. J., & Earthman, C. P. (2015). Bioimpedance at the bedside: current applications, limitations, and opportunities. *Nutrition in Clinical Practice*, 30(2), 180-193.
- Naranjo-Hernández, D., Reina-Tosina, J., & Min, M. (2019). Fundamentals, recent advances, and future challenges in bioimpedance devices for healthcare applications. *Journal of Sensors*, 2019.
- Nasser, S. A., Sharma, A., Saraf, A., Parulekar, A. M., Haria, P., & Sethi, A. (2023). Transforming Breast Cancer Diagnosis: Towards Real-Time Ultrasound to Mammogram Conversion for Cost-Effective Diagnosis. *arXiv preprint arXiv:2308.05449*.
- Nayak, V., Patra, S., Singh, K. R., Ganguly, B., Kumar, D. N., Panda, D., . . . Sharma, R. (2023). Advancement in precision diagnosis and therapeutic for triple-negative breast cancer: Harnessing diagnostic potential of CRISPR-cas & engineered CAR T-cells mediated therapeutics. *Environmental Research*, 235, 116573.
- Nguyen, D., Kosobrodov, R., Barry, M., Chik, W., Jin, C., Oh, T., . . . McEwan, A. (2013). *Electrode-Skin contact impedance: In vivo measurements on an ovine model*. Paper presented at the Journal of Physics: Conference Series.
- Noveletto, F., Bertemes-Filho, P., & Dutra, D. (2016). *Analog front-end for the integrated circuit AD5933 used in electrical bioimpedance measurements*. Paper presented at the II Latin American Conference on Bioimpedance: 2nd CLABIO, Montevideo, September 30-October 02, 2015.
- Null, M., & Agarwal, M. (2023). Anatomy, lymphatic system. In *StatPearls [Internet]*: StatPearls Publishing.
- Oremus, M., Walker, K., Dayes, I., & Raina, P. (2015). Diagnosis and treatment of secondary lymphedema.
- Pauliukaite, R., Ghica, M. E., Fatibello-Filho, O., & Brett, C. M. (2010). Electrochemical impedance studies of chitosan-modified electrodes for application in electrochemical sensors and biosensors. *Electrochimica Acta*, 55(21), 6239-6247.
- Petrek, J. A., & Heelan, M. C. (1998). Incidence of breast carcinoma-related lymphedema. *Cancer: Interdisciplinary International Journal of the American Cancer Society*, 83(S12B), 2776-2781.
- Petrek, J. A., Senie, R. T., Peters, M., & Rosen, P. P. (2001). Lymphedema in a cohort of breast carcinoma survivors 20 years after diagnosis. *Cancer*, 92(6), 1368-1377.
- Pfeiffer, D., Lord, M., Lamb, C., Damrill, K., Stewart, K., & Rock, D. T. (2021). Abstract PS9-34: Initial experience using the SOZO bio-impedance device over a 2 year surveillance period for identifying subclinical breast cancer related lymphedema

(BCRL) in patients attending a multidisciplinary breast clinic. *Cancer Research*, 81(4_Supplement), PS9-34-PS39-34.

- Powles, J. (1993). Cole-Cole plots as they should be. *Journal of molecular liquids*, 56, 35-47.
- Qin, E. S., Bowen, M. J., & Chen, W. F. (2018). Diagnostic accuracy of bioimpedance spectroscopy in patients with lymphedema: A retrospective cohort analysis. *Journal of Plastic, Reconstructive & Aesthetic Surgery*, 71(7), 1041-1050.
- Qin, E. S., Bowen, M. J., James, S. L., & Chen, W. F. (2020). Multi-segment bioimpedance can assess patients with bilateral lymphedema. *Journal of Plastic, Reconstructive & Aesthetic Surgery*, 73(2), 328-336.
- Ridner, S. H., Bonner, C. M., Doersam, J. K., Rhoten, B. A., Schultze, B., & Dietrich, M. S. (2014). Bioelectrical impedance self-measurement protocol development and daily variation between healthy volunteers and breast cancer survivors with lymphedema. *Lymphatic research and biology*, 12(1), 2-9.
- Ridner, S. H., Dietrich, M. S., Boyages, J., Koelmeyer, L., Elder, E., Hughes, T. M., . . . Abramson, V. G. (2022). A comparison of bioimpedance spectroscopy or tape measure triggered compression intervention in chronic breast cancer lymphedema prevention. *Lymphatic research and biology*, 20(6), 618-628.
- Ridner, S. H., Dietrich, M. S., Cowher, M. S., Taback, B., McLaughlin, S., Ajkay, N., . . . Wagner, J. (2019). A randomized trial evaluating bioimpedance spectroscopy versus tape measurement for the prevention of lymphedema following treatment for breast cancer: interim analysis. *Annals of surgical oncology*, 26(10), 3250-3259.
- Ridner, S. H., Dietrich, M. S., Deng, J., Bonner, C. M., & Kidd, N. (2009). Bioelectrical impedance for detecting upper limb lymphedema in nonlaboratory settings. *Lymphatic research and biology*, 7(1), 11-15.
- Ridner, S. H., Dietrich, M. S., Spotanski, K., Doersam, J. K., Cowher, M. S., Taback, B., . . . Koelmeyer, L. (2018). A prospective study of L-Dex values in breast cancer patients pretreatment and through 12 months postoperatively. *Lymphatic research and biology*, 16(5), 435-441.
- Ridner, S. H., Shah, C., Boyages, J., Koelmeyer, L., Ajkay, N., DeSnyder, S. M., . . . Dietrich, M. S. (2020). L-Dex, arm volume, and symptom trajectories 24 months after breast cancer surgery. *Cancer medicine*, 9(14), 5164-5173.
- Rockson, S. G. (2001). Lymphedema. *The American journal of medicine*, 110(4), 288-295.
- Rockson, S. G. (2018). Lymphedema after breast cancer treatment. *New England Journal of Medicine*, 379(20), 1937-1944.
- Rockson, S. G., Keeley, V., Kilbreath, S., Szuba, A., & Towers, A. (2019). Cancer-associated secondary lymphoedema. *Nature Reviews Disease Primers*, 5(1), 1-16.

- Romero, R. (1999). *Lymphedema and the nurse practitioner*. Paper presented at the Nurse practitioner forum.
- Roy, M., Biswas, J., & Datta, A. (2023). Breast Cancer: Epidemiology, Types, Diagnosis, and Treatment. In *Genetics and Epigenetics of Breast Cancer* (pp. 1-24): Springer.
- Sander, A. P., Hajer, N. M., Hemenway, K., & Miller, A. C. (2002). Upper-extremity volume measurements in women with lymphedema: a comparison of measurements obtained via water displacement with geometrically determined volume. *Physical therapy, 82*(12), 1201-1212.
- Sanders, J. E., Moehring, M. A., Rothlisberger, T. M., Phillips, R. H., Hartley, T., Dietrich, C. R., . . . Cagle, J. C. (2015). A bioimpedance analysis platform for amputee residual limb assessment. *IEEE Transactions on Biomedical Engineering, 63*(8), 1760-1770.
- Santambrogio, L. (2018). The lymphatic fluid. *International review of cell and molecular biology, 337*, 111-133.
- Santoso, D. R., Pitaloka, B., Widodo, C. S., & Juswono, U. P. (2020). Low-cost, compact, and rapid bio-impedance spectrometer with real-time Bode and Nyquist plots. *Applied Sciences, 10*(3), 878.
- Sardinha, L. B., Rosa, G. B., Hetherington-Rauth, M., Correia, I. R., Magalhães, J. P., Silva, A. M., & Lukaski, H. (2023). Development and validation of bioelectrical impedance prediction equations estimating regional lean soft tissue mass in middle-aged adults. *European journal of clinical nutrition, 77*(2), 202-211.
- Sayed, S., Ngugi, A. K., Nwosu, N., Mutebi, M. C., Ochieng, P., Mwenda, A. S., & Salam, R. A. (2023). Training health workers in clinical breast examination for early detection of breast cancer in low-and middle-income countries. *Cochrane Database of Systematic Reviews*(4).
- Sbrignadello, S., Göbl, C., & Tura, A. (2022). Bioelectrical impedance analysis for the assessment of body composition in sarcopenia and type 2 diabetes. *Nutrients, 14*(9), 1864.
- Scagliusi, S. F., Giménez, L., Pérez, P., Martín, D., Medrano, F. J., Huertas, G., & Yúfera, A. (2023). Bioimpedance Spectroscopy-based Edema Supervision Wearable System for Non-invasive Monitoring of Heart Failure. *IEEE Transactions on Instrumentation and Measurement*.
- Scharfetter, H., Hartinger, P., Hinghofer-Szalkay, H., & Hutten, H. (1998). A model of artefacts produced by stray capacitance during whole body or segmental bioimpedance spectroscopy. *Physiological measurement, 19*(2), 247.
- Schrenk, P., Rieger, R., Shamiyeh, A., & Wayand, W. (2000). Morbidity following sentinel lymph node biopsy versus axillary lymph node dissection for patients with breast carcinoma. *Cancer, 88*(3), 608-614.

- Seoane, F., Ferreira, J., Sanchez, J. J., & Bragós, R. (2008). An analog front-end enables electrical impedance spectroscopy system on-chip for biomedical applications. *Physiological measurement*, 29(6), S267.
- Seward, C., Skolny, M., Brunelle, C., Asdourian, M., Salama, L., & Taghian, A. G. (2016). A comprehensive review of bioimpedance spectroscopy as a diagnostic tool for the detection and measurement of breast cancer-related lymphedema. *Journal of Surgical Oncology*, 114(5), 537-542.
- Sharkey, A. R., King, S. W., Kuo, R. Y., Bickerton, S. B., Ramsden, A. J., & Furniss, D. (2018). Measuring limb volume: accuracy and reliability of tape measurement versus perometer measurement. *Lymphatic research and biology*, 16(2), 182-186.
- Shigaki, C. L., Madsen, R., Wanchai, A., Stewart, B. R., & Armer, J. M. (2013). Upper extremity lymphedema: Presence and effect on functioning five years after breast cancer treatment. *Rehabilitation psychology*, 58(4), 342.
- Siaravas, K. C., Katsouras, C. S., & Sioka, C. (2023). Radiation Treatment Mechanisms of Cardiotoxicity: A Systematic Review. *International Journal of Molecular Sciences*, 24(7), 6272.
- Siconolfi, S. F., Gretebeck, R. J., Wong, W. W., Pietrzyk, R. A., & Suire, S. S. (1997). Assessing total body and extracellular water from bioelectrical response spectroscopy. *Journal of Applied Physiology*, 82(2), 704-710.
- Sierla, R., Dylke, E. S., Shaw, T., Poon, S., & Kilbreath, S. L. (2020a). Assessment of Upper Limb Lymphedema: A Qualitative Study Exploring Clinicians' Clinical Reasoning. *Lymphatic research and biology*.
- Sierla, R., Dylke, E. S., Shaw, T., Poon, S., & Kilbreath, S. L. (2020b). Clinician assessment of upper limb lymphedema: An observational study. *Lymphatic research and biology*.
- Simic, M. (2013). *Realization of complex impedance measurement system based on the integrated circuit AD5933*. Paper presented at the 2013 21st Telecommunications Forum Telfor (TELFOR).
- SITZIA, J. (1995). Volume measurement in lymphoedema treatment: examination of formulae. *European journal of cancer care*, 4(1), 11-16.
- Smoot, B. J., Wong, J. F., & Dodd, M. J. (2011). Comparison of diagnostic accuracy of clinical measures of breast cancer-related lymphedema: area under the curve. *Archives of physical medicine and rehabilitation*, 92(4), 603-610.
- Songkakul, T., Wu, S., Ahmmed, P., Reynolds, W. D., Zhu, Y., & Bozkurt, A. (2021). *Wearable Bioimpedance Hydration Monitoring System using Conformable AgNW Electrodes*. Paper presented at the 2021 IEEE Sensors.
- Soran, A., Ozmen, T., McGuire, K. P., Diego, E. J., McAuliffe, P. F., Bonaventura, M., . . . Johnson, R. (2014). The importance of detection of subclinical lymphedema for the prevention of breast cancer-related clinical lymphedema after axillary lymph

node dissection; a prospective observational study. *Lymphatic research and biology*, 12(4), 289-294.

- Springer, B. A., Levy, E., McGarvey, C., Pfalzer, L. A., Stout, N. L., Gerber, L. H., . . . Danoff, J. (2010). Pre-operative assessment enables early diagnosis and recovery of shoulder function in patients with breast cancer. *Breast cancer research and treatment*, 120(1), 135-147.
- Sukul, D. K., Den Hoed, P., Johannes, E., Van Dolder, R., & Benda, E. (1993). Direct and indirect methods for the quantification of leg volume: comparison between water displacement volumetry, the disk model method and the frustum sign model method, using the correlation coefficient and the limits of agreement. *Journal of biomedical engineering*, 15(6), 477-480.
- Sun, F., Skolny, M. N., Swaroop, M. N., Rawal, B., Catalano, P. J., Brunelle, C. L., . . . Taghian, A. G. (2016). The need for preoperative baseline arm measurement to accurately quantify breast cancer-related lymphedema. *Breast cancer research and treatment*, 157(2), 229-240.
- Svensson, B., Dylke, E., Ward, L., & Kilbreath, S. (2015). Segmental impedance thresholds for early detection of unilateral upper limb swelling. *Lymphatic research and biology*, 13(4), 253-259.
- Svensson, B. J., Dylke, E. S., Ward, L. C., & Kilbreath, S. L. (2017). Segmental bioimpedance informs diagnosis of breast cancer-related lymphedema. *Lymphatic research and biology*, 15(4), 349-355.
- Swedborg, I. (1977). Volumetric estimation of the degree of lymphedema and its therapy by pneumatic compression. *Scandinavian journal of rehabilitation medicine*, 9(3), 131-135.
- Taji, B., Shirmohammadi, S., Groza, V., & Batkin, I. (2013). Impact of skin–electrode interface on electrocardiogram measurements using conductive textile electrodes. *IEEE Transactions on Instrumentation and Measurement*, 63(6), 1412-1422.
- Tan, P. H. (2023). Refining the classification of breast phyllodes tumours. *Pathology*.
- Tanaka, N. I., Miyatani, M., Masuo, Y., Fukunaga, T., & Kanehisa, H. (2007). Applicability of a segmental bioelectrical impedance analysis for predicting the whole body skeletal muscle volume. *Journal of Applied Physiology*, 103(5), 1688-1695.
- Taylor, R., Jayasinghe, U. W., Koelmeyer, L., Ung, O., & Boyages, J. (2006). Reliability and validity of arm volume measurements for assessment of lymphedema. *Physical therapy*, 86(2), 205-214.
- Ter, S.-E., Alavi, A., Kim, C. K., & Merli, G. (1993). Lymphoscintigraphy. A reliable test for the diagnosis of lymphedema. *Clinical nuclear medicine*, 18(8), 646-654.
- Thomas, T. H. (2023). What signs of breast cancer are there other than a lump? Retrieved from <https://www.medicalnewstoday.com/articles/322832>

- Thurlow, S., Taylor-Covill, G., Sahota, P., Oldroyd, B., & Hind, K. (2018). Effects of procedure, upright equilibrium time, sex and BMI on the precision of body fluid measurements using bioelectrical impedance analysis. *European journal of clinical nutrition*, 72(1), 148-153.
- Tierney, S., Aslam, M., Rennie, K., & Grace, P. (1996). Infrared optoelectronic volumetry, the ideal way to measure limb volume. *European journal of vascular and endovascular surgery*, 12(4), 412-417.
- Tiwari, A., Cheng, K.-S., Button, M., Myint, F., & Hamilton, G. (2003). Differential diagnosis, investigation, and current treatment of lower limb lymphedema. *Archives of surgery*, 138(2), 152-161.
- Tobin, M. B., Lacey, H. J., Meyer, L., & Mortimer, P. S. (1993). The psychological morbidity of breast cancer-related arm swelling. Psychological morbidity of lymphoedema. *Cancer*, 72(11), 3248-3252.
- Tokumoto, H., Akita, S., Kosaka, K., Nakamura, R., Yamamoto, N., Kubota, Y., & Mitsukawa, N. (2023). Differences in Transient Fluid Retention and Lymphedema With Breast Cancer Treatment for Lymphatic Microsurgery. *Annals of plastic surgery*, 91(1), 104-108.
- Tonello, S., Zacchini, A., Galli, A., Narduzzi, C., Golparvar, A., Meimandi, A., & Carrara, S. (2023). *In-Vivo Validation of Smart Device for on Body Hydration Monitoring*. Paper presented at the 2023 IEEE International Workshop on Metrology for Industry 4.0 & IoT (MetroInd4. 0&IoT).
- Tucker, A. S., Fox, R. M., & Sadleir, R. J. (2012). Biocompatible, high precision, wideband, improved Howland current source with lead-lag compensation. *IEEE transactions on biomedical circuits and systems*, 7(1), 63-70.
- Uchiyama, T., Ishigame, S., Niitsuma, J., Aikawa, Y., & Ohta, Y. (2008). Multi-frequency bioelectrical impedance analysis of skin rubor with two-electrode technique. *Journal of tissue viability*, 17(4), 110-114.
- Unno, N. a., Nishiyama, M., Suzuki, M., Yamamoto, N., Inuzuka, K., Sagara, D., . . . Konno, H. (2008). Quantitative lymph imaging for assessment of lymph function using indocyanine green fluorescence lymphography. *European journal of vascular and endovascular surgery*, 36(2), 230-236.
- Van Stralen, K. J., Stel, V. S., Reitsma, J. B., Dekker, F. W., Zoccali, C., & Jager, K. J. (2009). Diagnostic methods I: sensitivity, specificity, and other measures of accuracy. *Kidney international*, 75(12), 1257-1263.
- Van Zanten, M., Piller, N., & Ward, L. C. (2016). Inter-changeability of impedance devices for lymphedema assessment. *Lymphatic research and biology*, 14(2), 88-94.
- Vassard, D., Olsen, M. H., Zinckernagel, L., Vibe-Petersen, J., Dalton, S. O., & Johansen, C. (2010). Psychological consequences of lymphoedema associated with breast cancer: a prospective cohort study. *European journal of cancer*, 46(18), 3211-3218.

- Vicini, F., Shah, C., Lyden, M., & Whitworth, P. (2012). Bioelectrical impedance for detecting and monitoring patients for the development of upper limb lymphedema in the clinic. *Clinical breast cancer, 12*(2), 133-137.
- Vosika, Z. B., Lazovic, G. M., Misevic, G. N., & Simic-Krstic, J. B. (2013). Fractional calculus model of electrical impedance applied to human skin. *PloS one, 8*(4), e59483.
- Wanchai, A., Armer, J. M., Stewart, B. R., & Lasinski, B. B. (2016). Breast cancer-related lymphedema: A literature review for clinical practice. *International Journal of Nursing Sciences, 3*(2), 202-207.
- Wang, H., Li, D., Liuya, J., Dylke, E. S., Ward, L. C., Jia, J., & Kilbreath, S. L. (2017). Reference ranges using bioimpedance for detection of lymphedema in chinese women. *Lymphatic research and biology, 15*(3), 268-273.
- Ward, L., Bunce, I., Cornish, B., Mirolo, B., Thomas, B., & Jones, L. (1992). Multi-frequency bioelectrical impedance augments the diagnosis and management of lymphoedema in post-mastectomy patients. *European journal of clinical investigation, 22*(11), 751-754.
- Ward, L., Dylke, E., Czerniec, S., Isenring, E., & Kilbreath, S. (2011). Confirmation of the reference impedance ratios used for assessment of breast cancer-related lymphedema by bioelectrical impedance spectroscopy. *Lymphatic research and biology, 9*(1), 47-51.
- Ward, L., Dylke, E., & Kilbreath, S. (2012). Measurement of hand volume by bioelectrical impedance spectroscopy. *Lymphatic research and biology, 10*(2), 81-86.
- Ward, L., Fuller, N., Cornish, B., Elia, M., & Thomas, B. (1999). A Comparison of the Siconolfi and Cole-Cole Procedures for Multifrequency Impedance Data Analysis. *Annals of the New York Academy of Sciences, 873*(1), 370-373.
- Ward, L., Kilbreath, S., & Cornish, B. (2008). Bioelectrical impedance analysis for early detection of lymphedema. *Lymphedema diagnosis and therapy, 502-517*.
- Ward, L. C. (2006). Bioelectrical impedance analysis: proven utility in lymphedema risk assessment and therapeutic monitoring. *Lymphatic research and biology, 4*(1), 51-56.
- Ward, L. C. (2015). Bioelectrical impedance spectrometry for the assessment of lymphoedema: principles and practice. In *Lymphedema* (pp. 123-132): Springer.
- Ward, L. C. (2018). Early diagnosis in latent phase. In *Lymphedema* (pp. 197-203): Springer.
- Ward, L. C., Czerniec, S., & Kilbreath, S. L. (2009). Operational equivalence of bioimpedance indices and perometry for the assessment of unilateral arm lymphedema. *Lymphatic research and biology, 7*(2), 81-85.

- Ward, L. C., Degnim, A. C., Dylke, E. S., & Kilbreath, S. L. (2020). Bioimpedance spectroscopy of the breast. *Lymphatic research and biology*, 18(5), 448-454.
- Ward, L. C., Kilbreath, S. L., & Dylke, E. (2015). Letter to the Editor Re: Bundred et al. "Comparison of multi-frequency bioimpedance with perometry for the early detection and intervention of lymphoedema after axillary node clearance for breast cancer". *Breast cancer research and treatment*, 152(1), 227-228.
- Warren, A. G., Janz, B. A., Slavin, S. A., & Borud, L. J. (2007). The use of bioimpedance analysis to evaluate lymphedema. *Annals of plastic surgery*, 58(5), 541-543.
- Watanabe, R., Miura, A., Inoue, K., Haeno, M., Sakamoto, K., & Kanai, H. (1989). EVALUATION OF EDEMA USING A MULTIFREQUENCY IMPEDANCE METER INPATIENTS WITH LYMPHATIC OBSTRUCTION. *Lymphology*, 22(2), 85-92.
- Wernicke, A. G., Rosenblatt, R., Rasca, M., Parhar, P., Christos, P. J., Fischer, A., . . . Nori, D. (2009). Quantitative Assessment of Radiation-Induced Fibrosis of the Breast with Tissue Compliance Meter, Palpation, and Radiological Imaging: Preliminary Results. *The breast journal*, 15(6), 583-592.
- White, E. A., Orazem, M. E., & Bunge, A. L. (2013). Characterization of damaged skin by impedance spectroscopy: mechanical damage. *Pharmaceutical research*, 30(8), 2036-2049.
- Whitworth, P. W., & Cooper, A. (2018). Reducing chronic breast cancer-related lymphedema utilizing a program of prospective surveillance with bioimpedance spectroscopy. *The breast journal*, 24(1), 62-65.
- Whitworth, P. W., Shah, C., Vicini, F., & Cooper, A. (2018). Preventing breast cancer-related lymphedema in high-risk patients: the impact of a structured surveillance protocol using bioimpedance spectroscopy. *Frontiers in oncology*, 8, 197.
- Winterhalter, M., Schiller, J., Münte, S., Bund, M., Hoy, L., Weilbach, C., . . . Rahe-Meyer, N. (2008). Prospective investigation into the influence of various stressors on skin impedance. *Journal of clinical monitoring and computing*, 22(1), 67-74.
- Witte, C. L., Witte, M. H., Unger, E. C., Williams, W. H., Bernas, M. J., McNeill, G. C., & Stazzone, A. M. (2000). Advances in imaging of lymph flow disorders. *Radiographics*, 20(6), 1697-1719.
- Yamazaki, Z., Idezuki, Y., Nemoto, T., & Togawa, T. (1988). Clinical Experiences Using Pneumatic Massage Therapy bfor Edematous Limbs Over the Last 10 Years. *Angiology*, 39(2), 154-163.
- Yang, Y., Wang, J., Yu, G., Niu, F., & He, P. (2006). Design and preliminary evaluation of a portable device for the measurement of bioimpedance spectroscopy. *Physiological measurement*, 27(12), 1293.
- Yildiz, E. D., Bakar, Y., & Keser, I. (2022). What do lymphedema patients expect from a treatment and what do they achieve? A descriptive study. *Journal of Vascular Nursing*, 40(1), 59-65.

- York, S., Ward, L., Czerniec, S., Lee, M., Refshauge, K., & Kilbreath, S. (2009). Single frequency versus bioimpedance spectroscopy for the assessment of lymphedema. *Breast cancer research and treatment*, 117, 177-182.
- Yu, Q., Xu, Y., Yu, E., & Zheng, Z. (2022). Risk of cardiovascular disease in breast cancer patients receiving aromatase inhibitors vs. tamoxifen: A systematic review and meta-analysis. *Journal of Clinical Pharmacy and Therapeutics*.
- Zaleska, M. T., Olszewski, W. L., Durlík, M., Kaczmarek, M. K., & Freidenrich, B. (2018). Tonometry of deep tissues for setting effective compression pressures in lymphedema of limbs. *Lymphatic research and biology*, 16(2), 193-200.
- Zhuang, L., Chen, H., Zheng, X., Wu, S., Yu, Y., Lan, L., . . . Fan, H. (2022). Bioelectrical impedance analysis for early screening of upper limb subclinical lymphedema: A case-control study. *PloS one*, 17(9), e0274570.
- Zompanti, A., Cicco, R., Ciarrocchi, D., Santonico, M., & Pennazza, G. (2023). *Design, realization and test of a low-cost electrical impedance spectroscopy analyzer for biological samples*. Paper presented at the 2023 9th International Workshop on Advances in Sensors and Interfaces (IWASI).
- Zou, L., Liu, F.-h., Shen, P.-p., Hu, Y., Liu, X.-q., Xu, Y.-y., . . . Tian, Y. (2018). The incidence and risk factors of related lymphedema for breast cancer survivors post-operation: a 2-year follow-up prospective cohort study. *Breast Cancer*, 25(3), 309-314.